2018

The SHOC2 phosphatase complex as a therapeutic target for ERK pathway inhibition in RAS-driven tumors

Submitted in fulfilment of the requirements
for the Degree of

Doctor of Philosophy

UNIVERSITY COLLEGE LONDON (UCL)

’Imagination is the only weapon in the war against reality’’

Lewis Carroll

Abstract

Targeted inhibition of the ERK-MAPK pathway, upregulated in the majority of human cancers, has been hindered in the clinic by drug resistance and on-target toxicity. The MRAS-SHOC2-PP1 complex plays a key, but underexplored role in RAF-ERK pathway activation, by dephosphorylating a critical inhibitory site on RAF-kinases. In this body of work we present a preferential requirement for the SHOC2-phosphatase complex, specifically for Receptor Tyrosine Kinase (RTK), and anchorage-independent (tumorigenic) growth stimulated ERK-activation. We highlight that this context-dependent signalling bias has functional consequences in RAS-mutant cells, by specifically inhibiting anchorage-independent, but not 2D-adhered cell growth. Strikingly we show *in vivo* that SHOC2 deletion suppresses tumour initiation in KRAS-driven lung cancer models, and significantly extends overall survival. Additionally, SHOC2 inhibition selectively sensitizes KRAS- and EGFR-mutant Non-small cell lung carcinoma (NSCLC) cells to MEK inhibitors. Mechanistically we show this is because SHOC2 is required for feedback-induced RAF dimerization, and as such combined MEK inhibition and SHOC2 suppression leads to more potent and sustained ERK-pathway repression, driving a BIM-dependent apoptosis. Crucially, systemic SHOC2 ablation in adult mice is relatively well tolerated compared with other, core, ERK-pathway signalling nodes. These results present a rationale for the generation of SHOC2 targeted therapies, both as a monotherapy, and to widen the therapeutic index of MEK inhibitors.

Impact Statement

The insight provided in the breath of this project provides a strong rationale for the generation of targeted agents against the SHOC2 phosphatase complex, with clinical indications, not least, for NSCLC. The SHOC2 phosphatase complex is required for context dependent ERK-pathway activation. This places a unique requirement on SHOC2 for the tumorigenic properties of ERK-MAPK pathway addicted cancers, as well as in the acquisition of resistance to frontline small molecule inhibitor treatment with MEK inhibitors. We present extensive *in vitro* and *in vivo* experimental work that demonstrates genetic inhibition of SHOC2 selectively perturbs the tumorigenic growth of RAS-mutant cells, and significantly extends overall survival in murine models of RAS-driven LUng ADenocarcinoma (LUAD). In contrast SHOC2 is not required for ERK-signalling in 2D-adhered 'normal' cell growth, and systemic SHOC2 ablation is well-tolerated in adult mice. Furthermore genetic inhibition of SHOC2 prevents feedback relief ERK-pathway activation on MEKi treatment, lowering the concentration of MEKi required to drive cytotoxic responses in RAS- and EGFR-mutant tumour models. By driving a robust apoptotic response, combined MEK inhibition and SHOC2 suppression drive marked tumour regressions in xenograft models. We posit this will mitigate the acquisition of resistance, typically attributed to the otherwise cytostatic effects of MEKi's in the clinic, whose doses are constrained due to on-target toxicities. To surmise we propose that a SHOC2 targeted inhibitor would not only serve clinical utility as a monotherapy, but would also serve to widen the therapeutic index of MEK's, without providing any additional toxicity. Given that ERK-MAPK addicted cancers are not limited to NSCLC, but include both pancreatic and ColoRectal Cancers (CRC), we believe that SHOC2 therapies may have broader clinical indications beyond NSCLC. Collectively these cancers encompass those that are in the top 10 causes of mortality in the western world, and which present with poor progression free survival rates of <5-years. These cancers represent a huge unmet clinical need in an ageing world, where age represents the biggest predisposing risk factor for these diseases. Such distinct disease aetiologies all share an internal signalling network that may present an opportunity for shared therapeutic intervention. Research efforts that further our understanding of the core signalling networks and unique perturbations they present for therapeutic interventions is an area of research which commands further efforts.

Research Highlights

- Genetic inhibition of SHOC2 perturbs the tumorigenic properties of RAS-mutant cells.
- Loss of SHOC2 sensitizes RAS- and EGFR-mutant NSCLC cells to MEKi's.
- SHOC2 suppression transforms reversible cytostatic effects of MEKi's to cell death.
- SHOC2 is required for feedback-induced RAF dimerization and ERK reactivation on MEK inhibitor treatment.
- SHOC2 ablation inhibits LUAD development in RAS-driven mouse models.
- Systemic SHOC2 deletion in adult mice is well tolerated.

Table of Contents

List of Figures and Tables

Abbreviations

Anova	ANalysis Of VAriance
AF6	ALL1-fused gene from chromosome 6 protein
BAD	BCL-XL/BCL2-associated death promoter
BIM	B-cell lymphoma 2-interacting mediator of cell death
BSA	Bovine Serum Albumin
cDNA	complementary deoxyribonucleic acid
CMV	cytomegalovirus
CR1/2/3	conserved region 1/2/3
CRC	Colorectal Cancer
CRD	cysteine rich domain
DMEM	Dulbecco's Modified Eagle's Medium
DMSO	DiMethyl SulfOxide
dNTPs	deoxyribose nucleoside triphosphate
DTT	DiThioThreitol
DUSP	Dual-specificity phosphatase
ECL	Enhanced ChemiLuminescence
EDTA	EthyleneDiamineTetraAcetic acid
EGF	epidermal growth factor
EGFR	epidermal growth factor receptor
EMT	epithelial-mesenchymal transition
ERK	extracellular signal-regulated kinase
FBS	Fetal bovine serum
FDA	Food and Drug Administration
FGF	fibroblast growth factor
FGFR	fibroblast growth factor receptor
GAP	GTPase activating protein
GDP	guanosine diphosphate
GEF	guanine nucleotide exchange factors
GEMM	Genetically engineered mouse model
GFP	green fluorescent protein
GPCR	G-protein coupled receptor
GRB2	Growth Factor Receptor Bound Protein 2
GTP	guanosine triphosphate
H&E	Hematoxylin and eosin
HEAT	huntingtin-elongation-A subunit-TOR
HEK-293	human embryonic kidney-293
HTS	High throughput screen
HVR	hypervariable region
IVIS	*In vivo* imaging system
IP	Immunoprecipitation
IRES	Internal Ribosomal Entry Site

JNK	JUN N-terminal kinase
KSR	kinase suppressor of ras
LRR	leucine rich repeat
LRR	Leucine-Rich Repeats
LSL	lox-stop-lox
MAPK	Mitogen-Activated Protein Kinase
MEK	MAPK/ERK kinase
mESC	mouse embryonic stem cell
mRNA	messenger ribonucleic acid
MOMP	mitochondrial outer membrane permeabilisation
NOS	NSCLC Not otherwise specified
NT	Non-Targeting
NF1	neurofibromatosis type 1
NSCLC	non-small cell lung cancer
PAGE	PolyAcrylamide Gel Electrophoresis
PBS	Phopsphate Buffered Saline
PCR	polymerase chain reaction
PDAC	Pancreatic Ductal Adenocarcinoma
PDX	Pateint Derived Xenograft
PDZ	PSD-95 DLG1 ZO-1
PI3K	phosphatidylinositol 3-kinase
PP1	protein phosphatase 1
PP2A	protein phosphatase 2A
PP5	protein phosphatase 5
PTEN	Phosphatase and TENsin homolog
PTK	protein tyrosine kinase
RAF	Rapidly Accelerated Fibrosarcoma
RAS	c-Rat Sarcoma Viral Oncogene Homolog
RBD	ras binding domain
RFP	red fluorescent protein
RNA	ribonucleic acid
ROS	reactive oxygen species
RT	room temperature
RTK	receptor tyrosine kinase
SCID	Severe combined immunodeficiency
shRNA	small hairpin RNA
siRNA	small silencing RNA
SH2	scr homology 2
SHC	Src Homology 2 Domain Containing) Transforming Protein
SHOC2	Soc-2 Suppressor Of Clear Homolog
SOS	Son Of Sevenless Homolog
STAT	Signal transducer and activator of TranScription
SW1/2	Switch1/2
TAP	tandem affinity purification

Chapter 1

Introduction

1.1 Introduction

1.1.1 RAS – The Apical GTPase in Tumorigenesis

Oncogenic mutations in c-Rat Sarcoma Viral Oncogene Homolog (RAS) genes are found in over 30% of human cancers; including lung, colon and pancreatic adenocarcinomas. Cancers with RAS mutations make up some of the hardest to treat cancers, and as such currently represent both the 4th, and 7th largest causes of mortality in high income countries, for Non Small Cell Lung Carcinomas (NSCLCs) and ColoRectal Cancers (CRCs) respectively (Figure 1.1A). There are three canonical RAS isoforms, H/N and KRAS, of which KRAS is the most frequently deregulated in human malignancies (Figure 1.1C) (Forbes et al. 2011). In addition, RAS proteins play a key role in many more cancers through indirect activation, for example, as a result of aberrant signalling by receptor tyrosine kinases (RTKs), activation of Guanine nucleotide Exchange Factors (GEFs) (eg. Son Of Sevenless 1 SOS), by inactivation of negative regulators, such as the NF1 tumour suppressor gene, or mutations of downstream effectors, including BRAF in Melanoma and Hairy cell leukaemia, or PIK3CA in breast cancer (Downward 2003; Hobbs et al. 2016a).

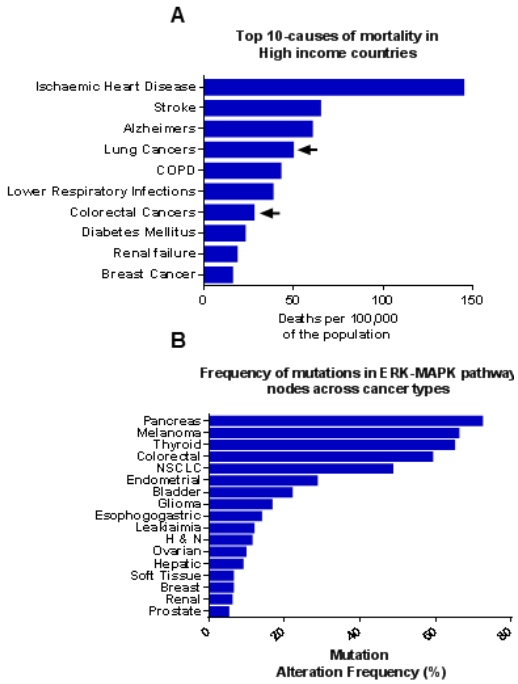

Figure 1.1 RAS – A disease of humanity

(**A**) Both NSCLCs and CRCs are recognised as top 10 causes of mortality in high income countries. (**B**) Driver mutation in the ERK-pathway are found across a breath

of cancers, including both NSCLCs and CRCs. Generated from data compiled from WHO website.

RAS exists as a binary molecular switch GTPase at the inner leaflet of the plasma membrane, cycling between an active GTP- and inactive GDP-bound form. RAS activation proceeds via Receptor Tyrosine Kinases (RTKs), G-Protein Coupled Receptors (GPCRs) and cytokine receptors. RTK activation by ligand engagement (eg. Epidermal growth factor receptor - EGFR) directs the phosphorylation of intracellular docking sites, allowing the recruitment of adaptor proteins (eg. Growth Factor Receptor Bound Protein 2 - GRB2) that in turn activate Guanine nucleotide Exchange Factors (GEFs) eg. SOS (Buday and Downward 1993). GEFs stimulate a structural reorientation in two highly conserved RAS regions 'Switch 1' and 'Switch 2' (SW1/2) which drive the exchange of GDP to the ten-fold more abundant GTP on RAS (Milburn et al. 1990). Active RAS-GTP now provides a landscape over which interaction and activation with effector proteins, including Rapidly Accelerated Fibrosarcoma (RAF) and Phosphatidylinositol-3-kinases (PI3K) can proceed (Vojtek et al. 1993; Rodriguez-Viciana et al. 1994). Slow intrinsic GTPase activity means RAS activity is largely attenuated by GTPase activating proteins (GAPs)(eg. Neurofibromin 1 - NF1) which potentiate GTP hydrolysis returning RAS to its inactive GDP form (Xu et al. 1990).

The canonical RAS family of GTPases, H,N,K share 90% sequence similarity. In all cases RAS-activity is orchestrated from the plasma membrane where it is anchored by a CAXX motif at its C-terminus. Post-translational modification of the C-terminus by farnesyl transferase and palimitoyl transferases govern spatial distribution of H,N,KRAS at the inner leaflet of the plasma membrane (Reiss et al. 1990; Hancock and Parton 2005; Tsai et al. 2015). KRAS is unique among the canonical RAS family members in that it encodes two splice variants, KRAS4A and 4B. Variation in their hypervariable regions (HVR) means that KRAS4B does not require these post-translational modifications for membrane targeting. Instead this polybasic HVR (unique among RAS isoforms) means KRAS4B is localised to distinct disordered lipid microdomains through an electrostatic interaction, as opposed to lipid rafts for the other RAS isoforms (Ehrhardt et al. 2002). It has also been suggested that KRAS4B preferentially binds BRAF as it negates the repulsion of negatively charged residues in BRAF's RAS binding domain (RBD) (Unpublished Data - Kota P et al 2018). Subtle sequence variations in the HVR region of canonical RAS family members may be functionally important, as different localisation may dictate specific effector pathway

engagement of different RAS-isoforms. This may have wider implications for predicting response to small molecule inhibitors targeting different RAS-effector pathways.

RAS functions as a master switch or regulator, governing gene transcriptional changes concerned with pro-mitogenic functions, including growth, survival and proliferation, (Figure 1.2). As such, RAS is frequently mutated in human cancer (Figure 1.1). 98% of RAS mutations cluster at three well defined sites in codons 12,13 and 61, the largest proportion (80%) in KRAS occurring in codon 12 (Parada et al. 1982; Taparowsky et al. 1982; Hobbs et al. 2016a). These mutations serve to inhibit GTP hydrolysis of RAS, either intrinsically, or by blocking GAP function, thus trapping RAS in its active state. This increase in active RAS across the inner leaflet of the cell membrane, due to reduced cycling, leads to hyperactivation of downstream effector pathways as the RAS switch is trapped in its 'on' state.

Mutations in RAS GTPases, including NF1, also lead to a reduced rate of GTP hydrolysis, ensuring RAS remains in its GTP bound or 'on' state for longer (Cichowski and Jacks 2001). As such patients with familial mutations in NF1 often present with benign or malignant tumours of the peripheral or central nervous system. In addition to direct mutations in RAS or NF1 mutations, overexpression of upstream RTKs, including EGFR, represent a means of ensuring persistent RAS activation. EGFR mutations cluster at two hotspots, a short deletion in exon 19 and a point mutation, 'L858R' in exon 21. Both are found within the kinase domain of EGFR, disrupt auto-inhibition of the RTK, and render EGFR constitutively active. Active EGFR's intracellular domain provides a platform to which Src Homology 2 (SH2) and phosphotyrosine binding (PTB) recruitment of adaptor proteins proceeds, including GRB2 (Scaltriti and Baselga 2006). GRB2 recruits SOS which in turn increases active RAS-GTP levels through its GEF function. Both NF1 and EGFR driver mutations are found in ~11% of NSCLC patients (Cancer Genome Atlas Research 2014).

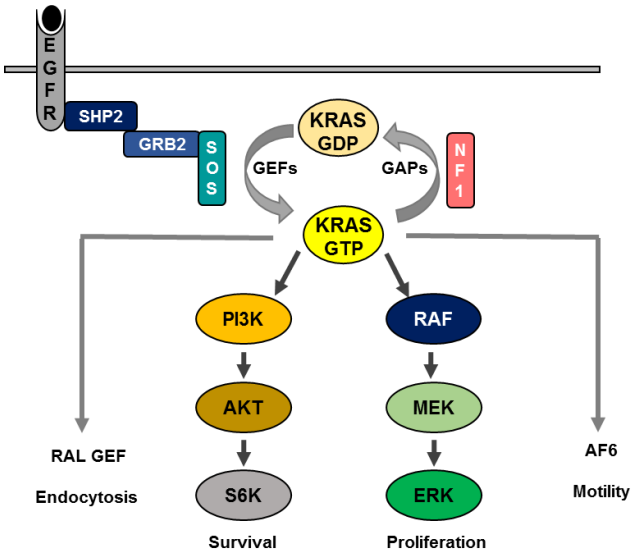

Figure 1.2 RAS – The Apex GTPase

RAS-GTP activates a number of effector pathways of which the ERK-MAPK and PI3K/AKT-pathway and the most frequently deregulated in human cancer.

1.1.2 RAF – the most frequently deregulated RAS-effector in cancer

RAF kinases are the primary kinase of the extracellular signal–regulated kinase (ERK)-MAPK-pathway, downstream of active RAS, and comprise three family members, A,B and CRAF (CRAF also frequently termed RAF1). RAF kinases are essential for normal ERK-MAPK-pathway activation. Activating mutations in RAF are associated with a variety of human cancers, as well as the related developmental RASopathy disorders; Noonan, LEOPARD, and cardiofaciocutaneous (CFC) syndromes (Molzan et al. 2010). RAF mutant cancers can be grouped into two distinct clusters: BRAF V600 mutant cancers, where ERK signalling is driven by a RAS-independent catalytic BRAF monomer, as is the case in melanoma, or p-loop BRAF mutants. The second cluster have low intrinsic kinase activity and instead promote heterodimerization with CRAF to drive aberrant ERK signalling that retains its RAS dependency, as is more common in NSCLC (Yao et al. 2015; Yao et al. 2017).

Activation of RAF kinases is a highly complex, multistep, cyclic process which requires multiple coordinate inputs, of which the mechanistics are still incompletely understood. What is known is that RAF transitions from an auto-inhibited cystolic monomer in which the N-terminus contacts the C-terminus, to an active homo-/ hetero-dimer bound to RAS at the plasma membrane (Cutler et al. 1998; Lavoie and Therrien 2015). Recruitment of RAF to the RAS Binding Domain (RBD) of RAS-GTP at the plasma

membrane is generally appreciated to be an early step in RAF activation (Figure 1.3). Further preliminary steps in RAF activation include the dephosphorylation of a conserved inhibitory site in the N-terminal regulatory domain (ARAF S214, BRAF S365, CRAF S259, hereby referred as 'S259) that facilitates 14-3-3 dissociation, re-localisation and, RAF dimerization (Morrison et al. 1993; Rommel et al. 1996; Jaumot and Hancock 2001; Dhillon et al. 2002; Lavoie and Therrien 2015). The S259 site in CRAF has been shown to be a phosphorylation-dependent binding motif for 14-3-3 proteins. The current model of activation suggests that auto-inhibition is at least partially stabilised by 14-3-3 proteins, binding to both the S259 site and an additional site, S621. Dephosphorylation of the S259 site then mediates the reorientation of 14-3-3 proteins to instead favour stabilization of the RAF dimer (Figure 1.3). The importance of the N-terminal RAF segment for RAF auto-inhibition and regulation is highlighted by oncogenic RAF fusion events that couple the RAF kinase domain to the N-terminus of a distant protein to de-couple RAF kinase activity from its own auto-inhibition, and thus de-repress RAF activity (Ciampi et al. 2005; Jones et al. 2008). Additionally, although rare in human cancers, hot spot mutations cluster at the S259 locus in various RASopathies, highlighting the importance of this site in maintaining 14-3-3 binding for RAF auto-inhibition (Molzan et al. 2010).

In addition to phosphatase-mediated RAF activation steps, phosphorylation events by kinases have been shown to regulate RAF activation. Indeed the aforementioned S621 site must be phosphorylated for 14-3-3 binding (Dhillon et al. 2002). Although highly homologous in their C-terminal kinase domain, subtle sequence variations in N-terminal regions of the three RAF isoforms permit divergent regulation. Both ARAF and CRAF have been shown to require phosphorylation of two sites at a conserved motif, 'SSYY' for activation by SRC or PAK, that BRAF does not require at its homologous 'SSDD' motif (Cleghon and Morrison 1994; Marais et al. 1995; Marais et al. 1997; Mason et al. 1999). In addition, CRAF but not BRAF requires an additional phosphorylation for its activation at S338 (S445 in BRAF), and both PAK and CK2 have been implicated in mediating this (Chaudhary et al. 2000; Ritt et al. 2007). The divergent N-terminal motifs, leading to two less regulatory requirements for BRAF activation, have been suggested to be responsible for the higher basal kinase activity of BRAF. Indeed the absence of these regulatory regions may be the reason BRAF is the chosen RAF frequently mutated in human disease, where one point mutation is sufficient to render BRAF constitutively active. The extra level of regulation imposed on CRAF, combined with high kinase activity compared to both BRAF and ARAF, may

suggest different functional consequences attributed to these layers of regulation, which may have important implications in aberrant RAF signalling (Marais et al. 1997).

The final significant event in RAF activation is RAS-driven RAF dimerization. Evidence for RAF dimerization being critical for RAS-mediated ERK signalling came from studies which identified that oncogenic mutations in BRAF that are catalytically inactive were able to drive hyperactive ERK-activation, due to an increased ability to associate with CRAF (Wan et al. 2004; Garnett et al. 2005; Heidorn et al. 2010). In this physiological scenario, downstream ERK-activation was both dependent on active RAS and CRAF, but not BRAF kinase activity, demonstrating the importance of one RAF monomer activating a second RAF monomer as part of the dimer *in situ*. This situation was analogous to KSR-induced RAF activation in *drosophila melanogaster* (Douziech et al. 2006). Further evidence includes: (i) Causal mutations of RAF found in RASopathies require dimerization (Molzan et al. 2010) (ii) RAF inhibitors have been shown to drive paradoxical ERK-activation through sterically supporting RAF dimerization (Hatzivassiliou et al. 2010; Poulikakos et al. 2010) (iii) Frontline RAF inhibitor resistance mechanisms have been reported to proceed through RAS-dependent RAF dimerization (Nazarian et al. 2010; Kaplan et al. 2012; Whittaker et al. 2013; Whittaker et al. 2015).

Following RAF dimerization MEK must be phosphorylated and the jury is still out on exactly how this proceeds. A compelling set of investigations proposes that MEK exists in the cytosol in inactive complexes bound to BRAF and/or KSR in a face-to-face heterodimer in which BRAF-BRAF, or KSR-KSR binding bridges the tetramer. Crystal structures of KSR-MEK complexes demonstrate that the MEK activation sites ‘S218 and S222’ lie at the dimer interface and thus KSR masks these sites from RAF (Brennan et al. 2011). In one KSR model it is proposed that a second RAF molecule must bind KSR, outcompete the KSR homodimer, and in doing so liberate MEK to be activated by a distinct RAF dimer, bound to RAS at the plasma membrane (Brennan et al. 2011; Dhawan et al. 2016). Alternatively, in the BRAF-MEK model, inactive complexes are directly recruited to RAS at the membrane in response to RAS activation (Haling et al. 2014). These models are far from complete, and it is unclear how much RAF exists in these scenarios as compared to in auto-inhibited RAF monomers, and which of these pools is more physiologically relevant in normal or aberrant RAF signalling. At least for BRAF p-loop mutant cells which require RAS-dependent dimerization for ERK-activation, the model suggests these cells have reduced inactive RAF-MEK complexes in favour of preformed RAF-RAF complexes

which drives their oncogenicity (Haling et al. 2014). These findings therefore suggest that RAF-dimerization represents the rate-limiting step for ERK-activation in RAS-mutant cancers, rather than MEK-recruitment to RAF, a limitation overcome by p-loop BRAF mutant cancers, and as such is an area of research which commands a much greater depth of understanding.

MEK1/2 mediate the transmission of RAS-RAF activation by phosphorylation of ERK at conserved residues 'Thr202/Tyr204'. ERK requires the phosphorylation of both sites for activation in contrast to MEK (Ferrell and Bhatt 1997). ERKs are proline-directed kinases which go on to phosphorylate an array of targets, including kinases and transcription factors concerned with pro-mitogenic functions. One family of ERK-targets worth mentioning are Ribosomal Protein S6 Kinases (RSKs), a family of ubiquitously expressed kinases which, like RAF, demonstrate auto-inhibition. Binding of ERK at the extreme C-terminus of RSK proteins, and subsequent phosphorylation at Thr573 is the first event in their activation. This phosphorylation activates the C-terminal kinase domain which, subsequently, auto-phosphorylates an additional activation site, S380. Further phosphorylation events by PDK1 (Dalby et al. 1998) lead to full RSK activation and dissociation of ERK from RSK, allowing RSK to bind, phosphorylate and activate secondary targets, both nuclear and cystolic, in part driving amplification and divergence of the ERK signal (Roux et al. 2003; Kidger and Cook 2018).

Ultimately ERK activity is transient and is tightly controlled both spatially and temporally. ERK signalling is attenuated in part by negative feedback loops from ERK to upstream pathway components, including, RTKs, SOS, MEK, and RAF itself (Corbalan-Garcia et al. 1996; Li et al. 2008; Lake et al. 2016). Phosphorylation of both BRAF and CRAF by ERK has been shown to disrupt both the RAS-RAF interaction and RAF dimerization, attenuating MEK phosphorylation by RAF and subsequent ERK activity (Rushworth et al. 2006; Ritt et al. 2010). Both SPRY (Sprouty) proteins and DUSPs (Dual Specificity phosphatases) are induced on ERK-activation and provide a more latent wave of ERK-pathway inactivation, including by direct cleaving of phospho-ERK 'pT-E-pY' motifs (Caunt et al. 2015).

1.1.3 SHOC2 – An underexplored ERK-pathway modulator

SHOC2/Sur-8 was originally identified in *C.elegans* as a positive modulator of the RTK-RAS-ERK pathway. Unlike RAF/Lin-45, MEK or ERK/Sur-1 genes, SHOC2 in *C.elegans* is not essential for organ development but SHOC2 deletion potently suppresses the phenotype of mutant RAS or high RTK (Fibroblast growth factor receptor - FGFR) signalling (Selfors et al. 1998; Sieburth et al. 1998). Thus, *C.elegans* genetics infer that targeting modulator nodes of the ERK-pathway such as SHOC2 may have milder toxicity, and thus provide better therapeutic margins than current targeting of core ERK-pathway modules (Moghal and Sternberg 2003).

Conflicting roles for SHOC2 function have been proposed. Some groups propose SHOC2 serves the role of a scaffold, bridging the RAS-RAF interaction (Matsunaga-Udagawa et al. 2010; Yoshiki et al. 2010). Others, including our group do not observe this direct interaction with RAS and/or RAF and instead recognise both MRAS and PP1 as SHOC2 binding partners (Rodriguez-Viciana et al. 2006; Jeoung et al. 2013; Young et al. 2013; Young et al. 2018). We demonstrate ‘S259’ RAF dephosphorylation is mediated by the ternary phosphatase complex comprised of SHOC2, MRAS and PP1 (SHOC2 complex) (Figure 1.4) (Rodriguez-Viciana et al. 2006). Evidence for this includes the fact that causal gain-of-function mutations in Noonan Syndrome patients are found to cluster at the S259 site in CRAF and are also found in all three members of the MRAS, SHOC2, PP1 complex, underscoring the importance of the SHOC2 phosphatase complex in modulating RAF-mediated ERK-pathway activation (Razzaque et al. 2007; Cordeddu et al. 2009; Molzan et al. 2010; Gripp et al. 2016; Higgins et al. 2017; Zambrano et al. 2017)

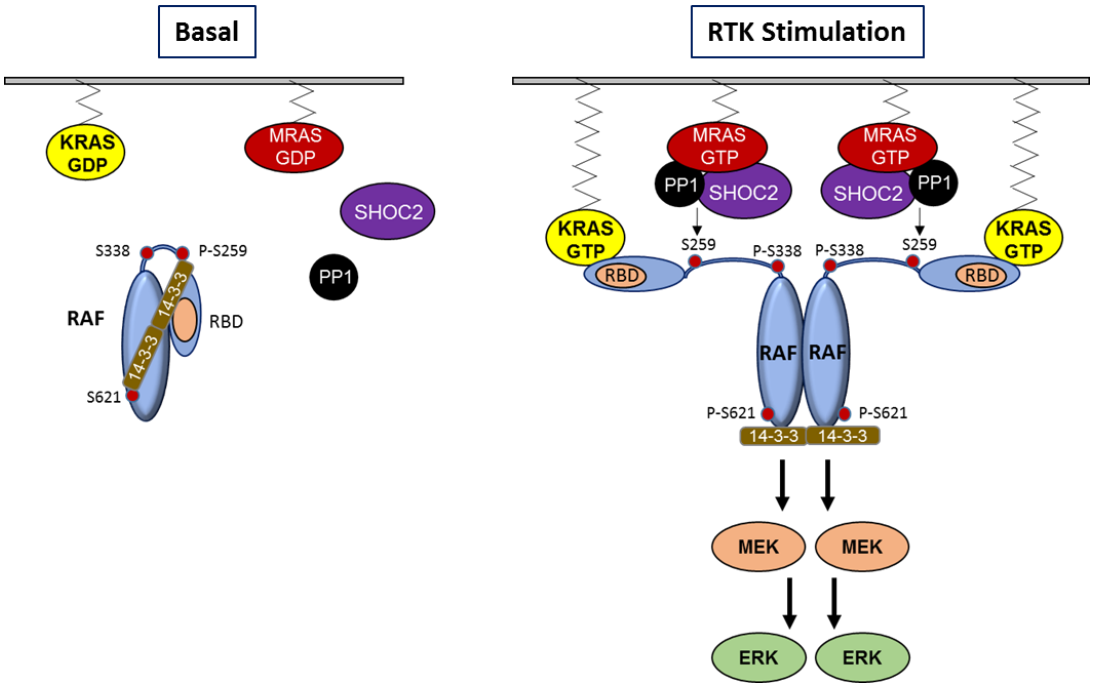

Figure 1.3 The SHOC2 phosphatase complex

The SHOC2 phosphatase complex dephosphorylates a site on RAF – 'S259' critical for RAF activation.

SHOC2 is comprised of leucine-rich repeats (LRR) - an 11-residue repeat sequence with the following consensus LxxLxLxxNxL (x can be any amino acid and L and N positions can be occupied by other hydrophobic amino acids). Leucine rich repeats are typically composed of 2 or 3 repeats and so form ~20-30 amino acid solenoid structures that are particularly adept to mediate protein-protein interactions. These protein-protein interactions are proposed to mediate SHOC2's interaction with MRAS and PP1, as well as other known effectors including SCRIB (Young et al. 2013). Loss of function point mutants of SHOC2 originally identified in *C.elegans* pinpointed regions of SHOC2 critical for mediating the interaction with MRAS, resulting in the recruitment of PP1 and dephosphorylation of S259 on RAF (Rodriguez-Viciana et al. 2006). Furthermore these original screens highlighted mutations that could uniquely disrupt SHOC2's interaction with either MRAS or PP1 whilst preserving other interacting properties and roles, notably with the scaffold protein SCRIB (Figure 1.5). This presents unique SHOC2 mutant tools (SHOC2 D175N) with which to disentangle the roles of SHOC2 *in vitro* and *in vivo* as part of the MRAS-SHOC2-PP1, or other complexes.

SHOC2 itself is predicted to be a horse-shoe shaped protein with flexible hinge regions similar to that of the PP2A subunit of the PP2 phosphatase. Like the MRAS-SHOC2-PP1 phosphatase complex, PP2 is, at least in one guise, also shown to form a trimeric holoenzyme complex comprising the regulatory 'A' subunit, catalytic 'C' subunit and a substrate recognition or further regulatory subunit 'B'. Here the 'A' subunit provides a similar horse-shoe shaped scaffold on which the 'B' and 'C' subunits converge, and changes in the flexible structure of 'A' permitted by the hinge regions allow a reduced or enhanced landscape on which the complex can assemble in response to cues (Groves et al. 1999; Cho and Xu 2007). It is predicted that the flexible structure of SHOC2 may allow such an interaction and complex assembly on binding active MRAS-GTP to permit PP1 binding to both components of the complex.

In vivo SHOC2 ablation is embryonically lethal at E8.5. Conditional deletion of SHOC2 specifically in endothelial cells causes embryonic lethality at a slightly delayed P13.5 due the requirement of SHOC2 for vasculature development. Intriguingly BRAF knockout (KO) mice have a similar time point of embryonic lethality. BRAF lethality is similarly attributed to disrupted vasculature, with both SHOC2 and BRAF KO embryos being notably smaller than wildtype littermates as well as presenting with sporadic haemorrhaging and subcutaneous oedema, due to incomplete formation of an endothelial layer lining the vessels. Given the requirement of SHOC2 for S259 dephosphorylation and RAF dimerization, the implication of this data suggests that intact SHOC2-dependent BRAF dimer signalling is required for normal vasculature development during embryogenesis (Wojnowski et al. 1997; Yi et al. 2010).

In cancer SHOC2 was recently identified as one of five genes necessary for viability of RAS mutant, but not RAS wild-type Acute Myeloid Leukaemia (AML) cell lines (Wang et al. 2017), demonstrating the preferential requirement of SHOC2 for viability in RAS mutant hematopoietic cells. In further studies SHOC2 has also been shown in RAF mutant colorectal and melanoma cell lines to drive resistance to front line RAF inhibitor therapies - PLX4720 (a vemurafenib analog). Resistance proceeded through RAS-activating events, including the acquisition of RTK/RAS mutations, amplification or NF1 loss-of function mutations. These resistance mechanisms reinstate ERK-activity through RAS-dependent RAF dimerization, and exemplify the importance of both CRAF and SHOC2 in this process, which are otherwise redundant with RAS-independent BRAF mutant monomers that activate ERK as dimerization-independent single catalytic units (Kaplan et al. 2012; Whittaker et al. 2015). The essential gene relationship between SHOC2 and CRAF is especially important considering CRAF is

reported to be the most essential RAF isoform for ERK-activation in RAS-driven tumorigenesis (Blasco et al. 2011; Karreth et al. 2011; Sanclemente et al. 2018).

1.1.4 MRAS – RAS a family of more than just three

MRAS belongs to the greater RAS family of GTPases with over 150 family members. MRAS constitutes the effector GTPase of the SHOC2 phosphatase complex. It is the most closely related RAS family member to the canonical RAS genes, and is similarly activated by growth factor treatment, cycling between an inactive GTP and inactive GDP form, with similar GEF/GAP specificity to the canonical RAS genes (Ehrhardt et al. 2002; Rodriguez-Viciana et al. 2004). Like the canonical RAS genes, MRAS has transforming capabilities, but contrastingly is rarely mutated in human cancer (Kimmelman et al. 1997). Causal mutations in Noonan syndrome patients are however found in MRAS and it is also upregulated in some cancers including Small Cell Lung Carcinoma (SCLC) (Gripp et al. 2016). MRAS shares a similar HVR to KRAS4B, a polybasic region that poses the idea they may be similarly located to disordered membrane microdomains and therefore may be required for co-engagement and activation of the same downstream effectors (Ehrhardt et al. 2002). This co-localisation may have important functional consequences in human cancer where driver mutations in KRAS are far more frequent than H/NRAS (Hobbs et al. 2016a).

1.1.5 No longer undruggable RAS – A tale of a RAS in a trap

The function of RAS and the layers of regulation that result in its cycling have been the subject of intensive research efforts with the hope of generating pharmacological inhibitors against RAS itself (Ostrem and Shokat 2016). In short, past research efforts attempted to generate GTP-competitive inhibitors for RAS, but these failed due to the high picomolar affinity of RAS for GTP, which is in stark contrast to ATP-competitive inhibitor success for kinase inhibitors, whose affinity for ATP is in a low nanomolar range. Subsequent efforts were aimed at preventing RAS recruitment to its active site at the plasma membrane. Farnesyl transferase inhibitors were the first of this kind but redundancy of a farnesyl membrane localisation tag with geranylgeranyltransferase circumvented the utility of this class of inhibitors (Whyte et al. 1997).

More recent efforts have seen early success with the KRAS G12C inhibitors which sequester KRAS G12C in its inactive state, by irreversible covalent occupancy of the 12 cysteine position (Ostrem et al. 2013). This class of inhibitor binds a novel pocket beneath SW2, adjacent, but distinct from the nucleotide binding pocket, circumventing the need to compete against the picomolar affinity of RAS for GTP. This research

highlighted that despite the G12C mutation RAS still transitioned between both an inactive GDP- and active GTP-bound state, allowing the inhibitors to 'trap' the inactive RAS state and slowly deplete RAS-GTP levels, thus exhausting the active conformation (Lito et al. 2016). Optimisation of tool compounds to those with desirable pharmacokinetics (PK) and rapid on-target kinetics to sequester the transient GDP-RAS during *in situ* cycling has shown that these inhibitors work *in vivo* to inhibit ERK and PI3K signalling, driving tumour regressions specifically in Patient Derived Xenograft (PDX) KRASG12C models (Janes et al. 2018). Currently this strategy exclusively relies on the cysteine warhead for covalent interference, and is limited to only a subset of KRAS mutant cancers with G12C mutations, 11-16% of NSCLC and <4% of PDACs (Hobbs et al. 2016b). Expanding this to other mutation subtypes is an area of active interest, ever more prevalent as research is beginning to illuminate both structural and functional differences in specific KRAS isoform mutations (Nussinov et al. 2018). Targeting mutant isoforms is a promising future avenue of research as these drugs may have more restrained toxicities - binding only the mutant subtype of RAS. This is an important consideration as deletion of all 3-canonical RAS isoforms or KRAS4B alone is embryonically lethal in mice (Johnson et al. 1997; Esteban et al. 2001; Plowman et al. 2003). As such Pan-RAS inhibitors or even sole inhibition of wildtype KRAS would be expected to have unacceptable toxicities reflecting the diversity of downstream effector pathways and outputs they would impinge on.

Data collected using the G12C inhibitor ARS-1620 highlighted that the inhibitor was much more effective against RAS mutant cells *in vivo* or in 3D anchorage-independent growth assays *in vitro* compared to 2D-adhered culture conditions (Janes et al. 2018). This fact resonates throughout the field of small molecule inhibitors targeting nodes of the ERK-MAPK pathway, and serves as a useful point of context to illustrate the transition of the field from 2D inhibitor screening platforms to organoids or anchorage-independent growth assays, and PDX models (Zhang et al. 2006; Fujita-Sato et al. 2015; Patricelli et al. 2016; Ambrogio et al. 2018; Sanclemente et al. 2018; Wong et al. 2018). It exemplifies the importance of 3D culture *in vitro,* and murine models in target validation projects, to uncover effects that, although clinically relevant, may be missed by conventional 2D assay platforms. This is something we have carefully considered in the scope of this research project. Although generally accepted and more clinically relevant, the field still has progress to make in explaining why RAS-mutant cells are more sensitive to ERK-pathway inhibition in 3D and we also attempt to make headway with this in the scope of this report.

1.1.6 EGFR – A demonstration in 'oncogene addiction' for small molecule inhibition

EGFR driver mutations are found in up to 11% of patients with NSCLC and lead to increased levels of active RAS-GTP (Cancer Genome Atlas Research 2014). EGFR has proved a much more tractable drug target than RAS, and EGFR small molecule inhibitors represent frontline therapeutics in EGFR-mutant NSCLC. Such inhibitors include the ATP-competitive inhibitors Gefitinib and Erlotinib, which are used in the first instance and show potent, but transient tumour regressions (Scaltriti and Baselga 2006). Unfortunately patients relapse and these are not durable beyond several months. Ultimately the EGFR receptor acquires a secondary mutation, most frequently at T790M in exon 20 that increases the affinity of the receptor for ATP and out-competes the inhibitor (Kobayashi et al. 2005). More recently inhibitors have been described that inhibit T790M EGFR, and these inhibitors are being incorporated into the clinic (Ward et al. 2018). Other resistance mechanisms that are acquired to reinstate RAS signalling include MET amplification, such persistent reactivation of RAS signalling serves to demonstrate the oncogene addiction of these cancers to EGFR-RAS signalling (Turke et al. 2010). There is still a great deal of work to be done, but the potent first response to small molecule therapies in examples such as EGFR inhibitors demonstrates the relevance of oncogene addiction in guiding the next generation of novel small molecule inhibitors that yield truly translational benefits.

1.1.7 Targeting RAS effectors – An alternative to direct targeting of RAS

RAS proteins have been challenging drug targets and extensive efforts have focused on targeting RAS effector pathways as a more tractable alternative (Cox et al. 2014; Downward 2015). Multiple lines of evidence, including mutual exclusivity of RAS and BRAF mutations in many cancers, highlight the RAF-MEK-ERK kinase cascade (ERK-MAPK pathway) as a key effector of RAS oncogenic properties, and multiple small molecule inhibitors of this pathway have been developed (Samatar and Poulikakos 2014). However, RAS-driven tumours remain intractable to targeted therapies. Whereas clinical progress has been made targeting BRAF V600E mutant tumours with first generation RAF inhibitors that specifically target the ATP binding pocket of the autonomous catalytic BRAF monomer, efforts to target BRAF wildtype/ RAS mutant, or RAS-dependent non-V600E, BRAF p-loop mutant tumours have had less success (Chapman et al. 2011; Ascierto et al. 2013). This is largely due to the requirement of these mutant subtypes on RAF dimerization and CRAF activation for downstream MEK/ERK-activation (Weber et al. 2001; Heidorn et al. 2010; Hu et al. 2013; Haling et

al. 2014). Mechanisms of RAF resistance mediated by RAF dimerization have been described, including both RTK-dependent/ independent RAS activation, as well as RTK-mediated activation of other mitogenic pathways, independent of RAS (Nazarian et al. 2010; Xing et al. 2012; Solit and Rosen 2014).

First generation RAF inhibitors designed to catalytically inhibit the BRAF V600E kinase have been shown to suffer two shortfalls in inhibiting RAF dimer-dependent ERK-pathway activation: (i) paradoxical ERK-activation by sterically supporting RAF dimerization, and (ii) 'negative cooperativity', both contraindicating their clinical use for RAS mutant tumours (Hatzivassiliou et al. 2010; Poulikakos et al. 2010). First generation RAF inhibitors typically fall into the DFG-IN/αC-OUT class based on structural studies. Vemurafenib, the first clinically approved RAF inhibitor for the treatment of BRAF V600E driven Melanoma belongs to this class. Early evidence found that this compound was unable to effectively inhibit RAS-GTP/RAF dimerization-dependent ERK-signalling, despite its potency in inhibiting the catalytic monomer, BRAF V600E (Yao et al. 2015; Yao et al. 2017). This was later shown to be in part due to negative cooperativity induced by this class of inhibitor. The binding of one molecule of Vemurafenib in the RAF dimer drives a conformation in the bound RAF that sterically hinders binding of the drug molecule on the second RAF protomer in the dimer, and additionally limits the duration of occupancy of the drug in the catalytic site. In contrast, second generation PanRAF inhibitors, as well as peptide blockers of the RAF-RAF interface, have demonstrated potent tumour regressions in RAS mutant cell lines, as well as RAS-mutant PDXs (Freeman et al. 2013; Peng et al. 2015). Second generation PanRAF inhibitors suppress the kinase activity of all three RAF isoforms and fall into the DFG-OUT/αC-IN class of RAF inhibitors. PanRAF inhibitors still counterintuitively stabilise the BRAF-CRAF dimers but due to their ability to inhibit all 3 RAF isoforms (A/B/C), and avoid negative cooperativity they have found greater utility across a range of cancer types, with driver RAS, BRAF V600E and non V600E mutations (Heidorn et al. 2010). However recent evidence has shown this class of inhibitors to paradoxically disrupt RAF auto-inhibition, increasing the pool of preformed RAF dimers in the cytosol. In quiescent cells (non-RAS mutant) this is without consequence, however in RAS-mutant cells this increases the proportion of RAS bound to RAF, and is modelled to paradoxically increase active signalling clusters of RAF dimers (Freeman et al. 2013; Peng et al. 2015; Karoulia et al. 2016; Jin et al. 2017). As a result of these caveats it is thought PanRAF inhibitors will have to be used at high concentrations to ensure both RAF protomers within the dimer are bound at any one time, which may lend this class of inhibitors to have a narrow therapeutic index. This is especially

important given that they will target both aberrant and 'normal' RAF signalling unlike first generation BRAF-selective inhibitors (Peng et al. 2015).

MEK inhibitors (MEKis) are highly selective due to their allosteric mechanism of action, but have shown minimal clinical efficacy against RAS-driven tumours, despite the fact that RAS mutant cells have been shown to be specifically sensitive to MEK inhibition. This is mainly due to drug resistance and on-target toxicity. The ERK-pathway is regulated by negative feedbacks at multiple levels including phosphorylation of negative regulatory sites on RTKs, as well as in RAF kinases that inhibit RAF dimerization and binding to RAS (Dougherty et al. 2005; Ritt et al. 2010; Sato et al. 2013; Lake et al. 2016). Relief of these negative feedbacks by pharmacological ERK-pathway inhibition results in paradoxical signalling rebound and intrinsic resistance. In addition, the ERK-pathway is a key mediator of G1/S transition, and as such MEKi's have a predominant cytostatic response that is likely permissive for an environment that facilitates acquisition of drug resistance mechanisms (Sale and Cook 2013b). Strikingly, in both RAS- and BRAF-mutant cells, most, if not all resistance mechanisms lead to ERK-pathway reactivation, highlighting the strong oncogene addiction of these cancers to ERK signalling (Johannessen et al. 2010; Nazarian et al. 2010; Whittaker et al. 2013). However ultimately, the potent pathway suppression required for antitumor activity is limited by the doses of MEKi that can be administered safely because of on-target toxicity (Bollag et al. 2010; Caunt et al. 2015).

ERK activity is essential for normal tissue homeostasis, highlighting the difficulties of inhibiting the ERK-pathway within a therapeutic index (Blasco et al. 2011). The core components of the ERK-pathway have been shown to be essential for embryonic development (Pritchard et al. 1996; Wojnowski et al. 1997; Wojnowski et al. 1998). Significantly, conditional deletion of A,B,CRAF/ MEK1/2/ ERK1/2 genes in adult mice also leads to rapid deterioration and death within 2-weeks of induction (Sanclemente et al. 2018). As a result of the essential role of the ERK-pathway in development and in normal healthy physiology in adult mice, drugs that target these nodes for the treatment of human cancers are expected to have a constrained therapeutic index. Therefore it is important novel targets of tumorigenic ERK-pathway activation are found that are more specific to cancer cells and spare surrounding healthy tissue for better clinical application of inhibitors that target such a core signalling axis. Alternative approaches have led research groups to use combinations of small molecule inhibitors to exploit unique signalling requirements or synthetic lethalities in cancer.

1.1.8 It takes 2 when it comes to killing cancer

The principle of synthetic lethal interaction is that targeted inhibition of two distinct effectors causes lethality by targeting a unique vulnerability in the cancer, whereas individual targeting of either effector alone may have little or no effect. Identifying synthetic lethalities has been the subject of intensive drug discovery efforts in the RAS field due to three reason (i) the oncogene addiction demonstrated by RAS-mutant tumours (ii) to identify RAS-effector co-targeting strategies that negate the need to target 'undruggable' RAS (iii) to provide a wide therapeutic index by perturbation of a unique pathway that the RAS cancer uniquely relies upon, overcoming toxicity limitations.

Given the reality that MEKi's have predominantly cytostatic responses at therapeutically relevant concentrations, and given the propensity of cancers to overcome MEK inhibition by reinstating ERK activity through pathway rewiring and upregulation of RTKs or KRAS amplification (Solit and Rosen 2014), co-targeting of MEK with secondary inhibitor combinations has been an active area of research. People have sought to identify synthetic lethalities, co-targeting two kinases of the ERK-pathway (vertical inhibition) and co-targeting different RAS-effector pathway kinases (Molina-Arcas et al. 2013; Lamba et al. 2014; Sun et al. 2014; Manchado et al. 2016; Merchant et al. 2017). Key among the second type of combinations was the co-targeting of RAS and PIK3CA pathways. With the exception of BRAF, PIK3CA mutations contribute the largest proportion of driver mutations in a RAS-effector pathway, with inactivation of PTEN further contributing to aberrant PI3K activation (Engelman et al. 2006). Point mutations in p110α cluster at 2 hotspots, (i) E545 in the helical phosphatidylinositol kinase homology domain, (ii) H1047 near the end of the catalytic domain, and both confer hyperphosphorylation of AKT in the absence of ligand stimulation (Samuels et al. 2004; Samuels et al. 2005). Early data demonstrated that disrupting RAS-p110α interaction decelerated tumour growth in KRAS-driven murine LUAD, but significantly only the combination of PI3K inhibitors with MEK inhibitors caused robust tumour regressions (Gupta et al. 2007; Engelman et al. 2008; Castellano et al. 2013).

Another MEK co-targeting strategy that is very topical at the time of writing this thesis is MEK + SHP2 inhibitors. SHP2 (PTPN-11 Tyrosine-protein phosphatase non-receptor type 11) is a phosphatase that positively regulates RAS. Activating mutations in RTKs, including in EGFR, lead to enhanced KRAS activity through phosphorylation

of adaptor proteins including the SHP2 phosphatase (PTPN11). Moreover, negative feedback loops from ERK to upstream RTKs lead to SHP2 addiction in the context of MEKi treatment, where RTK amplification serves as a resistance mechanism to reinstate ERK reactivation. SHP2 inhibitors have been extensively published in recent months to synergise with MEKi's in RAS-mutant, NSCLC, CRCs, and PDACs, as well as cancers with amplified KRAS, including, Gastric and Oesophageal cancers. SHP2 inhibitors serve to provide the first high impact validation of combined MEKi + phosphatase vertical inhibition in driving marked tumour regressions in RAS-mutant cancers (Mainardi et al. 2018; Ruess et al. 2018; Wong et al. 2018). Critically the data put forward by other research groups shows us, although SHP2 inhibitors alone have no effect on Kras.P53-driven PDAC or LUAD murine models, and MEKi monotherapy only provides a cytostatic benefit, the combination of both can drive robust and durable tumour regressions. This data highlights the redundancy of the phosphatase in RAS-mediated signalling until in the context of MEKi, where negative feedback loops upregulate RTK signalling to reinstate ERK activity via SHP2, driving a synthetic lethality. Although SHP2 inhibitors are currently at the forefront of novel therapies targeting RAS-mutant cancers, the critical role of SHP2 in normal cardiac physiology remains a huge clinical limitation to this class of inhibitors (Nakamura et al. 2007; Princen et al. 2009). Indeed causal mutations in SHP2 have been shown to drive congenital heart defects in LEOPARD syndrome (Lauriol et al. 2015). SHP2 inhibitors provide a demonstration of the power of combining kinase and phosphatase inhibition of the same pathway as a small molecule therapeutic alternative to targeting of two kinases which has traditionally been the norm.

Co-targeting two nodes of the same RAS-effector pathway (vertical inhibition) or two nodes of different RAS effector pathways has shown exciting preclinical data. Lessons learned from combination strategies teach us that if you deliver a robust enough cytotoxic effect at first insult it is possible to drive durable tumour regressions of established lesions *in vivo*. The proof of concept of these combination lies in their ability to provide a therapeutic index at concentrations that are not otherwise toxic in the clinic. Pre-clinical and early clinical data causes the field to progress cautiously as toxicity has been reported for MEK + PI3K and MEK + SHP2 combinations (Li et al. 2011; Castellano et al. 2013; Jokinen and Koivunen 2015). There is therefore still a rationale for the development of small molecule inhibitors against novel nodes of the ERK-pathway, alone or in combination with MEKi's, that are more specifically required for tumorigenesis, and therefore may demonstrate more sparing toxicity profiles.

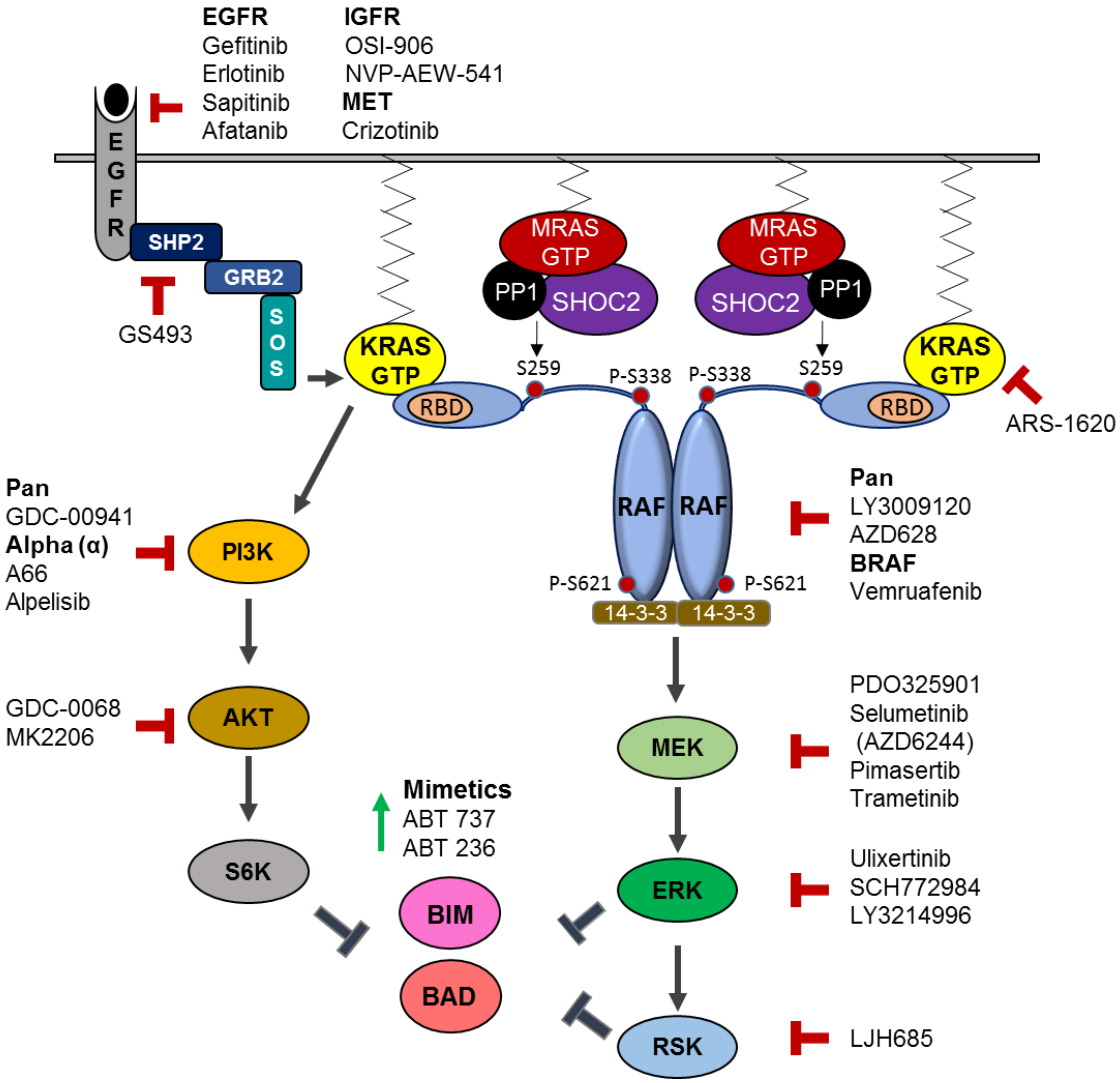

Figure 1.4 Past and present efforts to target RAS and its effectors

Due to difficulties in targeting RAS directly, efforts have been directed against RAS-effector pathways, notably the RAF-ERK and PI3K-AKT pathways, the two most frequently deregulated RAS-effector pathways in human cancer. Given the requirement of the SHOC2-phosphatase complex for RAF-mediated ERK-activation we propose this complex could present a novel therapeutic target for ERK-pathway inhibition. RED – Inhibitors/ Green – Mimetics/ Grey – Activating or inactivating pathway phosphorylation events.

1.1.9 ERK-dependent regulation of the intrinsic apoptotic pathway

Apoptosis is a form of programmed cell death characterised by cell rounding, shrinking, DNA fragmentation and membrane blebbing (Hengartner 2000). Apoptosis is an essential biological function during embryonic development and tissue homeostasis (Haanen and Vermes 1996). Apoptosis blockade is one of the hallmarks of cancer (Hanahan and Weinberg 2000), and efforts to reinstate apoptosis in cancer therapies to drive cytotoxic responses to small molecule inhibitor therapies is an active area of investigation. Apoptosis is divided into both the extrinsic and intrinsic apoptosis pathways and the focus of this section due to later findings and the role of ERK is focused on the intrinsic apoptotic pathway.

ERK activity has been shown to modulate the BCL-2-dependent intrinsic apoptosis pathway. The intrinsic apoptosis pathway relies on a critical balance between both pro and anti-apoptotic proteins that maintains the integrity of the outer mitochondrial membrane. Pro-survival BCL-2 family members comprise a subfamily of related anti-apoptotic proteins (BCL-2, BCL-XL, BCL-S, MCL1) that reside on the outer mitochondrial membrane. Conversely BCL-2 family members of the BH3 only subfamily are less structurally similar (BIM, BID, BAD, BAX, NOXA, PUMA and others) and are found in the cytosol. Various cellular assaults trigger the intrinsic apoptosis pathway that leads to the binding and sequestering of pro-survival BCL-2 family members by pro-apoptotic BH3 family members. This then permits the death effector proteins BAX and BAK to drive mitochondrial outer membrane permeabilisation (MOMP). MOMP releases cytochrome C from the inner membrane space of the mitochondria driving formation of the apoptosome, which in turn activates executioner caspases that go on to cleave a host of cellular substrates (Cook et al. 2017). Critically only BIM and PUMA have the capacity to bind and sequester all pro-survival proteins (Kuwana et al. 2005). MEKi's inhibit the phosphorylation of ERK, and in doing so have been shown to govern both transcriptional and protein level regulation of the intrinsic apoptotic pathway (Bonni et al. 1999). Of note ERK phosphorylates proapoptotic proteins BIM (B-cell lymphoma 2-interacting mediator of cell death) and BAD (BCL-XL/BCL2-associated death promoter). ERK- and/or RSK-mediated phosphorylation of BIM labels BIM for ubiquitination and degradation by the proteasome, similarly phosphorylation of BAD by ERK (and suggested more recently by RSK) at S112 promotes its inactivation, either by proteasomal degradation or sequestration by 14-3-3 proteins (Scheid et al. 1999; Ley et al. 2003; Fueller et al. 2008). Despite the regulation of ERK-pathway activity by MEKi's, they rarely induce apoptosis within a therapeutic index. There are many explanations for this, including the fact that many

intrinsic apoptotic pathway factors require coordinate inputs from other pathways. Indeed BAD requires coordinate phosphorylation by MEK and AKT for 14-3-3 sequestration (Datta et al. 1997). This may in part explain the pre-clinical success of combination strategies that target both the PI3K-AKT and ERK-MAPK axes to indirectly modulate BH3-proapoptotic proteins (Engelman et al. 2008; Castellano et al. 2013). Additionally many cancers have been found to upregulate pro-survival BCL-2 factors shifting the balance of the intrinsic apoptotic pathway mediators to permit survival even in the harsh tumour environment (Certo et al. 2006; Akgul 2009). As such there is a rationale for combining MEKi's with modulators of this pathway. Indeed combining MEKi's with BH3 mimetics, including ABT-737 & ABT-236, which bind and sequester pro-survival BCL-2 family proteins has shown large preclinical success, leading to marked on-target tumour regressions in RAS-mutant mouse models of lung and pancreatic cancers (Corcoran et al. 2013; Tan et al. 2013). The cytostatic effects of MEKi monotherapy have been suggested to provide an environment that is permissive for rapid selection of treatment-resistant cells, thus combination strategies that ensure a robust enough primary apoptotic response that prevents this are essential for the design of future therapeutic strategies.

Due to the limitations of targeting MEK as a monotherapy: (i) on-target toxicities constraining therapeutic concentrations in the clinic, (ii) predominantly cytostatic effects at these therapeutically applicable concentrations and (iii) resistance through RAS/RTK amplification or mutation that reinstate ERK activity, there is still a rationale for the generation of therapies that target novel nodes of the ERK-pathway alone, or in combination with MEKi's to widen their therapeutic index. Given the underexplored role for the SHOC2 phosphatase complex in mediating RAF dimer-dependent ERK-activation this project aimed to generate a body of evidence to validate SHOC2 as a therapeutic target for ERK-pathway inhibition in RAS-driven tumours.

1.2 Project Aims

SHOC2 deletion has previously been identified to selectively perturb the growth of KRAS-mutant AML suspension cell lines (Wang et al. 2017), and selectively perturb the growth of RAS mutant MDA-MB-231 cells in anchorage-independent growth conditions (Young et al. 2013). Given this information my primary aims were:

(i) Use genetic inhibition (shRNA/CRISPR) of SHOC2 to assess how SHOC2 suppression/deletion effects both the 2D-adhered and 3D-anchorage-independent growth of RAS-mutant NSCLC cells, expanding observations in MDA-MB-231 cells to a more clinically relevant cell system.

(ii) To take candidate RAS-mutant cell lines that respond *in vitro* and test the effect of SHOC2 suppression/deletion on *in vivo* growth assays in immunocompromised mice (subcutaneous/ IV-tail vein injections).

(iii) To determine the role of both SHOC2, and further still, the SHOC2 phosphatase complex on the initiation/progression of RAS-driven LUAD in two-autochthonous mouse models (introduced in 8.1.3).

Targeting of core ERK-MAPK nodes is limited in its therapeutic application by on-target toxicities, predicted by the essential role of these nodes for viability in adult mice (Blasco et al. 2011; Sanclemente et al. 2018). In addition to on-target toxicities therapeutic windows are often short due to the acquisition of secondary mutations that drive acquired resistance to frontline monotherapies, and serve to reinstate ERK-activity. As such various combinations of small molecule agents have been published to drive enhanced suppression of ERK-activity and provide more durable tumour stasis/regressions (1.1.8). The great limitations of many of these combination strategies is that their therapeutic index is predicted to be constrained by on-target toxicity (Castellano et al. 2013). However given the oncogene addiction of RAS-mutant cancers, affirmed by acquired resistance, there is still a rationale to develop agents that target novel nodes of the ERK-pathway, that provide a better therapeutic index, both as a monotherapy, and/or as part of combination strategies.

Given the redundancy of SHOC2 in *c.elegans* (Selfors et al. 1998; Sieburth et al. 1998) and that SHOC2 has been identified as a candidate gene that drives resistance to RAF inhibitor treated colorectal cancers (Whittaker et al. 2015) my aims were four-fold:

(i) Use genetic inhibition (shRNA/CRISPR) of SHOC2 to assess how SHOC2 suppression/deletion changes the response of RAS-mutant cell lines to RTK-stimulation.

(ii) Use genetic inhibition (shRNA/CRISPR) of SHOC2 to assess how SHOC2 suppression/deletion shifts the IC50 of RAS-mutant cells lines to a panel of candidate small molecule inhibitors, and expand these findings to other genetic drivers of ERK-activation in NSCLC eg. EGFR- and BRAF-mutant cell lines.

(iii) Determine how combined inhibition of SHOC2 and secondary inhibitor combinations effects both ERK-activity and correlate this to readouts of both cell cycle arrest and apoptosis.

(iv) Expand *in vitro* findings to *in vivo* subcutaneous xenograft assays.

All aims will be carried out using multiple means of genetic inhibition, given a SHOC2 inhibitor is yet to be developed. These genetic inhibition approaches will be complemented by rescue experiments using a combination of sophisticated *C-elegans* and/or human genetics that have identified point mutations that uniquely enhance or prevent SHOC2 phosphatase complex assembly (Figure 1.5). These tools will enable us to disentangle effects attributed to the role of SHOC2, both as an individual unit, and more specifically, as part of the SHOC2 phosphatase complex, described in section 1.1.3 (Figure 1.4).

Chapter 2

Methods

2.1 Methods

2.1.1 Cell culture and Generation of stable cell lines

HEK293 (UCL) and NSCLC cells (Table 1) obtained from the CRUK Central Cell Services facility (Francis Crick) were cultured in DMEM supplemented with 10% FBS at 37°C under 5% CO2. Cells were confirmed mycoplasma negative by PCR. For EGF stimulation, cells were serum-starved in DMEM/0% FBS for at least 6 hours followed by treatment with 25 ng/ml EGF.

Lentiviruses shSHOC2 or shSCR were generated by transient transfection of HEK293 cells with the lentiviral construct, pMD.G (VSV-G expresser) and p8.91 (gag-pol expresser) packaging vectors. Cells were transfected 4h after seeding with plasmid DNA and 1 mg/ml polyethylenimine (PEI, Polysciences) mixed at a 1:4 ratio in OptiMEM (Life Technologies). Virus-containing medium was harvested 24h, 48h, and 72h after transfection and supplemented with 5 µg/ml Polybrene (hexadimethrine bromide, Millipore Sigma). Cells were infected with lentivirus and where required, selection was carried out with either 2.5µg/ml puromycin (Sigma), 200µg/ml Hygromycin, Neomycin (Sigma). Ecotropic retroviruses were generated by transient transfection of the Phoenix ecotropic cell line and virus was collected as above. Cell lines expressing the ecotropic receptor EcoR were generated by transduction with amphotropic EcoR retroviruses and selection with 10µg/ml Blasticidin (Sigma).

SHOC2 knockout (KO) cells were generated by transient transfection with the pSpCas9(BB)-2A-GFP (PX458), (Addgene plasmid #48138), containing a GFP expression cassette and the following gRNA-encoding sequence targeting exon 3 of SHOC2: 5`-gRNA-`3 GAGCTACATCCAGCGTA, PAM: ATG. GFP-positive cells were sorted by FACS into 96-well plates and single-cell clones were amplified and analysed by Western blot to assess SHOC2 protein levels. SHOC2 KO cells were then transduced with lentivirus expressing an empty vector, FLAG-SHOC2 WT or the FLAG-SHOC2^{D175N}, under puromycin selection.

siRNA experiments were performed with a pool of 2 oligos at final concentration of 20nM. Oligos were mixed with optimum and RNAiMax (Fischer) and added to cells while cells are undergoing attachment. Lysates were harvested 72hours after si transfection. For sequences see materials and reagents in supplementary data.

2.1.2 Cell proliferation assays 2D-Adhered and 3D Spheroid culture

Cells with stable in-cooperation of shRNAs, or CRISPR knockout cells were seeded in 24-well plates and imaged on the IncuCyte (Essen BioScience). Pictures were taken every 2hrs of the cells to generate a growth curve of (%) confluency as determined as an average of 4-images per well at each time interval.

For anchorage-independent growth assays, cells were seeded as 8-replicates in low attachment 384-well plates (Greiner). Plates were read on day 7 post seeding by Alamar Blue after 3hours of incubation. Cell seeding was optimised so all lines maintained linear growth over this time.

2.1.3 Cell Viability

Cells were seeded in 384-well plates (Greiner) and left o/n to adhere. Cell seeding was optimised so all lines maintained linear growth over this time. Specifically H358, H520, H727 were seeded at 2000 cells per well, whereas all other lines, including MEFs were seeded at a density of 1000 cells per well. The following day drugs were prepared at 10X concentration as serial dilutions for single or combination inhibitor treatments. Cells are incubated in the presence of the drug for 96hrs. Cell viability was determined using Cell Titer Glo (Promega) by incubation with the cells for 10mins. Cell viability was determined by normalizing inhibitor-treated samples to DMSO controls. In the case of combination experiments cell viability was normalised to the viability of the MEK inhibitor alone. Alternatively cells were seeded for colony assays in 6-wells at very low confluency, incubated in the presence of drug for 96hrs before adding fresh media and staining with crystal violet 7-days after removing the drug.

2.1.4 Synergy Scores

For synergy calculations we derived the bliss score using *Challice Bioinformatic software Horizon*- http://chalice.horizondiscovery.com/analyzer-server/cwr/. The Bliss score is defined as the difference between observed and predicted growth inhibition values for drug combinations within cancer cell lines (Zhao et al. 2014). Predicted combination values are determined from the single agent dose responses of each compound and any effect beyond this prediction is given a score above ‘0’, indicative of synergy. Synergy scores for the combinations were determined over a 10 x 5 matrix and is representative of n=3 experiments. Synergy scores were additionally derived for a panel of SHOC2 KO NSCLC cell lines H358, A549, A427, H1792, H2009 and are

representative of 2 replicate experiments. Differences in Figure 5.9A are plotted as changes in raw synergy score and standard deviation between the 5 cell lines.

2.1.5 Flow Cytometry

Cells were treated for 48hr after being left to adhere o/n. Inhibitors were dissolved in >1% DMSO. Attached and floating cells were captured after 48hr, resuspended in DPBS and stained with Annexin V-FITC. Cells were sorted by FACS analysis into 4 groups, Viable, early apoptosis, late apoptosis and debris determined by their uptake of PI, Annexin V or the combination of both.

2.1.6 Immunoprecipitation (IP)

Cells were lysed with PBS-E lysis buffer (PBS/1% Triton-X-100/1 mM EDTA/Protease Inhibitors (Roche)/Phosphatase Inhibitors/1 mM DTT (dithiothreitol)) or PBS-M lysis buffer for RAS-GTP IPs (as before but with 5 mM MgCl2 instead of EDTA) (PBS/1% Triton-X-100/1 mM EDTA/Protease Inhibitors (Roche)/Phosphatase Inhibitors/1 mM DTT (dithiothreitol). Endogenous IPs were performed using 15µg of antibody with10µl of packed Protein A /G beads (GE Healthcare). Lysates were incubated for 6hours before 2 X washes in 1ml PBS-E lysis buffer to remove non-bound protein. Immunoprecipitates were drained on the final wash by aspiration and resuspended in NuPAGE LDS sample buffer (Life Technologies). Samples were run on western blot for downstream analysis.

2.1.7 Western Blot – SDS PAGE

Western blot analysis began by by heating samples to 70°C for 10 minutes and loading onto 4-12% NuPAGE Bis-Tris gels (Invitrogen) along with Pre-stained Protein Standards (Bio-Rad). Gels were run at 180 V for 1.5h using MOPS running buffer (50 mM MOPS, 50 mM Tris base, 0.2% SDS, 1 mM EDTA). Transfer was set up using either PVDF (for chemiluminescent visualisation) or Nitrocellulose (for fluorescent imaging using the Li-COR system) and run at 15 V for 15h at 4°C in Transfer Buffer (25 mM Bicine, 25 mM Bis-Tris, 1 mM EDTA, 10% Methanol). PVDF membrane was stained with Coomassie Stain (50% Methanol, 10% Acetic Acid, 0.2% Brilliant Blue R250) and background staining was removed by multiple washes with Coomassie Destain (50% Methanol, 10% Acetic Acid). Nitrocellulose membranes were stained with Ponceau Solution (0.1% Poneau S, 5% Acetic Acid) and rinsed with PBS-T (PBS, 0.1% Tween 20).

Membranes were incubated in primary antibody (see Table 8 below), diluted in 3% BSA/PBS-T/Azide for 1h at RT or o/n at 4°C. Membranes were washed 3 x 5 minutes with PBS-T followed by a 1h incubation with a species-specific secondary antibody diluted in blocking buffer. Membranes were washed 3 x 5 minutes with PBS-T and signal was visualised by either chemiluminescence or by using the Li-COR scanner.

For chemiluminescent signal where secondary antibodies conjugated to HRP were used, membranes were incubated with LumiGLO susbtrate for one minute and placed inside a film cassette within a protective plastic sheet. X-Ray film was exposed to the membranes for various lengths of time and developed using a film developer. Films were scanned to generate a digital image, and where used, densitometry analysis was performed using ImageJ software.

In some circumstances secondary antibodies conjugated to IRDyes (680 and 700) were used and an Odyssey scanner was used to image the membranes. The two main advantages of this system are that two species of primary antibody can be imaged at the same time (e.g. a phospho-specific and an antibody recognising total protein) and the sensitivity of the system means that the signals can be accurately quantified. Image analysis was performed using ImageStudio Lite software (Li-COR).

2.2.1 Xenografts

A427 KRAS mutant NSCLC cells (2.5 * 10^6 cells) - & + shSHOC2 were injected subcutaneously into both flanks of female athymic nude mice (Charles River, UK). For inhibitor experiments once tumours were established (200mm^3), animals (5 per group) were randomised and treated with vehicle (4-hydroxypropyl methylcellulose), or Trametinib resuspended in vehicle (0.4 mg/kg daily) for 28-days (No treatment breaks). Tumours were measured twice weekly by digital callipers and mice were weighed weekly for adverse effect to treatments (Mice ~25g at the point of treatment start). Tumour volume was calculated using the following formula: tumour volume=(D × d2)/2, in which D and d refer to the long and short tumour diameter, respectively. Animals were culled in accordance with licence restrictions.

2.2.2 In vivo Bioluminescence imaging

A427 KRAS mutant NSCLC cells (2.5 * 10^6 cells) Parental and SHOC2 KO luciferase expressing cells were injected into the lateral tail vein of 6-week old female SCID/ Beige mice (Charles River). 10-days post tail vein injections mice were subject to Intraparietal injection with 150mg/kg (3mg per 20g mouse) of D-Luciferin (GoldBio)

dissolved in DPBS and syringe filtered at 0.2µM. Bioluminescence imaging (BLI) were acquired after 15minutes of luciferin injection at a 5-second exposure using the IVIS Lumina. Photons per second were quantified using the IVIS software.

2.2.3 Generation of SHOC2 KO and SHOC2^{D175N} KI mouse models

SHOC2 mice were generated by Taconic Artemis. SHOC2 KO model was generated by the insertion of Lox P sites into exon 4 of endogenous SHOC2. For the generation of the SHOC2^{D175N} knockin (KI) mouse model we employed a 'minigene' strategy where the wild-type SHOC2 allele is expressed in a cDNA configuration with a Flag-tag at the N-terminus under the control of the endogenous promoter. The wild type SHOC2 cDNA sequence is deleted after Cre-mediated recombination and replaced by the mutant SHOC2^{D175N} allele containing a Myc-tag. Both models are on a pure C57BL/6 background.

For SHOC2 KO and KI ERT2 C57BL/6 models 6-week old mice are subject to 80mg/kg tamoxifen treatment in corn oil (Sigma) for 10-days in 2, 5-day treatment windows with a week break in between.

2.2.4 Lung Tumour Model

Mixed-gender, 6-12week old KRAS^{G12D};p53^{R172H};SHOC2$^{wt/wt}$, SHOC2$^{fl/wt}$ or SHOC2$^{fl/fl}$ mice were intranasally infected with a single dose of 2×10^7 pfu Ad-Cre (University of Iowa Vector Core) to induce tumours. The generation of KRAS^{G12D};p53^{R172H}has been described previously (Jackson et al. 2001; DuPage et al. 2009).

Lungs were isolated at six months post AdenoCre infection. Tumour sections were fixed in 10% formalin (Sigma) o/n before paraffin processing and fractioning. Fractions were stained for H&E. Burden was quantified by determining the total percentage of lung fraction that was tumour at six months. All histopathological analyses were performed blind by an experienced pathologist.

Recombination efficiency of the SHOC2 allele was tested for by PCR in the largest lung tumour nodules from each KRAS^{G12D};p53^{R172H};SHOC2$^{fl/fl}$ mouse to look for 'escapers' (max 2 nodules per animal – where isolation of the nodule from surrounding tumour was easily permissible).

2.2.5 Mouse Embryonic Fibroblasts

Mouse Embryonic Fibroblasts (MEFs) were isolated from R26CreERT2 SHOC2$^{fl/wt}$ mice at p13.5 and plated under standard culture conditions (DMEM/0% FBS + 1%

Penicillin/Streptomycin P/S). MEFs were immortalised with FB-E6 and transformed with LXSP3 $KRAS^{G12V}$ SHOC2. MEFs were treated with 1µg/ml 4-OHT (Sigma) for 7-days for to induce Cre-recombination for SHOC2 deletion.

2.2.6 Animal Husbandry

All mice were maintained in individually ventilated cages (IVCs). Athymic nude mice received autoclaved food, water and bedding according to institutional guidelines. All *in vivo* experiments were performed under appropriate animal licenses and guidelines. Where appropriate mice were maintained in 4% isoflurane for anaesthesia and allowed to recover post procedure at 37´C in heated chambers.

2.2.7 Statistical Analysis

Data are presented as mean ± SD unless otherwise stated. Significance was determined with GraphPad Prism 7 software using the Student's t test where $*p < 0.05$, $**p < 0.01$ or $***p < 0.001$.

2.2 Materials and Reagents

2.2.1 Sequences

siRNA sequences - Stealth RNAi Negative Control Medium GC Duplex (Life Technologies) was used as control oligo. All other siRNAs were from Qiagen or Life Technologies. SHOC2-1 sense 5'-3' GCUGCGGAUGCUUGAUUUA antisense 5'-3' AUUUAGUUCGUAGGCGUCG/ SHOC2 -2 sense 5'-3' GAACUUGGACCAGUAUGGUAGAAUU antisense 5'-3' CUUGAACCUGGUCAUACCAUCUUAA/ BRAF-1 Sense 5'3' AAAGCUGCUUUUCCAGGGUUU antisense 5'3' AAACCCUGGAAAAGCAGCUUU/ BRAF-2 sense 5'3' AAAGAAUUGGAUCUGGAUCAU antisense 5'3' AUGAUCCAGAUCCAAUUCUUU CRAF-1 sense 5'3' AAGCACGCUUAGAUUGGAAUA antisense 5'3' UAUUCCAAUCUAAGCGUGCUU/ CRAF-2 sense 5'3' GGAUGUUGAUGGUAGUACA antisense 5'3' UGUACUACCAUCAACAUCC/ ARAF-1 5'3' sense CCGACUCAUCAAGGGACGAAA antisense 5'3' GGCUGAGUAGUUCCCUGCUUU

shRNA sequences - Clones were obtained from Thermo Scientific Scramble (non-silencing) sense 5'-3'CTCTCGCTTGGGCGAGAGTAAG antisense 5'-3'CTTACTCTCGCCCAAGCGAGAG/ SHOC2-1 sense 5'-3'CTGCTGAAATTGGTGAATT antisense 5'-3'GACGACTTTAACCACTTAA/ SHOC2–3 sense 5'-3' CCATTAATGTTTCTTATCT antisense 5'-3' AGATAAGAAACATTAATGG.

For more details see supplementary methods.

2.2.2 Inhibitors

Pimasertib (AS-703026) (S1475), PD0325901 (S1026), LY3009120 (S7842), Ulixertinib (7854), SCH772984 (S7101), OSI-906 (Linsitinib) (S1091), A66 (S2636), GDC-0941 (Pictilisib) (S1065), NVP-AEW541 (S1034), Erlotinib (S7786), Ponatinib (AP24534) (S1490), Afatanib (S1011), MK2206 (S1078), GDC-0068 (Ipatasertib) (S2808), Sapitinib (S2192), Gefitinib (S1025), LY3214996 (S8534), SHP099 HCL (S8278), PLX-4720 (S1152), BGJ398 (S2183), CH5126766 (S7170), RAF265 (S2161), Crizotinib (S1068), RAF265 (S2161), AZD628 (S2746), LY3009120 (S7842) were purchased from SelleckChem (Stratech UK distributor). Trametinib (GSK1120212) (871700-17-3), AZD6244 (Selumetinib) (606143-52-6) were

purchased from Generon. Drugs for *in vitro* studies were dissolved in DMSO and stored at −20 °C.

2.2.3 Cell Lines

	NSCLC	KRAS	BRAF	EGFR	STK11	TRP53	PIK3CA	Adeno/Squ/ Large
KRAS	A549	G12S			Q37*			NOS
	H460	Q61H			Q37*		E545K	Large
	H358	G12C						Broncho Adeno
	H23	G12C				M246I		Adeno
	H727	G12V				Q165_S166insYKQ		Carcinoid
	H1792	G12C						Adeno
	H2009	G12A				R273L		Adeno
	A427	G12D						Large
BRAF p-loop	CAL-12T		G466V			C135F		NOS
	H1395		G469V					Adeno
EGFR	PC9			E746_A750del		R248Q		Adeno
	PC9-er			E746_A750del *T790M				
	HCC827			E746_A750del		V218delV		Adeno
	HCC4006			E746_A750del				Adeno
ERK-MAPK WT	H522					P191fs*56		Adeno
	H226							Squ
	H520					W146*		Squ
	BREAST							
	MDA-MB-231	G13D	G464V	L469W		R280K		

Table 1.1

2.2.4 Antibody list

BRAF P-S365 was generated by immunisation of rabbits with a phoshpo-peptide corresponding to the appropriate region of BRAF (Epitomics/Abcam). SHOC2 antibody was generated as described (Rodriguez-Viciana et al. 2006).

Name	Company	Catalogue number	species
AKT (pan)	Cell Signaling Technology	2920	Mouse
AKT P-S473	Cell Signaling Technology	4060	Rabbit
ARAF	Santa Cruz	sc-166771	Mouse
ARAF	Santa Cruz	sc-408	Rabbit
β-Actin	Santa Cruz	sc-47778	Mouse
BAD S112	Cell Signaling Technology	9291	Rabbit
BIM	Cell Signaling Technology	2933	Rabbit
BRAF	Santa Cruz	sc-5284	Mouse
BRAF	Santa Cruz	sc-9002	Rabbit
BRAF P-T753	Abcam	ab138399	Rabbit
CRAF	Santa Cruz	sc-7267	Mouse
CRAF	BD Biosciences	610152	Mouse
CRAF	Santa Cruz	sc-133	Rabbit
CRAF P-S259	Santa Cruz	sc-101791	Rabbit
CRAF P-S289/296/301	Cell Signaling Technology	9431	Rabbit
EGFR	Santa Cruz	sc-373746	Mouse
EGFR P-T669	Cell Signaling Technology	3056 & 8808	Rabbit
ERK ½	Cell Signaling Technology	9102	Rabbit
ERK ½	Cell Signaling Technology	9107	Mouse
ERK 1/2 P-T202/Y204	Cell Signaling Technology	9101	Rabbit
FLAG	Sigma	F1365	Mouse
GAPDH	Genetex	GT239	Mouse
KSR1	Abcam	ab68483	Rabbit
KRAS	Santa Cruz	sc-30	Mouse
MEK1	Santa Cruz	sc-6250	Mouse
MEK2	Santa Cruz	sc-13159	Mouse
MEK ½	Cell Signaling Technology	4694	Rabbit
MEK 1/2 P-S217/221	Cell Signaling Technology	9121 & 9154	Rabbit
MYC-TAG	Cell Signaling Technology	9B11	Mouse
PARP	BD Biosciences	556494	Mouse
PARP (cleaved)	Cell Signaling Technology	9541	Rabbit
RPS6 P-S235/236	Santa Cruz	sc-293144	Mouse
RSK1	Santa Cruz	sc-231	Rabbit
RSK2	Santa Cruz	sc-9986	Mouse
RSK1 P-S380	Cell Signaling Technology	11989	Rabbit
YB1	Santa Cruz	sc-398340	Mouse
YB1 P-S102	Cell Signaling Technology	2900	Rabbit

Table 1.2

Chapter 3

Results

3.1 SHOC2 is required for the malignant properties of growth in RAS mutant cells

3.1.1 Introductory statement

SHOC2 has previously been shown to be specifically required for the malignant properties of RAS-mutant cells (Young et al. 2013). Using the MDA-MB-231 cells as a model system of a cell line that is ERK-MAPK addicted/ dependent due to the fact it has rare co-occurring mutations in both KRAS G13D and BRAF G464V, we sort to recapitulate published data using two shRNA and three siRNA oligo's. Validation of the molecular tools at my disposal was critical from the outset of the project given the remit of this project is 'target validation', and as such an inhibitor for SHOC2 is yet to be developed.

3.1.2 SHOC2 is required for basal ERK-pathway signalling in MDA-MB-231 cells

Initially western blot analysis was performed of MDA-MB-231's cells transfected with either one of three siRNA oligo's, or transduced with one of two inducible (TRIPZ), or constitutive (GIPZ) lenti-viral shRNA oligo's. Each approach provides unique opportunities for experimental design. siRNA provides rapid but transient knockdown (KD) for high throughput pilot screening, but comes with the shortfall of variability between experiments, and cell lines, dependent on their inherent transfection efficiency. The constitutive GIPZ Lenti shRNA approach with a GFP tag enables visual conformation of transduction, and furthermore, selection under a puromycin cassette enables the stable generation of stable SHOC2 KD cell lines for longer term studies. In cases where it may be desired to inducibly express shRNA's targeted against SHOC2 for temporal control of SHOC2 inhibition, we utilised a TRIPZ construct (Figure 3.1A-B), Here after establishing the stable cell line with puromycin selection as above the shRNA and RFP are jointly expressed only upon doxycycline addition to the cell culture media (Figure 3.1A-B). Pilot experiments optimised peak SHOC2 deletion to occur after 72hrs of doxycycline exposure, at a concentration of 1µg/ml. Western blot analysis of the various knockdown approaches demonstrated that SHOC2 inhibition leads to increased phosphorylation of BRAF-S365 compared with all controls, in agreement with its role as part of the MRAS-SHOC2-PP1 complex (Rodriguez-Viciana et al. 2006). This increase in P-S365 BRAF occurred simultaneously with marked ERK-pathway inhibition at the level of P-MEK, and a partial reduction in basal levels of P-ERK (Figure 3.1C).

3.1.3 SHOC2 is required for the 3D-anchorage-independent, but not 2D-adhered growth of MDA-MB-231 cells

To explore a role for SHOC2 on 2D-adhered growth of MDA-MB-231 cells we performed incucyte proliferation experiments. Cells are seeded sparsely and allowed to reach confluency - while images captured at regular time intervals plot confluency of the growing cells over time. SHOC2 inhibition by three siRNA and two shRNA oligo's had no effect on the rate of growth of MDA-MB-231 cells in 2D-adhered culture conditions, compared to non-targeting controls, despite partial inhibition of ERK-pathway readouts by western blot (Figure 3.1D-E). In sharp contrast SHOC2 KD led to marked inhibition of 3D-anchorage-independent growth of MD-MB-231 cells by 75% using siRNA approaches, and 60% using two shRNA oligo's in low attached plate growth assays (Figure 3.1E-F). In agreement with this both induction of SHOC2 shRNA's pre and post implantation in nude mice prevented the growth/ establishment of MDA-MB-231 xenografts (Figure 3.1H). In contrast KD by siRNA of KRAS partially perturbed the growth of MDA-MB-231 cells in both 2D-adhered, and anchorage-independent cell growth (Figure 3.1D,F). These findings suggest a degree of specificity for SHOC2-dependent ERK-pathway signalling that is not seen by broadly hitting ERK-activation at the level of mutant RAS.

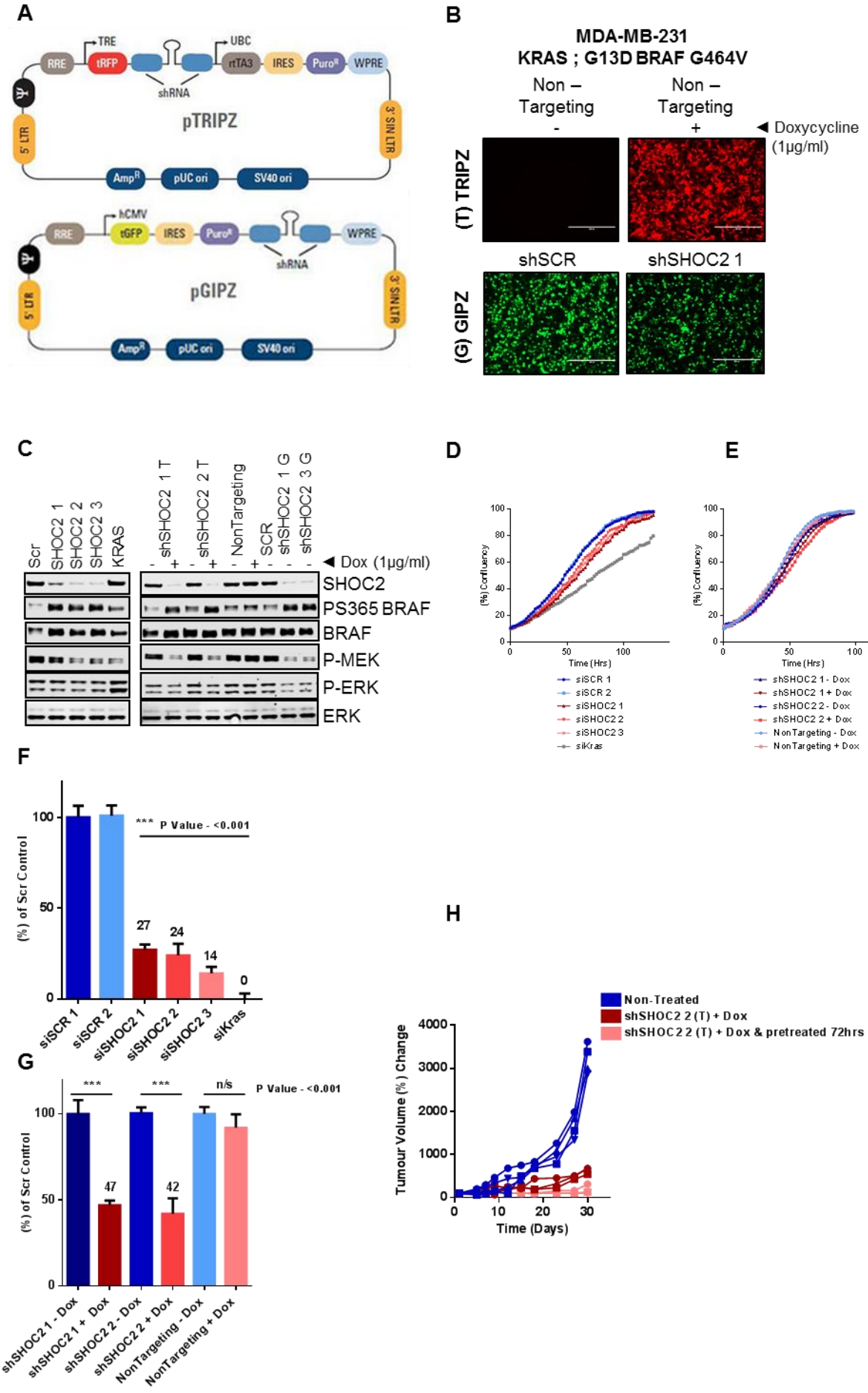
A
TRE
UBC
RRE
tRFP
shRNA
rtTA3
IRES
Puro^R
WPRE
pTRIPZ
5' LTR
3' SIN LTR
Amp^R
pUC ori
SV40 ori
hCMV
tGFP
pGIPZ
B
MDA-MB-231
KRAS ; G13D BRAF G464V
Non – Targeting
Non – Targeting
Doxycycline (1µg/ml)
(T) TRIPZ
shSCR
shSHOC2 1
(G) GIPZ
C
Scr
SHOC2 1
SHOC2 2
SHOC2 3
KRAS
shSHOC2 1 T
shSHOC2 2 T
NonTargeting
SCR
shSHOC2 1 G
shSHOC2 3 G
Dox (1µg/ml)
SHOC2
PS365 BRAF
BRAF
P-MEK
P-ERK
ERK
D
(%) Confluency
Time (Hrs)
siSCR 1
siSCR 2
siSHOC2 1
siSHOC2 2
siSHOC2 3
siKras
E
shSHOC2 1 - Dox
shSHOC2 1 + Dox
shSHOC2 2 - Dox
shSHOC2 2 + Dox
NonTargeting - Dox
NonTargeting + Dox
F
(%) of Scr Control
*** P Value - <0.001
27
24
14
0
siSCR 1
siSCR 2
siSHOC2 1
siSHOC2 2
siSHOC2 3
siKras
G
*** P Value - <0.001
n/s
47
42
shSHOC2 1 - Dox
shSHOC2 1 + Dox
shSHOC2 2 - Dox
shSHOC2 2 + Dox
NonTargeting - Dox
NonTargeting + Dox
H
Non-Treated
shSHOC2 2 (T) + Dox
shSHOC2 2 (T) + Dox & pretreated 72hrs
Tumour Volume (%) Change
Time (Days)

Figure 3.1 SHOC2 is required for the anchorage-independent growth of MDA-MB-231 cells but it's not required for 2D-adhered growth

A Construct map for pGIPZ and pTRIPZ constructs containing shRNAs targeted against SHOC2.

B RFP and GFP images for MDA-MB-231 cells transduced with either pGIPZ or pTRIPZ constructs - & + 72hr incubation in 1µg/ml Doxycycline. Scale bar represents 400µM.

C KD of SHOC2 by siRNA or shRNA increases S365 BRAF and decreases P-MEK. Lysates were harvested after 72hrs in the presence of siRNA, or shRNA + 1µg/ml Doxycycline, and lysates probed with indicated antibodies by western blot analysis.

D SHOC2 inhibition by siRNA has no effect on the growth of MDA-MB-231 cells in 2D. Incucyte curves of MDA-MB-231 cells growing in the presence of 3 different siRNAs targeting SHOC2 for depletion.

E As above for shRNAs targeting SHOC2 for depletion.

F SHOC2 inhibition perturbs the anchorage-independent growth of MDA-MB-231 cells. Growth of MDA-MB-231 cells in soft agar after 7-days with 3 different siRNAs targeting SHOC2 for depletion.

G As above for shRNAs targeting SHOC2 for depletion.

H SHOC2 inhibition perturbs the growth of MDA-MB-231 cells in a xenograft assay. 5*10^6 MDA-MB-231 cells with shRNA Non-Targeting, shRNA SHOC2 pre-treated for 72hrs with Doxycycline, or with no pre-treatment were seeded in the flanks of Athymic nude mice. Mice drank water containing Doxycycline, 2mg/kg supplemented with 8% sucrose. Tumour volume was determined over 4-weeks by digital calliper measurements.

3.1.4 NSCLC provides a powerful system for exploration of a role for SHOC2 in ERK-pathway activation

NSCLC represents the largest subtype of lung adenocarcinoma (85%), compared to small cell carcinoma (SCLC) which constitutes just 15%. 75% of NSCLC cases present with a driver mutation in an ERK-MAPK pathway node, including KRAS (32%), EGFR (11%), NF1 (11%) and BRAF (7%), demonstrating the oncogene addiction of NSCLC to ERK-signalling. These mutations are almost always mutually exclusive with respect to one another, but can regularly co-occur with mutations in p53 or STK11 (Figure 3.2A-B). The largest risk factor for NSCLC is smoking, but exposure to chemicals, asbestos, radiation, pollution, and a prior history of lung disease, such as chronic obstructive pulmonary disease (COPD) are contributing factors. Given that 5-year survival rate for patients diagnosed with stage IV NSCLC are ~1%, NSCLC represents a huge unmet clinical need. Wanting to expand our findings in MDA-MB-231 cells to a more clinically relevant/ tractable system we sought to establish a panel of NSCLC cell lines with stable SHOC2 inhibition that captured the mutational landscape of the human disease. Cell lines summarised in (Table 1).

We employed two approaches for the generation of these cell lines, stable shRNA knockdown (KD) by Lenti transduction (described above) and CRISPR-mediated SHOC2 deletion/ knockout (KO). Clustered Regularly Interspaced Short Palindromic Repeats (CRISPR) uses a predesigned gRNA against your target gene (in our case SHOC2) to target a cas9 nuclease to the gene to generate double-stranded breaks in the DNA, resulting, in our example, with a truncated non-functional SHOC2 protein. A complete KO approach was sought to obtain full SHOC2 deletion due to the concerns that a lack of functional response may simply be because the KD efficiency is not enough using shRNA approaches. KD versus KO of SHOC2 are shown by western blot for a panel of NSCLC cell lines (Figure 3.2C). For the majority of cell lines we use a combination of KD and KO approaches to strengthen our findings, but in some cases data is only from the various KD approaches available to us as these cells were unable to grow from single cells as part of the process of generating single CRISPR KO clones (eg. HCC4006, H522, CAL12T).

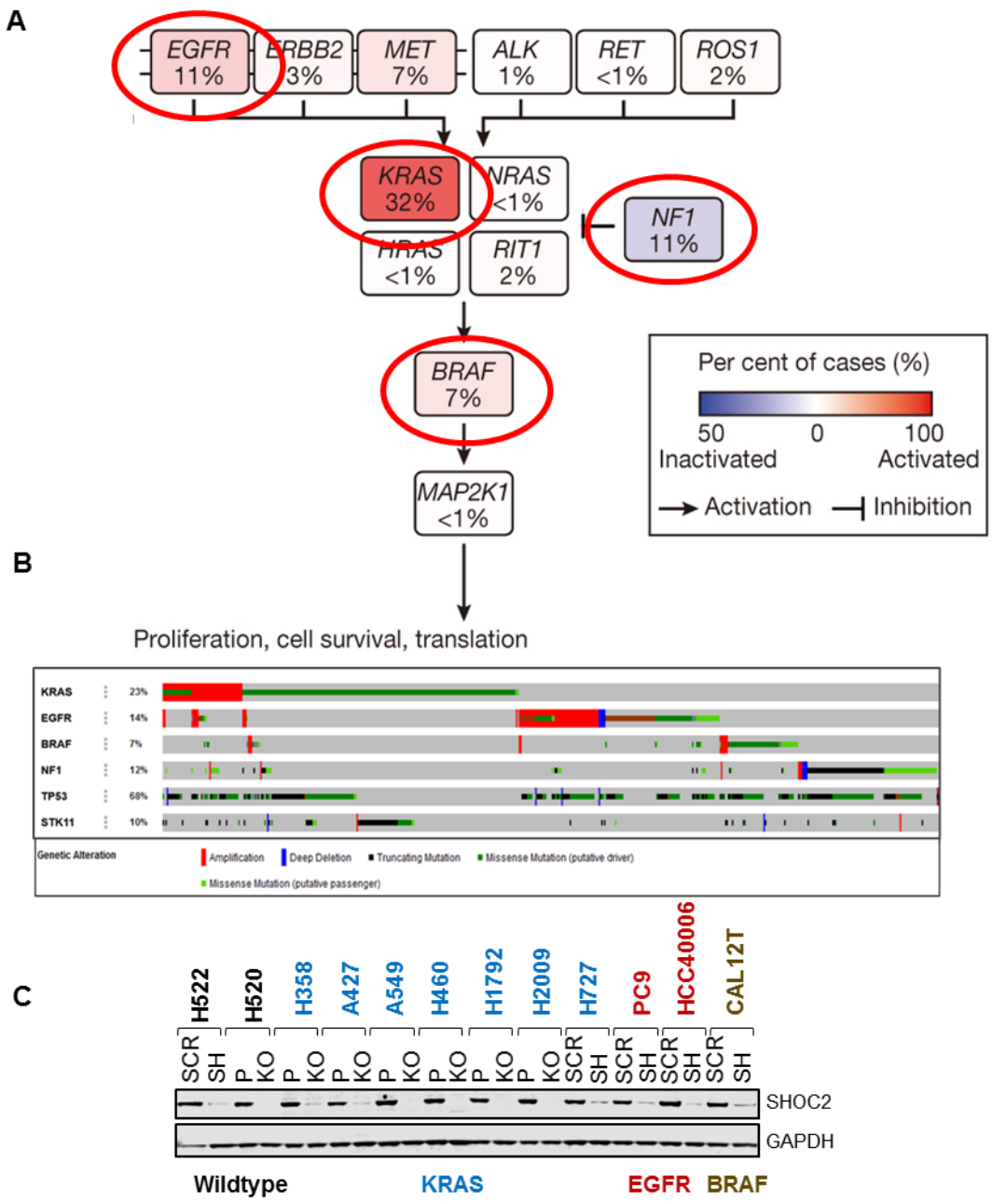

Figure 3.2 NSCLC – An ERK-pathway addicted cancer

A 75% of NSCLC's have a driver mutation in an ERK-pathway node. (Cancer Genome Atlas Research 2014)

B Oncoprint derived from Pan-Lung Cancer (TCGA, Nat Genet 2016) data set for selected gene of the ERK-MAPK pathway. (http://www.cbioportal.org/)

C Lysates of SHOC2 KO clones are compared alongside shRNA knockdown for a panel of NSCLC cell lines encompassing the diversity of ERK-pathway driver events in human LUAD.

3.1.5 SHOC2 is selectively required for tumorigenic growth of a subset of KRAS-mutant NSCLC cell lines

Expanding observations obtained in MDA-MB-231 cells we performed 2D-adhered and 3D-spheorid growth assays in a panel of SHOC2 KO or KD NSCLC lines. Consistent with both MDA-MB-231 data and previously published data we observed no effect of SHOC2 inhibition on growth of our cell lines on 2D-adhered incucyte growth curves, but found SHOC2 inhibition severely impaired the growth of half of our NSCLC lines in 3D-spheroid assays (Figure 3.3A-C), (Figure 3.1) (Young et al. 2013). Furthermore there was a good correlation between the inhibition of spheroid growth and growth of cell lines as subcutaneous xenografts, with SHOC2 KD having no effect on the ability of A427 cells to grow as xenografts, but completely preventing the growth of H358 xenografts (Figure 3.3E-F). Importantly re-expression of wildtype (WT) SHOC2, but not the D175N SHOC2 mutant in SHOC2 KO H358 cells was sufficient to rescue the 3D-growth deficit (Figure 3.3D). This demonstrates the requirement of SHOC2 for anchorage-independent growth is dependent upon its role as part of the MRAS-SHOC2-PP1 complex, previously described (Rodriguez-Viciana et al. 2006).

Although SHOC2 was not required for the 3D-anchorage-independent growth of A427 cells as spheroids, or as subcutaneous xenografts, SHOC2 inhibition did fully prevent lung colonisation by A427 cells after injection into the lateral tail vein of immunocompromised mice (Figure 3.4). This suggests although a subset of RAS-mutant NSCLC cell lines are resistant to SHOC2 inhibition for growth as a primary tumour mass in 3D, SHOC2 inhibition may broadly prevent the metastatic dissemination and/or re/seeding of cells at a distal site.

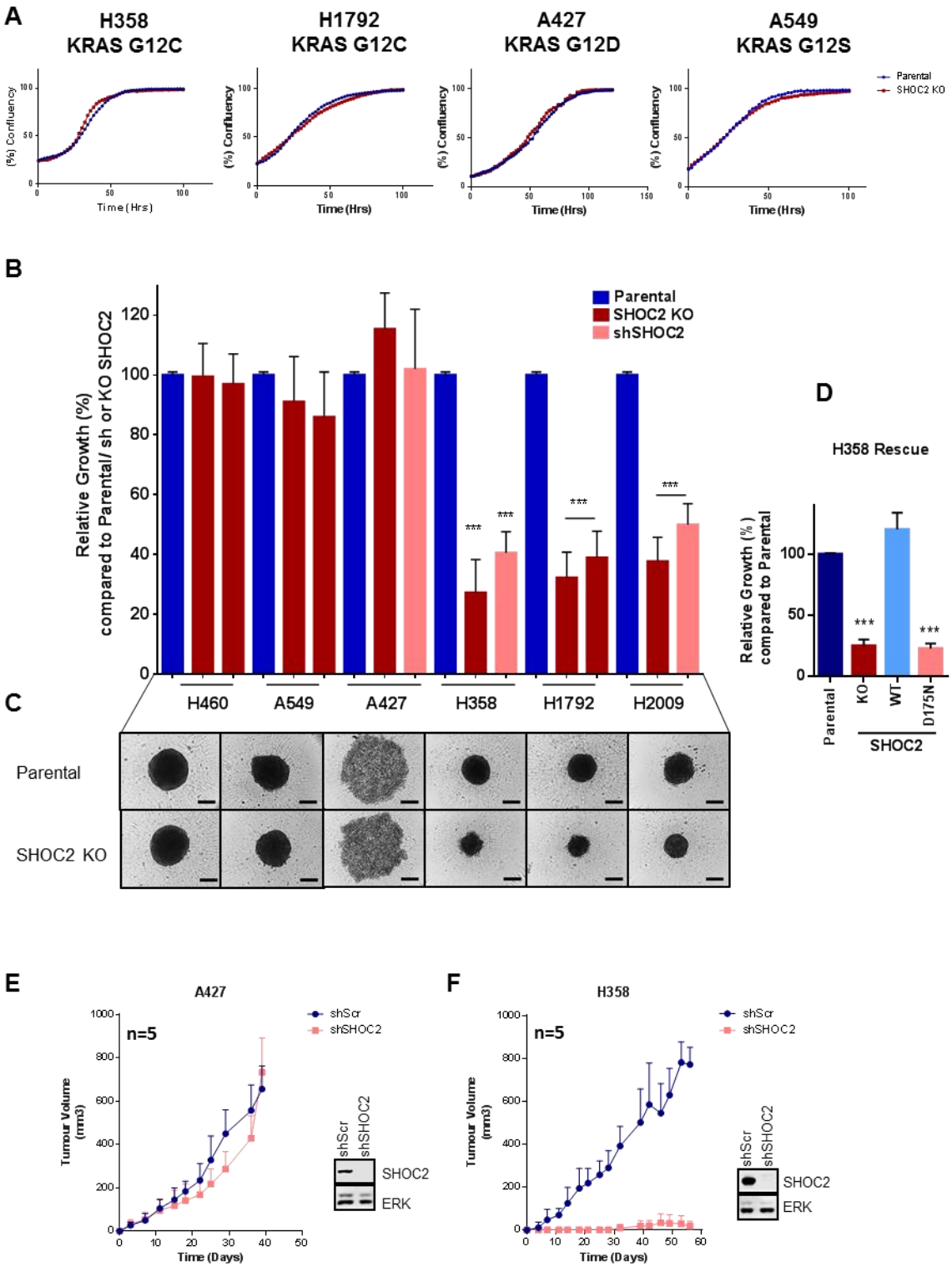
A
H358
KRAS G12C
H1792
KRAS G12C
A427
KRAS G12D
A549
KRAS G12S
(%) Confluency
Time (Hrs)
Parental
SHOC2 KO
B
Relative Growth (%)
compared to Parental/ sh or KO SHOC2
Parental
SHOC2 KO
shSHOC2
H460
A549
A427
H358
H1792
H2009
C
Parental
SHOC2 KO
D
H358 Rescue
Relative Growth (%)
compared to Parental
Parental
KO
WT
D175N
SHOC2
E
A427
n=5
shScr
shSHOC2
Tumour Volume
(mm3)
Time (Days)
SHOC2
ERK
F
H358
n=5
shScr
shSHOC2
Tumour Volume
(mm3)
Time (Days)
SHOC2
ERK

Figure 3.3 SHOC2 is selectively required for tumorigenic growth of a subset of KRAS-mutant NSCLC cell lines

A SHOC2 inhibition has no effect on the growth of RAS mutant NSCLC cells in 2D. Incucyte curves of a panel of RAS mutant NSCLC cells - & + SHOC2 KO. Representative n=3 experiments.

B SHOC2 inhibition perturbs the 3D-anchorage-independent growth of a subset of RAS-mutant NSCLC cell lines. Parental, SHOC2 KO clones, or shSHOC2 cells were seeded in low attachment plates and growth at D5 measured by alamar blue staining (mean ± SD) (n=4). Significance is determined using a two tailed T-test $*p < 0.05$, $**p < 0.01$ or $***p < 0.001$.

C P/C images of representative spheroids measured in (B) at D5. Scale bar = 200µm.

D Inhibition of 3D-anchorage-independent growth in SHOC2 KO H358 cells is rescued by re-expression of WT, but not the D175N SHOC2. H358 parental, and SHOC2 KO cells with stable re-expression of wildtype (WT) SHOC2, D175N SHOC2 or Empty vector control were seeded as (B).

E SHOC2 inhibition does not affect growth of A427 cells. shSCR or shSHOC2 $2.5*10^6$ A427 cells were injected subcutaneously per flank in immunocompromised mice and tumour growth measured twice weekly (mean ± SD) (n=5 animals per group).

F SHOC2 inhibition prevents xenograft growth of H358 cells. shSCR or shSHOC2 $5*10^6$ H358 cells were injected subcutaneously per flank in immunocompromised mice and tumour growth measured twice weekly (mean ± SD) (n=5 animals per group).

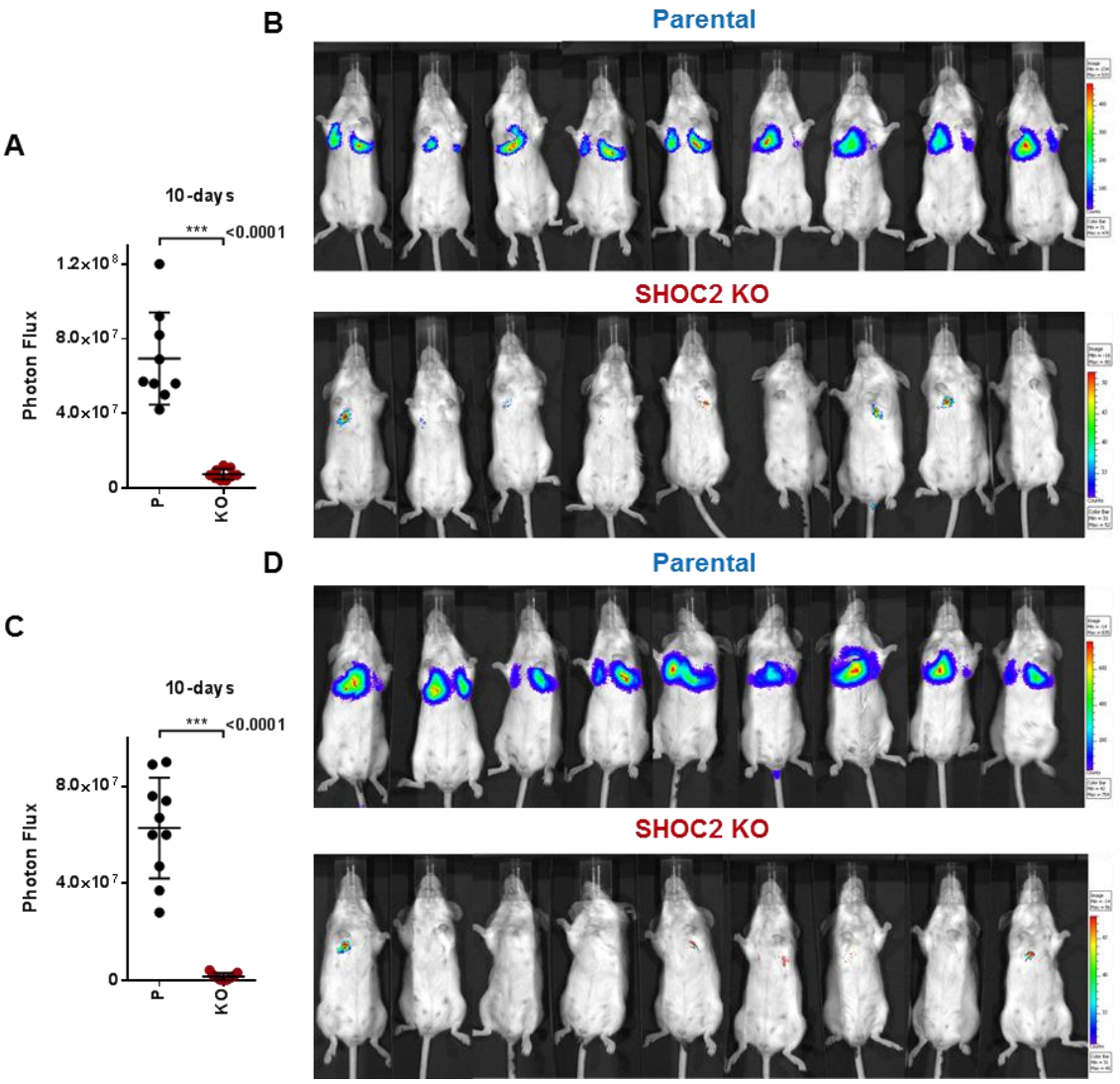

Figure 3.4 SHOC2 inhibition prevents lung colonisation of A427 cells following tail vein injection

A SCID/beige mice were injected with 2 × 10^6 A427 P or SHOC2 KO cells stably expressing luciferase into the lateral tail vein. Tumour burden was assessed after 10 days via bioluminescence imaging (BLI) and quantification of photon flux at a **5**-second exposure using IVIS n = 9/group.

B BLI Images captured by IVIS at a 5-second exposure are shown for (A).

C As (A) **10**-second exposure after tail vein injections.

D As (B) **10**-second exposure after tail vein injections.

3.1.6 3D – Anchorage-Independent growth reveals a SHOC2 dependency for ERK-signalling

A panel of KRAS-mutant NSCLC cells, - & + SHOC2 KO were seeded on polyHEMA coated plates to maintain cells in suspension, or on tissue culture (TC) treated plates and left overnight (o/n) to adhere, before lysates were collected and ran on western blot. We validated the KO of SHOC2 in these lines by western blot and ascertained the effect on downstream ERK-MAPK signalling. Crucially there was very little effect attributed to SHOC2 KO on basal ERK-pathway signalling in NSCLC cell lines (Figure 3.5), in contrast to MDA-MB-231 cells (Figure 3.1C). Conversely there was a marked increase in ERK-signalling readouts, P-MEK and P-RSK when cells were in suspension compared to 2D-adhered culture conditions, and an inverse reduction in signalling nodes of the PI3K-AKT axis – P-AKT, P-S6 and P-AF6, consistent with a loss of adhered integrin signalling (King et al. 1997; Martin et al. 2006; Vachon 2011; Riedl et al. 2017). This enhanced emphasis on ERK-MAPK signalling on cells in suspension revealed a SHOC2 contribution to ERK-signalling not seen in adhered growth conditions (Figure 3.5). In 3D-anchorage-independent culture conditions SHOC2 was required for P-MEK, P-ERK and downstream P-RSK activation in contrast to its apparent redundancy in 2D-adhered culture conditions.

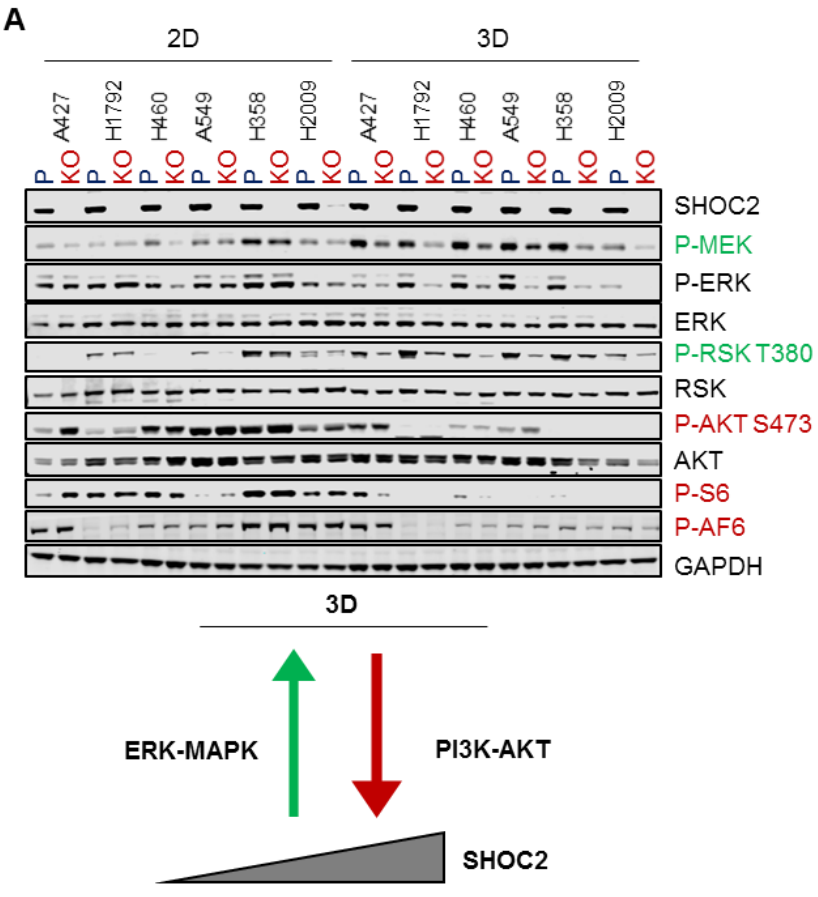

Figure 3.5 3D – Anchorage-Independent growth reveals a SHOC2 dependency for ERK-signalling

A SHOC2 selectively contributes to ERK-signalling in anchorage-independent conditions. Parental and SHOC2 KO cells were seeded in regular or poly-HEMA coated plates for 24hr and lysates probed for indicated signalling markers.

Given that there seemed to be a partial correlation between cell lines resistant to 3D-growth inhibition, and those with incomplete inhibition of P-AKT S473 on 3D lysates, it was reasonable to assume that blocking this residual AKT would prevent anchorage-independent growth of these cell lines. Indeed treatment of H460 but not A549 cell lines with both the PI3Kα inhibitor A66, and the AKT inhibitor, MK2206 was able to perturb anchorage-independent growth, however this was SHOC2-independent (Figure 3.6). This suggests that residual P-AKT levels are not fully responsible for the resistance to growth inhibition on SHOC2 knockdown and that others factor must be at play.

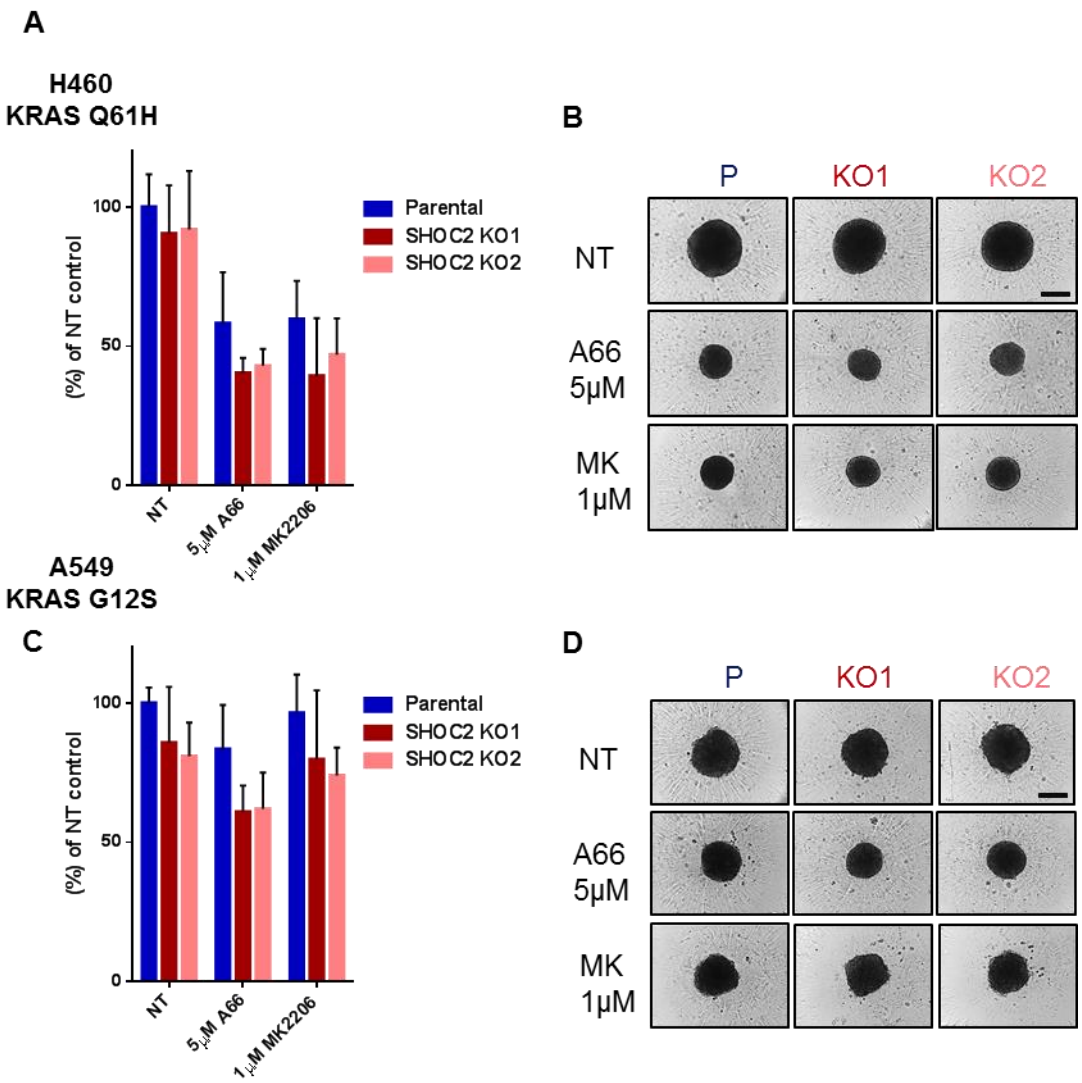

Figure 3.6 PI3K-AKT inhibition perturbs growth of H460 cells as spheroids but not A549 cells in a SHOC2-independent manner

A PI3Kα or AKTi treatment inhibits the growth of H460 cells in 3D-independently of SHOC2. Parental or SHOC2 KO clones were seeded in low attachment plates, treated 24hrs later with indicated treatments and growth at D5 measured by alamar blue staining (mean ± SD) (n=4). Significance is determined using a two tailed T-test $*p < 0.05$, $**p < 0.01$ or $***p < 0.001$.

B P/C images of representative spheroids measured in C at D5. Scale bar = 200μm.

C AS (B) for A549 cells.

D As (C) for A549 cells.

3.1.7 Conclusions

SHOC2 plays a critical role in the basal-MAPK signalling of MDA-MB-231 cells but did not in a panel of NSCLC cell lines. Instead we observe that ERK-signalling is elevated in anchorage-independent growth conditions, at the same time as a reduction in PI3K signalling. 3D-anchorage-independent growth reveals a specific SHOC2-dependent contribution to ERK-MAPK signalling. Significantly consistent with these signalling observations, SHOC2 inhibition has no effect on 2D 'normal' adhered growth of a panel of NSCLC cell lines, but specifically perturbs 3D –anchorage-independent, tumorigenic growth of these cell lines both *in vitro* and *in vivo*.

Chapter 4

SHOC2 is required for ERK-MAPK pathway activation by RTK-stimulation

4.1 SHOC2 is required for ERK-MAPK pathway activation by RTK stimulation

4.1.1 Introductory statement

Chapter 3, as well as work by others has shown that 3D-anchorage-independent growth reveals a SHOC2 dependency for ERK-signalling, whereas conversely SHOC2 has been shown to be redundant for ERK-signalling in 2D-adhered culture conditions (Young et al. 2013; Wang et al. 2017). This suggests that SHOC2 may specifically modulate ERK-signalling only in response to certain stimuli. SHOC2 has been shown through the MRAS-SHOC2-PP1 complex to mediate the dephosphorylation of 'S259' site on RAF, critical for ERK-activation (Rodriguez-Viciana et al. 2006). The dephosphorylation of this site is shown to be a critical requirement for RTK-mediated ERK-MAPK pathway activation, therefore we set out to explore the role of SHOC2 to RTK ligand stimulus (Lavoie and Therrien 2015).

4.1.2 SHOC2 is required for EGF-mediated ERK-pathway activation

To set out we took three KRAS-mutant NSCLC cell lines (A549, H1792 and H460), with two different SHOC2 KO clones for each of the cell lines, to exclude effects attributed to clonal variability after the CRISPR process. We then treated them, and their matched SHOC2 parental controls with EGF for indicated time points of between 2.5 and 60minutes to determine the response of the ERK-pathway to EGF-stimulation overtime. We observed that SHOC2 deletion completely blunted the ERK-pathway response to EGF-stimulation of RAS-mutant cells, notably at the level of P-ERK and P-MEK and that these results were consistent across the two clones (Figure 4.1).

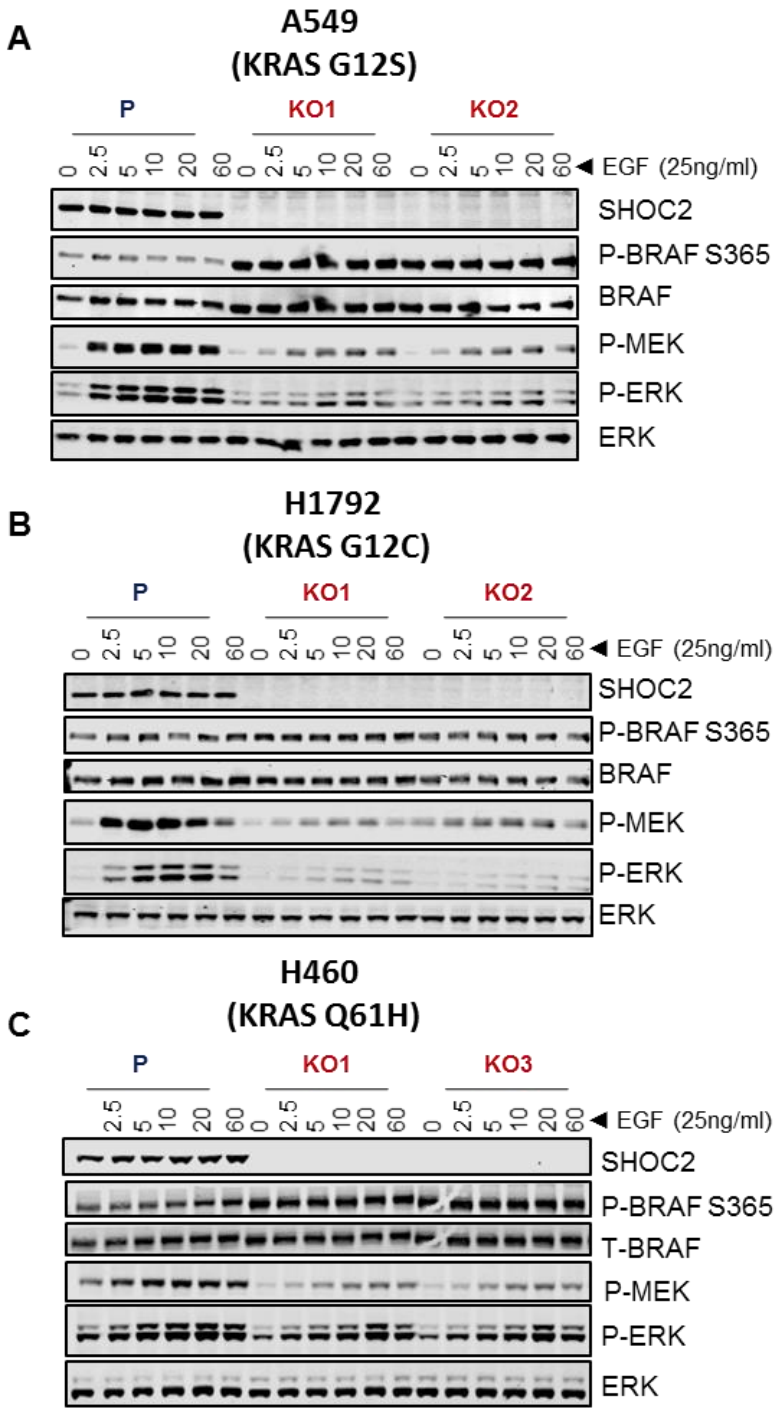

Figure 4.1 SHOC2 is required for EGF-mediated ERK-pathway activation

A SHOC2 is required for full ERK-pathway activation on EGF treatment. A549 parental, and 2 SHOC2 knockout (KO) clones were treated with 25ng/ml of EGF for indicated time points and then harvested for western blot analysis and probed with the indicated antibodies.

B As (A) for H1792 cells.

C As (A) for H460 cells.

4.1.3 The SHOC2 phosphatase complex is required for EGF-mediated ERK-pathway activation

To extend these observation we generated three NSCLC SHOC2 KO cell lines with stable expression of wildtype (WT) SHOC2 or the SHOC2 mutant D175N - previously shown to prevent formation of the MRAS-SHOC2-PP1 complex, but preserve other known scaffolding functions of SHOC2 (Figure 1.5)(Rodriguez-Viciana et al. 2006; Young et al. 2013). We then performed EGF time course experiments in 4.1.2. We observed a variable optimum stimulation of the ERK-MAPK pathway on EGF-treatment between 5-10minutes, in a cell line dependent manner. Upon EGF-stimulation P-BRAF S365 is dephosphorylated in both the parental and SHOC2 WT conditions, consistent with pathway activation. Indeed the higher levels of SHOC2 in rescued WT SHOC2 KO cells causes a more pronounced dephosphorylation than that of the parental cell line (Figure 4.2A,B). In agreement with the previously reported function of the MRAS-SHOC2-PP1 complex we observe both SHOC2 KO and expression of the D175N mutant leads to increased basal levels of S365 BRAF, and that dephosphorylation upon EGFR-activation is blocked even in the presence of active RAS (RAS mutant cells)(Figure 4.2)(Rodriguez-Viciana et al. 2006). Significantly we observe across all cell lines that the response of the ERK-MAPK pathway to EGF-stimulation is blunted/ reduced on SHOC2 inhibition, and that this is rescued by re-expression of WT SHOC2 but not expression of the SHOC2 D175N mutant. This demonstrates that it is the requirement of SHOC2 as part of the SHOC2 phosphatase complex that is required for RTK-driven ERK-activation. We observe this specifically for ERK-MAPK nodes, including P-MEK, PERK, and not with P-AKT, highlighting the specificity of SHOC2 for ERK-activity and not other RAS-effector pathways. Indeed P-AKT is elevated in SHOC2 KO and SHOC2 D175N cells. This may reflect modulation of the different pathways as a result of feedforward or feedback loops (Turke et al. 2012). Notably expression of the WT SHOC2 further stimulates ERK-MAPK activation over the parental cell line in response to EGF at the level of P-MEK in both H358 and A427 cell lines. This implies that the SHOC2 phosphatase complex may play an important role in modulating signalling flux through RAS to the ERK-pathway in response to RTK-stimulation.

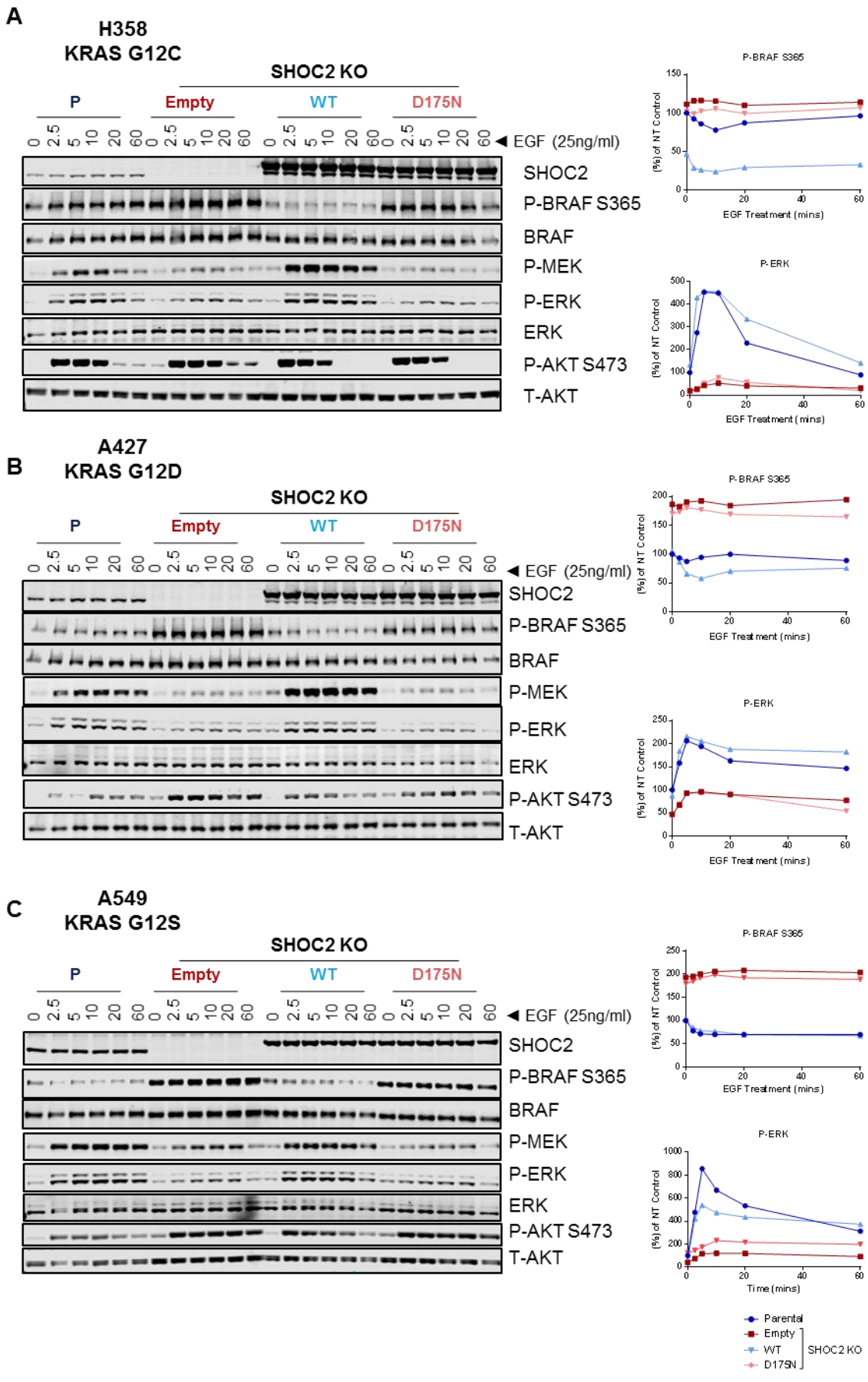
A
H358
KRAS G12C
SHOC2 KO
P
Empty
WT
D175N
0 2.5 5 10 20 60
EGF (25ng/ml)
SHOC2
P-BRAF S365
BRAF
P-MEK
P-ERK
ERK
P-AKT S473
T-AKT
P-BRAF S365
(%) of NT Control
EGF Treatment (mins)
P-ERK
B
A427
KRAS G12D
C
A549
KRAS G12S
Time (mins)
Parental
Empty
WT
D175N
SHOC2 KO

Figure 4.2 The SHOC2 phosphatase complex is required for EGF-mediated ERK-pathway activation

A SHOC2 is required for full ERK-pathway activation on EGF treatment through its role as part of the MRAS-SHOC2-PP1 complex. H358 parental, and SHOC2 knockout (KO) cells with stable re-expression of wildtype (WT) SHOC2, D175N SHOC2 or Empty vector control were treated with 25ng/ml of EGF for indicated time points and then harvested for western blot analysis and probed with the indicated antibodies. P-BRAF S365 and P-ERK levels are quantified by dividing by their respective totals at 0'mins of EGF stimulation for each cell line for the full length of the time course of EGF treatment.
B As (A) for A427 cells.
C As (A) for A549 cells.

4.1.4 Gain of function SHOC2 mutants are found in Noonan Syndrome

Expanding earlier observations we performed EGF time courses in H358 cells transduced with SHOC2 mutants found as causal mutations in the RASopathy Noonan syndrome (Cordeddu et al. 2009; Hannig et al. 2014). Both of these mutants have been shown to drive enhanced complex formation of the MRAS-SHOC2-PP1 complex (Unpublished data - Young et al 2018). We observe that both the SHOC2 S2G, and M173 led to almost complete dephosphorylation of the 'S365' on BRAF, in agreement with the SHOC2 phosphatase complex in mediating this dephosphorylation event. However we find that only the M173 is sufficient to restore ERK-signalling in response to EGF-stimulation (Figure 4.3). This may reflect their different subcellular localisation. The S2G mutant has been published to lead to aberrantly acquired N-myristoylation of the protein and subsequent constitutive membrane targeting, whereas the M173 proximally located to D175N site of SHOC2 is not membrane targeted (Cordeddu et al. 2009). Both point mutations highlight the importance of this region in mediating full SHOC2 complex activity for 'S259' dephosphorylation and support the notion that gain of function mutations in this complex drive aberrant ERK-activation in RASopathies.

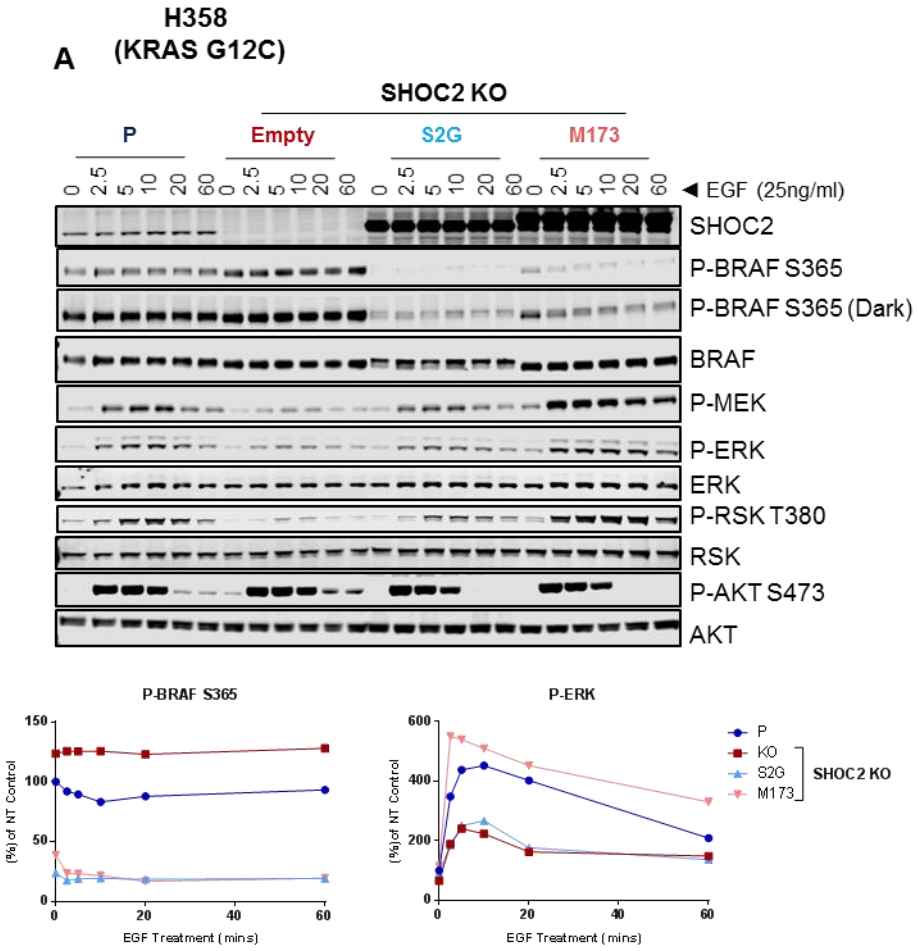

Figure 4.3 Gain of function SHOC2 mutants are found in Noonan Syndrome

A SHOC2 is required for full ERK-pathway activation on EGF treatment through its role as part of the MRAS-SHOC2-PP1 complex. H358 parental, and SHOC2 knockout (KO) cells with stable re-expression of, S2G or M173 SHOC2 or Empty vector control were treated with 25ng/ml of EGF for indicated time points and then harvested for western blot analysis and probed with the indicated antibodies. P-BRAF S365 and P-ERK levels are quantified by dividing by their respective totals at 0'mins of EGF stimulation for each cell line for the full length of the time course of EGF treatment.

4.1.5 SHOC2 is required for B-C RAF dimerization in response to EGF-stimulation

To explore the role of SHOC2 on both basal versus EGF-stimulated RAF dimerization we performed endogenous CRAF and/ or BRAF IPs and probed for either BRAF or CRAF in H358, A549, and DLD1 cell lines. DLD1 are a KRAS G13D mutant colorectal cell line and provide the opportunity to see if our effects stratify across tissue type.

Under basal conditions we only detected very low levels of RAF dimers. In contrast upon 10' EGF stimulation we observe a marked increase in BRAF-CRAF dimers, but no increase in ARAF-CRAF dimers (Figure 4.4) (Data not shown). Strikingly this induction of B-C dimers is completely abrogated in SHOC2 KO cells, and this correlates with diminished response of ERK-pathway readouts including P-MEK, ERK, RSK of all three cell lines to EGF-stimulation. In all three cell lines we also observe the corresponding SHOC2-independent increase in P-AKT and P-S6 previously discussed in relation to Figure 4.2.

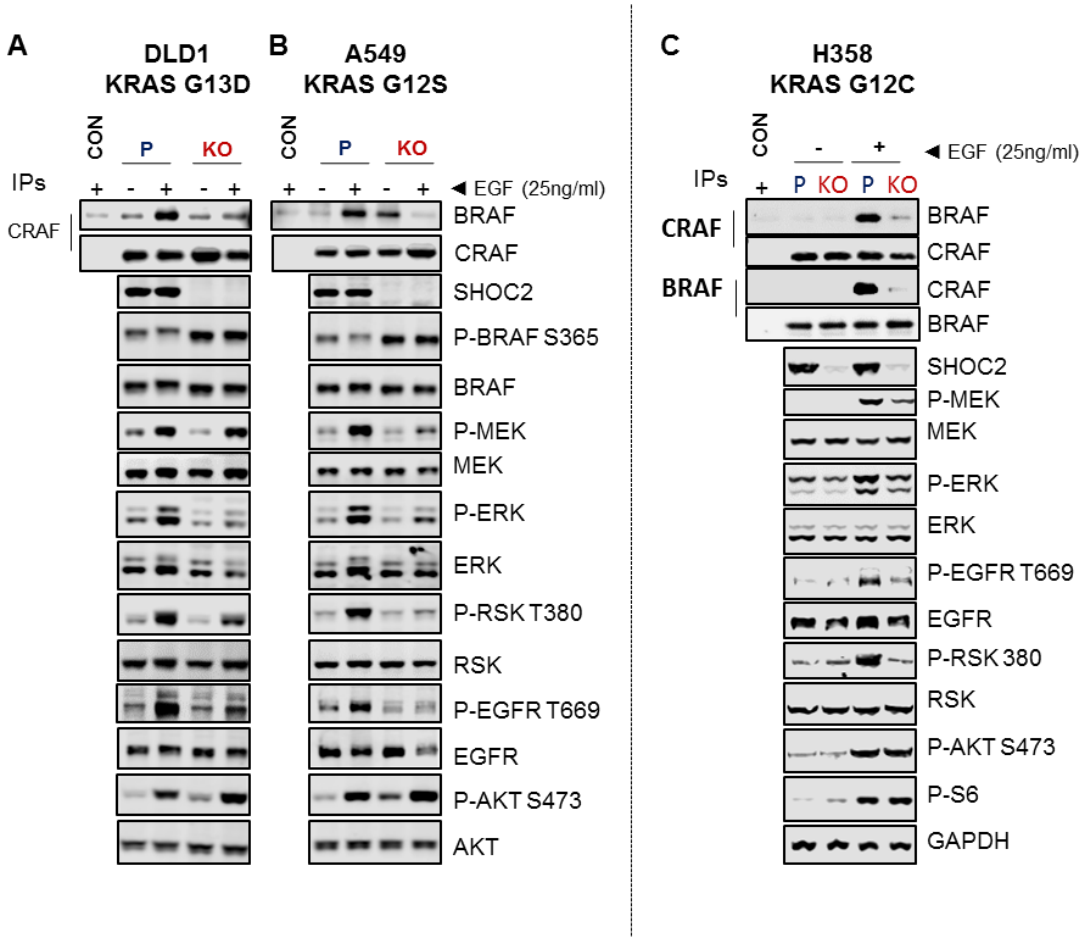

Figure 4.4 SHOC2 is required for B-CRAF dimerization in response to EGF-stimulation

A DLD1 parental, and SHOC2 knockout (KO) cells were treated with 25ng/ml of EGF for indicated 10minutes and then harvested for western blot analysis and endogenous CRAF IPs and probed with the indicated antibodies.

B As (A) for A549 cells.

C As (A) for H358 cells. *Note alternative loading pattern.

4.1.6 Conclusions

In summary, this data, as well as 2D- vs 3D-culture conditions in chapter 3 highlights the context-dependent nature of SHOC2-dependent ERK-signalling. SHOC2 is not required for 2D basal ERK-pathway activation, but conversely EGF treatment, reveals a striking SHOC2 phosphatase dependency for BRAF-CRAF dimer-mediated ERK-pathway activation on RTK-stimulation.

Chapter 5

SHOC2 inhibition selectively sensitizes KRAS- & EGFR-mutant NSCLC cells to MEKi's

5.1 SHOC2 inhibition selectively sensitizes KRAS- & EGFR-mutant NSCLC cells to MEKi's

5.1.1 Introductory statement

Targeting nodes of the ERK-MAPK pathway has been the subject of intensive drug discovery efforts. It is complicated by the essential requirement of the ubiquitous ERK-MAPK nodes for organism viability, both during embryonic development and in the adult (Blasco et al. 2011; Sanclemente et al. 2018). Although MEK inhibitors (MEKi's) are highly specific, they have shown little clinical benefit against RAS-driven tumours that remain clinically intractable. This is part due to drug resistance caused by feedback-induced ERK-reactivation that leads MEKi's to have a predominantly cytostatic response. Furthermore, on-target toxicity precludes the potent pathway suppression required for a clinical effect. Agents that serve to widen the therapeutic index of MEKi's may render them greater clinical utility. We know SHOC2 inhibition perturbs anchorage-independent tumour growth, but has no effect on growth/ viability in 2D-adhered culture conditions. How would SHOC2 inhibition alter the viability effects of already clinically available small molecule inhibitors?

5.1.2 SHOC2 inhibition enhances the effect of MEKi's in H358 cells

To ascertain the effect of SHOC2 inhibition in combination with other small molecule inhibitors, we transduced the KRAS mutant LUAD cell line H358 with two shRNAs targeting SHOC2 for depletion. We subsequently performed viability assays with each of the transduced cell lines compared to a shSCR control, against a candidate panel of inhibitors, encompassing inhibitors for RTKs, ERK-MAPK and PI3K-AKT pathway nodes (Figure 5.1). We determined the IC50 value as an average of the two shRNAs and calculated the fold change in IC50 value derived from the shSHOC2 compared to the shSCR control cells (Figure 5.2A). We identified a potent and selective sensitisation of H358 cells with SHOC2 inhibition to all four MEKi's within our candidate screen, using both shSHOC2 (Figure 5.2A) and SHOC2 KO (Figure 5.2B) approaches. These effects were reproduced in the KRAS mutant A549 cell lines (Figure 5.2C). Furthermore we observed no change in IC50 value of any other inhibitor tested to date, including other inhibitors of ERK-MAPK nodes, such as PanRAF and ERKi's when SHOC2 was concurrently inhibited in both cell lines. We did observe cells growing in 3D were more sensitive to MEKi's than in 2D-culture, but concurrent SHOC2 inhibition did not further enhance the activity of MEKi's anymore than cells growing in 2D (Data

not shown). As such all future investigation of combined MEK/ SHOC2 inhibition proceeded in 2D-experimental formats.

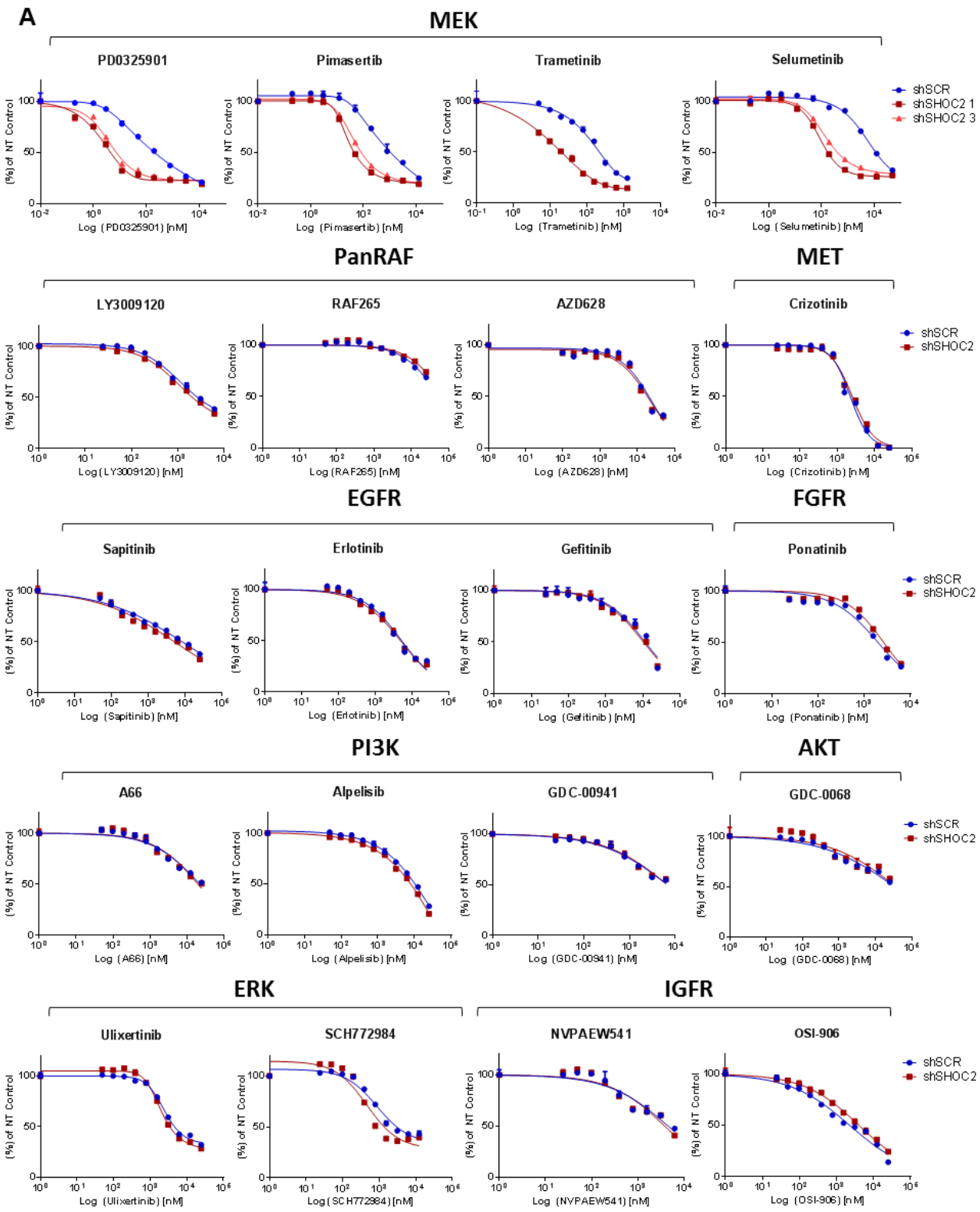

Figure 5.1 SHOC2 inhibition enhances the effect of MEKi's in H358 cells

A H358 cells transduced with either scrambled (shSCR) or 2-independent shSHOC2 oligos were treated with the indicated inhibitors at different doses and a dose-response curve derived for each of the inhibitors after a 96hr incubation using CellTiter-Glo viability reagent.

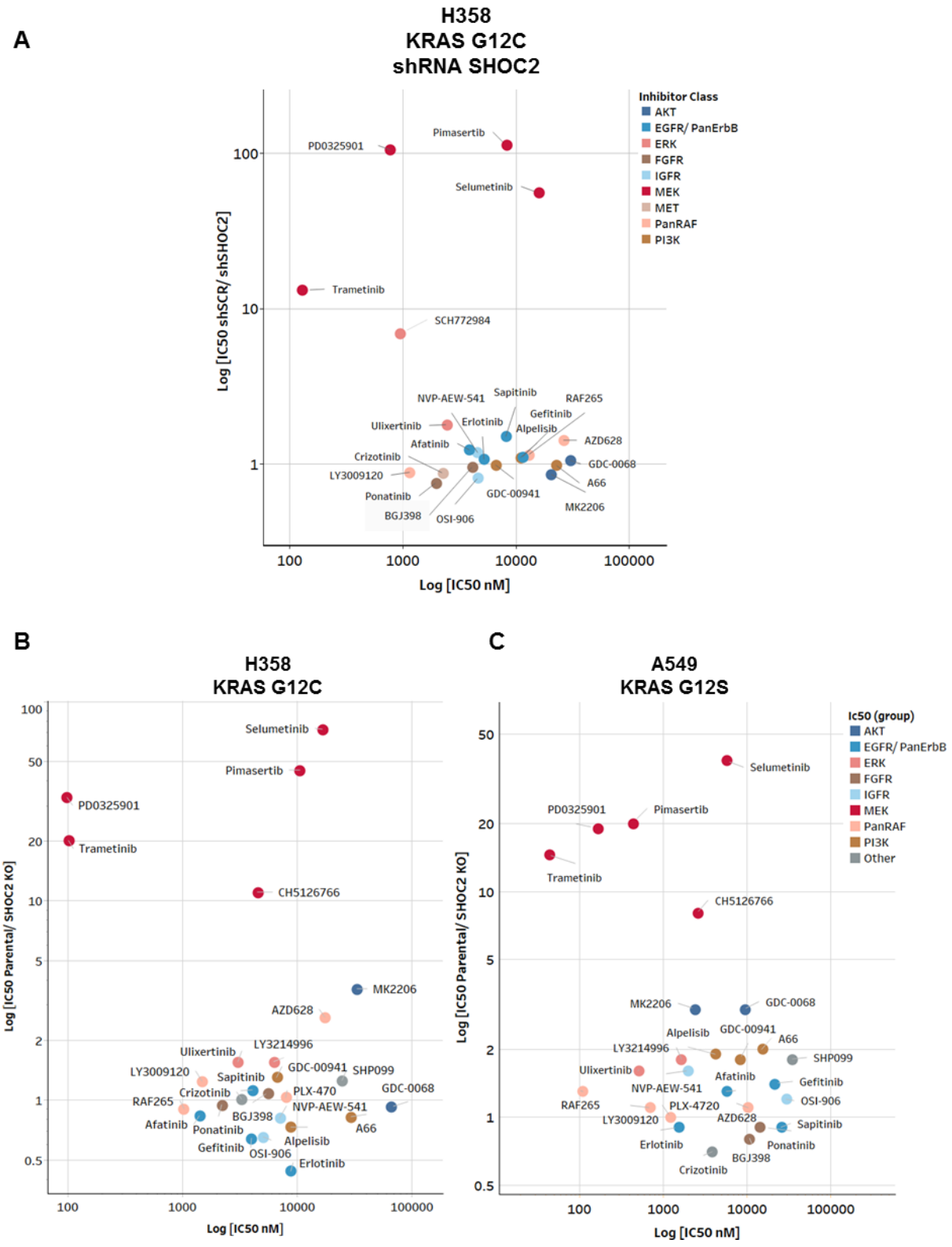
A
H358
KRAS G12C
shRNA SHOC2
Inhibitor Class
AKT
EGFR/ PanErbB
ERK
FGFR
IGFR
MEK
MET
PanRAF
PI3K
Log [IC50 shSCR/ shSHOC2]
Log [IC50 nM]
PD0325901
Pimasertib
Selumetinib
Trametinib
SCH772984
NVP-AEW-541
Sapitinib
RAF265
Gefitinib
Ulixertinib
Erlotinib
Alpelisib
AZD628
Afatinib
Crizotinib
GDC-0068
LY3009120
A66
Ponatinib
GDC-00941
MK2206
BGJ398
OSI-906
B
H358
KRAS G12C
Log [IC50 Parental/ SHOC2 KO]
Log [IC50 nM]
Selumetinib
Pimasertib
PD0325901
Trametinib
CH5126766
MK2206
AZD628
LY3214996
Ulixertinib
LY3009120
Sapitinib
GDC-00941
SHP099
Crizotinib
PLX-470
GDC-0068
RAF265
NVP-AEW-541
BGJ398
Afatinib
Ponatinib
A66
Alpelisib
Gefitinib
OSI-906
Erlotinib
C
A549
KRAS G12S
Ic50 (group)
AKT
EGFR/ PanErbB
ERK
FGFR
IGFR
MEK
PanRAF
PI3K
Other
Log [IC50 Parental/ SHOC2 KO]
Log [IC50 nM]
Selumetinib
PD0325901
Pimasertib
Trametinib
CH5126766
MK2206
GDC-0068
Alpelisib
GDC-00941
A66
LY3214996
SHP099
Ulixertinib
Afatinib
Gefitinib
NVP-AEW-541
OSI-906
RAF265
PLX-4720
LY3009120
AZD628
Sapitinib
Erlotinib
Ponatinib
BGJ398
Crizotinib

Figure 5.2 SHOC2 inhibition specifically sensitises H358 cells to MEKi's using both shRNA and CRISPR-mediated SHOC2 KD/KO approaches

A H358 Cells transduced with either scramble (shSCR) or 2-independent shSHOC2 oligos were treated with the indicated inhibitors at different doses and a dose-response curve derived for each of the inhibitors after a 96hr incubation using CellTiter-Glo viability reagent. For each inhibitor the fold change in IC50 between shSCR and an average of the 2-shSHOC2 cells is plotted.
B As (A) for Parental/ SHOC2 KO H358 cells.
C As (A) for Parental/ SHOC2 KO A549 cells.

5.1.3 SHOC2 inhibition enhances the effect of MEKi's in RAS- and EGFR-mutant cells

In order to determine the breath of this finding we repeated this across a panel of NSCLC cell lines, encompassing those with driver mutations in KRAS, EGFR, and BRAF, as well as cell lines wildtype for any known driver mutations in the ERK-MAPK pathway. SHOC2 inhibition sensitised the breath of KRAS mutant cell lines tested to the MEKi's Selumetinib (Figure 5.3A) and Trametinib (Figure 5.3B) with the exception of the cell line H727. We attribute this to a co-occurring ARAF mutation in this line, previously identified as an activating mutation (Baljuls et al. 2008). In addition, as in RAS mutant cells we found SHOC2 inhibition enhanced the response of MEKi's in EGFR mutant cell lines, but had no effect on BRAF mutant, or wildtype cell lines (Figure 5.4). Importantly SHOC2 inhibition sensitised EGFR mutant cell lines to MEKi's even after they had acquired a second hit mutation in T790M that renders them resistant to ATP competitive inhibitors such as Erlotinib and Gefitinib (PC9-er)(Figure 5.3A). We confirmed our findings with replicate experiments in H358, A427, A549 and H1792 SHOC2 KO cells to obtain significance scores (Figure 5.5A). These findings also reproduced in colony formation assays (Figure 5.5B).

A

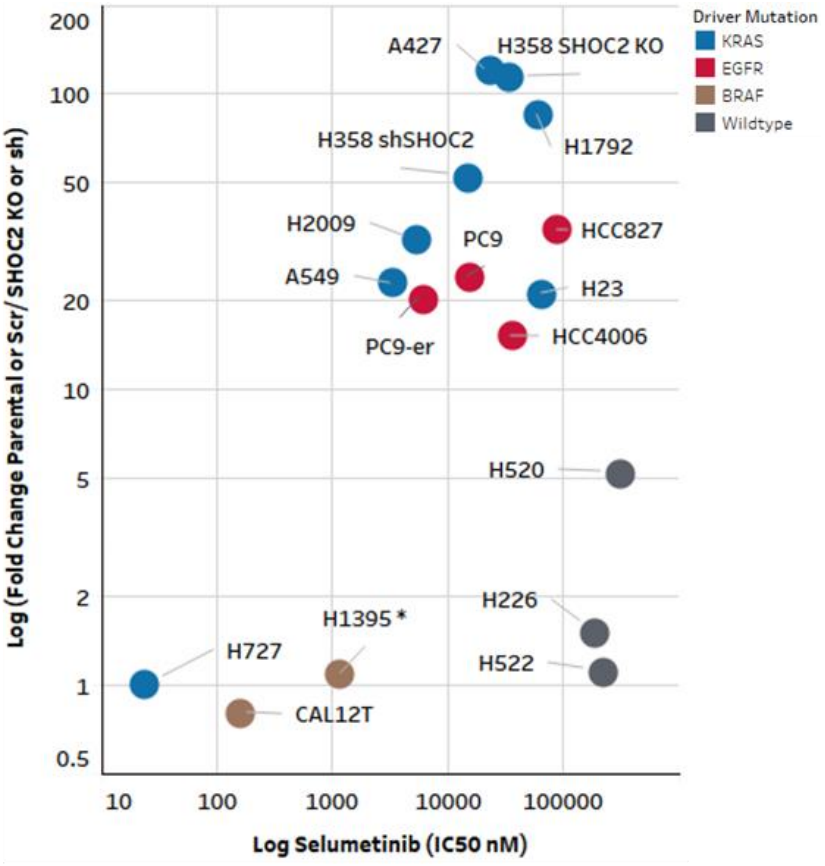
Driver Mutation
KRAS
EGFR
BRAF
Wildtype
Log (Fold Change Parental or Scr/ SHOC2 KO or sh)
200
100
50
20
10
5
2
1
0.5
A427
H358 SHOC2 KO
H358 shSHOC2
H1792
H2009
PC9
HCC827
A549
H23
PC9-er
HCC4006
H520
H226
H1395 *
H727
H522
CAL12T
10
100
1000
10000
100000
Log Selumetinib (IC50 nM)

B

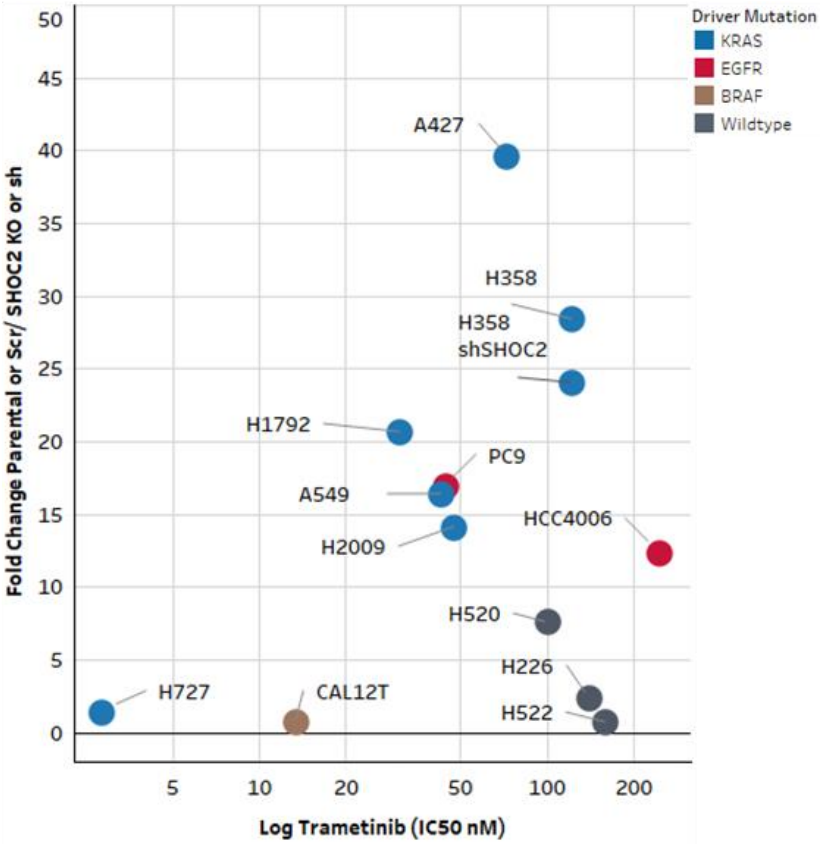
Driver Mutation
KRAS
EGFR
BRAF
Wildtype
Fold Change Parental or Scr/ SHOC2 KO or sh
50
45
40
35
30
25
20
15
10
5
0
A427
H358
H358
shSHOC2
H1792
PC9
A549
HCC4006
H2009
H520
H226
H727
CAL12T
H522
5
10
20
50
100
200
Log Trametinib (IC50 nM)

Figure 5.3 SHOC2 inhibition enhances the effect of MEKi's in RAS- and EGFR-mutant cells

A SHOC2 inhibition sensitises KRAS and EGFR mutant, but not BRAF or wildtype NSCLC cell lines to MEKi's. Viability assays for Selumetinib on a panel of NSCLC cell lines with different driver mutations. Fold change in IC50 between shSCR and shSHOC2 or Parental and SHOC2 KO cells plotted for each cell line. PC9-er (Erlotinib resistant)

*because of incomplete knockdown with shRNA, SHOC2 was inhibited in H1395 by siRNA. Cell lines are grouped by color code based on driver mutation.

B As (A) for the MEKi-Trametinib

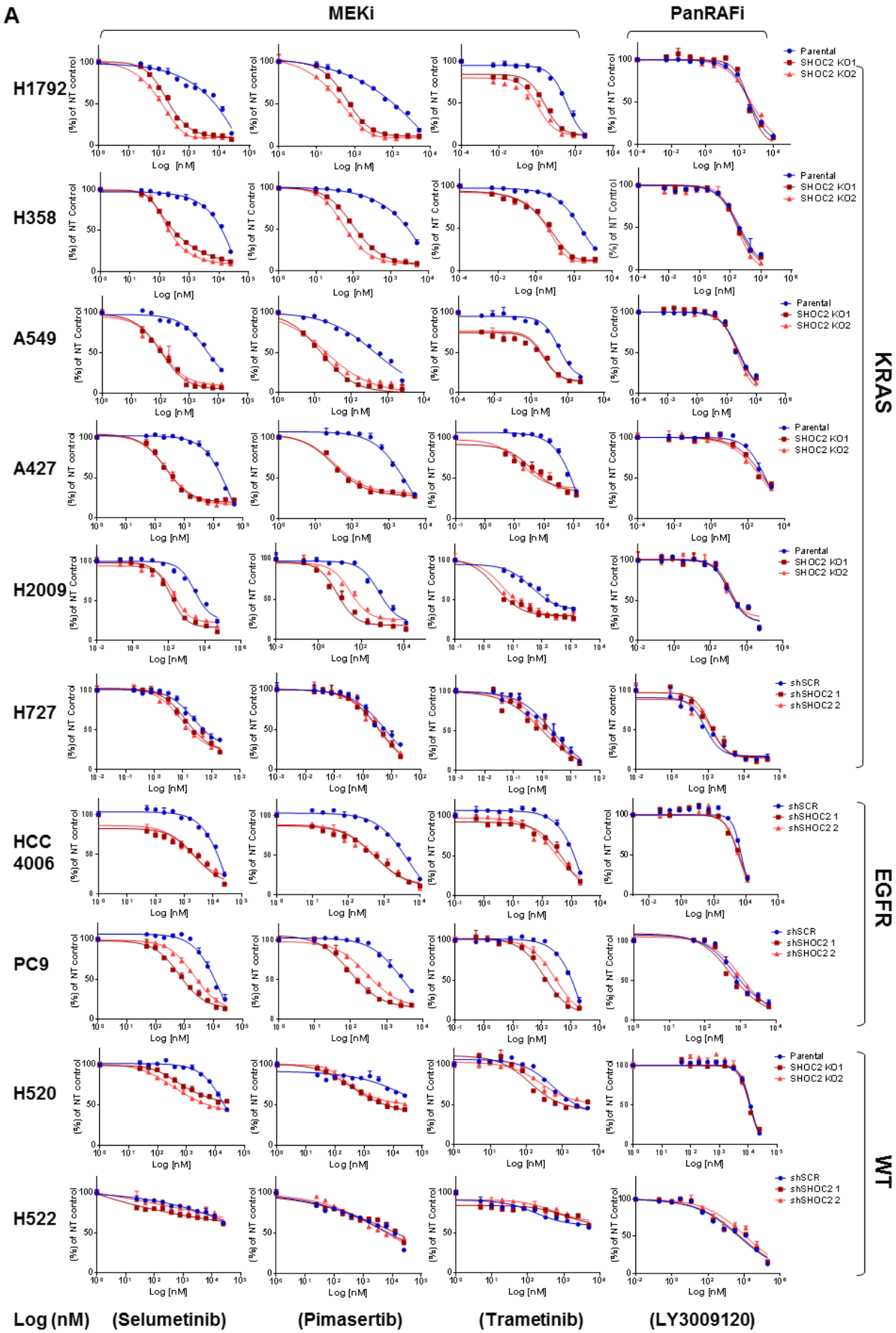
A
MEKi
PanRAFi
H1792
H358
A549
A427
H2009
H727
HCC 4006
PC9
H520
H522
KRAS
EGFR
WT
Parental
SHOC2 KO1
SHOC2 KO2
shSCR
shSHOC2 1
shSHOC2 2
[%] of NT control
Log [nM]
Log (nM)
(Selumetinib)
(Pimasertib)
(Trametinib)
(LY3009120)

Figure 5.4 SHOC2 inhibition sensitises RAS- and EGFR-mutant cells to MEK inhibitors, but not PanRAF or ERK inhibitors

A A panel of NSCLC cells encompassing both RAS, EGFR mutants, and cell lines wildtype for known ERK-MAPK drivers, - & + SHOC2 KO were treated with the indicated inhibitors at different doses and a dose-response curve derived for each of the inhibitors after a 96hr incubation using CellTiter-Glo viability reagent.

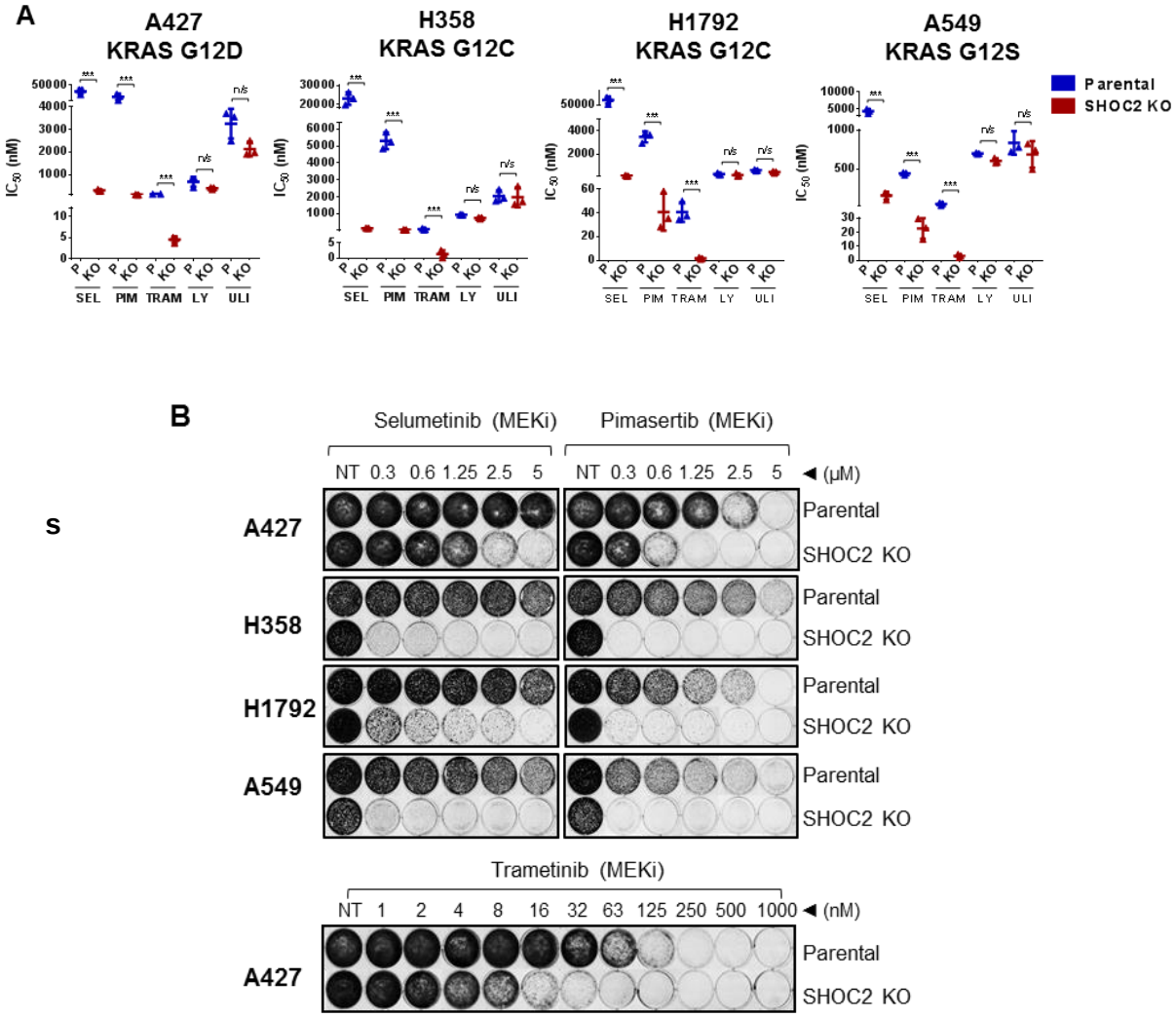

Figure 5.5 SHOC2 inhibition sensitises RAS- and EGFR-mutant cells to MEK, but not PanRAF or ERKi's, in both viability and colony formation assays

A SHOC2 inhibition selectively sensitises KRAS mutant NSCLC lines to MEKi (SEL - Selumetinib/ PIM – Pimasertib/ TRAM – Trametinib), but not PanRAF (LY – LY3009120) or ERKi's (ULI – Ulixertinib). Plot of IC50 values derived from viability assays of parental or SHOC2 KO cells treated with indicated inhibitors (mean ± SD) (n=3). Significance is determined using a two tailed T-test $*p < 0.05$, $**p < 0.01$ or $***p < 0.001$.

B Colony formation assays. 10,000 cells were seeded per well of the indicated cell line and treated with inhibitor for 96hrs as in viability assays. After inhibitor treatment for 4-days medium was replaced and cells were grown in the absence of inhibitor for a further 7-days before being stained with crystal violet.

5.1.4 Disruption of the SHOC2 phosphatase complex is sufficient to sensitise KRAS-mutant NSCLC cell lines to MEKi's

Re-expression of WT SHOC2 in SHOC2 KO cells was fully sufficient to rescue the sensitisation to MEKi's. However re-expression of the D175N SHOC2 mutant was unable to rescue this effect, attributing the enhancement of MEKi's on SHOC2 inhibition to the role of SHOC2 as part of the MRAS-SHOC2-PP1 complex (Figure 5.6B). In agreement with this, overexpression of phosphorylation deficient 'S259A' RAF mutants was sufficient to rescue the sensitisation of the KRAS mutant A427 and A549 cells, to both Selumetinib & Trametinib (Figure 5.7A,C). In agreement with the role of this dephosphorylation event in governing RAF-driven ERK-activation, expression of S259A phosphorylation deficient mutants led to hyperactivation of ERK-MAPK signalling by western blot (Figure 5.7B,D).

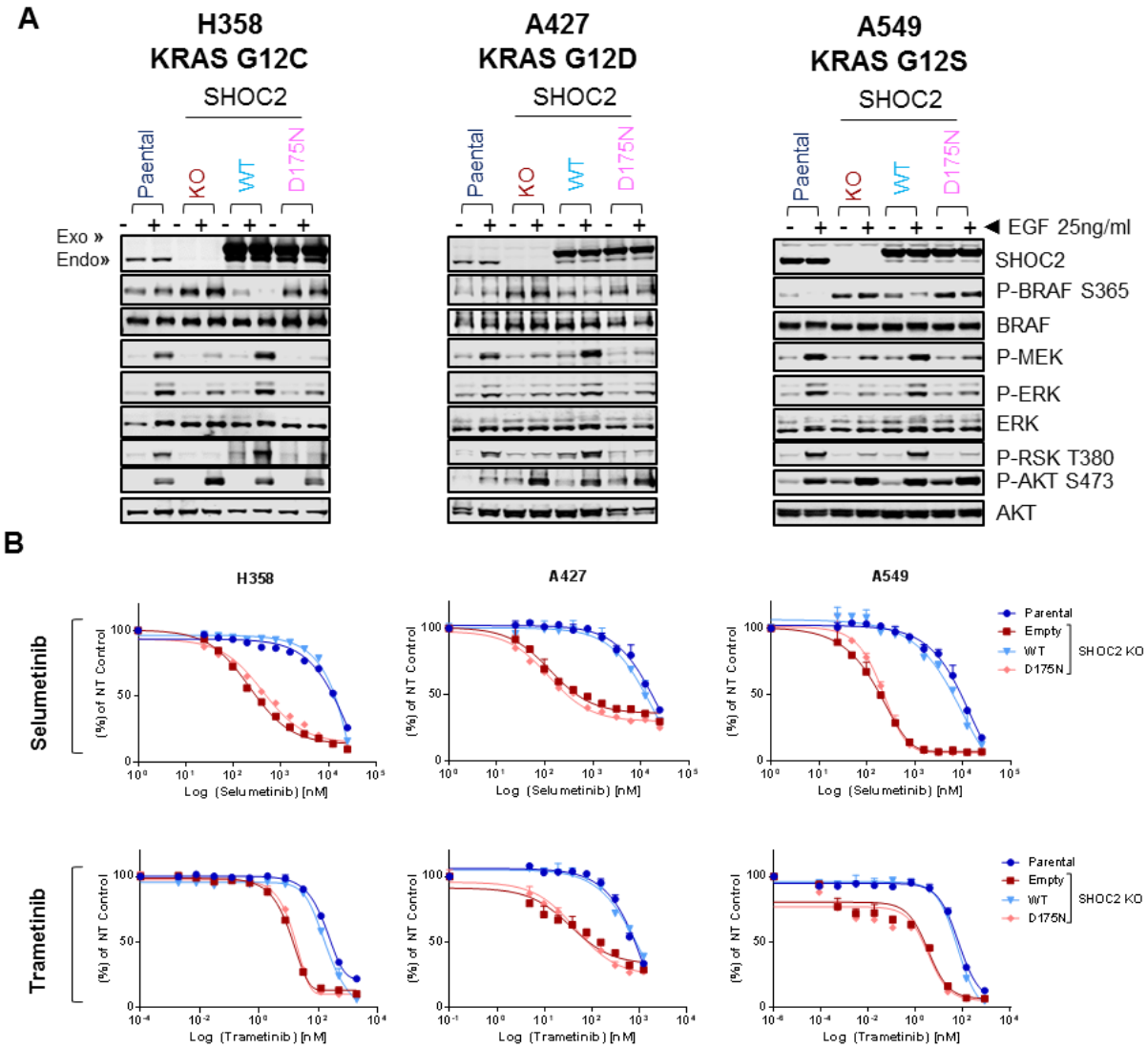

Figure 5.6 MEKi sensitisation on SHOC2 inhibition is dependent on the role of SHOC2 as part of the SHOC2 phosphatase complex

A SHOC2 inhibition impairs ERK-pathway activation by EGF. H358, A427, A549 parental, and SHOC2 knockout (KO) cells with stable re-expression of wildtype (WT) SHOC2, D175N SHOC2 or Empty vector control were treated with 25 ng/ml EGF for 10minutes. Lysates were probed with indicated antibodies and visualised by western blot.

B Cells described in (A) were treated with the indicated inhibitors at different doses and a dose-response curve derived for each of the inhibitors after a 96hr incubation using CellTiter-Glo viability reagent.

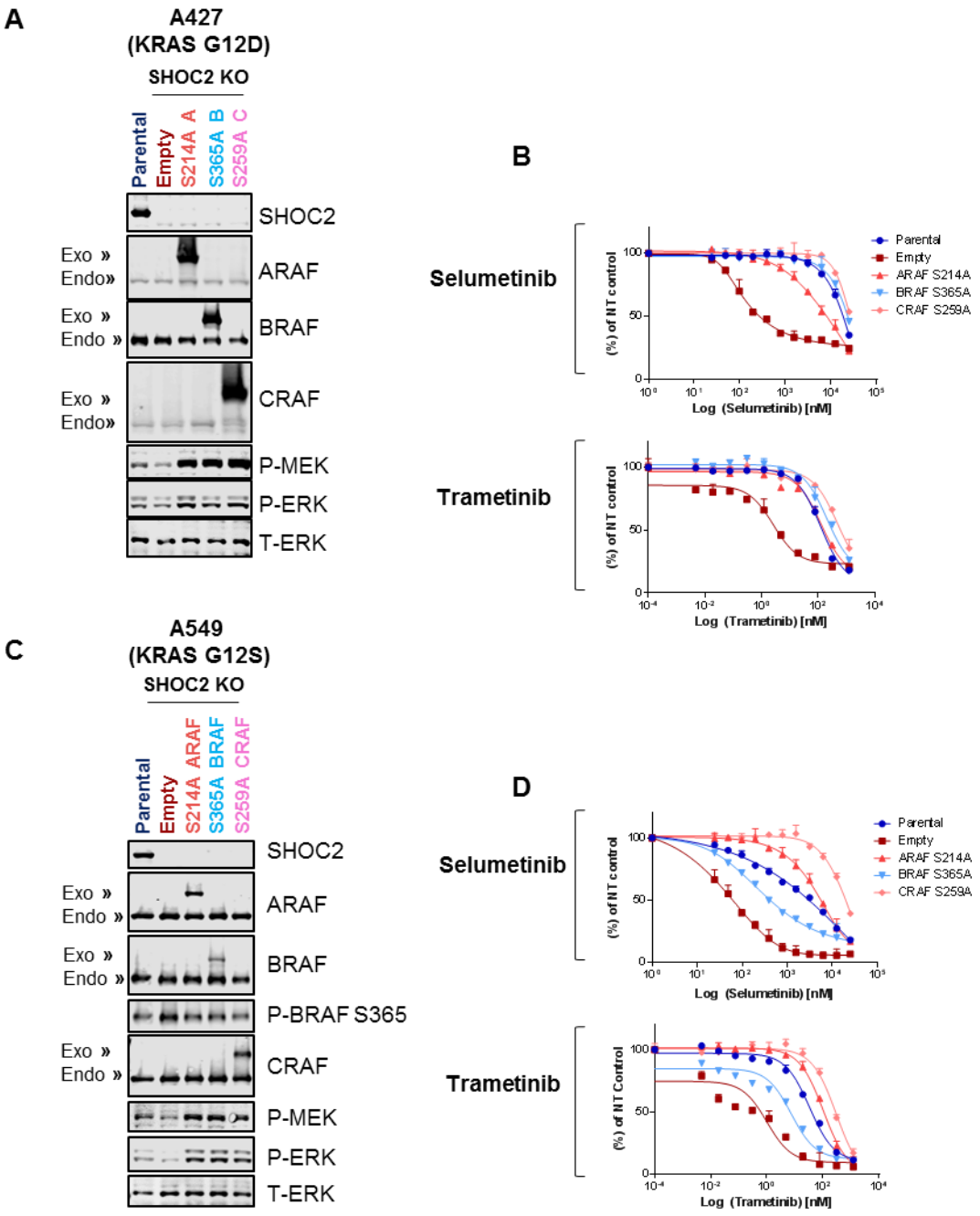

Figure 5.7 Sensitisation of SHOC2 knockout NSCLC cell lines to MEKi's is rescued by expression of RAF 'S259' phosphorylation-deficient mutants.

A A427 SHOC2 KO cells with stable re-expression of S214A ARAF, S365A BRAF, S259A CRAF or empty vector control. Lysates were probed for indicated antibodies.

B Cells described above were treated with the indicated inhibitors at different doses and a dose-response curve derived for each of the inhibitors after a 96hr incubation using CellTiter-Glo viability reagent.

C As (A) in A549 cells.

D As (B) in A549 cells.

5.1.5 Genetic inhibition of SHOC2 further sensitises NSCLC cells to pharma logical inhibition of MEKi + PI3K, IGFR and ERK, but not RAF combinations

Targeting of ERK-MAPK nodes has been fraught with complexity, and has been limited in therapeutic efficacy, in part due to rewiring and activation of compensatory mechanisms restoring ERK activity summarised in (Samatar and Poulikakos 2014). As a result of this, research efforts to identify and target resistance mechanisms is an area of research which has gained traction. Combination therapies have been shown to drive greater responses in KRAS mutant cancer models, and agents that co-target MEK + PI3K, IGFR, FGFR and ERB3, as well as nodes of the same pathway (vertical inhibition), MEK + PanRAF or ERK have been shown to induce apoptosis at much lower doses than single agent MEKi treatment, and so drive enhanced tumour regressions in *in vivo* lung and colon cancer models (Hatzivassiliou et al. 2012; Castellano et al. 2013; Molina-Arcas et al. 2013; Lamba et al. 2014; Whittaker et al. 2015; Manchado et al. 2016). Although promising preclinical data exists, the proof of these combinations as realistic therapeutic options will lie in their toxicity profiles. Given that SHOC2 inhibition substantially reduces the IC50 of the NSCLC cell lines to MEK inhibition, it's rational that co-targeting SHOC2 with these dual therapy options may enable these dual agents to be therapeutically applicable at lower concentrations; potentially also widening their therapeutic index.

To this end, we treated H358 cells with and without SHOC2 suppression to a 5*10 dose matrix of the MEKi Pimasertib + a second inhibitor (Figure 5.8). In agreement with previously published data we observe all combinations tested showed synergy with MEKi's, despite very low amounts of MEKi used in these assays (Figure 5.8B). However, in the case of each combination, we observed a variable further contribution with SHOC2 suppression. At very low doses of MEKi (50nM Pimasertib), we see that SHOC2 suppression further sensitises H358 cells most substantially to PI3K and IGFR combinations. SHOC2 suppression partially further contributes to MEK + ERK and EGFR combinations in H358 cells, but has no further contribution to MEK + PanRAF or MEK + Ponatinib, (a multi-targeted tyrosine kinase inhibitor) combinations. Expanding this observation across multiple KRAS mutant NSCLC cell lines, we derived the synergy score using the 'Bliss Independence model' for five NSCLC SHOC2 KO cell lines of MEK + PI3K, IGFR, ERK and PanRAF combinations (Figure 5.9). The data shows that although MEK + PI3K, IFGR and ERK have similar synergy scores, MEK + PanRAF scores are considerably higher. This demonstrates the importance of combined RAF + MEK inhibition for efficient viability inhibition in lung cancer cell lines. Critically, SHOC2 deletion synergises with MEK + PI3K, IGFR and

ERK combinations but does not with MEK + PanRAF inhibitor combinations in agreement with viability data obtained with H358 SHOC2 KD cells. Collectively this data demonstrates a rationale for combined SHOC2 inhibition with co-targeting of MEK + PI3K, IGFR, ERK inhibitors. The fact that we do not observe a further contribution to MEK + PanRAF synergy, even though we observe robust sensitisation to MEK monotherapy in our NSCLC cell lines suggests that some form of functional redundancy may exist between the PanRAF inhibitor and genetic inhibition of SHOC2. This is in agreement with the role of SHOC2 as part of the MRAS-SHOC2-PP1 complex in RAF activation. Should SHOC2 inhibition prevent RAF activation this would be functionally redundant in the context of PanRAF inhibition.

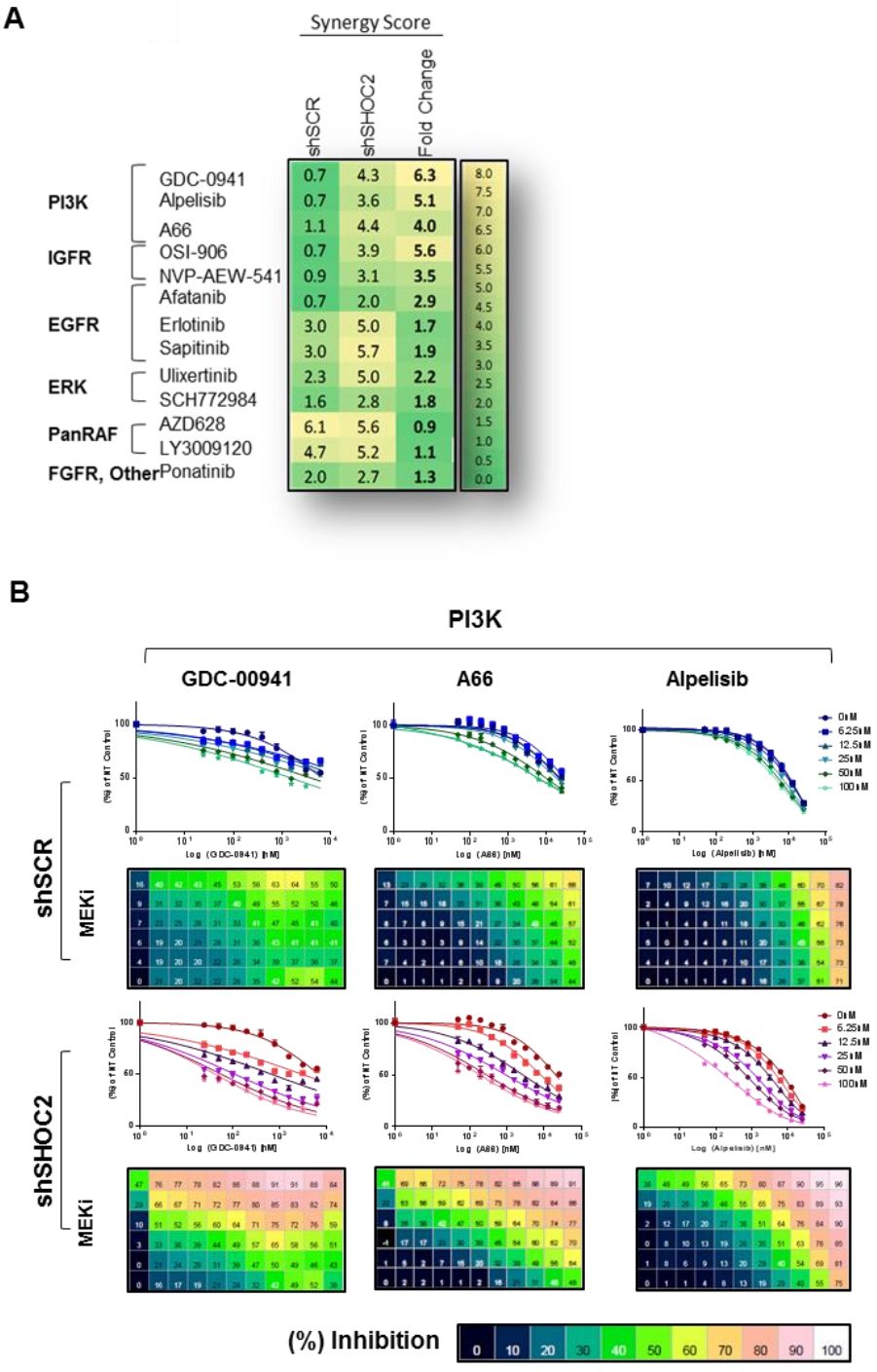
A
Synergy Score
shSCR
shSHOC2
Fold Change
PI3K
GDC-0941
Alpelisib
A66
IGFR
OSI-906
NVP-AEW-541
EGFR
Afatanib
Erlotinib
Sapitinib
ERK
Ulixertinib
SCH772984
PanRAF
AZD628
LY3009120
FGFR, Other
Ponatinib
0.7 4.3 6.3
0.7 3.6 5.1
1.1 4.4 4.0
0.7 3.9 5.6
0.9 3.1 3.5
0.7 2.0 2.9
3.0 5.0 1.7
3.0 5.7 1.9
2.3 5.0 2.2
1.6 2.8 1.8
6.1 5.6 0.9
4.7 5.2 1.1
2.0 2.7 1.3
8.0 7.5 7.0 6.5 6.0 5.5 5.0 4.5 4.0 3.5 3.0 2.5 2.0 1.5 1.0 0.5 0.0
B
PI3K
GDC-00941
A66
Alpelisib
shSCR
MEKi
shSHOC2
MEKi
0nM
6.25nM
12.5nM
25nM
50nM
100nM
(%) Inhibition
0 10 20 30 40 50 60 70 80 90 100

B Continued

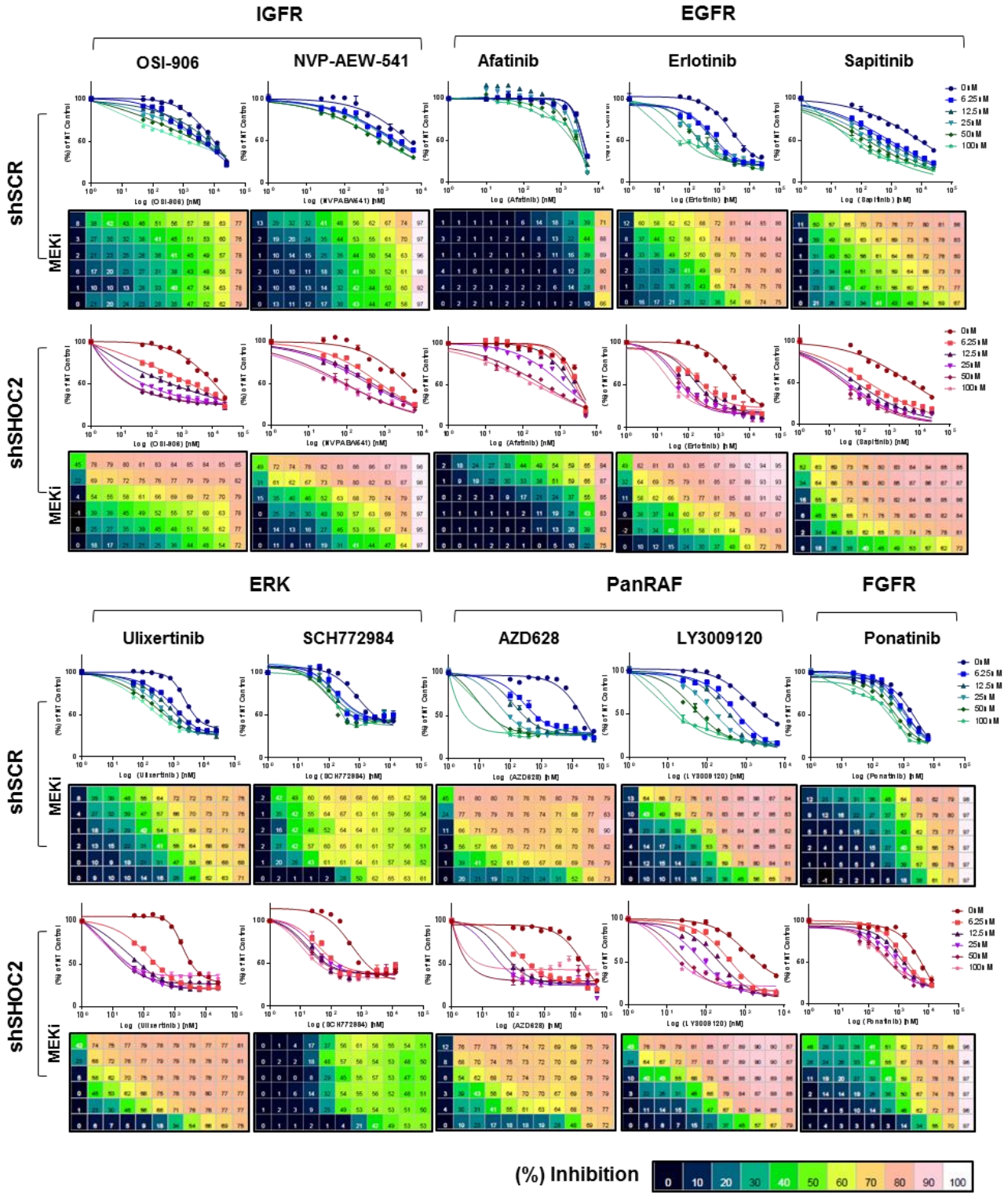
IGFR
EGFR
OSI-906
NVP-AEW-541
Afatinib
Erlotinib
Sapitinib
shSCR
shSHOC2
MEKi
0 nM
6.25 nM
12.5 nM
25 nM
50 nM
100 nM
ERK
PanRAF
FGFR
Ulixertinib
SCH772984
AZD628
LY3009120
Ponatinib
(%) Inhibition
0
10
20
30
40
50
60
70
80
90
100

Figure 5.8 SHOC2 suppression further sensitises H358 cells to MEKi + secondary inhibitor combinations

A SHOC2 suppression further sensitises H358 cells to combined inhibition of MEK with PI3K, IGFR, EGFR and ERK but not RAF inhibitors. H358 cells transduced with either shSCR or 2 independent shSHOC2 oligos were treated with a 10*5 point dose response of the indicated inhibitor, in combination with low doses of the MEK inhibitor Pimasertib and synergy scores for each inhibitor combination derived using the bliss independence model.
B Representative viability curves and % inhibition matrices for (A).

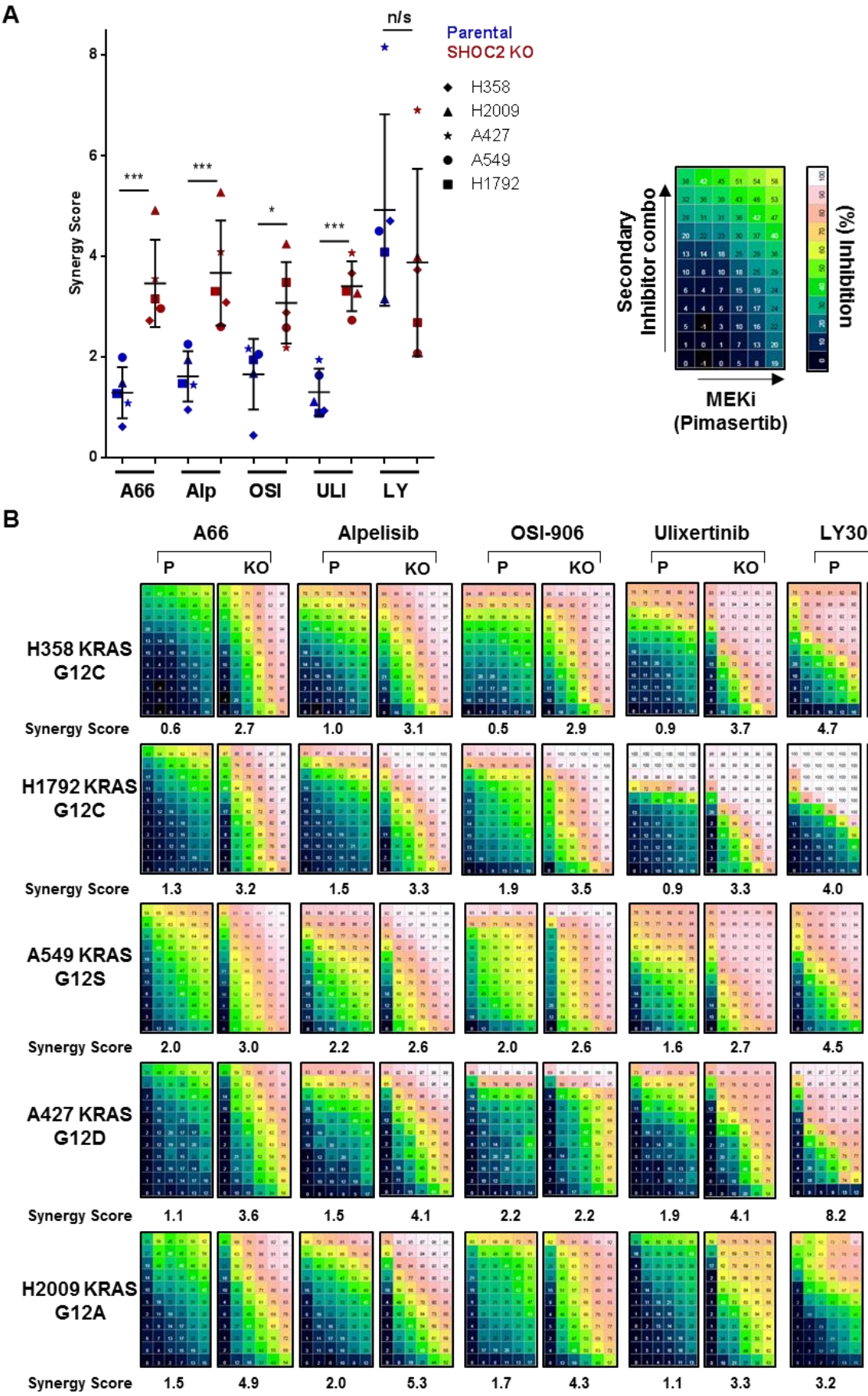
A
n/s
Parental
SHOC2 KO
H358
H2009
A427
A549
H1792
Synergy Score
0
2
4
6
8
***
***
*
***
A66
Alp
OSI
ULI
LY
Secondary Inhibitor combo
MEKi (Pimasertib)
(%) Inhibition
B
A66
Alpelisib
OSI-906
Ulixertinib
LY3009120
P
KO
H358 KRAS G12C
Synergy Score 0.6 2.7 1.0 3.1 0.5 2.9 0.9 3.7 4.7 3.7
H1792 KRAS G12C
Synergy Score 1.3 3.2 1.5 3.3 1.9 3.5 0.9 3.3 4.0 2.7
A549 KRAS G12S
Synergy Score 2.0 3.0 2.2 2.6 2.0 2.6 1.6 2.7 4.5 2.1
A427 KRAS G12D
Synergy Score 1.1 3.6 1.5 4.1 2.2 2.2 1.9 4.1 8.2 6.9
H2009 KRAS G12A
Synergy Score 1.5 4.9 2.0 5.3 1.7 4.3 1.1 3.3 3.2 4.0

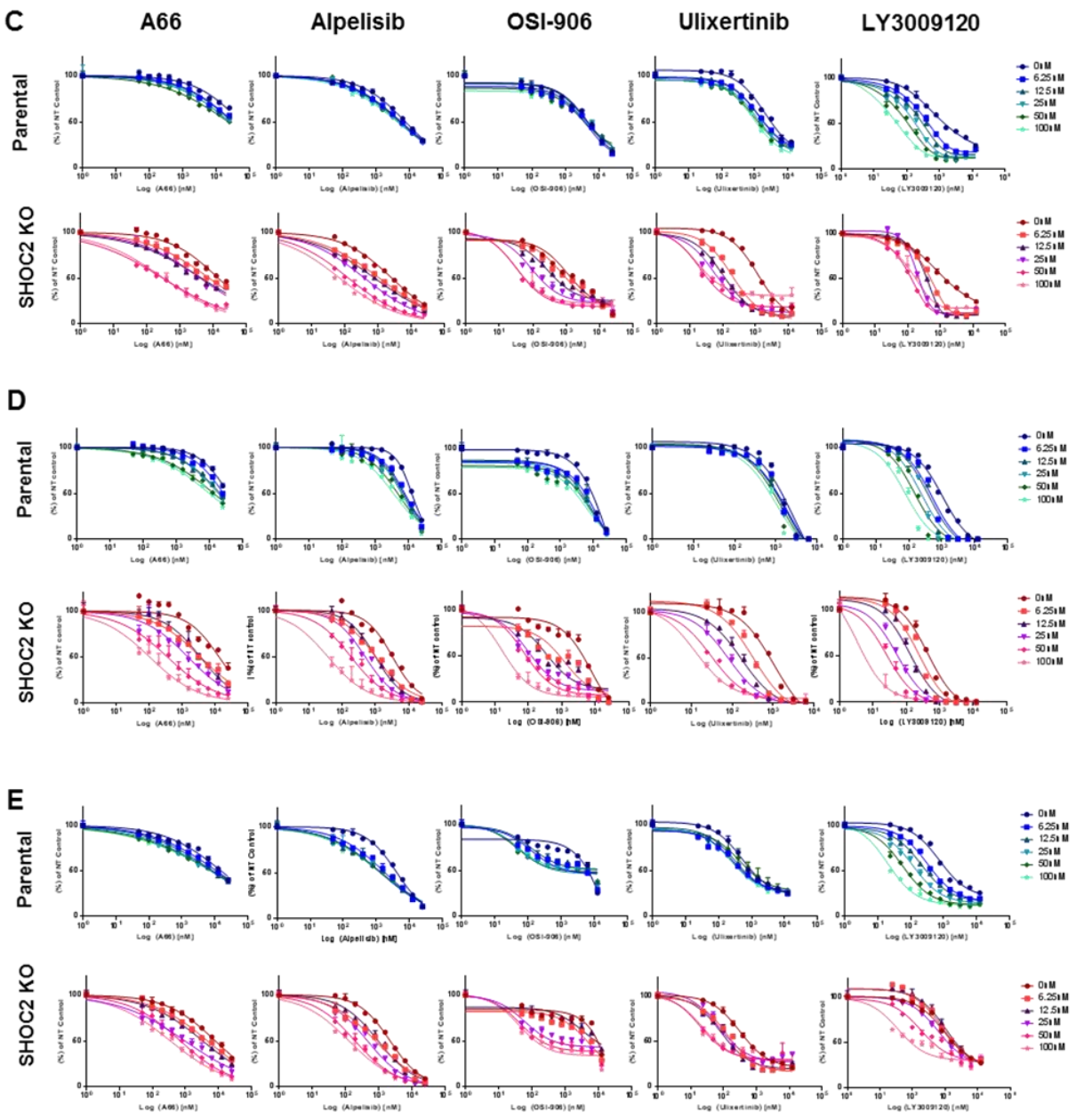
C
A66
Alpelisib
OSI-906
Ulixertinib
LY3009120
Parental
SHOC2 KO
0 nM
6.25 nM
12.5 nM
25 nM
50 nM
100 nM
D
Parental
SHOC2 KO
E
Parental
SHOC2 KO

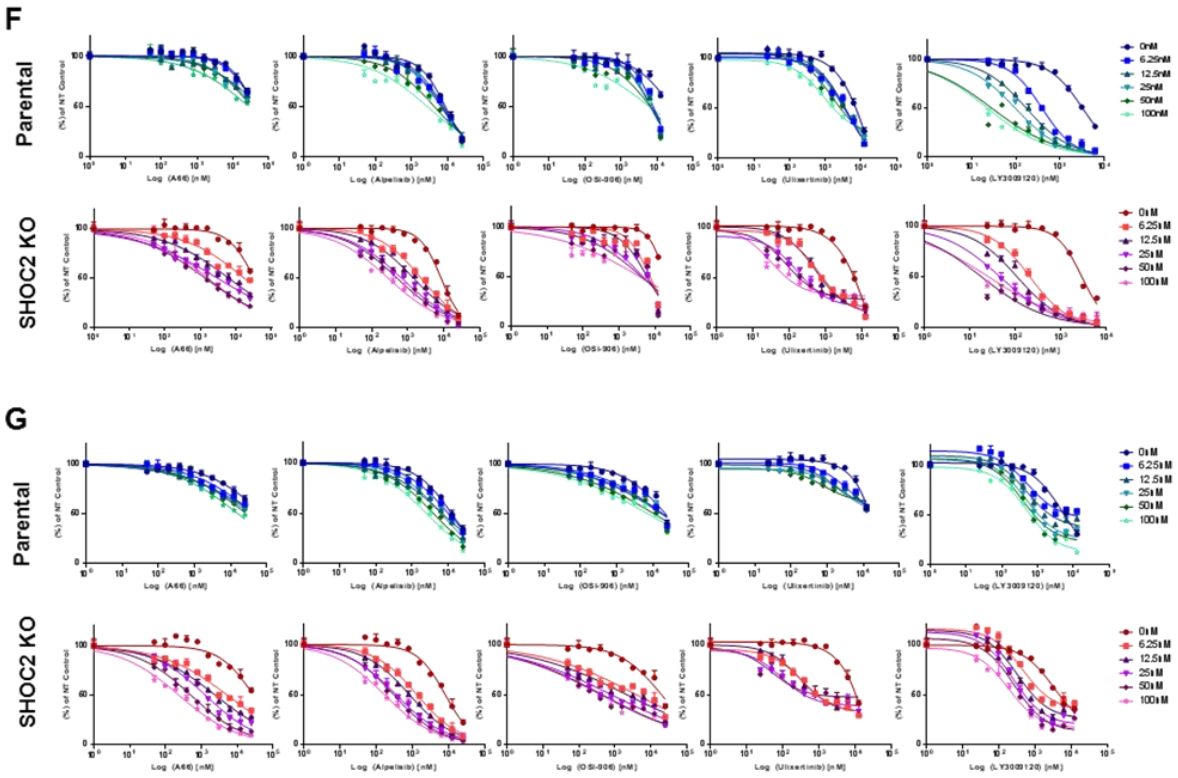

Figure 5.9 SHOC2 deletion further enhances the efficacy of MEKi + PI3K, MEK + IGFR, and MEK + ERK, but not MEK + RAF combinations, in a panel of NSCLC cell lines

A Synergy scores were derived using the bliss independence model (described in more detail in 2.1.14). In brief parental or SHOC2 KO cells were treated with a 10*5 point dose response of the indicated inhibitor, in combination with increasing concentration of the MEKi Pimasertib, (0-100nM). Values are plotted for 5-NSCLC cell lines (H358, A549, A427, H1792, H2009) (mean ± SD)(n=2). Significance is determined using a two tailed T-test $*p < 0.05$, $**p < 0.01$ or $***p < 0.001$. Representative of n=2 experiments.

B Representative (%) inhibition matrices for each of the cell lines described in (A).

C Representative dose-response viability curves for H358 cells in (A).

D Representative dose-response viability curves for H1792 cells in (A).

E Representative dose-response viability curves for A549 cells in (A).

F Representative dose-response viability curves for A427 cells in (A).

F Representative dose-response viability curves for H2009 cells in (A).

5.1.6 Conclusions

Collectively this data demonstrates that genetic inhibition of SHOC2 broadly sensitises both KRAS- and EGFR-mutant NSCLC cell lines to MEKi's. This enhancement of MEK-activity is dependent upon formation of the MRAS-SHOC2-PP1 complex and dephosphorylation of the S259 site on RAF. Critically, SHOC2 further decreases the IC50 value of KRAS- and EGFR-mutant cell lines to MEKi's without decreasing the IC50 for wildtype lines. This raises the possibility that SHOC2 inhibition may widen the therapeutic index of MEKi's. Combination therapies targeting other signalling nodes are synergistic with MEKi's in RAS mutant cells in preclinical models. However, it remains to be seen whether increased toxicity burden allows for a therapeutic index. We show SHOC2 suppression further contributes to MEKi + PI3Ki, IGFRi or ERKi combinations across a panel of NSCLC cell lines. It is thus possible that a SHOC2 targeted therapy would not only widen the therapeutic index of MEKi as single agent, but also in combination with other targeted therapies, enabling them more clinically viable.

Chapter 6

SHOC2 and MEK inhibition cooperate to induce apoptosis in KRAS-mutant cells

6.1 Genetic inhibition of SHOC2 lowers the concentration of MEKi required to induce apoptosis in KRAS-mutant cells

6.1.1 Introductory statement

Dose response viability assays, colony assays and live imaging techniques have shown SHOC2 inhibition sensitises RAS- & EGFR-mutant cells specifically to MEKi's. The steep drop of the slope in viability assays, as well as live imaging data suggests the reduction in viability may be due to cytotoxic not cytostatic effects, typically attributed to MEKi's, so we sought to characterise this further. MEKi's typically cause cytostatic effects that provide a permissive environment in which acquisition of second hit mutations in RAS cells selects to reinstate ERK-activity (Sale and Cook 2013b). ERK modulates apoptosis through the activity of pro-apoptotic BH3 family proteins including BIM and BAD, key mediators of the intrinsic apoptosis pathway (Luciano et al. 2003; Fueller et al. 2008; Dehan et al. 2009)

6.1.2 Combined MEK inhibition and/ SHOC2 deletion causes cytotoxicity of NSCLC cell lines

To determine if cytostatic versus cytotoxic effects were at play upon combined MEK inhibitor treatment with genetic inhibition of SHOC2 we generated incucyte growth curves for Parental and SHOC2 KO cells in the presence or absence of a dose response of the indicated MEKi, either Selumetinib or Trametinib (Figure 6.1). The cells were cultured in the presence of the inhibitor for 96hrs before the inhibitor was washed-out and the cells allowed to recover on addition of fresh media (media without drug). We observed, as previously (Figure 3.3A) that SHOC2 deletion has no effect on the growth of A427/ H358 cells by itself in 2D-adhered culture conditions, but in combination with MEK inhibition we observed that a lower dose of MEKi was required in the SHOC2 KO cells to cause growth inhibition. Furthermore when we washed-out the drug and allowed the cells to recover we observed SHOC2 deletion lowered the concentration of MEKi required to cause cytotoxicity in A427/ H358 cells – as determined by the absence of recovery of these cells on inhibitor wash-out, inferring cell death at these concentrations.

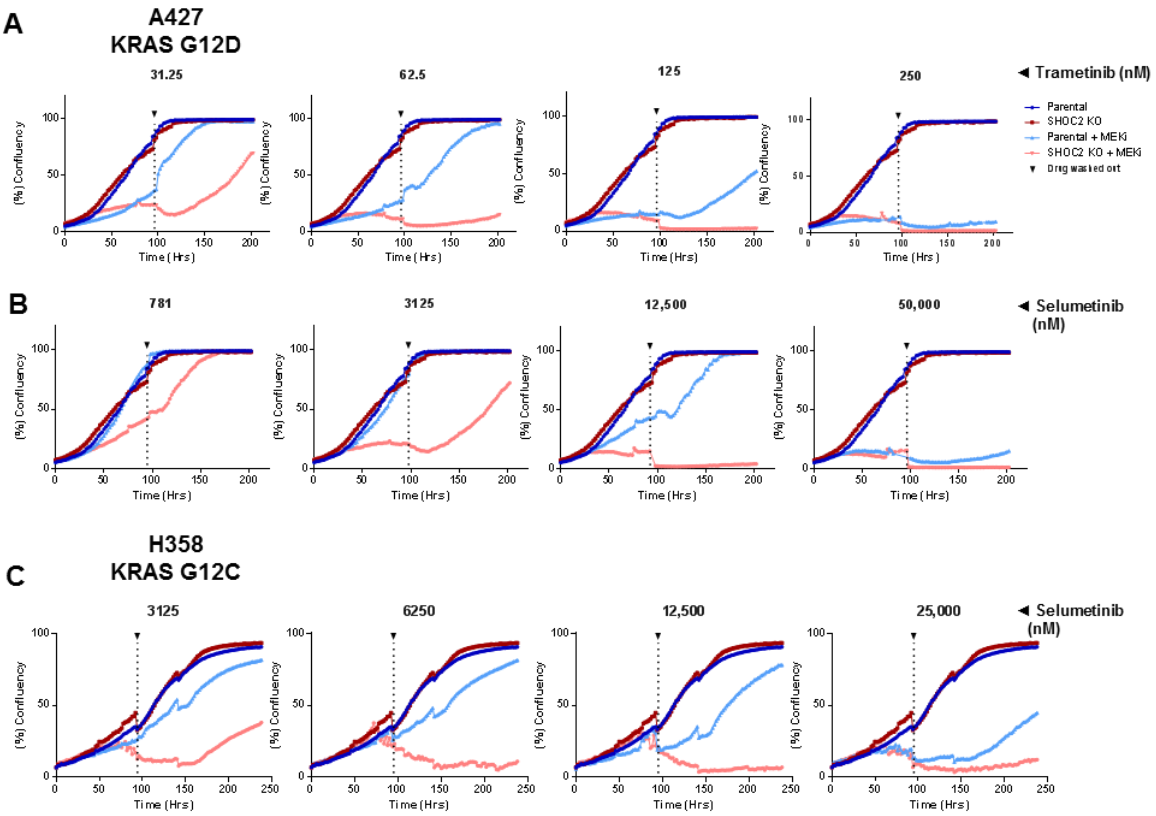

Figure 6.1 SHOC2 deletion lowers the concentration of MEKi required to prevent re-growth of NSCLC cells after inhibitor withdrawal

A Incucyte growth curves of parental or SHOC2 KO A427 (**A-B**) and H358 (**C**) cells grown in the presence of single addition of indicated concentrations of Trametinib or Selumetinib. After 96hrs the inhibitor was washed-out and cell growth measured for an additional 5-days by incucyte imaging. Representative of n=3.

Extending this observation we performed PI/ Annexin V staining of our cells in the presence of a dose response of the MEKi's, Selumetinib or Trametinib. In agreement with the incucyte observation we see SHOC2 deletion substantially lowers the concentration of MEKi required to induce apoptosis in these cells (Figure 6.2). Conversely apoptosis is only seen in the parental cells at the highest concentrations used, and even at these concentrations does not represent the largest proportion of cells, which remain viable. In agreement with these findings western blot analysis of H358 cells treated with a dose response of the MEKi selumetinib showed an increase in markers of both growth arrest and apoptosis in the SHOC2 KO cells, compared with the parental cells, including P21, C-PARP, BIM (Figure 6.3). We did not observe any induction of Caspase 3,8, or observe any changes in steady state of MCL-1 and Puma in this experiment (Data not shown).

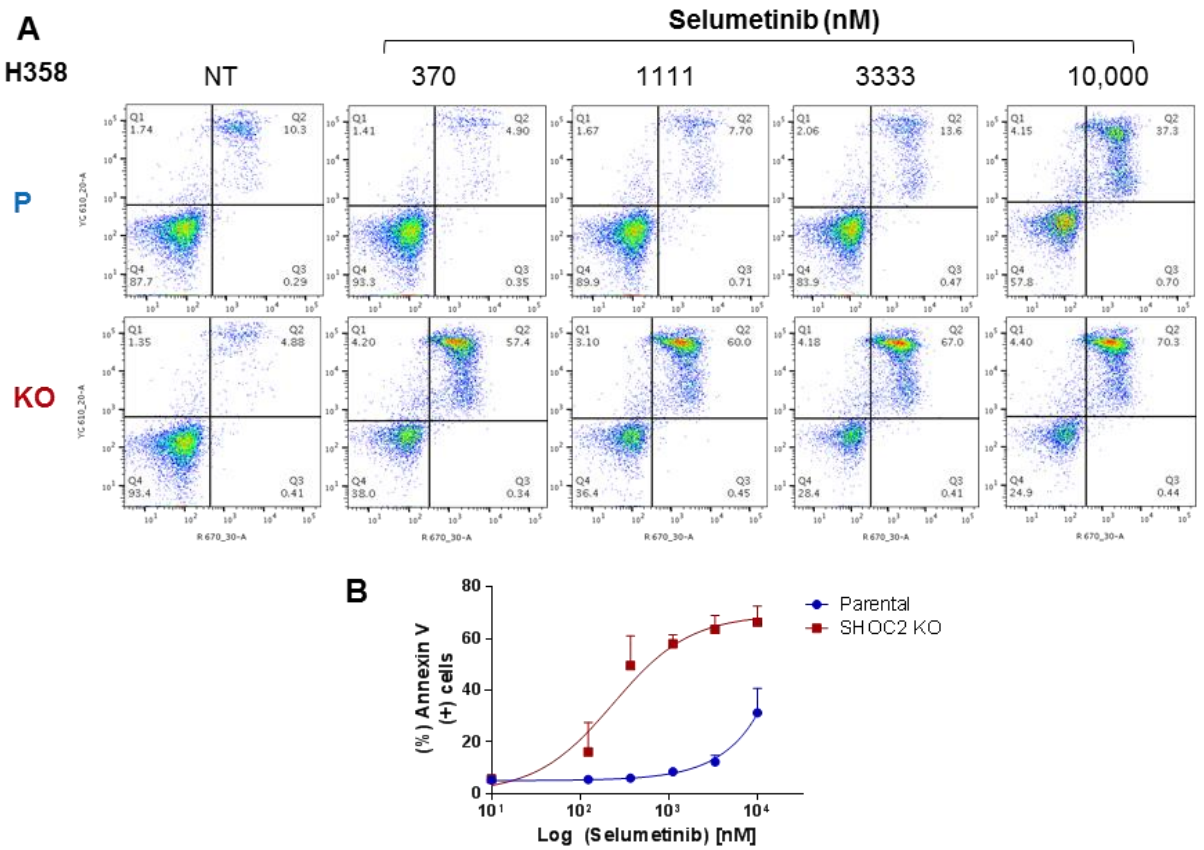
A
H358
Selumetinib (nM)
NT
370
1111
3333
10,000
P
KO
B
(%) Annexin V (+) cells
Log (Selumetinib) [nM]
Parental
SHOC2 KO

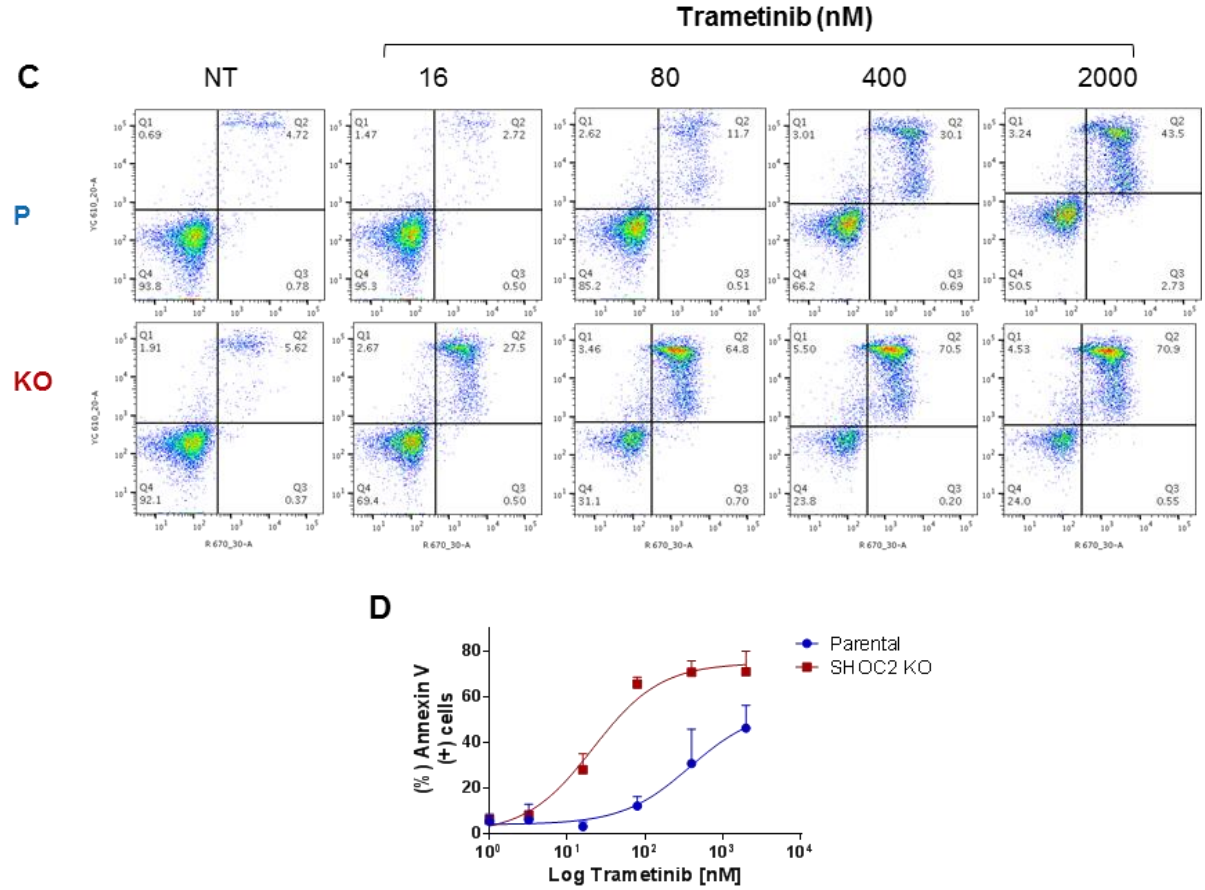
C
Trametinib (nM)
NT
16
80
400
2000
P
KO
D
(%) Annexin V (+) cells
Log Trametinib [nM]
Parental
SHOC2 KO

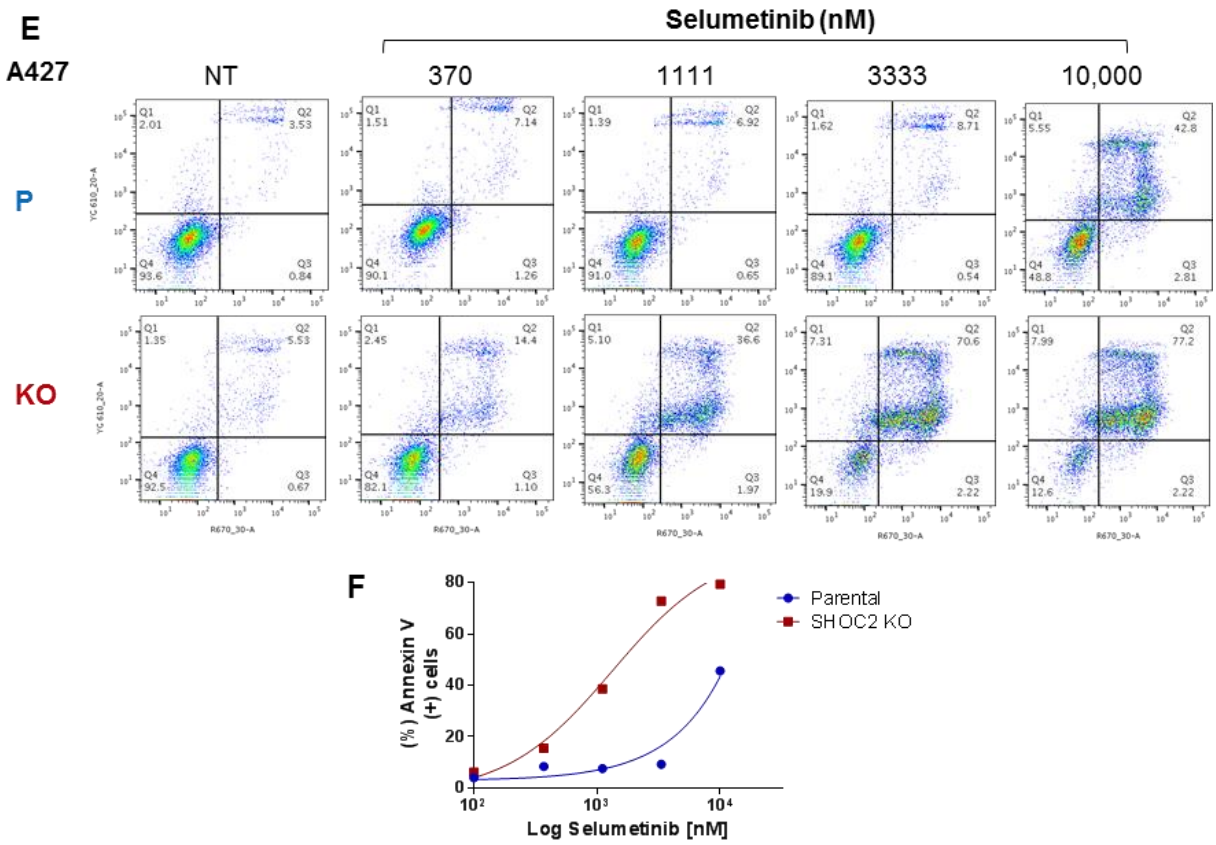
E
A427
Selumetinib (nM)
NT
370
1111
3333
10,000
P
KO
F
(%) Annexin V (+) cells
Log Selumetinib [nM]
Parental
SHOC2 KO

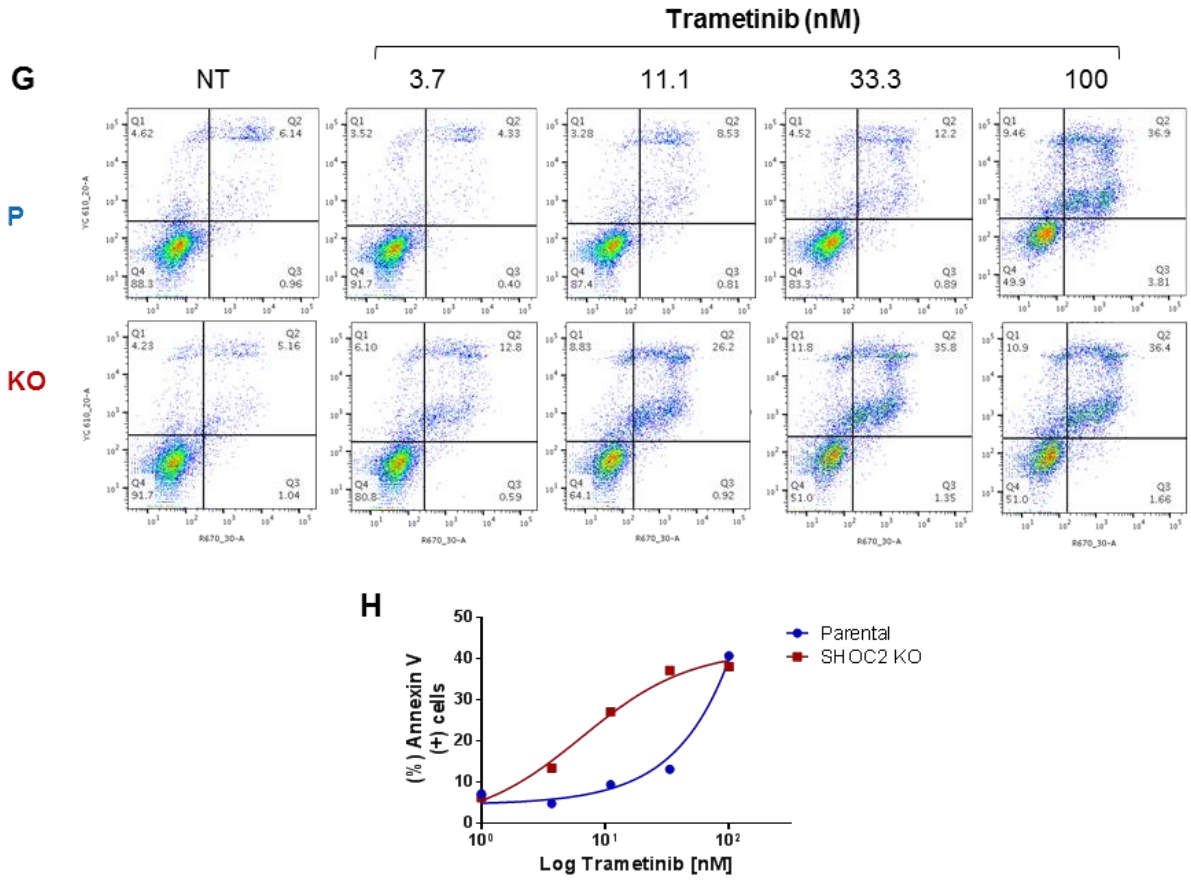
G
Trametinib (nM)
NT
3.7
11.1
33.3
100
P
KO
H
(%) Annexin V (+) cells
Log Trametinib [nM]
Parental
SHOC2 KO

Figure 6.2 SHOC2 lowers the concentration of MEKi required to induce apoptosis in NSCLC cell lines

A Parental or SHOC2 KO H358 cells were treated with the indicated concentrations of Selumetinib for 48hrs and analyzed by FACS after PI and Annexin V staining. Representative profiles from n=3 experiments.
B Quantification of % Annexin V + cells from (A) are plotted for both Parental and SHOC2 KO cells as an average of the n=3 experiments (Mean (+) SD).
C As (A) for the MEKi, Trametinib.
D As (B) for the MEKi, Trametinib.
E Parental or SHOC2 KO A427 cells were treated with the indicated concentrations of Selumetinib for 48hrs and analyzed by FACS after PI and Annexin V staining.
F Quantification of % Annexin V + cells from (E) is plotted for both Parental and SHOC2 KO cells. n=1
G As (E) for the MEKi, Trametinib.
H As (F) for the MEKi, Trametinib.

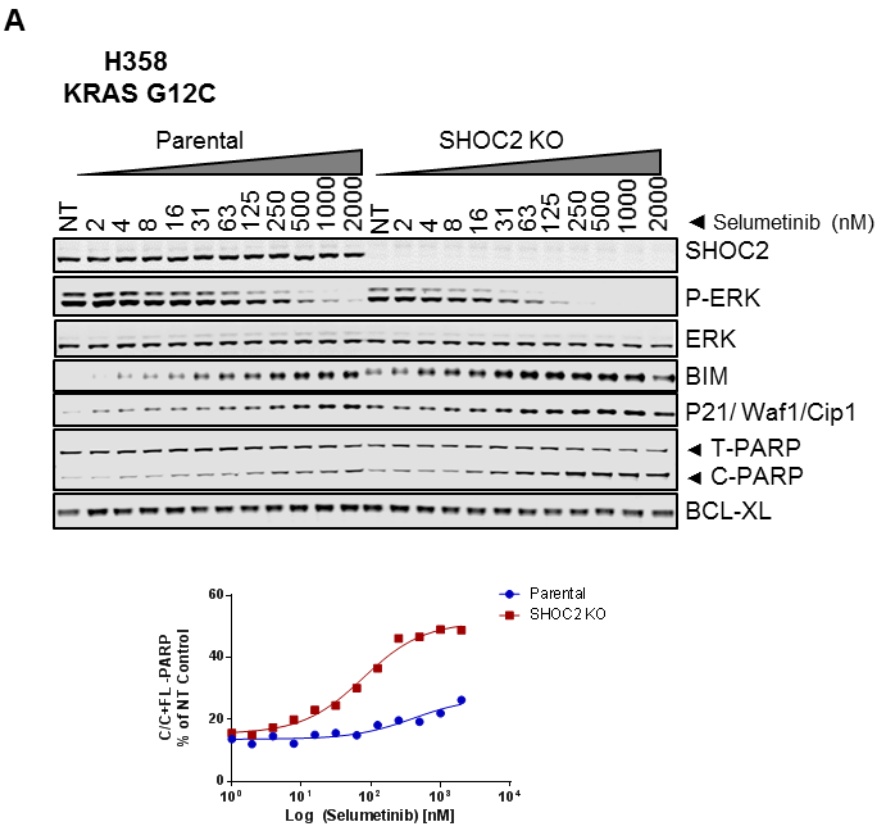

Figure 6.3 SHOC2 deletion lowers the concentration of MEKi required to induce markers of growth arrest and apoptosis in H358 cells

A Immunoblot analysis of lysates of H358 cells treated with Selumetinib for 12hr was performed using the Licor/Odyssey system for quantification of C-PARP/ C+FL-PARP. FL- Full length, C-cleaved.

6.1.3 Genetic suppression of SHOC2 lowers the concentration of MEKi required for BIM-dependent cytotoxicity in RAS mutant NSCLC lines

Given the published role of BIM in MEKi-mediated apoptosis and our observed increase in BIM at the level of western blot of H358 cells treated with coordinate MEK/ SHOC2 inhibition we sought to characterise whether the apoptosis we were observing was BIM-dependent. To do this we knocked down BIM using two independent siRNAs, both as single oligo's and a pool of the two. Using Parental and SHOC2 KO cells we performed dose response viability assays as Figure 5.1. Strikingly BIM either partially or fully rescued the sensitisation to MEKi's upon SHOC2 deletion, in a cell line

dependent manner (Figure 6.4). Additionally in both H358 and A549 KRAS-mutant NSCLC lines BIM KD further decreased the sensitivity of the Parental cell line to MEKi's (Figure 6.4A). These effects expanded to EGFR-mutant cell lines (Data not shown).

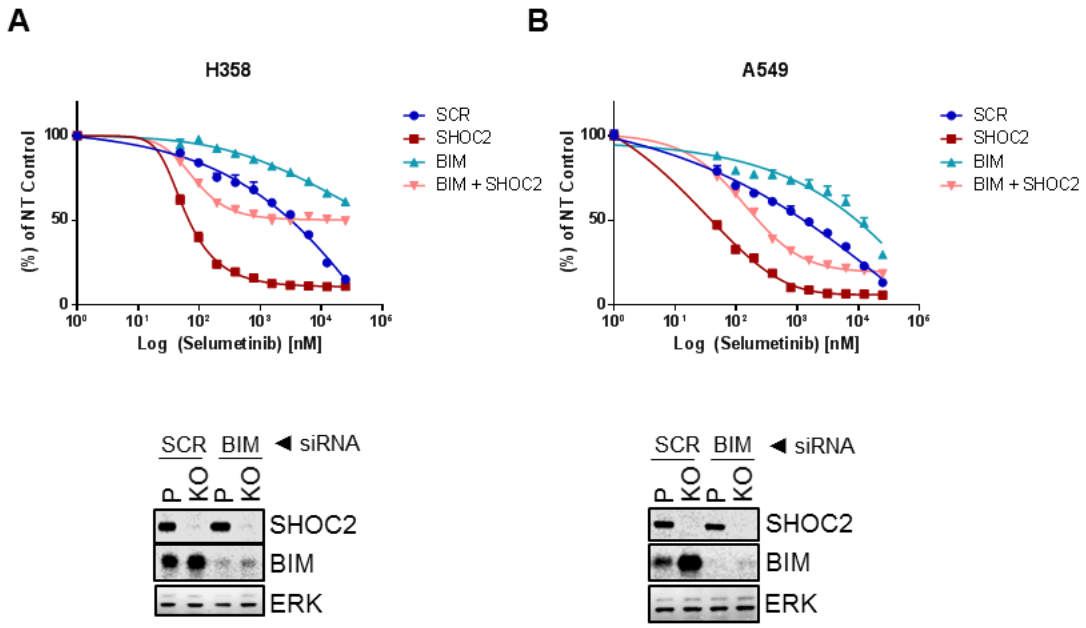

Figure 6.4 BIM suppression diminishes the sensitisation of NSCLC cell lines to combined genetic inhibition of SHOC2 with pharmacological inhibition of MEK

A H358 P and SHOC2 KO cells were transfected with SCR or BIM siRNA oligos. 2-days later cells were seeded for CTG-viability assays. On D3 cells were treated with different doses of the MEKi Selumetinib and a dose-response curve derived for the inhibitor after a 96hr incubation using CellTiter-Glo viability reagent. Lysates were harvested and probed for indicated antibodies to confirm knockdown efficiency using siRNAs. Representative of n=2 experiments and 2-independent siRNA oligo's. Data from a pool of the two is shown.
B As (A) for A549 cells.

To further explore the BIM-dependent nature of MEKi induced apoptosis we generated growth curves of Parental and SHOC2 KO H358 cells growing in the presence of MEKi, - & + Bim siRNA KD (Figure 6.5A). BIM KD provided a complete protection against cell death even at the highest concentration of MEKi tested, even in the context of combined MEK/ SHOC2 inhibition (Figure 6.5B,D), and in all cases after inhibitor removal these cells were able to recover and grow to confluency. This is in absolute contrast to siSCR controls where coordinate MEK/ SHOC2 inhibition causes irreversible cell death on inhibitor wash-out at very low doses of MEKi (6µM) (Figure 6.5D-E). This data places the emphasis of MEKi induced apoptosis on a single BH3

only apoptotic protein and suggests that SHOC2 potentiates the activity of the MEKi to drive a BIM-dependent apoptosis at lower concentrations of MEKi.

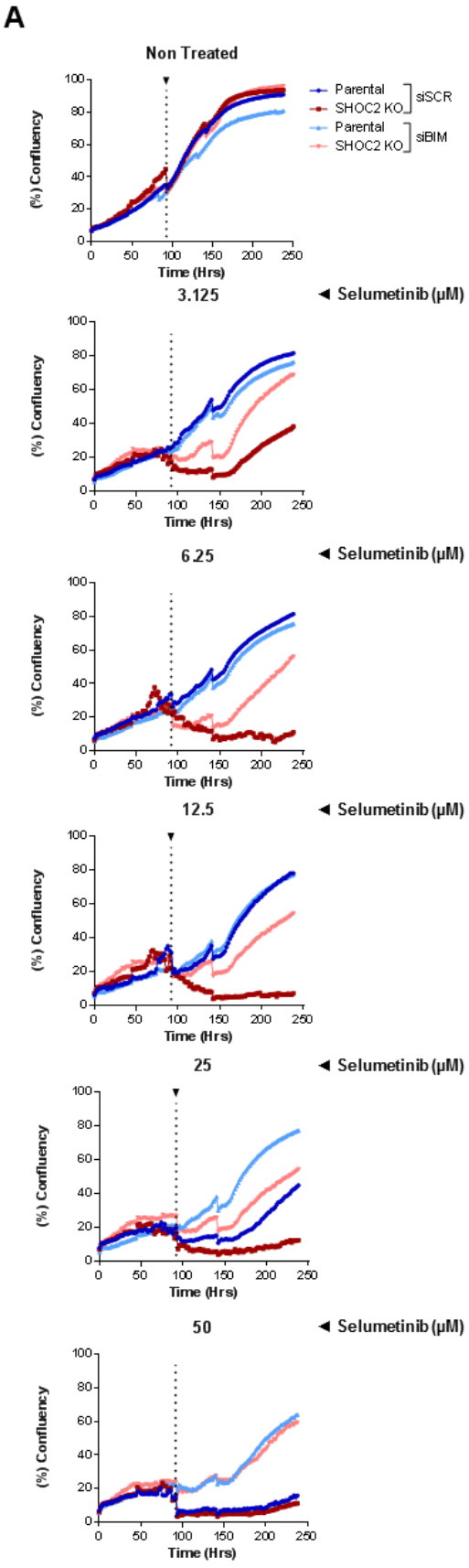
A
Non Treated
(%) Confluency
Time (Hrs)
Parental
SHOC2 KO
siSCR
Parental
SHOC2 KO
siBIM
3.125
Selumetinib (μM)
6.25
Selumetinib (μM)
12.5
Selumetinib (μM)
25
Selumetinib (μM)
50
Selumetinib (μM)

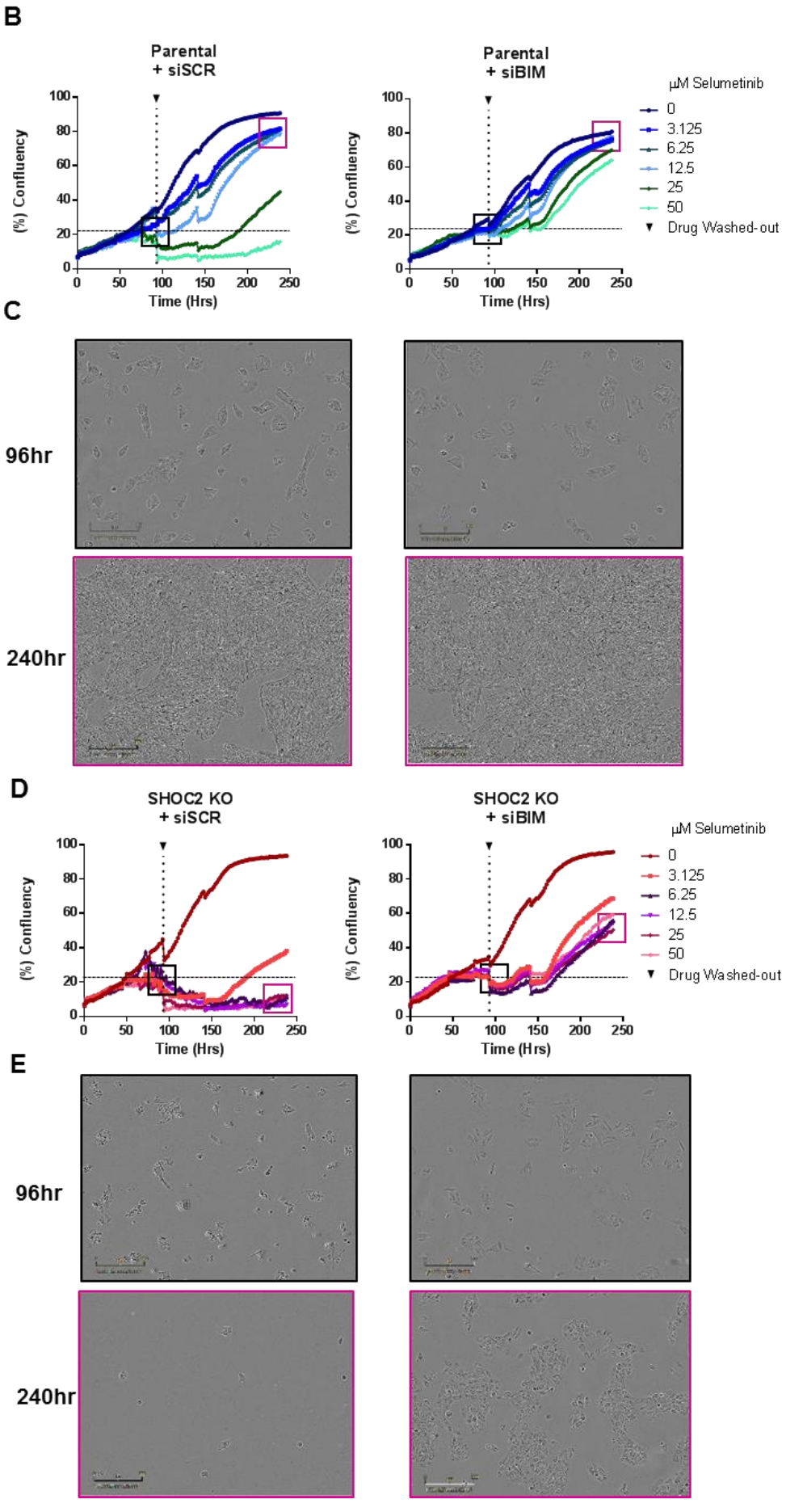
B
Parental
+ siSCR
Parental
+ siBIM
(%) Confluency
Time (Hrs)
µM Selumetinib
0
3.125
6.25
12.5
25
50
Drug Washed-out
C
96hr
240hr
D
SHOC2 KO
+ siSCR
SHOC2 KO
+ siBIM
(%) Confluency
Time (Hrs)
µM Selumetinib
0
3.125
6.25
12.5
25
50
Drug Washed-out
E
96hr
240hr

Figure 6.5 BIM KD prevents MEKi induced cell death of H358 cells even on coordinate MEK/ SHOC2 inhibition

A Incucyte growth curves of parental or SHOC2 KO H358 cells grown in the presence of single addition of indicated concentration of Selumetinib. After 96hrs the inhibitor was washed out and cell growth measured for an additional 7 days by incucyte imaging.
B As (A) plotting parental H358 cells with siRNA SCR or BIM with increasing doses of the MEKi Selumetinib (µM).
C P/C images of parental H358 cells after 96 and 240hrs of 12.5µM Selumetinib treatment. Scale bar is 300µm.
D As (B) for SHOC2 KO H358 cells.
E P/C images of SHOC2 KO H358 cells after 96 and 240hrs of 12.5µM Selumetinib treatment. Scale bar is 300µm.

6.1.4 Combined MEKi treatment and genetic suppression of SHOC2 drives marked tumour regressions in a xenograft model

To see if *in vitro* observations could be extended *in vivo* we performed xenograft assays using A427 cells, a cell line we previously identified to be SHOC2 insensitive for 3D growth assays and subcutaneous xenografts assays (Figure 6.6). Treatment with a low dose of the MEKi Trametinib had a partial effect on the growth rate of the control cell line shSCR, but in stark contrast, the same low dose of MEKi caused marked tumour regressions in shSHOC2 cells, in some cases full regressions that in all cases persisted beyond the treatment window (Figure 6.6B-C). In contrast the shSCR cell line quickly rebounded and reached the maximum tolerated tumour volume after treatment was removed (Figure 46.6C). The emphasis of this data lies in the ability to use much less of the MEKi to still drive marked tumour regressions. Indeed the concentration of MEKi is at least several fold below the commonly used standards for various Trametinib combinations in the field – 1-3mg/kg (Castellano et al. 2013; Sun et al. 2014; Manchado et al. 2016).

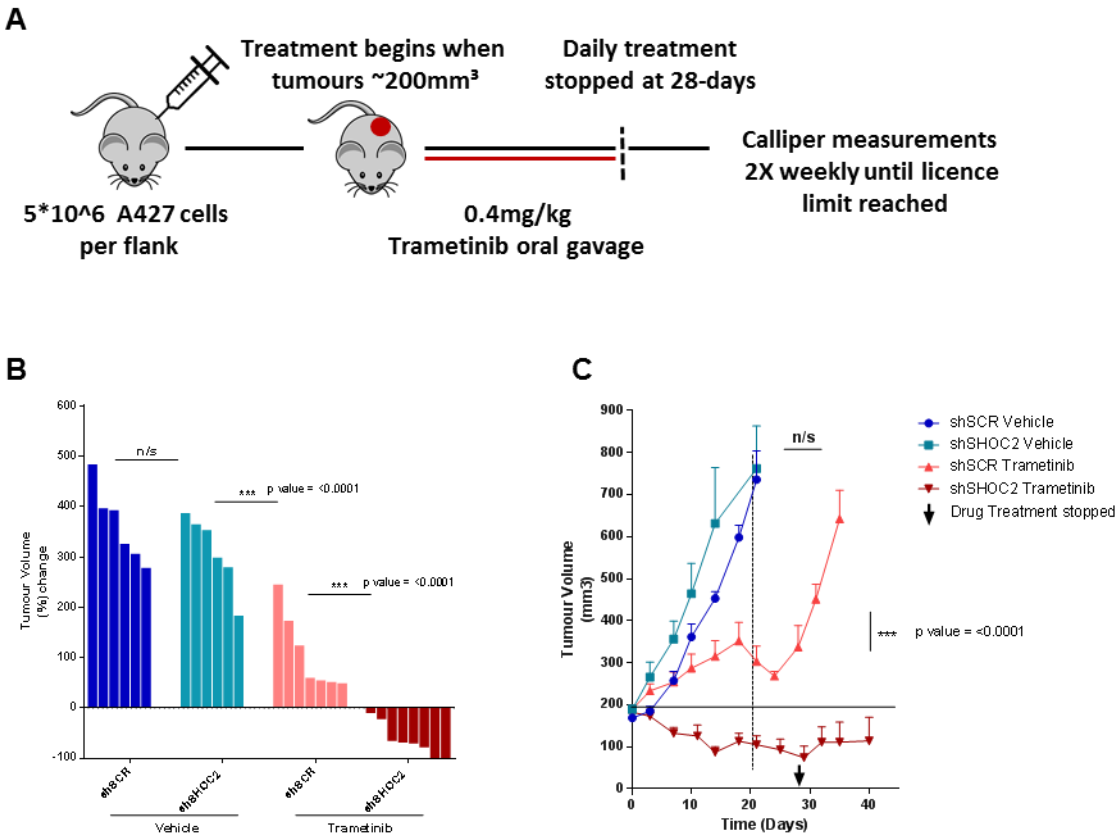

Figure 6.6 Genetic suppression of SHOC2 enhances the efficacy of Trametinib in xenograft models

A Schematic of xenograft experiment.

B Genetic suppression of SHOC2 enhances the efficacy of Trametinib in A427 xenograft assays. 2.5*10^6 shSCR or shSHOC2 A427 cells were injected into the flanks of nude mice and tumours allowed to reach 200mm³ before treatment with vehicle or 0.4mg/kg Trametinib. Change in tumour volume after 28-day treatment is presented as a waterfall plot of individual tumours. Significance is determined using a two tailed T-test $*p < 0.05$, $**p < 0.01$ or $***p < 0.001$.

C Change in tumour volume (mean ± SEM). Trametinib treatment was stopped after 28 days and tumour growth measured for additional 12 days. n=6 A427 shSCR/ A427 shSHOC2 vehicle, n=7 A427 shSCR Trametinib and n=8 shSHOC2 Trametinib tumours. Significance as above.

6.1.5 Conclusions

Taken together, these observations show that combined pharmacological inhibition of MEK with genetic suppression of SHOC2 potentiates the cytotoxic properties of MEKi's in a BIM-dependent manner, increasing antitumor efficacy in both lung cancer cell lines *in vitro,* as well as driving marked tumour regressions in an *in vivo* xenograft assay.

Chapter 7

SHOC2 is required for MEKi-induced feedback relief RAF dimerization and ERK-activation

7.1 SHOC2 is required for MEKi-induced feedback relief RAF dimerization and ERK-activation

7.1.1 Introductory statement

Negative feedback loops from ERK serve to maintain ERK-pathway homeostasis. Negative feedback ERK-target sites are found on BRAF, CRAF, SOS and upstream RTKs including EGFR (Corbalan-Garcia et al. 1996; Dougherty et al. 2005; Ritt et al. 2010; Lake et al. 2016). In part, negative feedback loops serve to disrupt RAF dimers and the RAS-RAF interaction. Loss of ERK negative feedback loops on MEKi treatment lead to a RAF dimerization-dependent ERK reactivation, even in the context of BRAF V600E mutant tumours, that otherwise signals as a catalytic monomer (Yao et al. 2015). In part ERK reactivation is responsible for the limited therapeutic activity of small molecule inhibitors and emergence of resistance networks (Samatar and Poulikakos 2014). We wanted to explore the contribution of SHOC2 to this dimerization-dependent pathway reactivation.

7.1.2 SHOC2 deletion impairs rebound MEK phosphorylation by Selumetinib in H358 cells in both a dose and time-dependent manner.

To characterize the molecular mechanisms of sensitization to MEKis by genetic inhibition of SHOC2, we measured ERK-pathway activation using a dose response with the MEKi Selumetinib in H358 cells, after both acute (0.5hrs), and longer treatment periods (12hrs) (Figure 7.1). IC50 values for MEK- and ERK-phosphorylation were unchanged after acute inhibitor treatment (Figure 7.1A-B). Thus, SHOC2 inhibition does not change the activity of Selumetinib to inhibit ERK-activity at early time-points. In contrast, a dose-dependent increase in MEK-phosphorylation was observed after 12hrs, and P-ERK levels were elevated compared with acute inhibitor treatment. Notably this dose-dependent rebound in P-MEK/ ERK levels, due to loss of feedback inhibition from P-ERK at later time points was impaired in SHOC2 KO cells (Figure 7.1C-D) (Lito et al. 2012; Yao et al. 2015).

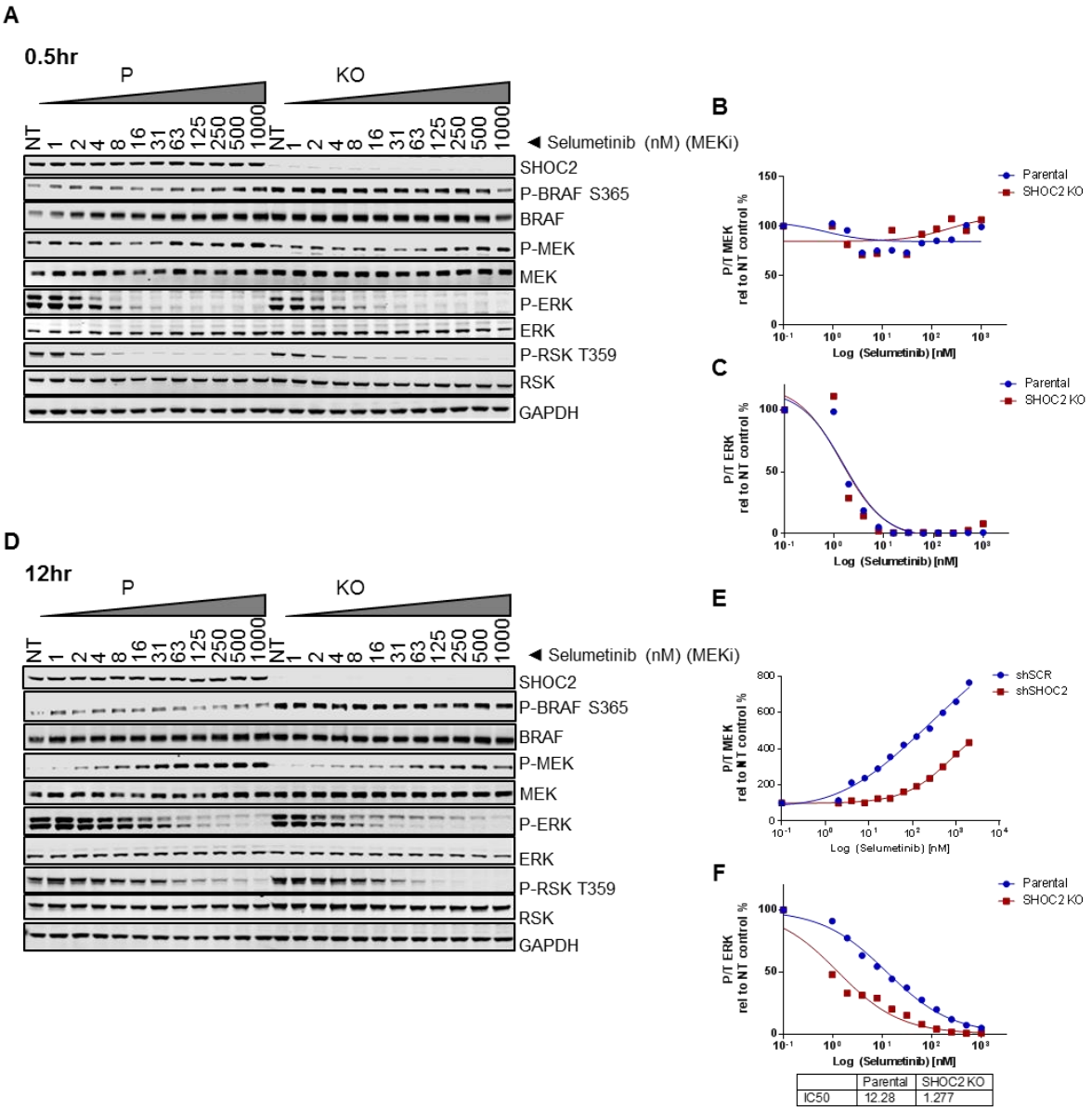

Figure 7.1 SHOC2 deletion impairs rebound MEK phosphorylation by Selumetinib in H358 cells in both a dose and time-dependent manner.

A Cells were treated for 0.5hrs with the indicated doses of Selumetinib.

B Quantification of P-MEK/ T-MEK in (A) relative to P-MEK NonTreated (NT).

C Quantification of P-ERK/ T-ERK in (A) relative to P-ERK NT.

D Cells were treated for 12hrs with the indicated doses of Selumetinib.

E Quantification of P-MEK/ T-MEK in (D) relative to P-MEK NT.

F Quantification of P-ERK/ T-ERK in (D) relative to P-ERK NT.

7.1.3 SHOC2 is required for MEKi-induced feedback relief ERK-activation

To directly observe if SHOC2 contributed to feedback relief MEK/ ERK reactivation after MEKi treatment we treated both KRAS- (A549, H358) and EGFR-mutant (HCC4006) SHOC2 KO cells with the MEKi Selumetinib (Figure 7.2A) and Trametinib (Figure 7.2B) over 72hrs. P-MEK rebounded after 12hr and P-ERK levels increased over the 72hr treatment window. Strikingly in SHOC2 KO cells both feedback relief P-MEK/ ERK were inhibited across the 72h treatment period which allowed the accumulation of the pro-apoptotic protein BIM.

To extend this observation we wanted to explore the effect of loss of feedback relays on ERK reactivation. While the MEKi is present at saturating concentrations ERK will remain inhibited. Therefore we performed wash-out experiments of MEKi pre-treated cells to observe pathway reactivation over time. As with the dose response and time course experiments we observe pre-treatment with MEKi induces P-MEK rebound, and that this is perturbed in SHOC2 KO cells (Figure 7.3A). Trametinib partially serves to mitigate this P-MEK rebound compared to the first generation MEKi selumetinib, in agreement with previously published data (Lito et al. 2014). This is as a result of its dual ability to also reduce RAF-mediated MEK activation upon feedback relief, but this action is not complete. Importantly SHOC2 inhibition is still able to further prevent P-MEK rebound even when using Trametinib (Figure 7.3A).

Once the inhibitor is removed (washed-out) there is a wave of P-ERK reactivation that spikes over steady state signalling levels before returning to this basal state as negative feedback loops are reinstated. We postulate that this wave of P-ERK is a result of the release of rebound P-MEK (activated but unable to phosphorylate ERK while the inhibitor is present at saturating concentrations). Critically SHOC2 inhibition fully prevents this wave of P-ERK reactivation and delays the reactivation of ERK-substrates. The inhibition of P-MEK rebound and elongation of P-ERK suppression are rescued by re-expression of WT SHOC2 but not mutant SHOC2 D175N in agreement for these observations being mediated by the role of SHOC2 as part of the MRAS-SHOC2-PP1 complex (Figure 7.4).

The effects observed are specific to MEKi's and we do not observe a delay in ERK reactivation upon SHOC2 inhibition when treating with the PanRAF inhibitors, LY3009120 and AZD628 (Figure 7.3B). ERKi's show a more differential response, likely due to the mechanism of action attributed to each inhibitor. In each case we observe a SHOC2-dependent rebound in P-MEK. However like PanRAFi's, P-ERK reactivation on Ulixertinib treatment is SHOC2-independent (Figure 7.3C). In contrast,

with SCH772984 we observe a partial SHOC2 contribution to ERK reactivation which is in agreement with a very slight sensitisation of this inhibitor in H358 cells on SHOC2 KD (Figure 5.2A).

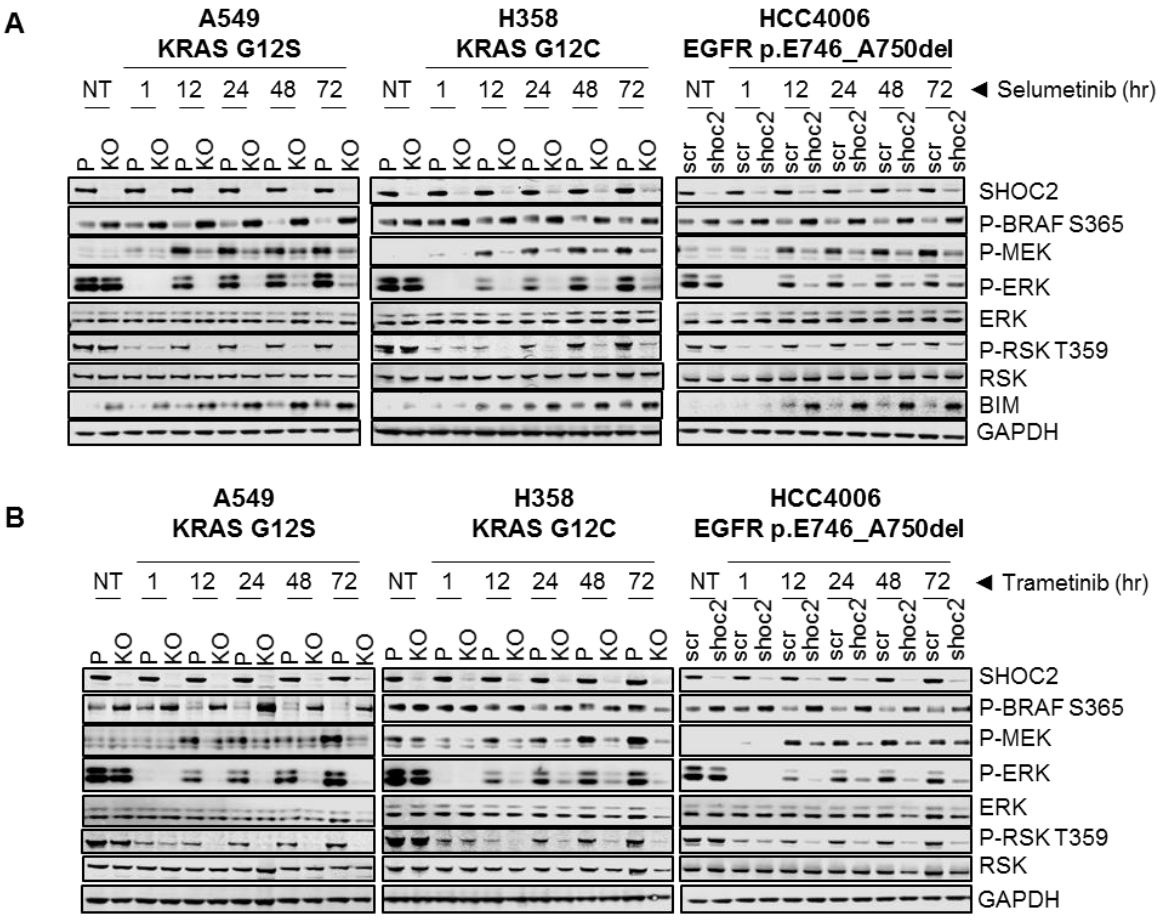

Figure 7.2 SHOC2 is required for feedback relief ERK-reactivation by MEKi's in both KRAS- and EGFR-mutant NSCLC cell lines.

A SHOC2 deletion impairs ERK-reactivation after treatment with Selumetinib. Indicated cells were treated with 1µM Selumetinib and lysates collected at indicated time points.

B Quantification of P-ERK/ T-ERK over time in (A) relative to P-ERK NT.

C SHOC2 deletion impairs ERK-reactivation after treatment with Trametinib. Indicated cells were treated with 100nM Tranetinib and lysates collected at indicated time points.

D Quantification of P-ERK/ T-ERK over time in (C) relative to P-ERK NT.

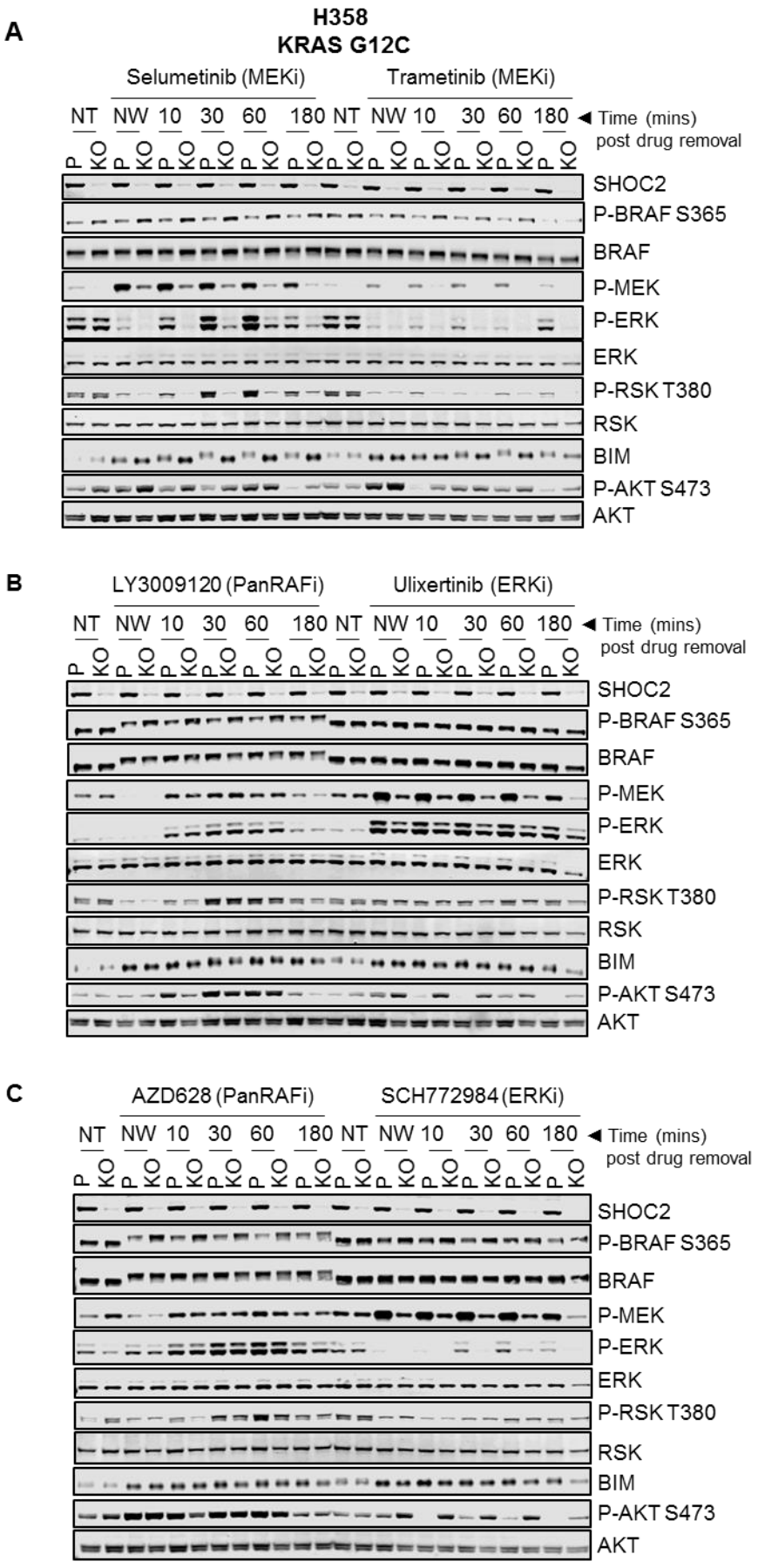
A
H358
KRAS G12C
Selumetinib (MEKi)
Trametinib (MEKi)
NT NW 10 30 60 180 NT NW 10 30 60 180
Time (mins) post drug removal
P KO
SHOC2
P-BRAF S365
BRAF
P-MEK
P-ERK
ERK
P-RSK T380
RSK
BIM
P-AKT S473
AKT
B
LY3009120 (PanRAFi)
Ulixertinib (ERKi)
C
AZD628 (PanRAFi)
SCH772984 (ERKi)

Figure 7.3 SHOC2 deletion impairs ERK-reactivation after treatment with MEK inhibitors, but not PanRAF or ERK inhibitors.

A H358 cells were pre-treated with either 1µM Selumetinib/ 100nM Trametinib/ (**B**) 2.5µM LY3009120/ 2.5µM Ulixertinib (**C**) 2.5µM AZD628/ 2.5µM SCH772984 for 9hrs. Cells were then either lysed (NT and NW), or inhibitor-containing media replaced with fresh media and lysates generated after the indicated time points (NT - Non Treated, NW - Non washed).

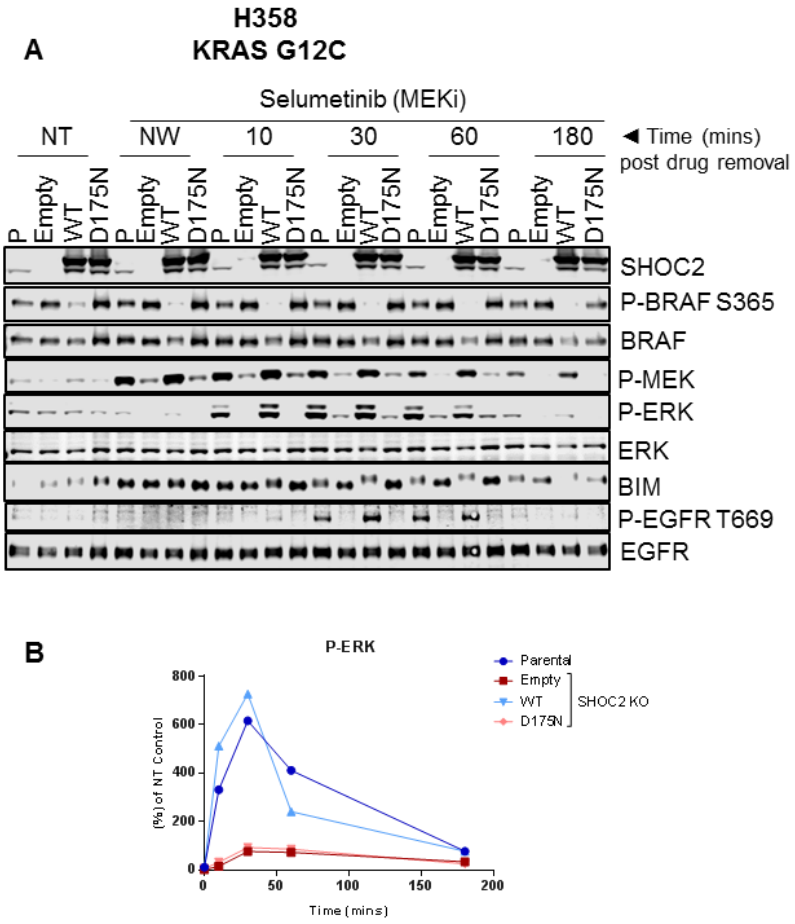

Figure 7.4 The SHOC2 phosphatase complex is required to mediate feedback relief ERK-activation on MEKi treatment

A Impaired MEKi induced signalling rebound and ERK reactivation in SHOC2 KO cells is rescued by re-expression of WT, but not D175N SHOC2. Wash experiments in H358 cells after 9hr treatment with 1µM Selumetinib were performed as in Figure 7.2.
B Licor Quantification of P-ERK (A). P-ERK is plotted as relative to P-ERK levels in NW 'treated' conditions and normalised to total ERK levels.

7.1.4 SHOC2 is preferentially required for MEKi-induced ERK-pathway feedback reactivation in KRAS- and EGFR-mutant, but not wildtype cells

Genetic inhibition of SHOC2 by KD/KO approaches sensitises both RAS- and EGFR-mutant cell lines to MEKi's (Figure 5.3). If we propose this is due to the requirement of SHOC2 for feedback relief ERK-activation in RAS-mutant H358 cells, then these effects should expand to additional RAS- and EGFR-mutant cell lines. We performed wash-out experiments as above in KRAS-mutant A549, A427 and EGFR-mutant, HCC4006, and PC9 cell lines. Significantly we observe SHOC2 inhibition suppresses P-ERK reactivation across multiple KRAS- and EGFR-mutant cell lines, using both Selumetinib and Trametinib (Figure 7.5A-D). Interestingly, despite SHOC2 deletion increasing steady state levels of PS365 BRAF in the wildtype cell lines, H520 and H522, we observe only a partial inhibition of P-MEK rebound and P-ERK reactivation (Figure 7.5E). Thus feedback-mediated pathway reactivation appears preferentially dependent on SHOC2 in KRAS- and EGFR-mutant cell lines when the pathway is inhibited at the level of MEK, but not at the level of RAF or ERK nodes. This is in agreement with viability assays where we see SHOC2 sensitises KRAS- and EGFR-mutant, but not wildtype cell lines to MEK, but not PanRAF or ERKi's (Figure 5.2-3A).

By sustaining P-ERK suppression, coordinate genetic inhibition of SHOC2 and pharmacological inhibition of MEK prevents ERK-mediated phosphorylation and clearance of the apoptotic factors BAD and BIM (Figure 7.2-7.5). We observe this using both Selumetinib and Trametinib. This is in contrast to PanRAF and ERKi's where phosphorylation of BAD, and total BIM levels are SHOC2-independent (Figure 7.3B-C). Taken together we surmise that combined SHOC2 and MEK inhibition leads to a deeper and more durable ERK-pathway inhibition that allows an apoptotic threshold to be reached by preventing the clearance of pro-apoptotic BH3 family member proteins, turning an otherwise reversible cytostatic response (typically attributed to MEKi's), into a BIM-dependent apoptosis.

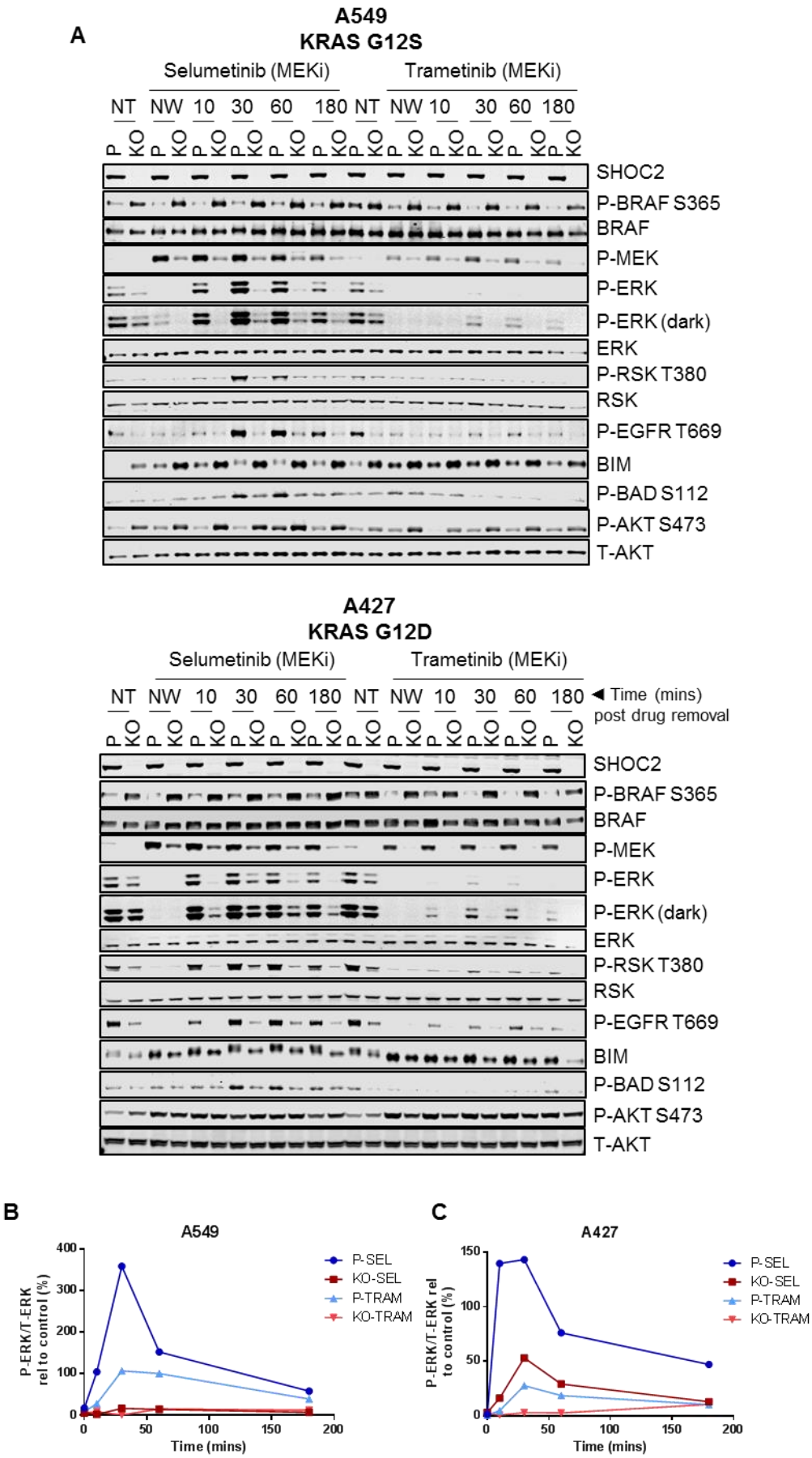
A
A549
KRAS G12S
Selumetinib (MEKi)
Trametinib (MEKi)
NT NW 10 30 60 180 NT NW 10 30 60 180
P KO P KO P KO P KO P KO P KO P KO P KO P KO P KO P KO P KO
SHOC2
P-BRAF S365
BRAF
P-MEK
P-ERK
P-ERK (dark)
ERK
P-RSK T380
RSK
P-EGFR T669
BIM
P-BAD S112
P-AKT S473
T-AKT
A427
KRAS G12D
Selumetinib (MEKi)
Trametinib (MEKi)
NT NW 10 30 60 180 NT NW 10 30 60 180
Time (mins) post drug removal
P KO P KO P KO P KO P KO P KO P KO P KO P KO P KO P KO P KO
SHOC2
P-BRAF S365
BRAF
P-MEK
P-ERK
P-ERK (dark)
ERK
P-RSK T380
RSK
P-EGFR T669
BIM
P-BAD S112
P-AKT S473
T-AKT
B
A549
P-ERK/T-ERK rel to control (%)
Time (mins)
P-SEL
KO-SEL
P-TRAM
KO-TRAM
C
A427
P-ERK/T-ERK rel to control (%)
Time (mins)
P-SEL
KO-SEL
P-TRAM
KO-TRAM

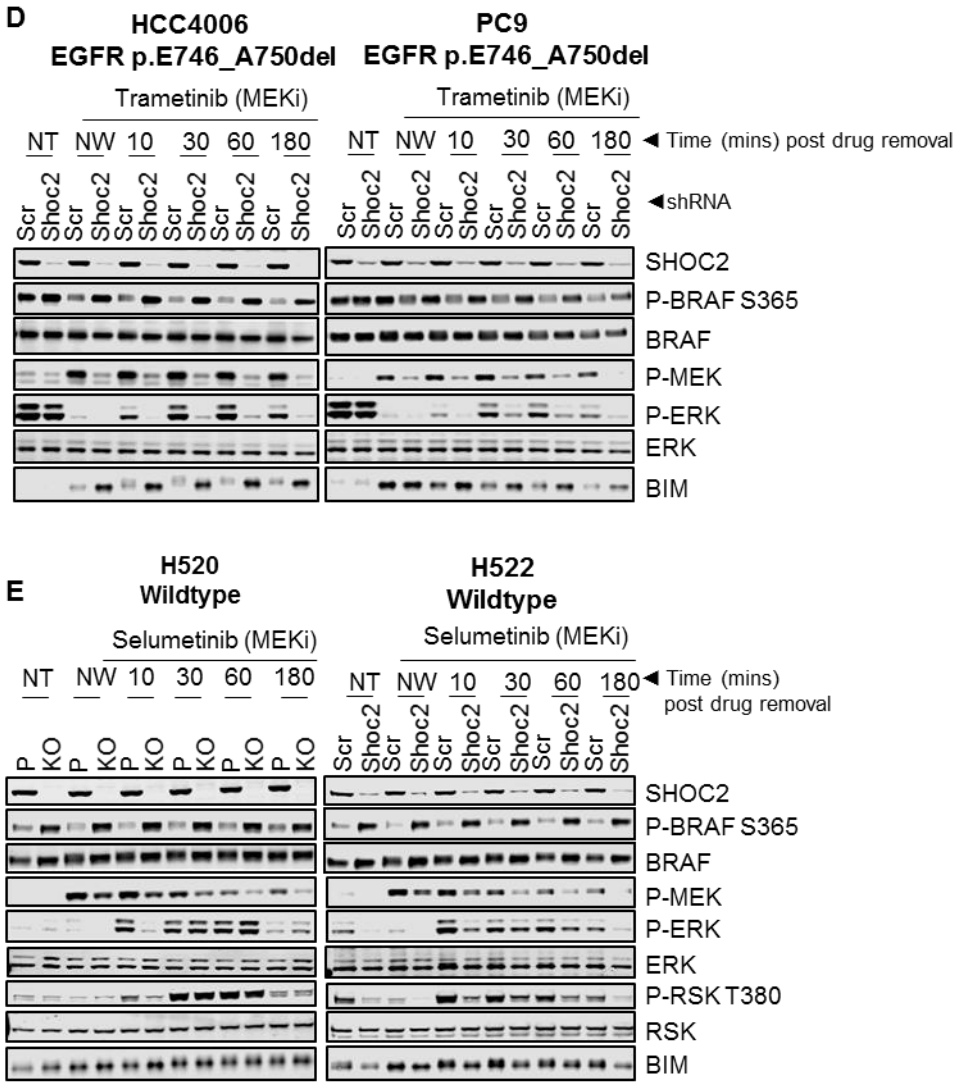

Figure 7.5 SHOC2 is preferentially required for MEKi-induced ERK-pathway feedback reactivation in KRAS- and EGFR-mutant, but not wildtype cells

A RAS-mutant A549 and A427 cells were pre-treated with either 1μM Selumetinib/ 100nM Trametinib. Cells were either lysed (NT and NW) or inhibitor-containing media replaced with fresh media and lysates generated after the indicated time points (NT - Non Treated, NW - Non washed).

B Quantification of P-ERK in A549 cells from (A). P-ERK is plotted as relative to P-ERK levels in NW 'treated' conditions and normalised to total ERK levels.

C Quantification of P-ERK in A427 cells from (A). P-ERK is plotted as relative to P-ERK levels in NW 'treated' conditions and normalised to total ERK levels.

D Wash-out experiments as (A) for EGFR mutant HCC4006, PC9 cell lines.

E Wash-out experiments as (B) for H520 and H522 wildtype cell lines.

7.1.5 SHOC2 is required for MEKi-induced feedback relief RAF dimerization

We next wanted to determine the contribution of SHOC2 and MEK inhibition to RAF dimerization. To this end we performed immunoprecipitation (IP) experiments of endogenous ARAF, BRAF and CRAF. As published MEKi treatment led to a striking induction of BRAF-CRAF dimers in KRAS mutant cells (Lamba et al. 2014), in parallel with this we observed an increase in BRAF-ARAF dimers. SHOC2 inhibition in H358 cells lowered basal BRAF-CRAF, and BRAF-ARAF dimers, but more strikingly SHOC2 inhibition almost fully abrogated the induction of both B-C and B-A dimers on MEKi treatment, using both Selumetinib, (Figure 7.6A) and Trametinib (Figure 7.8A). Dimerization of B-C and B-A occurs simultaneously with the wave of P-ERK rebound, (Figure 7.6B) but proceeds the wave of negative feedback phosphorylation by ERK of negative feedback sites, including T669 on EGFR (Figure 7.6C). Treatment with the ERKi, Ulixertinib also induces RAF dimerization, although more modestly than MEKi's, that is dependent on SHOC2. In contrast, however, the potent RAS-independent RAF dimerization induced by the RAFi LY3009120 (Peng et al. 2015; Jin et al. 2017) is not affected by loss of SHOC2, in agreement with LY3009120-induced ERK reactivation being independent of SHOC2 (Figure 7.6D).

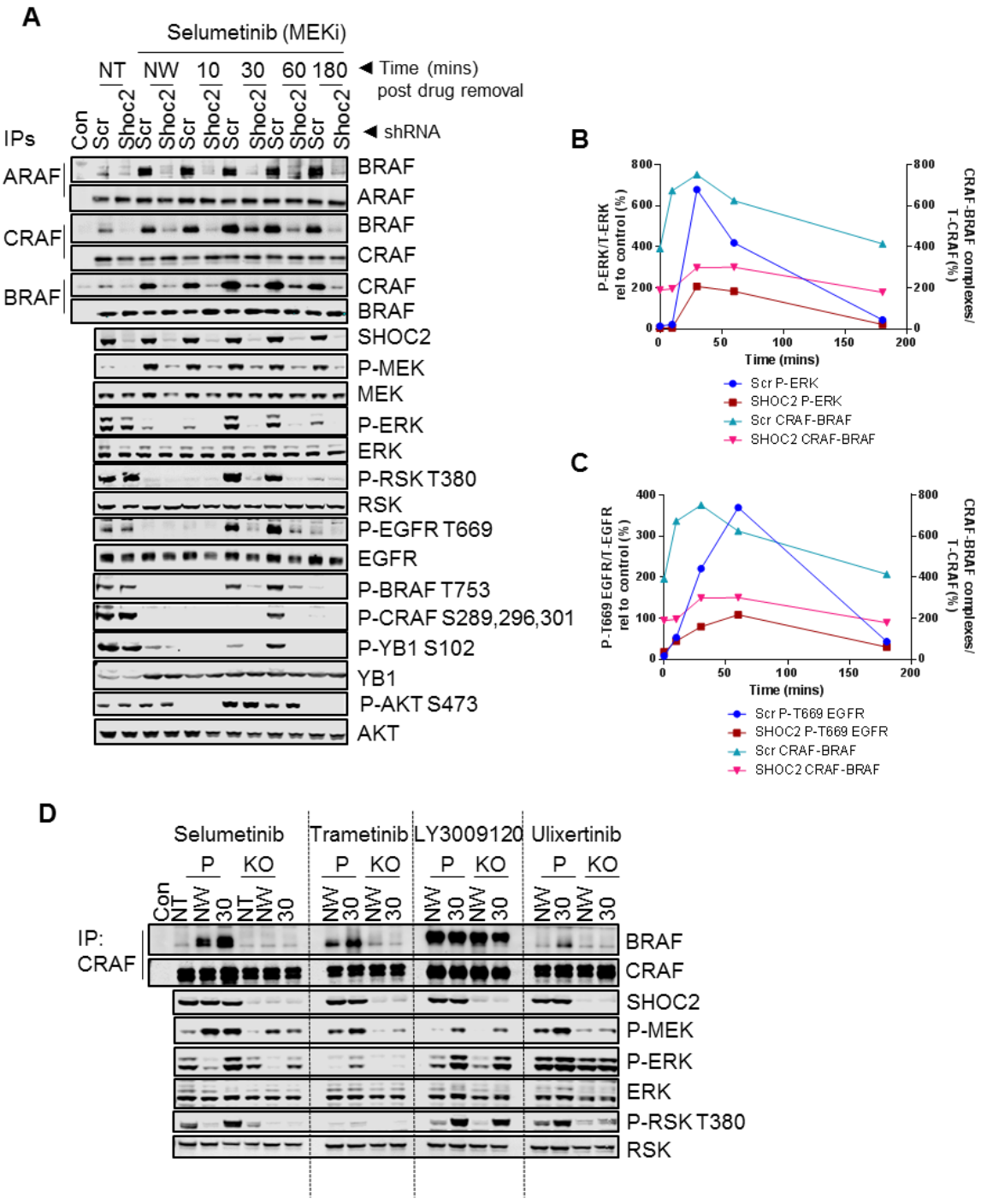

Figure 7.6 SHOC2 is required for MEKi-induced feedback relief RAF dimerization

A SHOC2 supression abrogates MEKi-induced RAF dimerization and impairs ERK-pathway reactivation after MEKi withdrawal. shSCR of shSHOC2 H358 cells were treated with 1µM Selumetinib and lysates used to perform endogenous RAF IPs or for immunoblot analysis using the licor/odyssey system. (NT - Non Treated, NW - Non washed). Con=IgG control IP.

B Quantification of P-ERK levels over time relative to B-CRAF dimers from (A)

C Quantification of P-EGFR T669 levels over time relative to B-CRAF dimers from (A)

D SHOC2 is required for MEKi, but not PanRAFi induced RAF dimerization. Parental and SHOC2 KO H358 cells were treated with 1μM Selumetinib, 100nM Trametinib, 2.5μM LY3009120 and Ulixertinib for 12hrs and inhibitor containing media replaced where indicated with fresh media for 30minutes. Lysates were used to IP endogenous CRAF or for immunoblot analysis. (NT - Non Treated, NW - Non washed). Con=IgG control IP.

7.1.6 Both BRAF and CRAF knockdown, but not ARAF knockdown partially phenocopy SHOC2 suppression

If SHOC2 enhances the effect of MEKi's by inhibiting RAF dimerization-dependent feedback relief ERK reactivation then these effects should be phenocopied by knocking down single RAF isoforms. Single RAF knockdown of BRAF or CRAF, but not ARAF partially perturbed P-MEK rebound on MEKi treatment with Selumetinib (Figure 7.7A-B) and Trametinib (Figure 7.8B). As well as resisting P-MEK rebound, BRAF and CRAF KD partially resisted the rebound wave of P-ERK and ERK-pathway targets, including P-RSK T380 when the inhibitor was washed off. Although both BRAF and CRAF partially phencopy SHOC2 inhibition, neither single isoform KD is as robust at inhibiting P-MEK rebound and reactivation of ERK as SHOC2 inhibition. This likely reflects the role of SHOC2 as a PanRAF dimer modulator. This is further supported by the fact that KD of either BRAF or CRAF, but not ARAF sensitise KRAS mutant NSCLC cells to MEKi's, however this effect is less than the sensitisation observed with SHOC2 KD (Figure 7.7C/7.8C). Collectively this data emphasises the importance of BRAF-CRAF dimers in overcoming MEK inhibition. By preventing dimer formation with SHOC2 inhibition or by knocking down BRAF or CRAF you can perturb this mechanism of resistance and enhance the therapeutic action of MEKi's. Although we place the emphasis on BRAF-CRAF dimer inhibition due to the fact ARAF KD does not sensitise KRAS mutant cells to MEKi's or perturb feedback relief pathway activation we cannot fully exclude a role of ARAF owing to the fact SHOC2 suppression also prevents the formation of ARAF-BRAF dimers (Figure 7.6A).

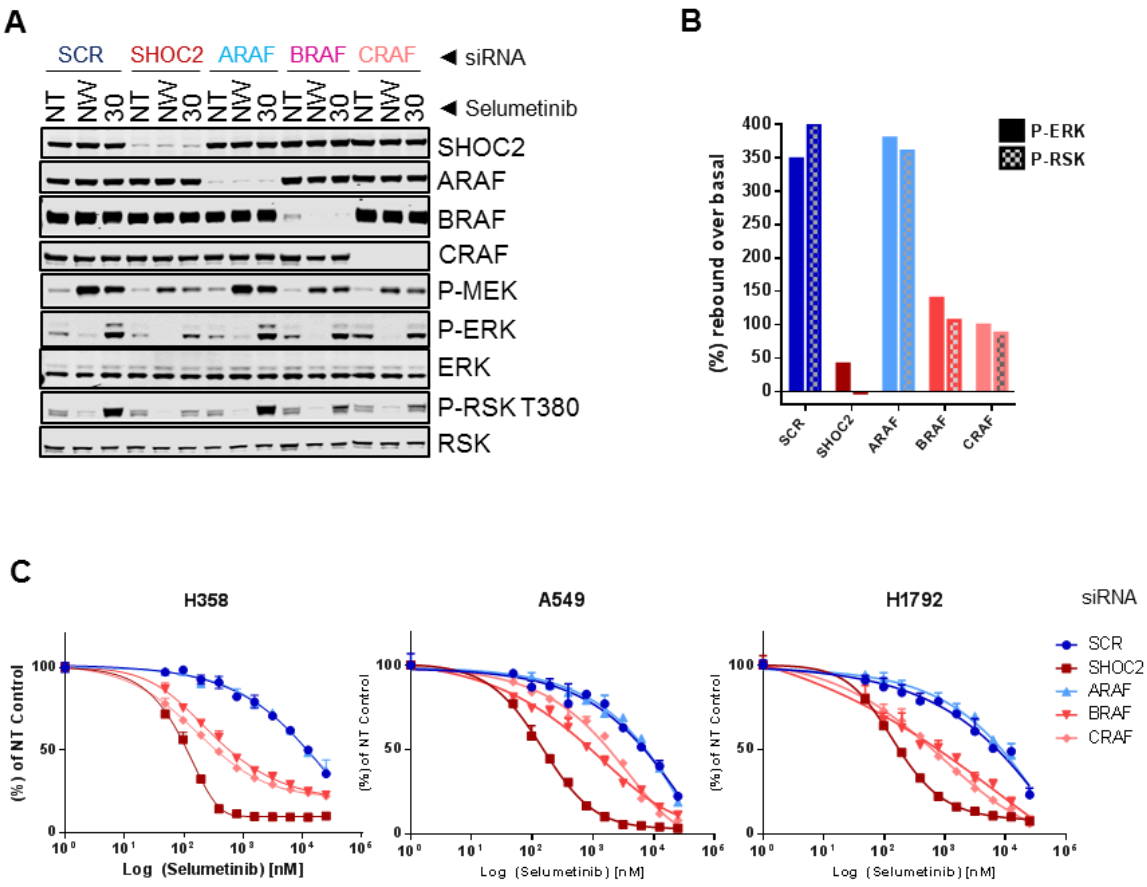

Figure 7.7 Both BRAF and CRAF, but not ARAF knockdown partially phenocopy SHOC2 inhibition

A BRAF and CRAF but not ARAF KD partially perturb MEKi induced signaling rebound and ERK re-activation, although not as strongly as SHOC2 KD. H358 cells transfected with indicated siRNAs were treated 3-days after transfection with 1µM Selumetinib for 9hrs before the inhibitor was washed out and replaced with fresh media for 30mins. (NT - Non Treated, NW - Non washed).

B Licor Quantification of P-ERK and P-T380 RSK in (C).

C BRAF and CRAF, but not ARAF knockdown sensitises NSCLC cells to Selumetinib, although to a lesser degree than SHOC2 KD. H358 cells transfected with siRNAs as in (A) were treated with Selumetinib on D2 post transfection and cell viability determined 4-days later.

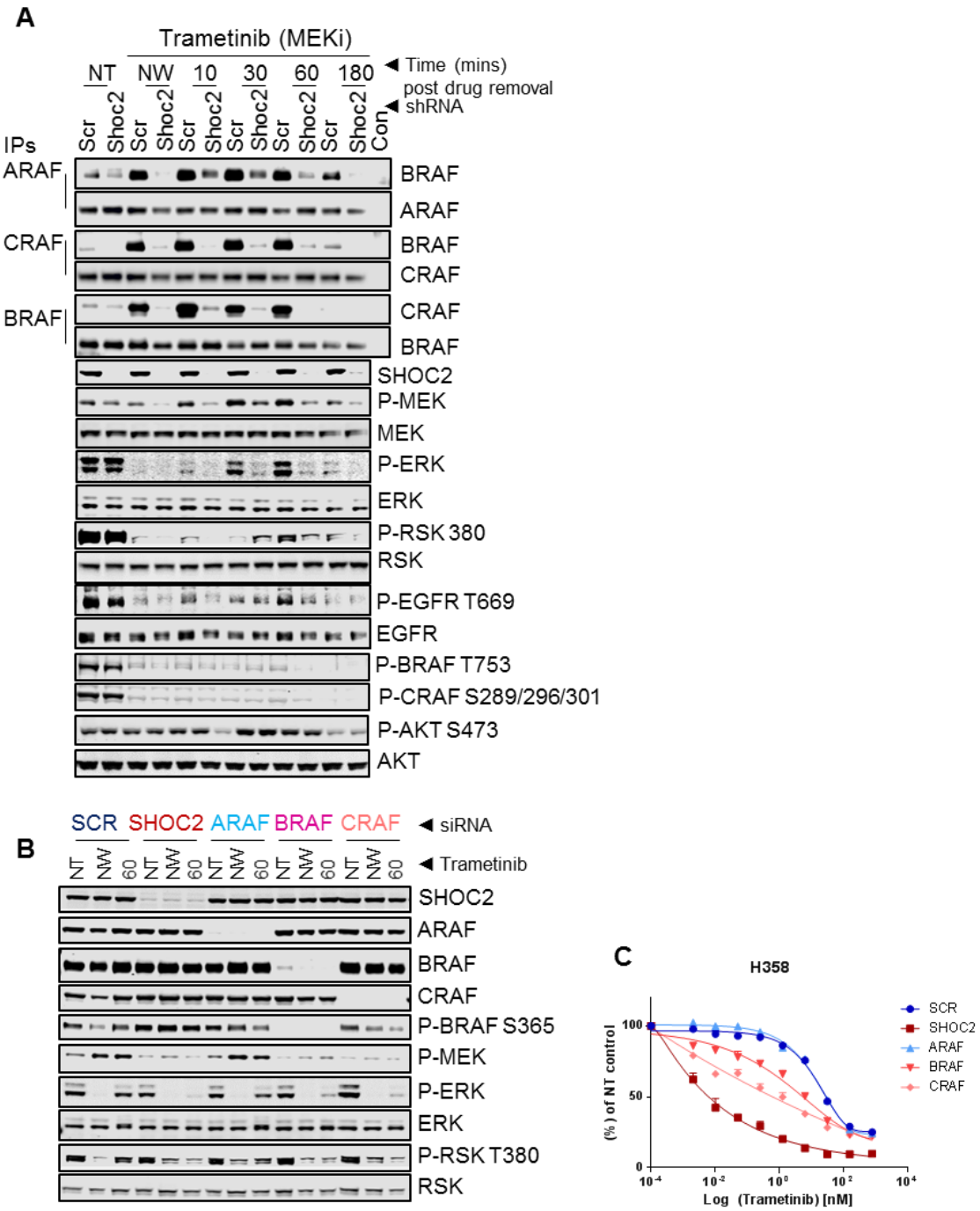

Figure 7.8 SHOC2 is required for Trametinib induced feedback relief RAF dimerization

A SHOC2 suppression abrogates MEKi-induced RAF dimerization and impairs ERK-pathway reactivation after MEKi withdrawal. shSCR of shSHOC2 H358 cells were treated with 100nM Trametinib and lysates used to perform endogenous RAF IPs, or for immunoblot analysis using the licor/odyssey system. (NT - Non Treated, NW - Non washed). Con=IgG control IP.

B BRAF and CRAF, but not ARAF KD partially perturb MEKi induced signaling rebound and ERK re-activation, although not as strongly as SHOC2 KD. H358 cells transfected with indicated siRNAs were treated 3-days later with 100nM Trametinib for 9hrs before the inhibitor was washed out and replaced with fresh media for 30mins. (NT - Non Treated, NW - Non washed).
C BRAF and CRAF but not ARAF KD sensitises NSCLC cells to Trametinib to a lesser degree than SHOC2 KD. H358 cells transfected with siRNAs as in (A) were treated with Trametinib on D2 post transfection and cell viability determined 4-days later.

7.1.7 SHOC2 is required for feedback relief RAF dimerization in KRAS-/ EGFR-mutant and wildtype cell lines

We have shown that SHOC2 is specifically required for feedback relief ERK-activation in KRAS- and EGFR-mutant cell lines but not wildtype cell lines. Mechanistically in RAS-mutant H358 cells we show this is because feedback relief ERK-activation requires SHOC2 phosphatase-dependent B-CRAF dimerization. Next we wanted to see if we observe this SHOC2-dependent BRAF-CRAF dimerization across different cell lines with different driver mutations. Robustly we see SHOC2 is absolutely required for MEKi induced B-CRAF dimerization in a KRAS-mutant (H358), EGFR-mutant (HCC4006) and more intriguingly a cell line wildtype for all known drivers in the ERK-MAPK pathway (H520) (Figure 7.9). There are several intriguing observations with the wildtype cell line: (i) we observe very low levels of P-ERK that remain largely SHOC2-independent upon washing-out the MEKi as shown previously (Figure 7.5E), (ii) with equal protein loading this cell line expresses high levels of CRAF and MEK, despite very low levels of basal P-ERK which infers these are inactive, and (iii), this cell line has a complete absence of EGFR. These observations and viability assay data suggest that rewiring of cellular signalling by oncogenic RAS (or high RAS-GTP levels by RTK signalling) creates a new requirement for combined MEK and SHOC2 inhibition to prevent ERK reactivation on MEKi treatment exploiting ERK-pathway addiction to drive a synthetic lethality of RAS- & EGFR-mutant cells. Intriguingly cell lines wildtype for any known driver mutations of the ERK-MAPK pathway are spared the synthetic lethality and despite the inhibition of MEKi induced RAF dimerization maintain very low P-ERK levels on pathway reactivation possibly reflecting their lack of requirement of the ERK-pathway for viability altogether.

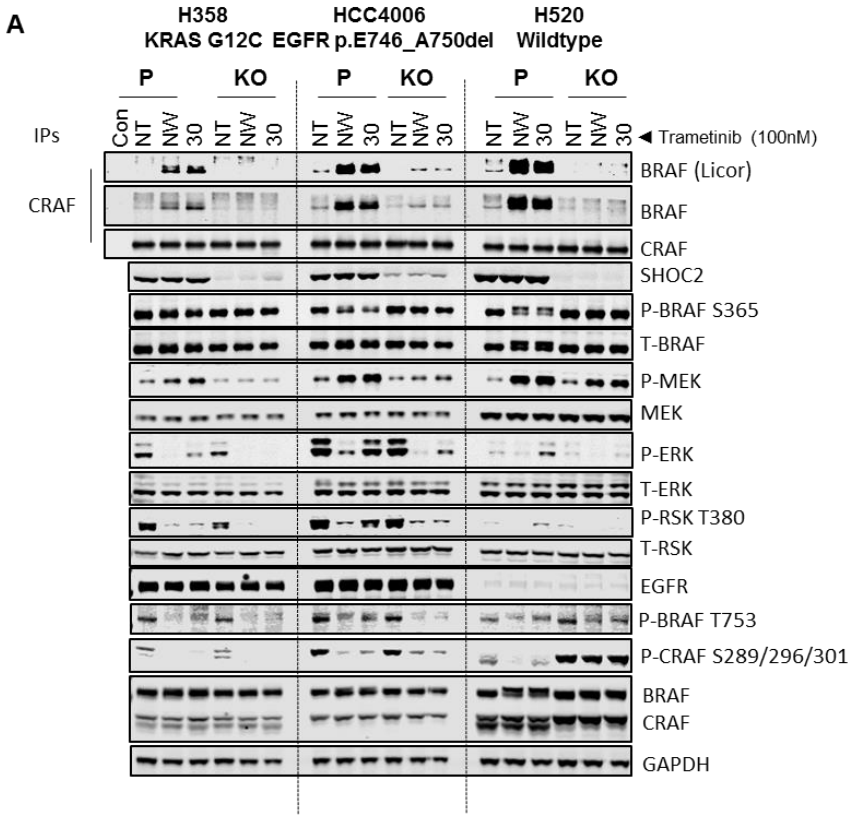

Figure 7.9 SHOC2 is required for feedback relief RAF dimerization in KRAS-/ EGFR-mutant and wildtype cell lines

A SHOC2 deletion abrogates MEKi-induced B-CRAF dimerization, and this correlates with impaired ERK-pathway reactivation after MEKi withdrawal. Parental and SHOC2 KO H358 cells were treated with 100nM Trametinib and lysates used to perform endogenous CRAF IPs or for immunoblot analysis using the lor/odyssey system. (NT - Non Treated, NW - Non washed). Con=IgG control IP.

7.1.8 SHOC2 inhibition leads to further dissociation of CRAF-MEK complexes on Trametinib treatment

Allosteric MEK inhibitors including PD032901 and Selumetinib have been show to drive the formation of RAF-MEK complexes (Lito et al. 2014). It has been suggested that MEK may be less susceptible to inhibition by these allosteric inhibitors while bound to RAF, compared to free MEK. Conversely to other allosteric MEKi's the more potent MEKi Trametinib disrupts RAF-MEK complexes, despite occupying the same binding pocket as PD0325901. As such it has been implied that its increased potency may in part be attributed to disrupting reactivated RAF contacting MEK, maintaining an increased cystolic pool of free MEK which the MEKi inhibitor is able to bind efficiently.

This work is ongoing in the lab at the time of writing but early experiments show, in agreement with published data, that Trametinib does indeed cause the dissociation RAF-MEK complexes (Figure 7.10A), in contrast to other allosteric MEKi's, such as Selumetinib which conversely drive enhanced association of RAF-MEK complexes (Figure 7.10B). Similarly both inhibitors lead to KSR-MEK dissociation (Brennan et al. 2011).

On Trametinib treatment SHOC2 deletion leads to an enhanced disruption of CRAF-MEK complexes, but not ARAF-MEK or BRAF-MEK complexes (Figure 7.10A). Furthermore as the inhibitor is washed-off and feedback relief pathway reactivation proceeds, there is a re-association of CRAF-MEK complexes to steady-state levels. However, intriguingly, coordinate genetic inhibition of SHOC2 and pharmacological inhibition of MEK leads to an sustained suppression of CRAF-MEK complexes. This effect is specific to CRAF-MEK complexes as ARAF-MEK, and BRAF-MEK complexes do not re-associate across the duration of the experiment, and as such their interaction appears SHOC2-independent. SHOC2 inhibition did not reduce the enhanced ARAF-MEK association seen with Selumetinib. Due to CRAF and BRAF levels remaining below detection levels on Selumetinib treatment we can only comment on ARAF-MEK complexes.

This data paves the way for furthering our understanding for the role of SHOC2 in mediating feedback relief ERK-activation. We have robustly demonstrated that coordinate MEK/ SHOC2 inhibition abrogates feedback relief RAF dimerization in the proceeding figures of this chapter, but this data suggests in an inhibitor-dependent manner SHOC2 may also elongate the suppression of CRAF-MEK complexes. In addition to the inhibition of feedback relief RAF dimerization this may in part reflect the enhanced sensitivity of RAS-mutant cells to coordinate Trametinib SHOC2 inhibition

in viability assays if we assume these CRAF-MEK complexes to be active (Figure 5.3B). Indeed CRAF-MEK re-association after Trametinib wash-out does proceed P-ERK reactivation in keeping with this model.

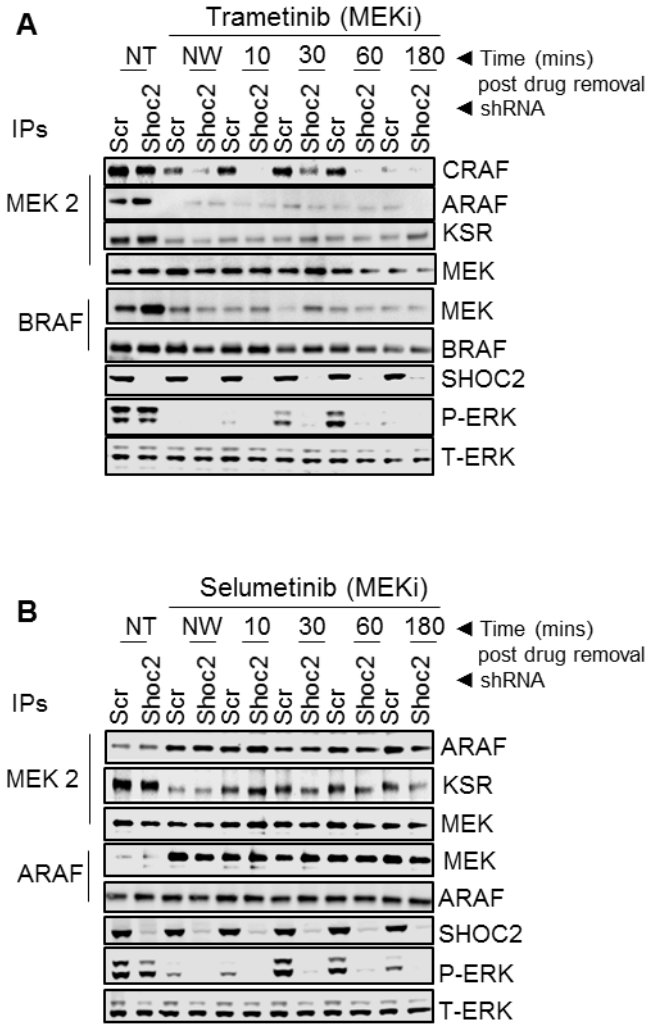

Figure 7.10 Combined genetic inhibition of SHOC2 and pharmacological inhibition of MEK leads to sustained dissociation of CRAF-MEK complexes

A H358 shSCR or shSHOC2 cells were pre-treated with either 100nM Trametinib for 9hrs. Cells were either NT and NW, or inhibitor-containing media replaced with fresh media and lysates generated after the indicated time points (NT - Non Treated, NW - Non washed). Cells were subject to endogenous MEK/RAF Ips or for immunoblot analysis using the licor/odyssey system. (NT - Non Treated, NW - Non washed).

B As (A) but H358 cells were treated with 1µM Selumetinib.

7.1.9 Conclusions

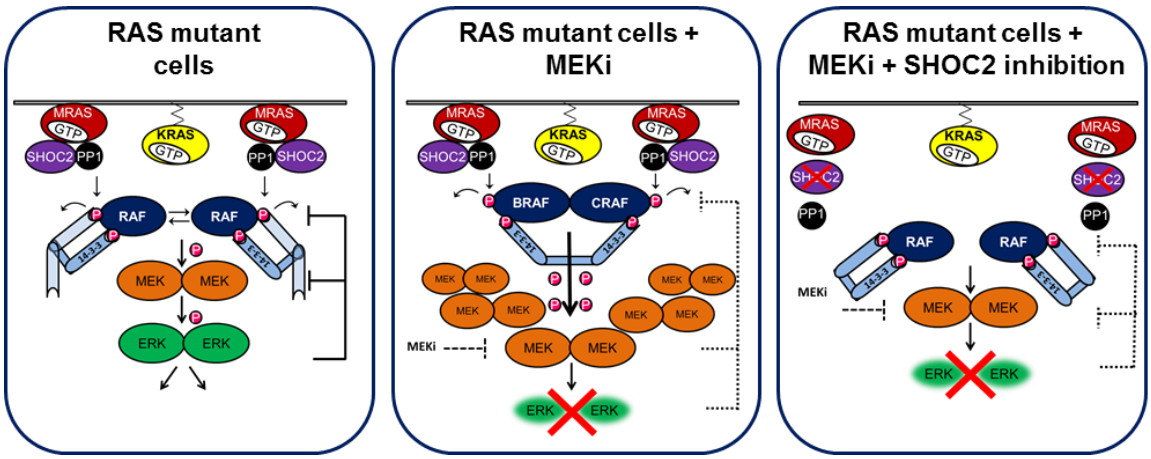

Figure 7.11 Model

ERK-activity in KRAS-mutant cells is maintained at a steady state by negative feedbacks at multiple levels, including RTK and RAF-pathway nodes. MEKi treatment leads to feedback relief RAF dimerization and P-MEK rebound that is dependent on both RAS-GTP and 'S259' RAF dephosphorylation by the SHOC2-phosphatase complex. On inhibitor withdrawal, release of this 'primed' P-MEK (phosphorylated but unable to activate ERK when inhibitor-bound) generates a wave of ERK phosphorylation (and subsequent waves of pathway substrates) that is dampened by negative feedbacks until a new steady state is reached. In the absence of SHOC2, even in the presence of active RAS, feedback relief RAF dimerization is abolished and P-MEK rebound suppressed to cause a more potent and durable ERK inhibition after inhibitor withdrawal.

Chapter 8

SHOC2 ablation inhibits LUAD development in RAS-driven mouse models

8.1 SHOC2 ablation inhibits LUAD development in RAS-driven mouse models

8.1.1 Introductory statement

SHOC2 ablation has been shown previously to be embryonic lethal in Genetically Engineered Mouse Models (GEMMs) (Yi et al. 2010). To this end we generated 2 mouse models: both a SHOC2 knockout (KO), and a knockin model (KI); the latter to specifically disrupt the formation of the MRAS-SHOC2-PP1 complex. We have shown *in vitro* that SHOC2 deletion prevents the growth of NSCLC cells in anchorage-independent growth assays in a cell line-dependent manner. Furthermore we have shown that broadly genetic inhibition of SHOC2 enhances the effect of MEKi's in both KRAS- and EGFR-mutant cells. We sought to cross our compound mice to CreER^{T2} and Kras.p53 mice to enable us to disentangle the effects of SHOC2 ablation on general homeostasis in adult mice, and more specifically in models of murine LUAD, to determine its value as a therapeutic target.

8.1.2 Systemic SHOC2 deletion in adult mice is well tolerated

The SHOC2 KO model was generated by flanking exon 4 of SHOC2 with loxP sites. For the generation of the SHOC2^{D175N} KI model we employed a 'minigene' strategy, where the wild-type SHOC2 allele is expressed in a cDNA configuration with a Flag-tag at the N-terminus under the control of the endogenous promoter. The wild type SHOC2 cDNA sequence is deleted after Cre-mediated recombination and replaced by the mutant D175N SHOC2 allele containing a Myc-tag (Figure 8.1A). This 'double tag' strategy will enable us to monitor recombination (and subsequent expression of SHOC2^{D175N}) by measuring loss of signal with Flag antibody, and gain-of-signal with a Myc-tag antibody (Figure 8.1B). Crucially this disrupts the formation of the SHOC2-MRAS-PP1 complex but preserves other scaffold functions of SHOC2, such as its known interaction with SCRIB (Young et al. 2013). We crossed our compound mouse strains to R26CreER^{T2} mice. Here the tamoxifen-inducible Cre-loxP system was used to overcome gene targeting that otherwise cause's embryonic lethality. Using the protocol surmised in Figure 8.1C, we observe good recombination across the breath of tissues tested – with the exception of the brain, in agreement with the inability of tamoxifen to efficiently cross the blood brain barrier (Valny et al. 2016). Crucially we observe no overt phenotype in both our KO and KI mouse models up to 8-weeks post tamoxifen treatment. At this point we observe mild to moderate phenotypes that seem to concern an inflammation phenotype, including splenomegaly. The homeostatic role

of SHOC2 is part of another project in the lab and is beyond the scope of this research project.

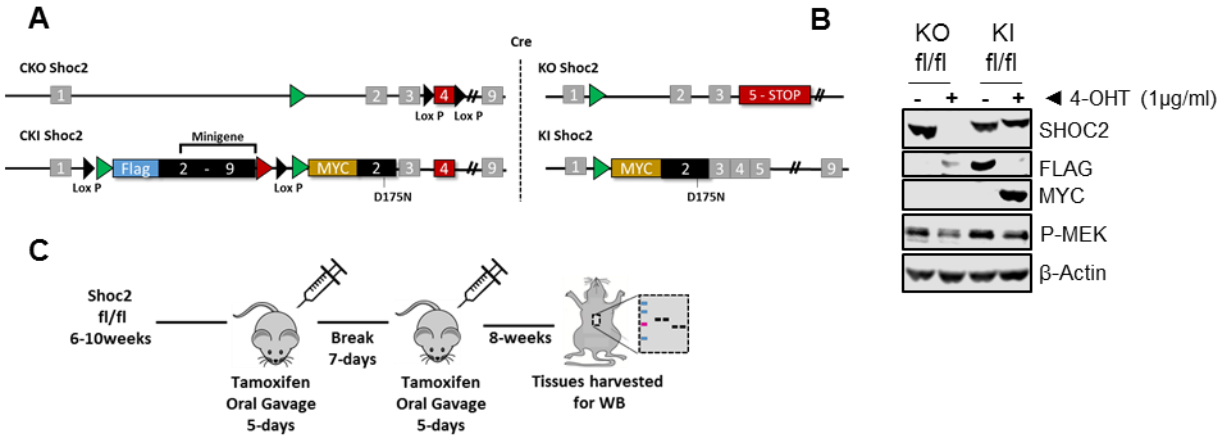

Figure 8.1 Systemic SHOC2 deletion in adult mice is well-tolerated

A Genetic strategy for the generation of Shoc2KO and Shoc2^{D175N} KI mouse models.

B Validation of recombination strategy. E6-immortalised Shoc2$^{fl/fl}$;CreER^{T2} MEFs were treated with 1µg/ml 4-OHT for 7-days and lysates analysed by western blot.

C Protocol schematic for systemic conditional Shoc2 deletion in adult mice.

8.1.3 SHOC2 ablation inhibits LUAD development in both Kras, and the more severe Kras.p53 mouse model

To study the role of SHOC2 within the context of a model that captures the human condition of NSCLC, it is essential to use animal models. The model in question LSL (Lox-Stop-Lox) Kras:p53, has been carefully chosen to faithfully capture the human affliction. Here Kras gain of function mutation and loss of function p53 are used to drive adenocarcinoma development in the mouse lung (Jackson et al. 2001)(Figure 8.2A). P53 is a common secondary mutation to KRAS in NSCLC and occurs in up to 50% of cases, often as a result of tobacco exposure (Toyooka et al. 2003; Gibbons et al. 2014). Expression of a dominant negative form of the tumour suppressor p53 is induced only after Cre-mediated removal of a transcriptional stop element which is floxed upon recombination. This model demonstrates a greater number of metastases and phenocopies a more aggressive pathology (Hingorani et al. 2005). Expression of the Kras^{G12D} mutation is induced only after Cre-mediated removal of a transcriptional termination Stop element and is maintained as a heterozygous mutation, allowing Kras^{G12D} expression to be representative of physiological levels (Jackson et al. 2001).

Cre is delivered to the lungs through intranasal administration of adenovirus expressing AdenoCre. The Kras.p53 model recapitulates many of the features of human KRAS-mutant lung cancer, and histological progression of these tumours progresses from hyperplasia to adenoma and ultimately adenocarcinoma, phenocopying the progression of human lung tumours (Jackson et al. 2001; Johnson et al. 2001). In addition autochthonous murine models in immune competent mice preserve the tumour microenvironment in the lungs which is otherwise absent in immunocompromised murine models of cancer. Given the emerging importance of the immune microenvironment in cancer this is an important consideration for the field for future research efforts and choosing animal models to best copy the human affliction (Schoenhals et al. 2017).

We crossed our SHOC2 KO and KI compound mice to LSL Kras.p53 mice. Here intranasal administration of Adeno Cre induces concomitant induction of gain of function Kras and p53 mutations at the same time as SHOC2 deletion in the mouse lung. This method of administration differs from tissue specific promoter driven Cre recombination in transgenic mice where there is recombination across all cells of the tissue. Instead AdenoCre exposure leads to recombination in only a patchwork of cells across the tissue of which timing and multiplicity can be controlled by viral titer. Using a previously published viral titer (Jackson et al. 2001; Karreth et al. 2011; von Karstedt et al. 2015) we inoculated the lungs of 6-8 week old Shoc2.Kras and Shoc2.Kras.p53 mice. Mice were sacrificed at 24-weeks post tumour induction and tumour burden determined using 2 parameters (i) lung weight and (ii) blind quantification of H&E stained fractions by a pathologist. SHOC2 inactivation, using either KO or KI models, significantly decreased overall tumour burden (Figure 8.2B-E) and significantly prolonged overall survival in both K and KP animals (Figure 8.2F-G). Kaplan-Meier survival curves are still in progress and we are collecting additional points on a rolling basis. Importantly using a published viral titer of AdenoCre our Kras.p53 animals demonstrated similar survival curves to what has been previously reported, with a median survival of Kras.p53 animals at 169 days and Kras animals at 216 days (Figure 8.2H) (Jackson et al. 2001). Strikingly, and in agreement with the role for SHOC2 is RAF activation, the survival extension attributed to Kras.Shoc2 knockout animals is overlapping with that reported for Kras.Craf knockout animals at ~100-days (Karreth et al. 2011). We did not observe a gene dosage effect for either the SHOC2 KO or KI model for the perturbation of SHOC2 ablation on LUAD development, indeed deletion of both copies of SHOC2 is essential for the reduced tumour burden (Figure 8.3A-B). In agreement with this when recombination of the floxed Shoc2 allele was analysed in

tumour nodules from Shoc2$^{fl/fl}$ KP mice, a band for the unrecombined Shoc2^{fl} allele could be detected to various levels in the majority of these tumours (Figure 8.3C) suggesting that at least a significant proportion of Shoc2$^{fl/fl}$ tumours are 'escapers' due to incomplete or no recombination (Ehrenreiter et al. 2009; Blasco et al. 2011; Karreth et al. 2011), further underscoring a key requirement for Shoc2 in lung tumour development.

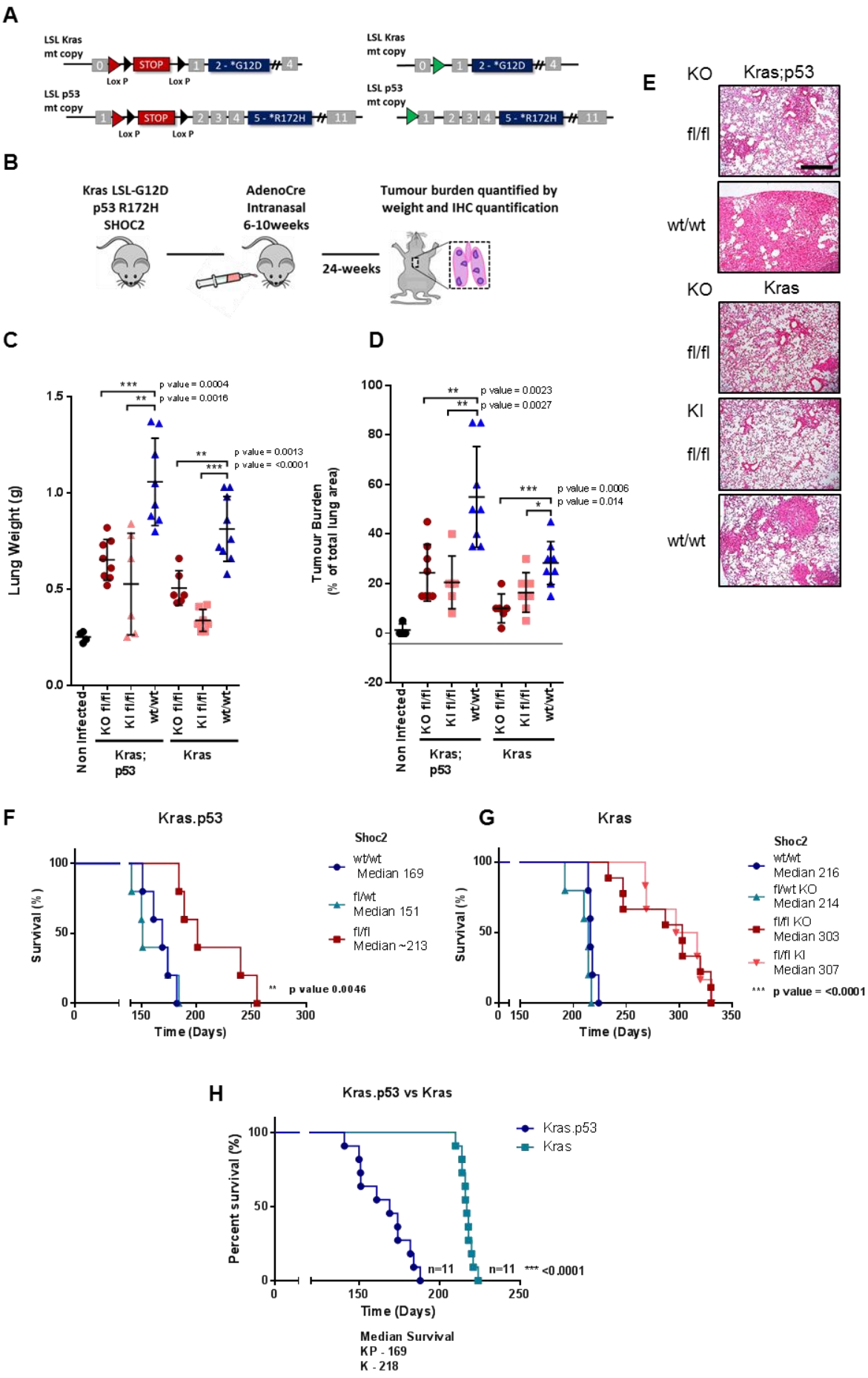
A
LSL Kras mt copy
STOP
Lox P
2 - *G12D
LSL p53 mt copy
5 - *R172H
B
Kras LSL-G12D p53 R172H SHOC2
AdenoCre Intranasal 6-10weeks
24-weeks
Tumour burden quantified by weight and IHC quantification
C
Lung Weight (g)
p value = 0.0004
p value = 0.0016
p value = 0.0013
p value = <0.0001
Non Infected
KO fl/fl
KI fl/fl
wt/wt
Kras; p53
Kras
D
Tumour Burden (% of total lung area)
p value = 0.0023
p value = 0.0027
p value = 0.0006
p value = 0.014
E
KO
Kras;p53
fl/fl
wt/wt
Kras
KI
F
Kras.p53
Shoc2
wt/wt Median 169
fl/wt Median 151
fl/fl Median ~213
p value 0.0046
Survival (%)
Time (Days)
G
Kras
wt/wt Median 216
fl/wt KO Median 214
fl/fl KO Median 303
fl/fl KI Median 307
p value = <0.0001
H
Kras.p53 vs Kras
Kras.p53
Kras
Percent survival (%)
n=11
n=11
<0.0001
Median Survival
KP - 169
K - 218

Figure 8.2 SHOC2 ablation inhibits LUAD development in RAS-driven mouse models

A Genetic strategy for the generation of Kras and Kras.p53 mouse models.

B Schematic for AdenoCre protocol.

C SHOC2 ablation perturbs the growth of $Kras^{G12D}$ and $Kras^{G12D}$;$p53^{R172H}$ mouse LUAD. Lung weight from indicated genotypes 24-weeks post AdenoCre infection. Significance is determined using a two tailed T-test *=<0.05 **=<0.01 ***=<0.001.

D Lung sections were stained with H&E and quantified for tumour burden as a % of total lung area. Significance as above.

E Representative H&E images from (D). Scale bar = 500µm.

F Kaplan-Meier survival curve of mice with indicated genotypes from the Kras;p53 mouse model. Statistics were determined by log-rank test *=<0.05 **=<0.01 ***=<0.001. n=5/6 animals per group – data in progress.

G Kaplan-Meier survival curve of mice with indicated genotypes from the Kras mouse model. Statistics were determined by log-rank test *=<0.05 **=<0.01 ***=<0.001. n=5/6 animals per group – data in progress**.**

H Kaplan-Meier survival curve of Kras;p53 vs Kras mouse model. Statistics were determined by log-rank test *=<0.05 **=<0.01 ***=<0.001. n=>11 animals per group

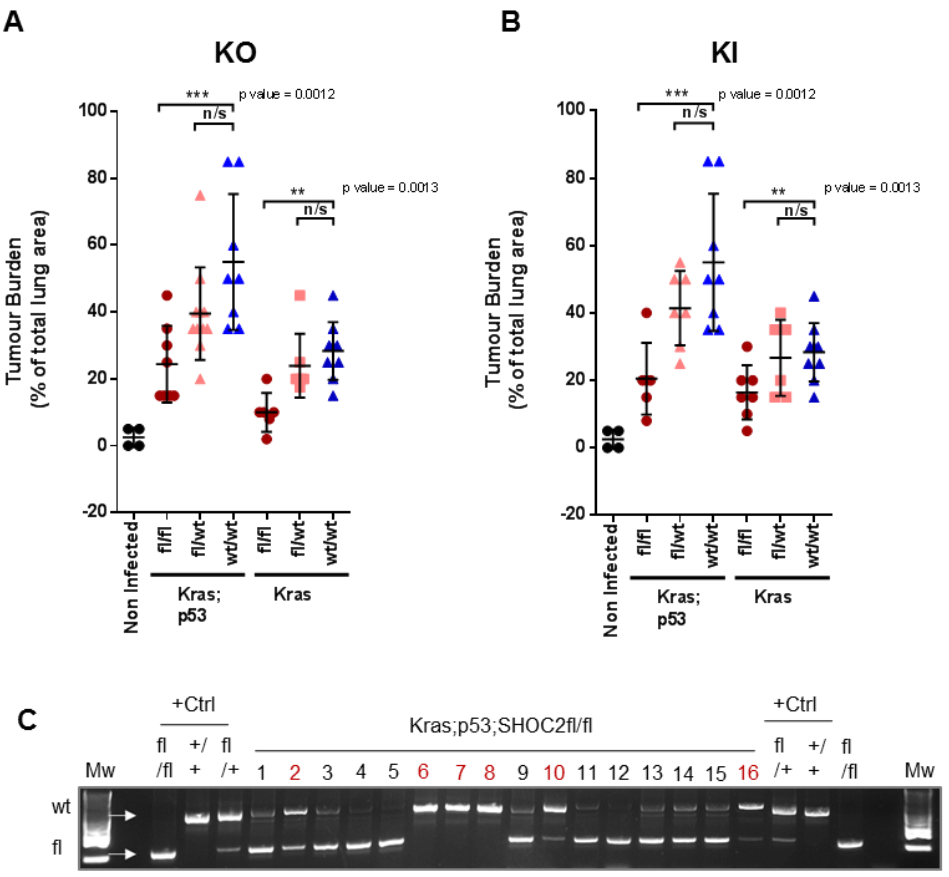

Figure 8.3 Deletion of both copies of SHOC2 is required for inhibition of LUAD development in RAS-driven mouse models

A Kras.p53 KO lung sections from KO fl/fl/ fl/wt/ wt/wt mice were stained with H&E and quantified for tumour burden as a % of total lung area. Significance is determined using a two tailed T-test *=<0.05 **=<0.01 ***=<0.001.

B As above for Kras.p53 KI D175N model.

C Incomplete Shoc2 recombination ('escapers') may account for a significant number of tumour arising in $Shoc2^{fl/fl}$ mice. Cre-mediated recombination was analysed by PCR in the largest nodules isolated from lungs of $Kras^{G12D}$;$p53^{R172H}$;$SHOC2^{fl/fl}$ mice 6-months post-adenocre.

8.1.4 SHOC2 ablation perturbs MEKi induced ERK reactivation & sensitises KRASG12V MEFs to MEKi's

To validate our mouse model we derived MEFs form Shoc2 KO and KI mice crossed to R26-CreER^{T2} mice. We transformed MEFs with a KrasG12V expression construct and treated the resulting transformed MEFs with 4-OHT to guide temporal SHOC2 deletion. We confirmed SHOC2 deletion by western blot and transformation by an increase in KRAS expression and hyperactivation of the ERK-pathway at the level of P-MEK (Figure 8.4A). Transformed cells demonstrated an increased growth rate in adhered culture conditions and loss of contact inhibition, as determined by the ability of cells to compact and grow beyond 100% confluency (Figure 8.4 B-C). Both growth rate and loss of contact inhibition was unaffected by loss of SHOC2. To validate the SHOC2 MEFs we performed EGF time courses, and as previously observed in Chapter 4 we see that SHOC2 inhibition blunted the ERK-MAPK pathway response to EGF-stimulation in both Empty- and KRAS-transformed MEFs (Figure 8.4D). Conversely KRAS-transformed MEFs demonstrated a preferential SHOC2 dependency for feedback relief ERK-pathway activation on MEKi treatment compared to Empty vector controls (Figure 8.4E). Crucially this correlated with viability assays where KRAS transformation specifically sensitised MEFs to combined MEK SHOC2 inhibition, not observed in non-transformed controls (Figure 8.4F).

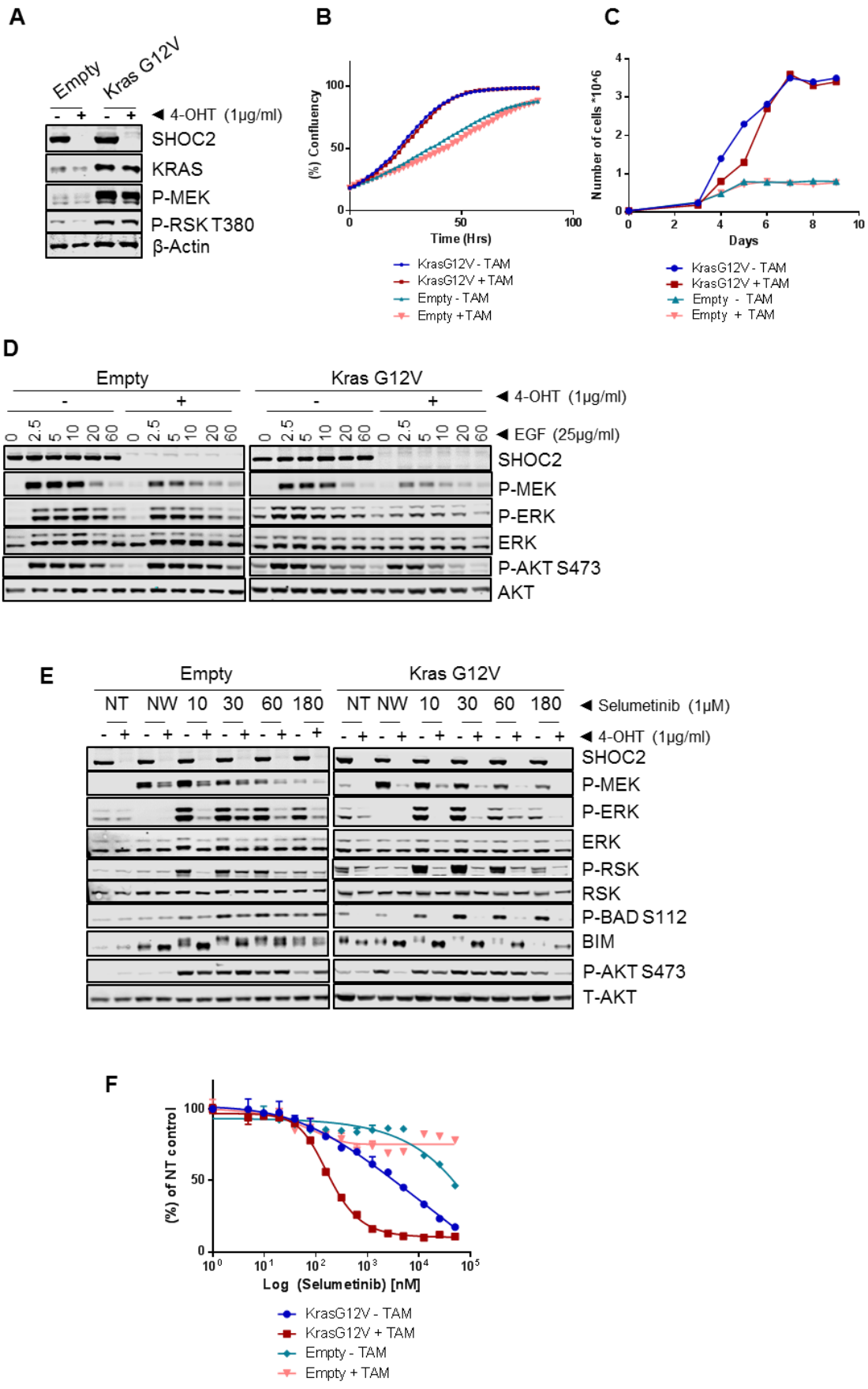
A
Empty
Kras G12V
- + - +
◀ 4-OHT (1µg/ml)
SHOC2
KRAS
P-MEK
P-RSK T380
β-Actin
B
(%) Confluency
Time (Hrs)
KrasG12V - TAM
KrasG12V + TAM
Empty - TAM
Empty + TAM
C
Number of cells *10^6
Days
KrasG12V - TAM
KrasG12V + TAM
Empty - TAM
Empty + TAM
D
Empty
Kras G12V
◀ 4-OHT (1µg/ml)
◀ EGF (25µg/ml)
SHOC2
P-MEK
P-ERK
ERK
P-AKT S473
AKT
E
Empty
Kras G12V
NT NW 10 30 60 180
◀ Selumetinib (1µM)
◀ 4-OHT (1µg/ml)
SHOC2
P-MEK
P-ERK
ERK
P-RSK
RSK
P-BAD S112
BIM
P-AKT S473
T-AKT
F
(%) of NT control
Log (Selumetinib) [nM]
KrasG12V - TAM
KrasG12V + TAM
Empty - TAM
Empty + TAM

Figure 8.4 Characterization of SHOC2$^{fl/fl}$ MEFs

A Lysates of E6-immortalized MEFs derived from Shoc2$^{fl/fl}$;CreER^{T2} mice infected with retrovirus expressing KrasG12V or empty vector control. Cells were treated with 1ug/ml 4-OHT for 5-days

B Kras^{G12V} transformed MEFs grow faster in 2D than non-transformed controls, and the growth rate of either is unaffected by Shoc2 deletion. MEFs as described were seeded sparsely and allowed to reach confluency. Confluency was determined by cell coverage as captured by incucyte.

C Kras^{G12V} transformed MEFs continue to grow past confluency as they do not demonstrate contact inhibition, whereas non-transformed MEFs do not. MEFs as described were seeded sparsely in 6-wells and cells counted each day over a 9-day period.

D Shoc2 KO blunts the ERK-MAPK pathway response to EGF stimulation in both Empty, and KrasG12V transformed MEFs. MEFs described in (A) were treated with 25ng/ml of EGF for indicated time points and then harvested for western blot analysis and probed with the indicated antibodies.

E Shoc2 is preferentially required for feedback relief ERK-pathway reactivation on MEKi treatment in KrasG12V transformed MEFs compared to non-transformed controls. MEFs as described were pre-treated with either 1µM Selumetinib for 9hrs. Cells were either lysed (NT and NW) or inhibitor-containing media replaced with fresh media and lysates generated after the indicated time points (NT - Non Treated, NW - Non washed).

F Shoc2 deletion sensitises KrasG12V transformed MEFs to MEKi's. MEFs were treated at different doses and a dose-response curve derived for each of the inhibitors after a 96hr incubation using CellTiter-Glo viability reagent.

8.1.5 Conclusions

Shoc2 ablation in both the LSL-Kras^{G12D} and more aggressive Kras^{G12D}Trp53^{R172H} LUAD mouse model, caused a marked delay in tumour development that significantly prolonged overall survival. This was phenocopied in a Shoc2 KI model, which more closely phenocopies pharmacological inhibition of SHOC2 in the clinic, and attributes the perturbation in KRAS-driven tumour initiation to the role of SHOC2 as part of the SHOC2 phosphatase complex. Crucially systemic Shoc2 deletion in adult mice is well tolerated compared to other nodes of the ERK-pathway. In addition Shoc2 ablation specifically sensitises KRAS-transformed, but not empty vector transformed MEFs, (derived from the R26-CreERT2 mouse model) to MEKi's. Taken together we suggest that SHOC2 may find utility as both a monotherapy in a subset of LUAD's, and otherwise serve to widen the therapeutic index of MEKi's without adding significant toxicity.

Chapter 9

Discussions & Future Perspectives

9.1 Discussion

This research project has sought to provide a rationale for a SHOC2 targeted therapy in NSCLC. We have uncovered that SHOC2 ablation inhibits growth of a subset of NSCLC cell lines under anchorage-independent growth conditions (spheroid assays). Interestingly even in non-responding cell lines in these assays SHOC2 did fully prevent lung colonisation of the same cells when injected into the lateral tail vein of immunocompromised mice (Figure 3.3-5). Furthermore in an *in vivo* autochthonous mouse model of LUAD we show that SHOC2 inhibition inhibits overall tumour burden, delays tumour progression, and as a result of this significantly increases overall survival in both the K, and more serve Kras.p53 mouse model, using both Shoc2 KO and a Shoc2 KI 'D175N' approach (Figure 8.2). This demonstrates that SHOC2 as part of the MRAS-SHOC2-PP1 complex (which the KI model prevents the assembly of) is required for tumour development in an initiation mouse model of LUAD. In extending this data it will be important to explore a role for SHOC2 in a tumour maintenance model i.e. once the tumours are established SHOC2 is deleted to determine the role of SHOC2 in already established lesions. We will make use of inducible recombinase systems, combining FRT and Cre technologies (Schonhuber et al. 2014). Experiments are underway for the maintenance model, we are using the FRT Kras.p53 LUAD mouse model crossed to Shoc2CreER^{T2} mice. This model permits oncogenic activation of Kras- and p53-driven by AdenoFlp infection, while SHOC2 deletion is controlled temporally by dosing of the animal with tamoxifen (Schonhuber et al. 2014; Sanclemente et al. 2018). This study will require the monitoring of individual tumours, and to this end Computed tomography (CT), or Positron electron tomography (PET) imaging techniques will be employed in collaboration with UCL-CABI to monitor the contribution of SHOC2 deletion to the progression of advanced tumours (Shackelford et al. 2013; Sanclemente et al. 2018). In cases where the effect of SHOC2 is purely cytostatic or only partial this project presents a strong rationale for combined genetic SHOC2 ablation with MEKi treatment, in this case we would expect robust tumour regressions based on our *in vitro* and xenograft observations (Figure 5.3-5/ 6.6). Tamoxifen treatment will cause conditional SHOC2 deletion in all tissues across the mouse model. As such combining systemic genetic inhibition SHOC2 with systemic pharmacological inhibition of MEK will enable us to observe the toxicity profile of the combination in the whole organism: (i) to ascertain if we really are able to use lower doses of MEKi on combined treatment and (ii) whether this really does provide a wider therapeutic index than has been observed in similar mouse models for other combination strategies (Castellano et al. 2013; Wong et al. 2018). Likewise these

studies could be incooperated into EGFR- or NF1-mutant mouse models, with the expectation from *in vitro* studies that if combined MEK/ SHOC2 inhibition causes tumour regressions of KRAS-driven tumours, the same combination strategy could be expanded to RTK and tumour suppressor drivers of aberrant RAS-signalling, so long as the particular driver requires RAF dimerization for its aberrant ERK-activation (Politi et al. 2006; Kwon and Berns 2013; Malone et al. 2017).

This research project has also furthered our understanding of why SHOC2 specifically seems to be preferentially required for the malignant (Anchorage-independent) growth of RAS mutant cells, demonstrated in this study and others (Young et al. 2013; Wang et al. 2017). In KRAS-mutant NSCLC cells, 3D-growth reveals a SHOC2-dependent contribution to ERK-signalling, as does EGF-stimulation, not observed in basal 2D-adhered growth conditions (Figure 3.5, 4.2). This suggests there must be redundant and/or SHOC2/ 'S259'-independent mechanisms of ERK-activation in basal 2D-conditions that are revealed in a context-dependent manner. Integrin signalling is known to provide a crucial contribution to PI3K/AKT pathway activation in adhered culture condtions that is lost in cells growing in suspension (King et al. 1997; Martin et al. 2006; Vachon 2011; Riedl et al. 2017), and it is possible that SHOC2-independent mechanisms of ERK-activation linked to integrin-signalling are similarly lost in suspension. This could be mediated by alternative mechanisms of RAF activation, perhaps through kinases activated by integrin signalling that regulate the N-region of CRAF, including SRC and PAK (Mason et al. 1999). Our results are consistent with a model where reduced cooperation from other signalling pathways enhances the dependency on SHOC2-dependent ERK-signalling for anchorage-independent growth (i.e. 'oncogene addiction to SHOC2 in 3D').

An important early observation was that although our autochthonous GEMM of NSCLC responded to SHOC2 ablation alone in an initiation model, not all RAS-mutant cell lines were SHOC2 sensitive for 3D-growth inhibition as spheroids (Figure 3.3). Interestingly each of the non-responding cell lines were those lines which had co-occurring mutations in STK11 (LKB1). LKB1 is a bona fide tumour suppressor gene that acts an activator of stress sensing AMPK, and as such mutations are loss of function mutations allowing advanced cancers to proliferate under low nutrient, or non-favourable growth conditions. In human LUAD, KRAS-driven cancers frequently co-occur with STK11 mutations (~11%) (Cancer Genome Atlas Research 2014). We have recently sourced constructs where we plan to rescue LKB1 expression in our RAS-mutant LKB1 null cells (A549 and A427) to see if we can reverse the resistance to

SHOC2 suppression for growth of cells in suspension by restoring LKB1-mTORC signalling. Like Kras.p53 LUAD models, Kras.Lkb1 mice demonstrate more aggressive and metastatic disease than Kras alone (Shackelford et al. 2013). If we hypothesise we observe a SHOC2-dependent growth in anchorage-independent conditions only in the absence of STK11 mutations then Shoc2 ablation should have no effect on the tumour development in this GEMM. This mouse model would further allow us to see if co-targeting strategies such as Shoc2/ MEK would work in this scenario, for which our *in vitro* data suggests it should, as genetic inhibition of SHOC2 sensitised KRAS-mutant NSCLC cells to MEKi's in all cases, including LKB1 null cells, suggesting that the enhanced efficacy of MEKi's on combined MEK/ SHOC2 inhibition is independent of LKB1 status (Figure 5.3).

Our study highlights that regardless of an individual cell lines sensitivity in anchorage-independent growth conditions to SHOC2 ablation/suppression in 2D-adhered, or 3D-suspension cell culture, genetic inhibition of SHOC2 broadly sensitises KRAS- and EGFR-mutant NSCLC cell lines to MEKi's. These effects also reproduced in MEFs with ectopic KRAS G12V expression and tamoxifen-mediated SHOC2 deletion (Figure 8.4F). Importantly genetic inhibition of SHOC2 did not sensitise NSCLC cancer cell lines with no known driver mutations in the ERK-pathway to MEKi's. This suggests that pathway rewiring as a result of ERK-pathway oncogene addiction at the level of RAS or RTK's that lead to increased RAS-GTP provide a unique vulnerability, or synthetic lethality that may be clinically relevant. The observed effects are specific to the role of SHOC2 as part of the MRAS-SHOC2-PP1 phosphatase complex (Figure 5.6-7), and in keeping with the role of this complex in RAF-activation we demonstrate that SHOC2 is required for MEKi-induced feedback relief RAF-dimerization and ERK-activation (Figure 7.3).

In the context of RAS-mutant cells, ERK-dependent feedback loops serve to regulate pathway activation; in part by inhibitory phosphorylation of BRAF and CRAF. This phosphorylation prevents the RASGTP-RAF interaction and RAF-dimerization, thus regulating further activation of MEK (Dougherty et al. 2005; Ritt et al. 2010). In the context of MEKi treatment these negative feedback loops are shut off with the inhibition of ERK. This leads to hyperactivation of upstream pathway components, with an increase in BRAF-CRAF dimerization, and subsequent rebound in P-MEK levels (Figure 7.6). Critically we identify a role for SHOC2 in mediating MEKi induced RAF-dimerization and activation upon feedback relief. Inhibition of SHOC2 prevents MEKi induced BRAF-CRAF dimerization and the rebound in P-MEK. By preventing feedback

relief RAF-dimerization and P-MEK rebound, SHOC2 inhibition serves to provide a more potent and sustained ERK-inhibition, and as a result of this dampen and delay the phosphorylation of downstream ERK-targets including RSK, as well as feedback sites on EGFR and RAF when the MEKi is washed-out (Figure 7.2-5).

Not all MEKi's have the same mechanism of action and comparing two distinct inhibitors we observe variations in our assays in agreement with these distinct mechanisms. Selumetinib (AZD6244) binds a discrete binding pocket of MEK1/2, distinct from the ATP-binding pocket or interacting sites of ERK1/2, and prevents downstream ERK-phosphorylation, causing feedback relief P-MEK rebound. Trametinib also inhibits ERK-phosphorylation, but mitigates the consequences of feedback relief P-MEK rebound by simultaneously preventing MEK contacting ERK (Ishii et al. 2013; Lito et al. 2014). As a result of this dual mechanism we observe that Trametinib has a much weaker P-MEK rebound than Selumetinib when compared side by side, and this correlates with a reduced sensitisation on SHOC2 inhibition in viability assays (Figure 5.2A/ 7.3A). However this inhibition is incomplete and like all MEKi's Trametinib does lead to feedback relief activation upstream of MEK and we observe a marked SHOC2 sensitive induction of BRAF-CRAF and BRAF-ARAF dimers with Trametinib treatment of H358 cells, comparable to Selumetinib (Figure 7.6D). We propose the broad requirement of SHOC2 for feedback relief RAF-activation, a consequence of all MEKi's, is responsible for our effects in viability assays. In agreement with this CRAF has been previously shown to be required for ERK-feedback reactivation (Lito et al. 2014; Merchant et al. 2017). Here we extend this observation to show that both BRAF- and CRAF-knockdown, but not ARAF-knockdown, impair signalling rebound and sensitize KRAS-mutant NSCLC cell lines to MEKi's, although not as strongly as SHOC2-knockdown (Figure 7.7). A more potent response of SHOC2 suppression compared to suppression of BRAF or CRAF is consistent with SHOC2 functioning as a PanRAF 'S259' phosphatase. In agreement with this, yet in contrast to other inhibitor combinations, synergy of a PanRAFi with MEKi is either not affected or mildly antagonized with suppression of SHOC2 (Figure 5.9), consistent with RAF and SHOC2 inhibition having redundant roles in their cooperation with MEKi. Collectively, this data is consistent with a key role for BRAF-CRAF dimers as primary mediators of signalling rebound and resistance to MEKi, although a role for ARAF cannot be fully excluded as genetic inhibition of SHOC2 also prevents ARAF-BRAF dimers (Figure 7.6A).

As well as modulating RAF-RAF dimers this research introduces the concept that SHOC2 may module RAF-MEK complexes. Trametinib treatment disrupts RAF-MEK

complexes, however upon feedback relief RAF-dimerization and pathway reactivation there is a re-association of CRAF-MEK complexes, but not A/BRAF-MEK complexes. This re-association correlates well with P-ERK reactivation and infers these CRAF-MEK complexes are active, and may be solely responsible for immediate feedback relief ERK-pathway activation (Lito et al. 2014). Intriguingly SHOC2 further supressed these CRAF-MEK complexes from re-association, and in doing so may explain in part the enhanced suppression of P-ERK, and increased sensitivity of RAS-mutant cells to combined Trametinib treatment with genetic inhibition of SHOC2.

BRAF-mutant NSCLC cell lines are not sensitised to MEKi's on SHOC2 suppression, in keeping with many features of what is known about these mutants in human cancer. BRAFV600E-mutant cells signal as catalytic monomers, independent of upstream activation and dimerization for MEK-phosphorylation (Lito et al. 2012; Chapman et al. 2014; Haling et al. 2014; Yao et al. 2015). Although BRAF driver mutations are found in NSCLC they are typically defined as non-V600E mutants, these p-loop mutants characteristically have low to no catalytic activity but instead stabilise RAF-hetero dimers and support CRAF-activation (Haling et al. 2014). We postulate that this increases the pool of preformed dimers (basal dimers) in these cancers that are independent of the SHOC2 phosphatase complex for activation. Although inhibition of SHOC2 will not be useful as a frontline treatment in combination with MEK inhibition for BRAF mutant tumours, it is worth noting that many resistance mechanisms to frontline RAFi therapies drive reactivation of ERK-signalling via dimerization-dependent, and therefore SHOC2-dependent mechanisms (Nazarian et al. 2010; Lito et al. 2012; Whittaker et al. 2013). These include, RTK-activation, NRAS activating mutations and loss of function NF1 tumour suppressor mutations (Nazarian et al. 2010; Whittaker et al. 2013). Indeed it is published that both CRAF and SHOC2 have been identified as targets of therapeutic resistance in RAS-driven colorectal and melanoma cancers (Kaplan et al. 2012; Whittaker et al. 2015).

The ERK-pathway is a key regulator of G1/S transition and MEKi's predominantly exert cytostatic effects, which likely contributes to their poor clinical efficacy and facilitates the selective pressure to acquire resistance mechanisms (Meloche and Pouyssegur 2007; Cook et al. 2017). Importantly, SHOC2 inactivation greatly potentiates apoptosis induced by MEKi's in KRAS-mutant NSCLC cells. This correlates with complete cytotoxic responses in tissue culture and with marked tumour regressions in a xenograft model, at MEKi concentrations that otherwise only induce a reversible cytostatic response in SHOC2-WT controls (Chapter 6).

ERK-signalling regulates multiple proteins involved in apoptosis and can control the balance of pro- and antiapoptotic BCL2 proteins to modulate the apoptotic threshold (Hata et al. 2015; Cook et al. 2017). ERK-phosphorylation of the pro-apoptotic BH3 proteins BAD and BIM leads to sequestration by 14-3-3 proteins and protein degradation (Zha et al. 1996; Meng et al. 2010; Sale and Cook 2013a; Sun et al. 2014). Combined genetic inhibition of SHOC2 and pharmacological MEK inhibition cooperate to decrease S112 BAD phosphorylation and increase BIM protein levels suggesting a biochemical mechanism to reach the apoptotic threshold (Figure 7.2-4/8.4E). Furthermore, suppressing BIM expression diminishes sensitisation to MEKi upon SHOC2 knockdown (Figure 6.4). Taken together our data is consistent with a model where the more potent and durable ERK suppression, achieved by co-targeting SHOC2 and MEK, allows pro-apoptotic BH3 proteins to accumulate to levels required to induce apoptosis.

Sensitisation to MEKi's upon SHOC2 inhibition is highly specific and SHOC2 inhibition does not sensitise RAS- or EGFR-mutant cells to any other inhibitors tested through the breath of our experiments, including other nodes of the ERK-pathway (Figure 5.2). Importantly sensitisation in viability assays correlates with ERK-suppression in wash-out experiments, where we see only complete ERK-pathway suppression on combined SHOC2 and MEK inhibition, but not SHOC2/ PanRAF, or SHOC2/ ERK inhibition (Figure 7.3). In the case of PanRAF inhibitors it is published that this class of inhibitors paradoxically stabilises BRAF-CRAF dimers and increases the RAS-RAF interaction independently of upstream RAS activation (Hatzivassiliou et al. 2010; Peng et al. 2015; Jin et al. 2017). In our own experiments we show that LY3009120 induces a striking increase in SHOC2-independent BRAF-CRAF dimerization (Figure 7.5D). This is in agreement with a lack of sensitisation to RAFi's on SHOC2 inhibition in viability assays and a large SHOC2-indpendent P-ERK reactivation in inhibitor wash-out experiments. Conversely to RAF inhibitors, ERK inhibitors induced a partial SHOC2 sensitive BRAF-CRAF dimerization but this induction was slight and ERK reactivation was largely SHOC2-independent, again in agreement with viability assays.

As seen with SHOC2, intrapathway dual inhibition (vertical inhibition) at the level of RAF or ERK (MEKi plus RAFi or MEKi plus ERKi) also impairs feedback reactivation, leads to more potent and sustained ERK-suppression, and promotes cytotoxicity/ tumour regression in preclinical models of RAS-mutant cells, consistent with our model (Figure 7.11) (Lamba et al. 2014; Whittaker et al. 2015; Merchant et al. 2017). It is also true that resistance to frontline MEKi treatment due to ERK feedback reactivation can

be overcome with ERKi therapies (Hatzivassiliou et al. 2012). However the clinical applicability of these combinations remains to be seen with on-target toxicities of these inhibitors limiting their therapeutic index. Mouse models already tell us that lethality attributed to genetic ablation of ERK-pathway nodes is not restricted to embryogenesis. Using a similar means of conditional ablation as our own CreER^{T2} model it has been shown that deletion of either A,B, CRAF/, MEK1/2/ and ERK1/2 in adult mice leads to rapid death due to multiple organ failure in ~2-weeks highlighting the critical relevance of these nodes in normal homeostasis (Blasco et al. 2011; Sanclemente et al. 2018). In contrast Shoc2 deletion in adult mice is remarkably well-tolerated with adult mice not presenting with any overt phenotype until ~8-weeks. Our study suggests that uniquely among other pathway nodes for vertical inhibition, SHOC2 inhibition may overcome MEKi resistance in RAS-mutant tumours without adding significant toxicity.

9.2 Future Perspectives

Our model suggests SHOC2 will sensitise any cell line to MEKi's which is dependent on RAF dimer driven ERK-activation and this likely includes multiple driver mutations at the level of RTK's including MET, and loss of NF1 tumour suppressor functions not shown in the scope of this study. Further still our study is limited to NSCLC but multiple other cancer types rely on ERK-pathway activation, including both colorectal and pancreatic cancers which have high rates of KRAS- or KRAS-effector driver mutations (~60% and 90% respectively). Preliminary data suggests our observations extend to at least one colorectal cancer cell line, HCT116 (data not shown). It is my belief that the notion that SHOC2 will sensitise any cell line that relies on RAF dimerization for ERK-activation is overly simplistic, in fact many RAS-mutant cell lines simply may not require the ERK-pathway for their oncogenic activity. Indeed observations of RAS-effectors, BRAF and PIK3CA as driver mutations found that PIK3CA driver mutations are found more commonly in CRC (11-13%) than both pancreatic (<1%) and NSCLC (1-2%). Similarly co-occurring EGFR/ PIK3CA mutations are more common in CRC than NSCLC (O'Byrne et al. 2011). This implies strong differential dependencies of RAS-effector pathways in certain cancer types. This will be an important consideration for the RAS field moving forward and more specifically for this project in discerning patients groups that may be more likely to respond to a SHOC2 targeted therapy. In the context of KRAS-mutations such a differential effector pathway bias may be governed at the level of the mutational variant itself. Early evidence for this comes from structural analysis of Q61 mutations which are most commonly found in NSCLC and favour a catalytically inactive RAS-GTP state only when RAS is bound to RAF, thus shifting the conformational equilibrium to favour RAF activation by RAS over other RAS-effectors (Buhrman et al. 2007). Delineating the engagement of different RAS-variants with specific RAS-effectors remains a highly active interest of many in the field, specifically with regard to predicting treatment responses.

Similarly to research being undertaken on identifying functional consequences of different mutant RAS-variants our own future research efforts may look to delineate the individual contribution of RAF isoforms as hetero or homo dimers in driving oncogenic signalling - to identify functional differences that may one day be able to be inhibited differentially. We propose that feedback relief-mediated ERK-pathway activation is mediated by B-CAF heterodimers, and that BRAF-CRAF dimerization in this context requires SHOC2 (Figure 7.6). Additionally we see that SHOC2 potentiates the dissociation of MEK-CRAF complexes on MEKi treatment but MEK-ARAF/BRAF

dissociation are independent of SHOC2 (Figure 7.10). This is in agreement with literature that implicates a role for BRAF and CRAF but not ARAF in cancer (Blasco et al. 2011; Karreth et al. 2011). Intriguingly although all three RAF isoforms have a highly conserved kinase domain at their c-terminus there is variability in their n-regions. As well as endowing RAF kinases with different levels of regulation that may influence their intrinsic kinase activity, it may provide RAF kinases with the ability to be differentially regulated both temporally, spatially, and in response to certain stimuli. Indeed we readily identify both A-BRAF and B-CRAF dimers on MEKi treatment but not A-CRAF (Data not shown). The field generally agrees that S259 dephosphorylation is required for all RAF activation (Lavoie and Therrien 2015), however it may be that SHOC2's requirement for S259 dephosphorylation and RAF-activation is more context-dependent and other holoenzyme phosphatase complexes may be required in other contexts (Abraham et al. 2000; Ory et al. 2003). This may help explain the preferential requirement of SHOC2 for both growth factor stimulated, anchorage-independent growth-mediated, and MEKi-driven ERK-activation. Additionally this may reflect the redundancy of SHOC2 in adult mice and have significant implications for a SHOC2-targeted therapy in mitigating problems of on-target toxicity that plagues targeting of core ERK-pathway nodules (Blasco et al. 2011; Sanclemente et al. 2018).

Our results highlight that the dephosphorylation of the 'S259' site by the MRAS-SHOC2-PP1 complex represents a rate limiting step for efficient ERK-pathway reactivation in response to loss of negative feedback loops on MEKi treatment, or RTK growth factor stimulation. SHOC2 inhibition abrogates dephosphorylation of this site, and as such blunts the ERK-pathway response to feedback relief ERK-activation and RTK-mediated ERK-activation. Mutations are found frequently to cluster at the 'S259' site and across all three components of the MRAS-SHOC2-PP1 complex in the RASopathy Noonan syndrome (Razzaque et al. 2007; Cordeddu et al. 2009; Molzan et al. 2010; Gripp et al. 2016; Higgins et al. 2017; Zambrano et al. 2017). Intriguingly mutations at this site are also found in cancer, albeit it infrequently and these mutations frequently co-occur with KRAS mutations (COSMIC-Data not shown). This may or may not be coincidence, I suspect not, but future work efforts could look to see if these mutations cooperate in KRAS-mutant tumour development – evidence towards this comes from phosphorylation deficient mutants of CRAF 'S259' and equivalent sites on ARAF and BRAF which even in RAS-mutant cells further increase levels of P-MEK and P-ERK (Figure 5.7). Alternatively mutations at the S259 site may become more relevant in acquired resistance of KRAS-mutant tumours to frontline MEKi or BRAFi treatment. Either way validation of this site as a bona-fide oncogenic mutation in RAF

would be expected to raise the profile and significance of the phosphatase complex that regulates this site. Indeed down the line it will be important in screening patients that may be expected to benefit form a SHOC2 targeted therapy as patients with these mutations would be expected to be resistant to these small molecule inhibitors.

An important factor that remains to be determined following a project focused on target validation is how feasible will it be to generate a drug that targets a phosphatase complex and what approach would be best to take. Phosphatases have long been thought undruggable due to their broad requirement across many physiological processes of which have been shown to even be opposing and context-dependent (St-Denis et al. 2016). We now know this early dogma failed to recognise that phosphatases often carry out their biological function as part of highly specific holoenzyme complexes, formed of the catalytic phosphatase and regulatory protein partners, that may govern the phosphatase activity both spatially and temporally (Bollen et al. 2010). PP1 is known to interact with over 200 regulatory proteins each providing unique substrate binding and holophosphatase activity, highlighting that phosphatases may represent underexplored targets for pharmacological inhibition for the treatment of many diseases (Bollen et al. 2010; De Munter et al. 2013; Peti and Page 2015). Indeed targeting the regulatory subunit of a protein phosphatase complex has already been shown to be effective for the treatment of protein misfolding neurodegenerative diseases (Das et al. 2015; Carrara et al. 2017).

MRAS activation and binding to GTP is thought to trigger the formation of the complex and the re-localisation of SHOC2 and PP1 to the plasma membrane (consensus model). This permits a unique opportunity to inhibit the catalytic function of the phosphatase at a site distinct from the phosphatase itself by disrupting complex formation. We also know that a single point mutation ‘D175N’ is sufficient to specifically disrupt the role of SHOC2 as part of the MRAS-SHOC2-PP1 complex without disrupting other interactions (Figure 1.5). This provides a rationale for specific targeting of SHOC2 as part of one complex but not another. Alternatively MRAS-SHOC2 have been shown to interact with the polarity protein SCRIB (Young et al. 2013). SCRIB antagonises ERK-activity in a model which assumes a competition for PP1 binding between SCRIB and the MRAS-SHOC2 complex, of which the latter has increased affinity only on MRAS activation and cycling to its GTP-bound state. An inhibitor which supported or stabilised the MRAS-SHOC2-SCRIB complex, reducing affinity of the complex for PP1 may find greater utility as an anti-tumour therapy. Inhibitors that stabilise specific conformational states have already shown utility for ERK-pathway inhibition. By stabilising the inactive state of KSR/ MEK Dar and colleagues were able

to prevent MEK phosphorylation and activation by RAF (Dhawan et al. 2016). Further still they observed that RAS-mutant cells were sensitised to MEKi's when treated with their KSR stabilising compound, through a mechanism they posited to be because their compound prevented feedback relief MEK phosphorylation by RAF, highly analogous to our own.

9.3 Conclusions

Our data highlights that conditional deletion of SHOC2 in the adult mouse is well tolerated up to 8-weeks, and that strikingly, SHOC2 ablation causes a marked inhibition of tumour development in KRAS mutant LUAD mouse models, significantly extending overall survival. Additionally we show that genetic inhibition of SHOC2 by KD/KO approaches specifically sensitises KRAS- and EGFR-mutant NSCLC cell lines to MEK inhibitors, while sparing wildtype cells - by lowering the concentration of MEKi required to drive BIM-dependent cytotoxicity. We propose these effects are driven by the role of SHOC2 as part of the MRAS-SHOC2-PP1 complex in mediating RAF dimerization. We show that SHOC2 is specifically required for feedback relief RAF dimerization-driven ERK reactivation on MEKi treatment, and that its inhibition elongates the therapeutic action of MEKi's by sustaining ERK suppression and stabilising pro-apoptotic ERK-targets. In summary we propose a SHOC2 targeted therapy may not only serve to perturb tumour growth as a monotherapy, but may also substantially enhance the efficacy of clinically available MEKi's, without adding significant toxicity.

Alice ‘’This is impossible

The Mad Hatter ‘’Only if you believe it is’’

Lewis Carroll

References

Abraham D, Podar K, Pacher M, Kubicek M, Welzel N, Hemmings BA, Dilworth SM, Mischak H, Kolch W, Baccarini M. 2000. Raf-1-associated protein phosphatase 2A as a positive regulator of kinase activation. *The Journal of biological chemistry* **275**: 22300-22304.

Akgul C. 2009. Mcl-1 is a potential therapeutic target in multiple types of cancer. *Cellular and molecular life sciences : CMLS* **66**: 1326-1336.

Ambrogio C, Kohler J, Zhou ZW, Wang H, Paranal R, Li J, Capelletti M, Caffarra C, Li S, Lv Q et al. 2018. KRAS Dimerization Impacts MEK Inhibitor Sensitivity and Oncogenic Activity of Mutant KRAS. *Cell* **172**: 857-868 e815.

Ascierto PA, Minor D, Ribas A, Lebbe C, O'Hagan A, Arya N, Guckert M, Schadendorf D, Kefford RF, Grob JJ et al. 2013. Phase II trial (BREAK-2) of the BRAF inhibitor dabrafenib (GSK2118436) in patients with metastatic melanoma. *Journal of clinical oncology : official journal of the American Society of Clinical Oncology* **31**: 3205-3211.

Blasco RB, Francoz S, Santamaria D, Canamero M, Dubus P, Charron J, Baccarini M, Barbacid M. 2011. c-Raf, but not B-Raf, is essential for development of K-Ras oncogene-driven non-small cell lung carcinoma. *Cancer cell* **19**: 652-663.

Bollag G, Hirth P, Tsai J, Zhang J, Ibrahim PN, Cho H, Spevak W, Zhang C, Zhang Y, Habets G et al. 2010. Clinical efficacy of a RAF inhibitor needs broad target blockade in BRAF-mutant melanoma. *Nature* **467**: 596-599.

Bollen M, Peti W, Ragusa MJ, Beullens M. 2010. The extended PP1 toolkit: designed to create specificity. *Trends in biochemical sciences* **35**: 450-458.

Bonni A, Brunet A, West AE, Datta SR, Takasu MA, Greenberg ME. 1999. Cell survival promoted by the Ras-MAPK signaling pathway by transcription-dependent and -independent mechanisms. *Science* **286**: 1358-1362.

Brennan DF, Dar AC, Hertz NT, Chao WC, Burlingame AL, Shokat KM, Barford D. 2011. A Raf-induced allosteric transition of KSR stimulates phosphorylation of MEK. *Nature* **472**: 366-369.

Buday L, Downward J. 1993. Epidermal growth factor regulates p21ras through the formation of a complex of receptor, Grb2 adapter protein, and Sos nucleotide exchange factor. *Cell* **73**: 611-620.

Buhrman G, Wink G, Mattos C. 2007. Transformation efficiency of RasQ61 mutants linked to structural features of the switch regions in the presence of Raf. *Structure* **15**: 1618-1629.

Cancer Genome Atlas Research N. 2014. Comprehensive molecular profiling of lung adenocarcinoma. *Nature* **511**: 543-550.

Carrara M, Sigurdardottir A, Bertolotti A. 2017. Decoding the selectivity of eIF2alpha holophosphatases and PPP1R15A inhibitors. *Nature structural & molecular biology* **24**: 708-716.

Castellano E, Sheridan C, Thin MZ, Nye E, Spencer-Dene B, Diefenbacher ME, Moore C, Kumar MS, Murillo MM, Gronroos E et al. 2013. Requirement for interaction of PI3-kinase p110alpha with RAS in lung tumor maintenance. *Cancer cell* **24**: 617-630.

Caunt CJ, Sale MJ, Smith PD, Cook SJ. 2015. MEK1 and MEK2 inhibitors and cancer therapy: the long and winding road. *Nature reviews Cancer* **15**: 577-592.

Certo M, Del Gaizo Moore V, Nishino M, Wei G, Korsmeyer S, Armstrong SA, Letai A. 2006. Mitochondria primed by death signals determine cellular addiction to antiapoptotic BCL-2 family members. *Cancer cell* **9**: 351-365.

Chapman PB, Hauschild A, Robert C, Haanen JB, Ascierto P, Larkin J, Dummer R, Garbe C, Testori A, Maio M et al. 2011. Improved survival with vemurafenib in melanoma with BRAF V600E mutation. *The New England journal of medicine* **364**: 2507-2516.

Chapman PB, Solit DB, Rosen N. 2014. Combination of RAF and MEK inhibition for the treatment of BRAF-mutated melanoma: feedback is not encouraged. *Cancer cell* **26**: 603-604.

Chaudhary A, King WG, Mattaliano MD, Frost JA, Diaz B, Morrison DK, Cobb MH, Marshall MS, Brugge JS. 2000. Phosphatidylinositol 3-kinase regulates Raf1 through Pak phosphorylation of serine 338. *Current biology : CB* **10**: 551-554.

Cho US, Xu W. 2007. Crystal structure of a protein phosphatase 2A heterotrimeric holoenzyme. *Nature* **445**: 53-57.

Ciampi R, Knauf JA, Kerler R, Gandhi M, Zhu Z, Nikiforova MN, Rabes HM, Fagin JA, Nikiforov YE. 2005. Oncogenic AKAP9-BRAF fusion is a novel mechanism of MAPK pathway activation in thyroid cancer. *The Journal of clinical investigation* **115**: 94-101.

Cichowski K, Jacks T. 2001. NF1 tumor suppressor gene function: narrowing the GAP. *Cell* **104**: 593-604.

Cleghon V, Morrison DK. 1994. Raf-1 interacts with Fyn and Src in a non-phosphotyrosine-dependent manner. *The Journal of biological chemistry* **269**: 17749-17755.

Cook SJ, Stuart K, Gilley R, Sale MJ. 2017. Control of cell death and mitochondrial fission by ERK1/2 MAP kinase signalling. *The FEBS journal* **284**: 4177-4195.

Corbalan-Garcia S, Yang SS, Degenhardt KR, Bar-Sagi D. 1996. Identification of the mitogen-activated protein kinase phosphorylation sites on human Sos1 that regulate interaction with Grb2. *Molecular and cellular biology* **16**: 5674-5682.

Corcoran RB, Cheng KA, Hata AN, Faber AC, Ebi H, Coffee EM, Greninger P, Brown RD, Godfrey JT, Cohoon TJ et al. 2013. Synthetic lethal interaction of combined BCL-XL and MEK inhibition promotes tumor regressions in KRAS mutant cancer models. *Cancer cell* **23**: 121-128.

Cordeddu V, Di Schiavi E, Pennacchio LA, Ma'ayan A, Sarkozy A, Fodale V, Cecchetti S, Cardinale A, Martin J, Schackwitz W et al. 2009. Mutation of SHOC2 promotes aberrant protein N-myristoylation and causes Noonan-like syndrome with loose anagen hair. *Nature genetics* **41**: 1022-1026.

Cox AD, Fesik SW, Kimmelman AC, Luo J, Der CJ. 2014. Drugging the undruggable RAS: Mission possible? *Nature reviews Drug discovery* **13**: 828-851.

Cutler RE, Jr., Stephens RM, Saracino MR, Morrison DK. 1998. Autoregulation of the Raf-1 serine/threonine kinase. *Proceedings of the National Academy of Sciences of the United States of America* **95**: 9214-9219.

Dalby KN, Morrice N, Caudwell FB, Avruch J, Cohen P. 1998. Identification of regulatory phosphorylation sites in mitogen-activated protein kinase (MAPK)-activated protein kinase-1a/p90rsk that are inducible by MAPK. *The Journal of biological chemistry* **273**: 1496-1505.

Das I, Krzyzosiak A, Schneider K, Wrabetz L, D'Antonio M, Barry N, Sigurdardottir A, Bertolotti A. 2015. Preventing proteostasis diseases by selective inhibition of a phosphatase regulatory subunit. *Science* **348**: 239-242.

Datta SR, Dudek H, Tao X, Masters S, Fu H, Gotoh Y, Greenberg ME. 1997. Akt phosphorylation of BAD couples survival signals to the cell-intrinsic death machinery. *Cell* **91**: 231-241.

De Munter S, Kohn M, Bollen M. 2013. Challenges and opportunities in the development of protein phosphatase-directed therapeutics. *ACS chemical biology* **8**: 36-45.

Dehan E, Bassermann F, Guardavaccaro D, Vasiliver-Shamis G, Cohen M, Lowes KN, Dustin M, Huang DC, Taunton J, Pagano M. 2009. betaTrCP- and Rsk1/2-mediated degradation of BimEL inhibits apoptosis. *Molecular cell* **33**: 109-116.

Dhawan NS, Scopton AP, Dar AC. 2016. Small molecule stabilization of the KSR inactive state antagonizes oncogenic Ras signalling. *Nature* **537**: 112-116.

Dhillon AS, Meikle S, Yazici Z, Eulitz M, Kolch W. 2002. Regulation of Raf-1 activation and signalling by dephosphorylation. *The EMBO journal* **21**: 64-71.

Dougherty MK, Muller J, Ritt DA, Zhou M, Zhou XZ, Copeland TD, Conrads TP, Veenstra TD, Lu KP, Morrison DK. 2005. Regulation of Raf-1 by direct feedback phosphorylation. *Molecular cell* **17**: 215-224.

Douziech M, Sahmi M, Laberge G, Therrien M. 2006. A KSR/CNK complex mediated by HYP, a novel SAM domain-containing protein, regulates RAS-dependent RAF activation in Drosophila. *Genes & development* **20**: 807-819.

Downward J. 2003. Targeting RAS signalling pathways in cancer therapy. *Nature reviews Cancer* **3**: 11-22.

-. 2015. RAS Synthetic Lethal Screens Revisited: Still Seeking the Elusive Prize? *Clinical cancer research : an official journal of the American Association for Cancer Research* **21**: 1802-1809.

DuPage M, Dooley AL, Jacks T. 2009. Conditional mouse lung cancer models using adenoviral or lentiviral delivery of Cre recombinase. *Nature protocols* **4**: 1064-1072.

Ehrenreiter K, Kern F, Velamoor V, Meissl K, Galabova-Kovacs G, Sibilia M, Baccarini M. 2009. Raf-1 addiction in Ras-induced skin carcinogenesis. *Cancer cell* **16**: 149-160.

Ehrhardt A, Ehrhardt GR, Guo X, Schrader JW. 2002. Ras and relatives--job sharing and networking keep an old family together. *Experimental hematology* **30**: 1089-1106.

Engelman JA, Chen L, Tan X, Crosby K, Guimaraes AR, Upadhyay R, Maira M, McNamara K, Perera SA, Song Y et al. 2008. Effective use of PI3K and MEK inhibitors to treat mutant Kras G12D and PIK3CA H1047R murine lung cancers. *Nature medicine* **14**: 1351-1356.

Engelman JA, Luo J, Cantley LC. 2006. The evolution of phosphatidylinositol 3-kinases as regulators of growth and metabolism. *Nature reviews Genetics* **7**: 606-619.

Esteban LM, Vicario-Abejon C, Fernandez-Salguero P, Fernandez-Medarde A, Swaminathan N, Yienger K, Lopez E, Malumbres M, McKay R, Ward JM et al. 2001. Targeted genomic disruption of H-ras and N-ras, individually or in combination, reveals the dispensability of both loci for mouse growth and development. *Molecular and cellular biology* **21**: 1444-1452.

Ferrell JE, Jr., Bhatt RR. 1997. Mechanistic studies of the dual phosphorylation of mitogen-activated protein kinase. *The Journal of biological chemistry* **272**: 19008-19016.

Forbes SA, Bindal N, Bamford S, Cole C, Kok CY, Beare D, Jia M, Shepherd R, Leung K, Menzies A et al. 2011. COSMIC: mining complete cancer genomes in the Catalogue of Somatic Mutations in Cancer. *Nucleic acids research* **39**: D945-950.

Freeman AK, Ritt DA, Morrison DK. 2013. Effects of Raf dimerization and its inhibition on normal and disease-associated Raf signaling. *Molecular cell* **49**: 751-758.

Fueller J, Becker M, Sienerth AR, Fischer A, Hotz C, Galmiche A. 2008. C-RAF activation promotes BAD poly-ubiquitylation and turn-over by the proteasome. *Biochemical and biophysical research communications* **370**: 552-556.

Fujita-Sato S, Galeas J, Truitt M, Pitt C, Urisman A, Bandyopadhyay S, Ruggero D, McCormick F. 2015. Enhanced MET Translation and Signaling Sustains K-Ras-Driven Proliferation under Anchorage-Independent Growth Conditions. *Cancer research* **75**: 2851-2862.

Garnett MJ, Rana S, Paterson H, Barford D, Marais R. 2005. Wild-type and mutant B-RAF activate C-RAF through distinct mechanisms involving heterodimerization. *Molecular cell* **20**: 963-969.

Gibbons DL, Byers LA, Kurie JM. 2014. Smoking, p53 mutation, and lung cancer. *Molecular cancer research : MCR* **12**: 3-13.

Gripp KW, Aldinger KA, Bennett JT, Baker L, Tusi J, Powell-Hamilton N, Stabley D, Sol-Church K, Timms AE, Dobyns WB. 2016. A novel rasopathy caused by recurrent de novo

missense mutations in PPP1CB closely resembles Noonan syndrome with loose anagen hair. *Am J Med Genet A* **170**: 2237-2247.

Groves MR, Hanlon N, Turowski P, Hemmings BA, Barford D. 1999. The structure of the protein phosphatase 2A PR65/A subunit reveals the conformation of its 15 tandemly repeated HEAT motifs. *Cell* **96**: 99-110.

Gupta S, Ramjaun AR, Haiko P, Wang Y, Warne PH, Nicke B, Nye E, Stamp G, Alitalo K, Downward J. 2007. Binding of ras to phosphoinositide 3-kinase p110alpha is required for ras-driven tumorigenesis in mice. *Cell* **129**: 957-968.

Haanen C, Vermes I. 1996. Apoptosis: programmed cell death in fetal development. *European journal of obstetrics, gynecology, and reproductive biology* **64**: 129-133.

Haling JR, Sudhamsu J, Yen I, Sideris S, Sandoval W, Phung W, Bravo BJ, Giannetti AM, Peck A, Masselot A et al. 2014. Structure of the BRAF-MEK complex reveals a kinase activity independent role for BRAF in MAPK signaling. *Cancer cell* **26**: 402-413.

Hanahan D, Weinberg RA. 2000. The hallmarks of cancer. *Cell* **100**: 57-70.

Hancock JF, Parton RG. 2005. Ras plasma membrane signalling platforms. *The Biochemical journal* **389**: 1-11.

Hannig V, Jeoung M, Jang ER, Phillips JA, 3rd, Galperin E. 2014. A Novel SHOC2 Variant in Rasopathy. *Human mutation* **35**: 1290-1294.

Hata AN, Engelman JA, Faber AC. 2015. The BCL2 Family: Key Mediators of the Apoptotic Response to Targeted Anticancer Therapeutics. *Cancer discovery* **5**: 475-487.

Hatzivassiliou G, Liu B, O'Brien C, Spoerke JM, Hoeflich KP, Haverty PM, Soriano R, Forrest WF, Heldens S, Chen H et al. 2012. ERK inhibition overcomes acquired resistance to MEK inhibitors. *Molecular cancer therapeutics* **11**: 1143-1154.

Hatzivassiliou G, Song K, Yen I, Brandhuber BJ, Anderson DJ, Alvarado R, Ludlam MJ, Stokoe D, Gloor SL, Vigers G et al. 2010. RAF inhibitors prime wild-type RAF to activate the MAPK pathway and enhance growth. *Nature* **464**: 431-435.

Heidorn SJ, Milagre C, Whittaker S, Nourry A, Niculescu-Duvas I, Dhomen N, Hussain J, Reis-Filho JS, Springer CJ, Pritchard C et al. 2010. Kinase-dead BRAF and oncogenic RAS cooperate to drive tumor progression through CRAF. *Cell* **140**: 209-221.

Hengartner MO. 2000. The biochemistry of apoptosis. *Nature* **407**: 770-776.

Higgins EM, Bos JM, Mason-Suares H, Tester DJ, Ackerman JP, MacRae CA, Sol-Church K, Gripp KW, Urrutia R, Ackerman MJ. 2017. Elucidation of MRAS-mediated Noonan syndrome with cardiac hypertrophy. *JCI insight* **2**: e91225.

Hingorani SR, Wang L, Multani AS, Combs C, Deramaudt TB, Hruban RH, Rustgi AK, Chang S, Tuveson DA. 2005. Trp53R172H and KrasG12D cooperate to promote chromosomal instability and widely metastatic pancreatic ductal adenocarcinoma in mice. *Cancer cell* **7**: 469-483.

Hobbs GA, Der CJ, Rossman KL. 2016a. RAS isoforms and mutations in cancer at a glance. *Journal of cell science* **129**: 1287-1292.

Hobbs GA, Wittinghofer A, Der CJ. 2016b. Selective Targeting of the KRAS G12C Mutant: Kicking KRAS When It's Down. *Cancer cell* **29**: 251-253.

Hu J, Stites EC, Yu H, Germino EA, Meharena HS, Stork PJS, Kornev AP, Taylor SS, Shaw AS. 2013. Allosteric activation of functionally asymmetric RAF kinase dimers. *Cell* **154**: 1036-1046.

Ishii N, Harada N, Joseph EW, Ohara K, Miura T, Sakamoto H, Matsuda Y, Tomii Y, Tachibana-Kondo Y, Iikura H et al. 2013. Enhanced inhibition of ERK signaling by a novel allosteric MEK inhibitor, CH5126766, that suppresses feedback reactivation of RAF activity. *Cancer research* **73**: 4050-4060.

Jackson EL, Willis N, Mercer K, Bronson RT, Crowley D, Montoya R, Jacks T, Tuveson DA. 2001. Analysis of lung tumor initiation and progression using conditional expression of oncogenic K-ras. *Genes & development* **15**: 3243-3248.

Janes MR, Zhang J, Li LS, Hansen R, Peters U, Guo X, Chen Y, Babbar A, Firdaus SJ, Darjania L et al. 2018. Targeting KRAS Mutant Cancers with a Covalent G12C-Specific Inhibitor. *Cell* **172**: 578-589 e517.

Jaumot M, Hancock JF. 2001. Protein phosphatases 1 and 2A promote Raf-1 activation by regulating 14-3-3 interactions. *Oncogene* **20**: 3949-3958.

Jeoung M, Abdelmoti L, Jang ER, Vander Kooi CW, Galperin E. 2013. Functional Integration of the Conserved Domains of Shoc2 Scaffold. *PloS one* **8**: e66067.

Jin T, Lavoie H, Sahmi M, David M, Hilt C, Hammell A, Therrien M. 2017. RAF inhibitors promote RAS-RAF interaction by allosterically disrupting RAF autoinhibition. *Nature communications* **8**: 1211.

Johannessen CM, Boehm JS, Kim SY, Thomas SR, Wardwell L, Johnson LA, Emery CM, Stransky N, Cogdill AP, Barretina J et al. 2010. COT drives resistance to RAF inhibition through MAP kinase pathway reactivation. *Nature* **468**: 968-972.

Johnson L, Greenbaum D, Cichowski K, Mercer K, Murphy E, Schmitt E, Bronson RT, Umanoff H, Edelmann W, Kucherlapati R et al. 1997. K-ras is an essential gene in the mouse with partial functional overlap with N-ras. *Genes & development* **11**: 2468-2481.

Johnson L, Mercer K, Greenbaum D, Bronson RT, Crowley D, Tuveson DA, Jacks T. 2001. Somatic activation of the K-ras oncogene causes early onset lung cancer in mice. *Nature* **410**: 1111-1116.

Jokinen E, Koivunen JP. 2015. MEK and PI3K inhibition in solid tumors: rationale and evidence to date. *Therapeutic advances in medical oncology* **7**: 170-180.

Jones DT, Kocialkowski S, Liu L, Pearson DM, Backlund LM, Ichimura K, Collins VP. 2008. Tandem duplication producing a novel oncogenic BRAF fusion gene defines the majority of pilocytic astrocytomas. *Cancer research* **68**: 8673-8677.

Kaplan FM, Kugel CH, 3rd, Dadpey N, Shao Y, Abel EV, Aplin AE. 2012. SHOC2 and CRAF mediate ERK1/2 reactivation in mutant NRAS-mediated resistance to RAF inhibitor. *The Journal of biological chemistry* **287**: 41797-41807.

Karoulia Z, Wu Y, Ahmed TA, Xin Q, Bollard J, Krepler C, Wu X, Zhang C, Bollag G, Herlyn M et al. 2016. An Integrated Model of RAF Inhibitor Action Predicts Inhibitor Activity against Oncogenic BRAF Signaling. *Cancer cell* **30**: 485-498.

Karreth FA, Frese KK, DeNicola GM, Baccarini M, Tuveson DA. 2011. C-Raf is required for the initiation of lung cancer by K-Ras(G12D). *Cancer discovery* **1**: 128-136.

Kidger AM, Cook SJ. 2018. De-RSKing ERK - regulation of ERK1/2-RSK dissociation by phosphorylation within a disordered motif. *The FEBS journal* **285**: 42-45.

Kimmelman A, Tolkacheva T, Lorenzi MV, Osada M, Chan AM. 1997. Identification and characterization of R-ras3: a novel member of the RAS gene family with a non-ubiquitous pattern of tissue distribution. *Oncogene* **15**: 2675-2685.

King WG, Mattaliano MD, Chan TO, Tsichlis PN, Brugge JS. 1997. Phosphatidylinositol 3-kinase is required for integrin-stimulated AKT and Raf-1/mitogen-activated protein kinase pathway activation. *Molecular and cellular biology* **17**: 4406-4418.

Kobayashi S, Boggon TJ, Dayaram T, Janne PA, Kocher O, Meyerson M, Johnson BE, Eck MJ, Tenen DG, Halmos B. 2005. EGFR mutation and resistance of non-small-cell lung cancer to gefitinib. *The New England journal of medicine* **352**: 786-792.

Kuwana T, Bouchier-Hayes L, Chipuk JE, Bonzon C, Sullivan BA, Green DR, Newmeyer DD. 2005. BH3 domains of BH3-only proteins differentially regulate Bax-mediated mitochondrial membrane permeabilization both directly and indirectly. *Molecular cell* **17**: 525-535.

Kwon MC, Berns A. 2013. Mouse models for lung cancer. *Molecular oncology* **7**: 165-177.

Lake D, Correa SA, Muller J. 2016. Negative feedback regulation of the ERK1/2 MAPK pathway. *Cellular and molecular life sciences : CMLS* **73**: 4397-4413.

Lamba S, Russo M, Sun C, Lazzari L, Cancelliere C, Grernrum W, Lieftink C, Bernards R, Di Nicolantonio F, Bardelli A. 2014. RAF suppression synergizes with MEK inhibition in KRAS mutant cancer cells. *Cell reports* **8**: 1475-1483.

Lauriol J, Jaffre F, Kontaridis MI. 2015. The role of the protein tyrosine phosphatase SHP2 in cardiac development and disease. *Seminars in cell & developmental biology* **37**: 73-81.

Lavoie H, Therrien M. 2015. Regulation of RAF protein kinases in ERK signalling. *Nature reviews Molecular cell biology* **16**: 281-298.

Ley R, Balmanno K, Hadfield K, Weston C, Cook SJ. 2003. Activation of the ERK1/2 signaling pathway promotes phosphorylation and proteasome-dependent degradation of the BH3-only protein, Bim. *The Journal of biological chemistry* **278**: 18811-18816.

Li L, Modi H, McDonald T, Rossi J, Yee JK, Bhatia R. 2011. A critical role for SHP2 in STAT5 activation and growth factor-mediated proliferation, survival, and differentiation of human CD34+ cells. *Blood* **118**: 1504-1515.

Li X, Huang Y, Jiang J, Frank SJ. 2008. ERK-dependent threonine phosphorylation of EGF receptor modulates receptor downregulation and signaling. *Cellular signalling* **20**: 2145-2155.

Lito P, Pratilas CA, Joseph EW, Tadi M, Halilovic E, Zubrowski M, Huang A, Wong WL, Callahan MK, Merghoub T et al. 2012. Relief of profound feedback inhibition of mitogenic signaling by RAF inhibitors attenuates their activity in BRAFV600E melanomas. *Cancer cell* **22**: 668-682.

Lito P, Saborowski A, Yue J, Solomon M, Joseph E, Gadal S, Saborowski M, Kastenhuber E, Fellmann C, Ohara K et al. 2014. Disruption of CRAF-mediated MEK activation is required for effective MEK inhibition in KRAS mutant tumors. *Cancer cell* **25**: 697-710.

Lito P, Solomon M, Li LS, Hansen R, Rosen N. 2016. Allele-specific inhibitors inactivate mutant KRAS G12C by a trapping mechanism. *Science* **351**: 604-608.

Luciano F, Jacquel A, Colosetti P, Herrant M, Cagnol S, Pages G, Auberger P. 2003. Phosphorylation of Bim-EL by Erk1/2 on serine 69 promotes its degradation via the proteasome pathway and regulates its proapoptotic function. *Oncogene* **22**: 6785-6793.

Mainardi S, Mulero-Sanchez A, Prahallad A, Germano G, Bosma A, Krimpenfort P, Lieftink C, Steinberg JD, de Wit N, Goncalves-Ribeiro S et al. 2018. SHP2 is required for growth of KRAS-mutant non-small-cell lung cancer in vivo. *Nature medicine*.

Malone CF, Emerson C, Ingraham R, Barbosa W, Guerra S, Yoon H, Liu LL, Michor F, Haigis M, Macleod KF et al. 2017. mTOR and HDAC Inhibitors Converge on the TXNIP/Thioredoxin Pathway to Cause Catastrophic Oxidative Stress and Regression of RAS-Driven Tumors. *Cancer discovery* **7**: 1450-1463.

Manchado E, Weissmueller S, Morris JPt, Chen CC, Wullenkord R, Lujambio A, de Stanchina E, Poirier JT, Gainor JF, Corcoran RB et al. 2016. A combinatorial strategy for treating KRAS-mutant lung cancer. *Nature* **534**: 647-651.

Marais R, Light Y, Paterson HF, Marshall CJ. 1995. Ras recruits Raf-1 to the plasma membrane for activation by tyrosine phosphorylation. *The EMBO journal* **14**: 3136-3145.

Marais R, Light Y, Paterson HF, Mason CS, Marshall CJ. 1997. Differential regulation of Raf-1, A-Raf, and B-Raf by oncogenic ras and tyrosine kinases. *The Journal of biological chemistry* **272**: 4378-4383.

Martin MJ, Melnyk N, Pollard M, Bowden M, Leong H, Podor TJ, Gleave M, Sorensen PH. 2006. The insulin-like growth factor I receptor is required for Akt activation and suppression of anoikis in cells transformed by the ETV6-NTRK3 chimeric tyrosine kinase. *Molecular and cellular biology* **26**: 1754-1769.

Mason CS, Springer CJ, Cooper RG, Superti-Furga G, Marshall CJ, Marais R. 1999. Serine and tyrosine phosphorylations cooperate in Raf-1, but not B-Raf activation. *The EMBO journal* **18**: 2137-2148.

Matsunaga-Udagawa R, Fujita Y, Yoshiki S, Terai K, Kamioka Y, Kiyokawa E, Yugi K, Aoki K, Matsuda M. 2010. The scaffold protein Shoc2/SUR-8 accelerates the interaction of Ras and Raf. *The Journal of biological chemistry* **285**: 7818-7826.

Meloche S, Pouyssegur J. 2007. The ERK1/2 mitogen-activated protein kinase pathway as a master regulator of the G1- to S-phase transition. *Oncogene* **26**: 3227-3239.

Meng J, Fang B, Liao Y, Chresta CM, Smith PD, Roth JA. 2010. Apoptosis induction by MEK inhibition in human lung cancer cells is mediated by Bim. *PloS one* **5**: e13026.

Merchant M, Moffat J, Schaefer G, Chan J, Wang X, Orr C, Cheng J, Hunsaker T, Shao L, Wang SJ et al. 2017. Combined MEK and ERK inhibition overcomes therapy-mediated pathway reactivation in RAS mutant tumors. *PloS one* **12**: e0185862.

Milburn MV, Tong L, deVos AM, Brunger A, Yamaizumi Z, Nishimura S, Kim SH. 1990. Molecular switch for signal transduction: structural differences between active and inactive forms of protooncogenic ras proteins. *Science* **247**: 939-945.

Moghal N, Sternberg PW. 2003. The epidermal growth factor system in Caenorhabditis elegans. *Experimental cell research* **284**: 150-159.

Molina-Arcas M, Hancock DC, Sheridan C, Kumar MS, Downward J. 2013. Coordinate direct input of both KRAS and IGF1 receptor to activation of PI3 kinase in KRAS-mutant lung cancer. *Cancer discovery* **3**: 548-563.

Molzan M, Schumacher B, Ottmann C, Baljuls A, Polzien L, Weyand M, Thiel P, Rose R, Rose M, Kuhenne P et al. 2010. Impaired binding of 14-3-3 to C-RAF in Noonan syndrome suggests new approaches in diseases with increased Ras signaling. *Molecular and cellular biology* **30**: 4698-4711.

Morrison DK, Heidecker G, Rapp UR, Copeland TD. 1993. Identification of the major phosphorylation sites of the Raf-1 kinase. *The Journal of biological chemistry* **268**: 17309-17316.

Nakamura T, Colbert M, Krenz M, Molkentin JD, Hahn HS, Dorn GW, 2nd, Robbins J. 2007. Mediating ERK 1/2 signaling rescues congenital heart defects in a mouse model of Noonan syndrome. *The Journal of clinical investigation* **117**: 2123-2132.

Nazarian R, Shi H, Wang Q, Kong X, Koya RC, Lee H, Chen Z, Lee MK, Attar N, Sazegar H et al. 2010. Melanomas acquire resistance to B-RAF(V600E) inhibition by RTK or N-RAS upregulation. *Nature* **468**: 973-977.

Nussinov R, Tsai CJ, Jang H. 2018. Oncogenic Ras Isoforms Signaling Specificity at the Membrane. *Cancer research* **78**: 593-602.

O'Byrne KJ, Gatzemeier U, Bondarenko I, Barrios C, Eschbach C, Martens UM, Hotko Y, Kortsik C, Paz-Ares L, Pereira JR et al. 2011. Molecular biomarkers in non-small-cell lung cancer: a retrospective analysis of data from the phase 3 FLEX study. *The Lancet Oncology* **12**: 795-805.

Ory S, Zhou M, Conrads TP, Veenstra TD, Morrison DK. 2003. Protein phosphatase 2A positively regulates Ras signaling by dephosphorylating KSR1 and Raf-1 on critical 14-3-3 binding sites. *Current biology : CB* **13**: 1356-1364.

Ostrem JM, Peters U, Sos ML, Wells JA, Shokat KM. 2013. K-Ras(G12C) inhibitors allosterically control GTP affinity and effector interactions. *Nature* **503**: 548-551.

Ostrem JM, Shokat KM. 2016. Direct small-molecule inhibitors of KRAS: from structural insights to mechanism-based design. *Nature reviews Drug discovery* **15**: 771-785.

Parada LF, Tabin CJ, Shih C, Weinberg RA. 1982. Human EJ bladder carcinoma oncogene is homologue of Harvey sarcoma virus ras gene. *Nature* **297**: 474-478.

Patricelli MP, Janes MR, Li LS, Hansen R, Peters U, Kessler LV, Chen Y, Kucharski JM, Feng J, Ely T et al. 2016. Selective Inhibition of Oncogenic KRAS Output with Small Molecules Targeting the Inactive State. *Cancer discovery* **6**: 316-329.

Peng SB, Henry JR, Kaufman MD, Lu WP, Smith BD, Vogeti S, Rutkoski TJ, Wise S, Chun L, Zhang Y et al. 2015. Inhibition of RAF Isoforms and Active Dimers by LY3009120 Leads to Anti-tumor Activities in RAS or BRAF Mutant Cancers. *Cancer cell* **28**: 384-398.

Peti W, Page R. 2015. Strategies to make protein serine/threonine (PP1, calcineurin) and tyrosine phosphatases (PTP1B) druggable: achieving specificity by targeting substrate and regulatory protein interaction sites. *Bioorganic & medicinal chemistry* **23**: 2781-2785.

Plowman SJ, Williamson DJ, O'Sullivan MJ, Doig J, Ritchie AM, Harrison DJ, Melton DW, Arends MJ, Hooper ML, Patek CE. 2003. While K-ras is essential for mouse development, expression of the K-ras 4A splice variant is dispensable. *Molecular and cellular biology* **23**: 9245-9250.

Politi K, Zakowski MF, Fan PD, Schonfeld EA, Pao W, Varmus HE. 2006. Lung adenocarcinomas induced in mice by mutant EGF receptors found in human lung cancers respond to a tyrosine kinase inhibitor or to down-regulation of the receptors. *Genes & development* **20**: 1496-1510.

Poulikakos PI, Zhang C, Bollag G, Shokat KM, Rosen N. 2010. RAF inhibitors transactivate RAF dimers and ERK signalling in cells with wild-type BRAF. *Nature* **464**: 427-430.

Princen F, Bard E, Sheikh F, Zhang SS, Wang J, Zago WM, Wu D, Trelles RD, Bailly-Maitre B, Kahn CR et al. 2009. Deletion of Shp2 tyrosine phosphatase in muscle leads to dilated cardiomyopathy, insulin resistance, and premature death. *Molecular and cellular biology* **29**: 378-388.

Pritchard CA, Bolin L, Slattery R, Murray R, McMahon M. 1996. Post-natal lethality and neurological and gastrointestinal defects in mice with targeted disruption of the A-Raf protein kinase gene. *Current biology : CB* **6**: 614-617.

Razzaque MA, Nishizawa T, Komoike Y, Yagi H, Furutani M, Amo R, Kamisago M, Momma K, Katayama H, Nakagawa M et al. 2007. Germline gain-of-function mutations in RAF1 cause Noonan syndrome. *Nature genetics* **39**: 1013-1017.

Reiss Y, Goldstein JL, Seabra MC, Casey PJ, Brown MS. 1990. Inhibition of purified p21ras farnesyl:protein transferase by Cys-AAX tetrapeptides. *Cell* **62**: 81-88.

Riedl A, Schlederer M, Pudelko K, Stadler M, Walter S, Unterleuthner D, Unger C, Kramer N, Hengstschlager M, Kenner L et al. 2017. Comparison of cancer cells in 2D vs 3D culture reveals differences in AKT-mTOR-S6K signaling and drug responses. *Journal of cell science* **130**: 203-218.

Ritt DA, Monson DM, Specht SI, Morrison DK. 2010. Impact of feedback phosphorylation and Raf heterodimerization on normal and mutant B-Raf signaling. *Molecular and cellular biology* **30**: 806-819.

Ritt DA, Zhou M, Conrads TP, Veenstra TD, Copeland TD, Morrison DK. 2007. CK2 Is a component of the KSR1 scaffold complex that contributes to Raf kinase activation. *Current biology : CB* **17**: 179-184.

Rodriguez-Viciana P, Oses-Prieto J, Burlingame A, Fried M, McCormick F. 2006. A phosphatase holoenzyme comprised of Shoc2/Sur8 and the catalytic subunit of PP1 functions as an M-Ras effector to modulate Raf activity. *Molecular cell* **22**: 217-230.

Rodriguez-Viciana P, Sabatier C, McCormick F. 2004. Signaling specificity by Ras family GTPases is determined by the full spectrum of effectors they regulate. *Molecular and cellular biology* **24**: 4943-4954.

Rodriguez-Viciana P, Warne PH, Dhand R, Vanhaesebroeck B, Gout I, Fry MJ, Waterfield MD, Downward J. 1994. Phosphatidylinositol-3-OH kinase as a direct target of Ras. *Nature* **370**: 527-532.

Rommel C, Radziwill G, Lovric J, Noeldeke J, Heinicke T, Jones D, Aitken A, Moelling K. 1996. Activated Ras displaces 14-3-3 protein from the amino terminus of c-Raf-1. *Oncogene* **12**: 609-619.

Roux PP, Richards SA, Blenis J. 2003. Phosphorylation of p90 ribosomal S6 kinase (RSK) regulates extracellular signal-regulated kinase docking and RSK activity. *Molecular and cellular biology* **23**: 4796-4804.

Ruess DA, Heynen GJ, Ciecielski KJ, Ai J, Berninger A, Kabacaoglu D, Gorgulu K, Dantes Z, Wormann SM, Diakopoulos KN et al. 2018. Mutant KRAS-driven cancers depend on PTPN11/SHP2 phosphatase. *Nature medicine*.

Rushworth LK, Hindley AD, O'Neill E, Kolch W. 2006. Regulation and role of Raf-1/B-Raf heterodimerization. *Molecular and cellular biology* **26**: 2262-2272.

Sale MJ, Cook SJ. 2013a. The BH3 mimetic ABT-263 synergizes with the MEK1/2 inhibitor selumetinib/AZD6244 to promote BIM-dependent tumour cell death and inhibit acquired resistance. *The Biochemical journal* **450**: 285-294.

-. 2013b. That which does not kill me makes me stronger; combining ERK1/2 pathway inhibitors and BH3 mimetics to kill tumour cells and prevent acquired resistance. *British journal of pharmacology* **169**: 1708-1722.

Samatar AA, Poulikakos PI. 2014. Targeting RAS-ERK signalling in cancer: promises and challenges. *Nature reviews Drug discovery* **13**: 928-942.

Samuels Y, Diaz LA, Jr., Schmidt-Kittler O, Cummins JM, Delong L, Cheong I, Rago C, Huso DL, Lengauer C, Kinzler KW et al. 2005. Mutant PIK3CA promotes cell growth and invasion of human cancer cells. *Cancer cell* **7**: 561-573.

Samuels Y, Wang Z, Bardelli A, Silliman N, Ptak J, Szabo S, Yan H, Gazdar A, Powell SM, Riggins GJ et al. 2004. High frequency of mutations of the PIK3CA gene in human cancers. *Science* **304**: 554.

Sanclemente M, Francoz S, Esteban-Burgos L, Bousquet-Mur E, Djurec M, Lopez-Casas PP, Hidalgo M, Guerra C, Drosten M, Musteanu M et al. 2018. c-RAF Ablation Induces Regression of Advanced Kras/Trp53 Mutant Lung Adenocarcinomas by a Mechanism Independent of MAPK Signaling. *Cancer cell* **33**: 217-228 e214.

Sato K, Shin MS, Sakimura A, Zhou Y, Tanaka T, Kawanishi M, Kawasaki Y, Yokoyama S, Koizumi K, Saiki I et al. 2013. Inverse correlation between Thr-669 and constitutive tyrosine phosphorylation in the asymmetric epidermal growth factor receptor dimer conformation. *Cancer science* **104**: 1315-1322.

Scaltriti M, Baselga J. 2006. The epidermal growth factor receptor pathway: a model for targeted therapy. *Clinical cancer research : an official journal of the American Association for Cancer Research* **12**: 5268-5272.

Scheid MP, Schubert KM, Duronio V. 1999. Regulation of bad phosphorylation and association with Bcl-x(L) by the MAPK/Erk kinase. *The Journal of biological chemistry* **274**: 31108-31113.

Schoenhals JE, Seyedin SN, Anderson C, Brooks ED, Li YR, Younes AI, Niknam S, Li A, Barsoumian HB, Cortez MA et al. 2017. Uncovering the immune tumor microenvironment in non-small cell lung cancer to understand response rates to checkpoint blockade and radiation. *Translational lung cancer research* **6**: 148-158.

Schonhuber N, Seidler B, Schuck K, Veltkamp C, Schachtler C, Zukowska M, Eser S, Feyerabend TB, Paul MC, Eser P et al. 2014. A next-generation dual-recombinase system for time- and host-specific targeting of pancreatic cancer. *Nature medicine* **20**: 1340-1347.

Selfors LM, Schutzman JL, Borland CZ, Stern MJ. 1998. soc-2 encodes a leucine-rich repeat protein implicated in fibroblast growth factor receptor signaling. *Proceedings of the National Academy of Sciences of the United States of America* **95**: 6903-6908.

Shackelford DB, Abt E, Gerken L, Vasquez DS, Seki A, Leblanc M, Wei L, Fishbein MC, Czernin J, Mischel PS et al. 2013. LKB1 inactivation dictates therapeutic response of non-small cell lung cancer to the metabolism drug phenformin. *Cancer cell* **23**: 143-158.

Sieburth DS, Sun Q, Han M. 1998. SUR-8, a conserved Ras-binding protein with leucine-rich repeats, positively regulates Ras-mediated signaling in C. elegans. *Cell* **94**: 119-130.

Solit DB, Rosen N. 2014. Towards a unified model of RAF inhibitor resistance. *Cancer discovery* **4**: 27-30.

St-Denis N, Gupta GD, Lin ZY, Gonzalez-Badillo B, Veri AO, Knight JDR, Rajendran D, Couzens AL, Currie KW, Tkach JM et al. 2016. Phenotypic and Interaction Profiling of the Human Phosphatases Identifies Diverse Mitotic Regulators. *Cell reports* **17**: 2488-2501.

Sun C, Hobor S, Bertotti A, Zecchin D, Huang S, Galimi F, Cottino F, Prahallad A, Grernrum W, Tzani A et al. 2014. Intrinsic resistance to MEK inhibition in KRAS mutant lung and colon cancer through transcriptional induction of ERBB3. *Cell reports* **7**: 86-93.

Tan N, Wong M, Nannini MA, Hong R, Lee LB, Price S, Williams K, Savy PP, Yue P, Sampath D et al. 2013. Bcl-2/Bcl-xL inhibition increases the efficacy of MEK inhibition alone and in combination with PI3 kinase inhibition in lung and pancreatic tumor models. *Molecular cancer therapeutics* **12**: 853-864.

Taparowsky E, Suard Y, Fasano O, Shimizu K, Goldfarb M, Wigler M. 1982. Activation of the T24 bladder carcinoma transforming gene is linked to a single amino acid change. *Nature* **300**: 762-765.

Toyooka S, Tsuda T, Gazdar AF. 2003. The TP53 gene, tobacco exposure, and lung cancer. *Human mutation* **21**: 229-239.

Tsai FD, Lopes MS, Zhou M, Court H, Ponce O, Fiordalisi JJ, Gierut JJ, Cox AD, Haigis KM, Philips MR. 2015. K-Ras4A splice variant is widely expressed in cancer and uses a hybrid membrane-targeting motif. *Proceedings of the National Academy of Sciences of the United States of America* **112**: 779-784.

Turke AB, Song Y, Costa C, Cook R, Arteaga CL, Asara JM, Engelman JA. 2012. MEK inhibition leads to PI3K/AKT activation by relieving a negative feedback on ERBB receptors. *Cancer research* **72**: 3228-3237.

Turke AB, Zejnullahu K, Wu YL, Song Y, Dias-Santagata D, Lifshits E, Toschi L, Rogers A, Mok T, Sequist L et al. 2010. Preexistence and clonal selection of MET amplification in EGFR mutant NSCLC. *Cancer cell* **17**: 77-88.

Vachon PH. 2011. Integrin signaling, cell survival, and anoikis: distinctions, differences, and differentiation. *Journal of signal transduction* **2011**: 738137.

Valny M, Honsa P, Kirdajova D, Kamenik Z, Anderova M. 2016. Tamoxifen in the Mouse Brain: Implications for Fate-Mapping Studies Using the Tamoxifen-Inducible Cre-loxP System. *Frontiers in cellular neuroscience* **10**: 243.

Vojtek AB, Hollenberg SM, Cooper JA. 1993. Mammalian Ras interacts directly with the serine/threonine kinase Raf. *Cell* **74**: 205-214.

von Karstedt S, Conti A, Nobis M, Montinaro A, Hartwig T, Lemke J, Legler K, Annewanter F, Campbell AD, Taraborrelli L et al. 2015. Cancer cell-autonomous TRAIL-R signaling promotes KRAS-driven cancer progression, invasion, and metastasis. *Cancer cell* **27**: 561-573.

Wan PT, Garnett MJ, Roe SM, Lee S, Niculescu-Duvaz D, Good VM, Jones CM, Marshall CJ, Springer CJ, Barford D et al. 2004. Mechanism of activation of the RAF-ERK signaling pathway by oncogenic mutations of B-RAF. *Cell* **116**: 855-867.

Wang T, Yu H, Hughes NW, Liu B, Kendirli A, Klein K, Chen WW, Lander ES, Sabatini DM. 2017. Gene Essentiality Profiling Reveals Gene Networks and Synthetic Lethal Interactions with Oncogenic Ras. *Cell* **168**: 890-903 e815.

Ward MC, Prabhu RS, Burri SH. 2018. Osimertinib in EGFR Mutation-Positive Advanced NSCLC. *The New England journal of medicine* **378**: 1261.

Weber CK, Slupsky JR, Kalmes HA, Rapp UR. 2001. Active Ras induces heterodimerization of cRaf and BRaf. *Cancer research* **61**: 3595-3598.

Whittaker SR, Cowley GS, Wagner S, Luo F, Root DE, Garraway LA. 2015. Combined Pan-RAF and MEK Inhibition Overcomes Multiple Resistance Mechanisms to Selective RAF Inhibitors. *Molecular cancer therapeutics* **14**: 2700-2711.

Whittaker SR, Theurillat JP, Van Allen E, Wagle N, Hsiao J, Cowley GS, Schadendorf D, Root DE, Garraway LA. 2013. A genome-scale RNA interference screen implicates NF1 loss in resistance to RAF inhibition. *Cancer discovery* **3**: 350-362.

Whyte DB, Kirschmeier P, Hockenberry TN, Nunez-Oliva I, James L, Catino JJ, Bishop WR, Pai JK. 1997. K- and N-Ras are geranylgeranylated in cells treated with farnesyl protein transferase inhibitors. *The Journal of biological chemistry* **272**: 14459-14464.

Wojnowski L, Stancato LF, Zimmer AM, Hahn H, Beck TW, Larner AC, Rapp UR, Zimmer A. 1998. Craf-1 protein kinase is essential for mouse development. *Mechanisms of development* **76**: 141-149.

Wojnowski L, Zimmer AM, Beck TW, Hahn H, Bernal R, Rapp UR, Zimmer A. 1997. Endothelial apoptosis in Braf-deficient mice. *Nature genetics* **16**: 293-297.

Wong GS, Zhou J, Liu JB, Wu Z, Xu X, Li T, Xu D, Schumacher SE, Puschhof J, McFarland J et al. 2018. Targeting wild-type KRAS-amplified gastroesophageal cancer through combined MEK and SHP2 inhibition. *Nature medicine*.

Xing F, Persaud Y, Pratilas CA, Taylor BS, Janakiraman M, She QB, Gallardo H, Liu C, Merghoub T, Hefter B et al. 2012. Concurrent loss of the PTEN and RB1 tumor suppressors attenuates RAF dependence in melanomas harboring (V600E)BRAF. *Oncogene* **31**: 446-457.

Xu GF, O'Connell P, Viskochil D, Cawthon R, Robertson M, Culver M, Dunn D, Stevens J, Gesteland R, White R et al. 1990. The neurofibromatosis type 1 gene encodes a protein related to GAP. *Cell* **62**: 599-608.

Yao Z, Torres NM, Tao A, Gao Y, Luo L, Li Q, de Stanchina E, Abdel-Wahab O, Solit DB, Poulikakos PI et al. 2015. BRAF Mutants Evade ERK-Dependent Feedback by Different Mechanisms that Determine Their Sensitivity to Pharmacologic Inhibition. *Cancer cell* **28**: 370-383.

Yao Z, Yaeger R, Rodrik-Outmezguine VS, Tao A, Torres NM, Chang MT, Drosten M, Zhao H, Cecchi F, Hembrough T et al. 2017. Tumours with class 3 BRAF mutants are sensitive to the inhibition of activated RAS. *Nature* **548**: 234-238.

Yi J, Chen M, Wu X, Yang X, Xu T, Zhuang Y, Han M, Xu R. 2010. Endothelial SUR-8 acts in an ERK-independent pathway during atrioventricular cushion development. *Developmental dynamics : an official publication of the American Association of Anatomists* **239**: 2005-2013.

Yoshiki S, Matsunaga-Udagawa R, Aoki K, Kamioka Y, Kiyokawa E, Matsuda M. 2010. Ras and calcium signaling pathways converge at Raf1 via the Shoc2 scaffold protein. *Molecular biology of the cell* **21**: 1088-1096.

Young LC, Hartig N, Boned Del Rio I, Sari S, Ringham-Terry B, Wainwright JR, Jones GG, McCormick F, Rodriguez-Viciana P. 2018. SHOC2-MRAS-PP1 complex positively regulates RAF activity and contributes to Noonan syndrome pathogenesis. *Proceedings of the National Academy of Sciences of the United States of America*.

Young LC, Hartig N, Munoz-Alegre M, Oses-Prieto JA, Durdu S, Bender S, Vijayakumar V, Vietri Rudan M, Gewinner C, Henderson S et al. 2013. An MRAS, SHOC2, and SCRIB complex coordinates ERK pathway activation with polarity and tumorigenic growth. *Molecular cell* **52**: 679-692.

Zambrano RM, Marble M, Chalew SA, Lilje C, Vargas A, Lacassie Y. 2017. Further evidence that variants in PPP1CB cause a rasopathy similar to Noonan syndrome with loose anagen hair. *American journal of medical genetics Part A* **173**: 565-567.

Zha J, Harada H, Yang E, Jockel J, Korsmeyer SJ. 1996. Serine phosphorylation of death agonist BAD in response to survival factor results in binding to 14-3-3 not BCL-X(L). *Cell* **87**: 619-628.

Zhang Z, Jiang G, Yang F, Wang J. 2006. Knockdown of mutant K-ras expression by adenovirus-mediated siRNA inhibits the in vitro and in vivo growth of lung cancer cells. *Cancer biology & therapy* **5**: 1481-1486.

Zhao W, Sachsenmeier K, Zhang L, Sult E, Hollingsworth RE, Yang H. 2014. A New Bliss Independence Model to Analyze Drug Combination Data. *Journal of biomolecular screening* **19**: 817-821.

Supplementary Methods

Full SHOC2 Sequence

Homo sapiens SHOC2, leucine rich repeat scaffold protein (SHOC2), transcript variant 1, mRNA:

GAGTGGGGGAGGGGCGGGCGGGGGGCGGCGGTTGGGCAGCGTCGCTTCTTAGGAGGAGGAGGAAGAGGA
GGAAGGAGGGCGAGCGAGGAGGATGGCGGAGTCGGGGCTCCTGACGGAACTCTAATGAATCATTGATTG
ACCAGCACTATTTTACCAGTTGGAATGAATGATCAGAAATGGGCATAGTGCTTTTAGATCCAACATGTA
ACAGATGGATGTTACTCCATGCTGATTACTTCTTCAAGCCAGTACTTTTTTGATTGTGTAGGATCTTTG
TCTCTTCATCTTTGAATTCAATTACTGGAAAATAAAAGGAGTTCATGTAGTTTTTGTCCAGGCTTGAGT
CACCATGAGTAGTAGTTTAGGAAAAGAAAAAGACTCTAAAGAAAAAGATCCCAAAGTACCATCAGCCAA
GGAAAGAGAAAAGGAGGCAAAAGCCTCTGGAGGTTTTGGGAAAGAGAGCAAAGAAAAAGAACCTAAGAC
CAAAGGGAAAGATGCCAAAGATGGAAAGAAGGACTCCAGTGCTGCCCAACCAGGGGTGGCATTTTCAGT
TGACAATACGATCAAACGGCCAAACCCAGCACCTGGGACTAGAAAAAAATCCAGCAATGCAGAGGTGAT
TAAAGAGCTCAACAAATGCCGGGAAGAGAATTCAATGCGTTTGGACTTATCCAAGAGATCTATACACAT
ATTGCCATCATCAATCAAAGAGTTGACTCAATTAACAGAACTTTATTTATACAGTAACAAATTGCAGTC
CCTCCCAGCAGAGGTGGGATGTTTAGTAAATCTCATGACACTGGCTCTAAGTGAAAATTCACTTACCAG
TTTGCCTGACTCTCTTGATAACTTGAAGAAGCTGCGGATGCTTGATTTACGGCATAATAAACTGAGAGA
AATTCCTTCAGTGGTGTATAGGCTGGATTCTCTCACCACTCTTTACCTTCGCTTTAATCGTATAACTAC
TGTGGAAAAGGACATCAAAAACTTGTCAAAACTCAGCATGCTTAGCATTCGAGAGAACAAAATTAAACA
ACTACCTGCTGAAATTGGTGAATTATGTAACCTCATTACGCTGGATGTAGCTCACAATCAACTTGAACA
CCTTCCAAAGGAGATTGGAAACTGTACACAGATAACCAACCTTGACTTGCAGCACAATGAACTGCTAGA
CCTCCCAGATACTATAGGAAACCTGTCCAGTTTAAGTCGTCTTGGTCTGAGATATAACAGACTGTCAGC
AATACCCAGATCATTAGCAAAATGCAGTGCACTTGAAGAATTAAATTTAGAGAACAATAACATTTCTAC
TTTACCAGAGAGTCTTTTATCAAGTCTTGTGAAACTGAATAGTTTGACCTTAGCTAGAAATTGCTTCCA
GTTGTATCCAGTGGGTGGTCCATCTCAGTTTTCTACCATCTATTCCCTCAACATGGAACACAATCGAAT
CAACAAAATTCCATTTGGAATTTTCTCCAGAGCAAAAGTATTAAGTAAGCTGAATATGAAGGACAATCA
GTTAACATCACTTCCCTTGGATTTTGGAACTTGGACCAGTATGGTAGAATTGAATTTAGCCACTAATCA
GCTCACAAAGATCCCTGAGGATGTGTCTGGTCTCGTTTCTCTTGAGGTTCTTATCTTATCAAACAATCT
TCTAAAGAAGCTTCCCCATGGTCTTGGAAACCTTAGGAAGTTAAGAGAGTTGGATCTAGAAGAGAACAA
ATTGGAATCCTTGCCAAATGAAATTGCATATCTTAAGGATTTACAGAAATTAGTCTTGACAAACAACCA
GTTGACCACTCTTCCCAGAGGCATTGGTCACCTTACTAATCTCACACATCTGGGCCTTGGAGAGAACCT
ACTTACTCACCTTCCTGAAGAAATTGGTACACTCAACCTGCATAGCCTTCCCTTTGAGCTGGCACTCTG
CAGCAAGCTTTCAATCATGAGTATTGAGAACTGTCCACTCAGTCACCTTCCACCTCAGATTGTTGCTGG
GGGGCCTTCTTTCATCATTCAGTTCTTAAAGATGCAGGGTCCATATCGTGCCATGGTCTGATATAAATC
TGCTGGTCCCACACACTGTTCAAAAATAGACTGCCATTAATGTTTCTTATCTATATCTGTATCTATTTA
TGTAGATATTGGTATATGGCAGATTTATAAAAATTGCATTATGTGTTTCTGCTAATAGAGGAATCATAG
CCATTTAGAATTTTTTTTAAATTCTGTACAAAAGGCTTATATAAGTTTTCTTTGCTGAATTTGATGGAT
GTTTTTCTGTTGTGTAATCTGATATGCCAGTTTGCTTAAAACATTTGCCAACACATTATGAAGTTATTA
AATTTAAGGGACAGAGGTAGTATAGTTAGATATACTTTCTCTTAGGAAAAATAATGGGCAAAAATTTTT
GTTGCAACTTTTCATATATATTTTCCCCTTACCAATTGTTTTATCCTTATAGTATTGTAGGCCCTGAAA
GTAGAATTTTTCTTTAACTTATTTTGAGATTTGAGATTTAAATTTTATGTATTGTTTACAGTCAGAGTA
AATCACTGGATTTCTTTTGTTTGTTTTGATTTGCTCTGTTTTATTCAGTCAAATCTAGAGTTTGAATCC
TCTGCTAAAGAATTTGCATCCACTGGTGTAAACAGTGAAAGGTATTTGCTTGTTGAAAAAAAAAACTGG
CAAAGTGAAAAGATACAGTCAAAAATCTAGAATTTCTTTAATTTTGCTTCTCTGACGAGTTGTGAAGCA
AAATACCTGAAGTGAGTCTTTGGGTAGGGGAAGGGTATTGAGACCTTTTCTAGTATGAATATTTTTTAA
GTTTGGGGGAAGAGAAACTTGCAGTGAAAAGGAGTTTTTTCATTCCTGAAAGTTGCAGATCCACAAAAC
TAACAGGATAATTGGGCAAATAAATTACATATAAACACACACAATCTATATATGTATATACAATGCTAT
ATAGATATGTATTTATTATATCATAAACTACAGTAGGTAACTTTAAGGATTTCTTCCTATCCTTGTACA
ATGACATGAATGTCTTTCTTTGAAAACTGCAATGTATGTATGTTTCAAGGTTATTTAACAGTGTACTAT
GGTTTTATATCTTGACTTGCCTTGTACATCTTTCAATTCTGGAATATCTGTGTCTAAGCACAATATCTT
CACACTGTGCTGTATTGCTGCTGAACTAAATGCACTTTTCCCCACATATGGGGCACTGGCTTCAAACAA
TTCAGTTCAGTATCATTACTTTTAATCTCATCTTTCCTTTCTTGGTAGTTGTTAATACAGTTATGGAAA
AGAGGCACATTGCATAGAAGCCATTGGGGAGTTCAGTGGAAGTTCTGTAAGATGTGCATGTACTATTTG
ATGCGTTTTCTTTGCTTCACTGCTTTTAATACTTAGCAGTATTGTTGGTCTAAGTCAATTTGATTATTG
AGGAGTCTCAGAGCAAGGTGCGTTCTAGATGTCATCCTAAAAAACACTTCATATATAATTAATCACTAT
TTTGTATAATTACATATTGCTGCTTGTGTGTTTTTTTTTTTTCCATTTAGTTGGGCGTTGTGTTTTAC
ACAAAACCATTTTTGAATTAAGGCTATGATATTAAGATAGAAATTTGGACTGTTGTTCTGCTTTTCCTG
GCACTCAAATTCATGACTAGTTTTGAGGTCAAACCTATGTTCGTAATGAGAGATTTTATAAGGATCAAC

TAAGAAATGGAAGGCAGGTGAAGATATAAAACCCTAGAATGCTTAAATGTGCTGTAAAACTATTGTAGA
TGTCACTGGATTTTACCAAGTAATATCCTTTCTTTTTTTTTTCCCCCCATCTGCTGTGGCTTTTCAGTT
AAAATTTTGTTTATAAAAGGAATTTGTTTATTACAGCTCTACCTAGAAAAAAAAAAAAAAAA

SHOC2 coding sequence only

>SHOC2coding
ATGAGTAGTAGTTTAGGAAAAGAAAAAGACTCTAAAGAAAAAGATCCCAAAGTACCATCAGCCAAGGAA
AGAGAAAAGGAGGCAAAAGCCTCTGGAGGTTTTGGGAAAGAGAGCAAAGAAAAAGAACCTAAGACCAAA
GGGAAAGATGCCAAAGATGGAAAGAAGGACTCCAGTGCTGCCCAACCAGGGGTGGCATTTTCAGTTGAC
AATACGATCAAACGGCCAAACCCAGCACCTGGGACTAGAAAAAAATCCAGCAATGCAGAGGTGATTAAA
GAGCTCAACAAATGCCGGGAAGAGAATTCAATGCGTTTGGACTTATCCAAGAGATCTATACACATATTG
CCATCATCAATCAAAGAGTTGACTCAATTAACAGAACTTTATTTATACAGTAACAAATTGCAGTCCCTC
CCAGCAGAGGTGGGATGTTTAGTAAATCTCATGACACTGGCTCTAAGTGAAAATTCACTTACCAGTTTG
CCTGACTCTCTTGATAACTTGAAGAAGCTGCGGATGCTTGATTTACGGCATAATAAACTGAGAGAAATT
CCTTCAGTGGTGTATAGGCTGGATTCTCTCACCACTCTTTACCTTCGCTTTAATCGTATAACTACTGTG
GAAAAGGACATCAAAAACTTGTCAAAACTCAGCATGCTTAGCATTCGAGAGAACAAAATTAAACAACTA
CCTGCTGAAATTGGTGAATTATGTAACCTCATTACGCTGGATGTAGCTCACAATCAACTTGAACACCTT
CCAAAGGAGATTGGAAACTGTACACAGATAACCAACCTTGACTTGCAGCACAATGAACTGCTAGACCTC
CCAGATACTATAGGAAACCTGTCCAGTTTAAGTCGTCTTGGTCTGAGATATAACAGACTGTCAGCAATA
CCCAGATCATTAGCAAAATGCAGTGCACTTGAAGAATTAAATTTAGAGAACAATAACATTTCTACTTTA
CCAGAGAGTCTTTTATCAAGTCTTGTGAAACTGAATAGTTTGACCTTAGCTAGAAATTGCTTCCAGTTG
TATCCAGTGGGTGGTCCATCTCAGTTTTCTACCATCTATTCCCTCAACATGGAACACAATCGAATCAAC
AAAATTCCATTTGGAATTTTCTCCAGAGCAAAAGTATTAAGTAAGCTGAATATGAAGGACAATCAGTTA
ACATCACTTCCCTTGGATTTTGGAACTTGGACCAGTATGGTAGAATTGAATTTAGCCACTAATCAGCTC
ACAAAGATCCCTGAGGATGTGTCTGGTCTCGTTTCTCTTGAGGTTCTTATCTTATCAAACAATCTTCTA
AAGAAGCTTCCCCATGGTCTTGGAAACCTTAGGAAGTTAAGAGAGTTGGATCTAGAAGAGAACAAATTG
GAATCCTTGCCAAATGAAATTGCATATCTTAAGGATTTACAGAAATTAGTCTTGACAAACAACCAGTTG
ACCACTCTTCCCAGAGGCATTGGTCACCTTACTAATCTCACACATCTGGGCCTTGGAGAGAACCTACTT
ACTCACCTTCCTGAAGAAATTGGTACACTGGAGAACCTAGAAGAACTGTATTTGAATGACAACCCCAAC
CTGCATAGCCTTCCCTTTGAGCT**GG**CACTCTGCAGCAAGCTTTCAATCATGAGTATTGAGAACTGTCCA
CTCAGTCACCTTCCACCTCAGATTGTTGCTGGGGGGCCTTCTTTCATCATTCAGTTCTTAAAGATGCAG
GGTCCATATCGTGCCATGGTCTGA

CRSPR
CATTACGCTGGATGTAGCTC
Complementary Guide - GAGCTACATCCAGCGTAATG

shRNA-pGIPZ
>SH1GIPZ
CTGCTGAAATTGGTGAATT
>SH3GIPZ
CCATTAATGTTTCTTATCT

siRNA
>SHOC2-5Q
GCTGCGGATGCTTGATTTA
>STEALTH928
GAACTTGGACCAGTATGGTAGAATT